Beatriz Aguiar Moreiras Vicente dos Santos

Licenciatura em Engenharia Química e Bioquímica

Optimization of Sensing Materials for Gas Detection

Dissertação para obtenção do Grau de Mestre em
Engenharia Química e Bioquímica

Orientadora: A. Cecília Roque, Associate Professor, FCT-NOVA

FACULDADE DE CIÊNCIAS E TECNOLOGIA
UNIVERSIDADE NOVA DE LISBOA

Março, 2019

Optimization of Sensing Materials for Gas Detection

Acknowledgments

Firstly, I would like to thank my adviser, Professor Cecília Roque, for giving me the opportunity to integrate in her research team, and helping me grow on a personal and professional level, always encouraging me to pursue my ideas.

Next, I would like to thank Gonçalo Santos, my guide on the lab, who closely followed my work. Always helping me to keep my feet on the ground and dealing with the drawbacks.

A special thanks to Henrique Costa, one of my greatest friends and colleagues, to whom I have the greatest respect and consideration. Whenever I doubted my ideas, I would go to him for better clairvoyance and support.

To my partner, Óscar Campos, I would like to give a very special thanks, for always supporting me and never running away when things weren't so great. For believing in me and accompanying by my side, in every journey.

To my father, Emídio Santos, and mother, Helena Vicente, for always pushing me to go further and challenging me to do better. Always teaching me to be independent, but always reassuring that if I wanted they would be there.

To my uncle Luís Barrocas and aunt Patrícia Barrocas, for giving me a quiet and safe place whenever I needed, and a lot of support.

Lastly, but not least, I would like to thank all the Biomolecular Engineering Lab group, for giving a warm welcome, useful feedback, great help throughout this journey and, for taking interest in my work.

Abstract

Gas sensing devices are in crescent demand, due to their vast applicability in several fields of interest, such as Agriculture, Biomedical, Food and Beverages industries, among others. These devices employ different technologies, however some features are commonly desirable, such as portability, accuracy, robustness, selectivity and reusability, nonetheless some of these are difficult to achieve.

In this work, sensing gels employing liquid crystal doped with surfactant and immobilized on a biopolymeric matrix were produced and applied on an in-house built sensing device (e-nose) in order to detect Volatile Organic Compounds (VOCs).

Two main studies were conducted: (i) the effect of the surfactant on the sensing gels, and (ii) the impact of changing the pH during gels production. Both studies had the purpose to increase the stability, durability of the gels and enhance the selectivity of these sensors. On both studies the morphology of the liquid crystal droplets, and the response of the sensing gels on the e-nose were evaluated.

Five different surfactants were used to carry out these studies, [Bmim][DCA], [Bmim][Cl], [C12mim][Cl], SDS and [C12mim][DS].

Better stability and durability, as well as some selectivity were achieved with [C12mim][Cl]. The liquid crystal droplets doped with this surfactant, maintained most of their configuration after being exposed to 12 VOCs, and resisted even after 22 days. Moreover, a score over 85% on VOCs discriminations was achieved.

Keywords: Gas sensing devices, VOCs, surfactants, droplets

Resumo

Dispositivos para deteção de gases têm vindo a possuir uma procura crescente, devido à sua vasta empregabilidade em diversos campos de interesse, tais como, Agricultura, Biomédica, indústrias de Comidas e Bebidas, entre outros. Estes dispositivos utilizam diferentes tecnologias, contudo algumas características são comumente desejáveis, tais como, portabilidade, precisão, robustez, selectividade e reutilização, embora, algumas das mesmas são dificilmente alcançáveis.

Neste trabalho, géis que actuam como sensores, utilizando cristal líquido coberto com surfactante e imobilizado numa matriz biopolimérica, foram produzidos e aplicados num dispositivo de detecção, construído internamente com o objectivo de detectar Compostos Orgânicos Voláteis (VOCs).

Dois estudos principais foram realizados: i) o efeito do surfactante nos géis sensores, e ii) o impacto da mudança de pH durante a produção dos géis. Ambos os estudos tinham o propósito de aumentar a estabilidade, durabilidade dos géis e melhorar a selectividade destes sensores. Nos dois estudos, a morfologia das droplets de cristal líquido e a resposta, dos géis sensores, no e-nose foram avaliadas.

Cinco surfactants diferentes foram utilizados de forma a realizar estes estudos, [Bmim][DCA], [BmimCl] [C_{12}mim][Cl], SDS e [C_{12}mim][DS].

Uma melhor estabilidade e durabilidade, assim como, alguma selectividade foram conseguidas com [C_{12}mim][Cl. Droplets de cristal líquido cobertas com este surfactante, mantiveram maioritariamente a sua configuração após exposição a 12 VOCs e resistiram durante 22 dias. Ademais um resultado acima dos 85%, relativamente à discriminação de VOCs fora conseguido.

Termos-chave: Dispositivos de detecção de gás; VOCs; surfactantes, droplets

Table of Contents

Index of Figures

Index of Tables

List of Abbreviations

5CB: 4-Cyano-4'-pentylbiphenyl

8CB: 4′-Octyl-4-biphenylcarbonitrile

CB15: [4-(2-methylbutyl)-4-cyanobiphenyl]

E7: mixture of cyanobphenyls with long aliphatic tails

BAW: Bulk Acoustic Wave

[Bmim][Cl]: 1-Butyl-3-methylimidazolium chloride

[Bmim][DCA]: 1-Butyl-3-methylimidazolium dicyanamide

[C_{12}mim][Cl]: 1-Dodecyl-3-methylimidazolium chloride

[C_{12}mim][DS]: 1-Dodecyl-3-methylimidazolium dodecyl sulphate

CARG: Compound Annual Rate Growth

CB: Catalytic Bead

CMC: Critical Micellar Concentration

E-nose: Electronic Nose

EPA: Environmental Protection Agency

IL: Ionic Liquid

LC: Liquid Crystal

LEDs: Light-Emitting Diodes

MOS: Metal Oxide Semiconductors

PDs: PhotoDiodes

PVA: Polyvinyl alcohol

QMB: Quartz Crystal Microbalance

SAW: Surface Acoustic Wave

SDS: Sodium Dodecyl Sulphate

VOCs: Volatile Organic Compounds

1. Introduction

1.1. Artificial Olfaction and The Electronic Nose

The electronic nose (E-nose) is a device that was design and developed with the intent to mimic the mammalian olfactory system, in order to sense mixtures of Gaseous Analytes released from several sources, accurately discriminating and properly identifying them through a pattern recognition system. [1]–[5].

Since the e-nose concept was based on the olfactory system, it seems reasonable to make a comparison between the two, for a better understanding of the process. Hence, on table 1.1 it is possible to find the proper correspondence between the functions performed by the two systems mentioned, from the beginning when the mammalian nose enters in contact with the odour, to the final recognition and identification, which are performed by the brain. Then it is possible to comprehend how the e-nose reaches to the same conclusion [6]–[8].

Nevertheless, one difference is noticeable, the mammalian olfactory system can only sense the smell, or odour, in contrast the e-nose has the potential of sensing not only the odours, but as well as other Gaseous Analytes.

Table 1.1 Comparison between the functions of the mammalian olfactory system and the e-nose [1], [2]

Mammalian Olfactory System	Electronic Nose
Inhalation	Input of a sample with Gaseous Analytes
Interaction of odours with the olfactory receptors	Interaction of the Gaseous Analytes with the sensor array
Inducement of a reaction and generation of signals	Generation of signals from the reaction within the sensors
Transmission of the signals to the brain	Transmission of the signals to the pattern recognition mechanism
Recognition of the signal based on the memory	Match of the signal with the known patterns of the system
Identification of the odour	Identification of the Gaseous Analyte

A particular category of gases is the Volatile Organic Compounds. (VOCs). These are defined by the Environmental Protection Agency (EPA), “as any compound of carbon, excluding some compounds, such as carbon monoxide, carbon dioxide, among others, which participate in atmospheric photochemical reactions” [9]. For the purpose of the device employed on this work,

which is to be able to make an early non-invasive diagnostic, it should be noted that some microorganisms release, in their early stages, VOCs [10]. Thus, with this device (e-nose) it should be possible to detect some infectious diseases in their early stages, through a non-invasive and accurate method.

Regarding the technologies employed on the e-nose, and their components, there can be found several sorts, each on with their unique characteristics and features. However some features, such as rapid response, high sensitivity and selectivity, cost-effectiveness, portability among others are common and desirable, nonetheless these are considered some of the most harder features to properly achieve [2], [11], [12]. The most common technologies employed on these devices are the Metal Oxide Semiconductors (MOS), conducting polymers and surface acoustic wave, nonetheless, other technologies emerge and may also be applied for gas sensing devices. Table 1.2, based on the review *Applications and Advances in Electronic-Nose Technologies* by A. D. Wilson, indicates the several possible technologies, detection principles and respective materials that are applied to the e-noses systems [5], [7].

Table 1.2 Comparison between the different possible technologies employed on electronic noses systems.

Sensor Technology	Detection Principle	Sensitive Material
Metal Oxides Semi-Conducting (MOS)	Resistance change	Doped semi-conducting materials oxides (SnO_2, GaO)
Conducting Polymers	Resistance change	Modified conducting polymers
Quartz crystal microbalance (QMB)	Mass change (frequency shift)	Organic or inorganic film layers
Surface and Bulk acoustic wave (SAW & BAW)	Mass change (frequency shift)	Organic or inorganic film layers
Optical Sensors	Light modulation and optical changes	Photodiode and light-sensitive materials
Electrochemical sensors	Current or voltage change	Solid or liquid electrolytes
Fluorescence sensors	Fluorescent-light emissions	Fluorescence-sensitive detector
Colorimetric sensors	Colour changes, absorbance	Organic dyes
Catalytic field-effect sensors (MOSFET)	Electric field change	Catalytical metals
Calorimetric	Temperature or heat change (from chemical reactions)	Pellistor
Catalytic Bead (CB)	Temperature or heat change (from chemical reactions)	Pellistor
Infrared sensors	Infrared-radiation absorption	IR-sensitive detector

Regarding these technologies (table 1.2.), each possess their own advantages and disadvantages. Some technologies such as MOS, Conducting Polymers among others, are low cost, however, possess low or poor sensitivity. Contrastingly, high cost technologies, such as optical sensors,

have high sensitivity, thus, according to the desired application of the device the appropriate technology should be employed.

A representation of the e-nose system employed on this work can be found on figure 1.1. In this system the liquid sample which contains the VOC(s) that will be delivered to the detection device, need to be heated to approximately 37 ºC in order to evaporate the VOC(s), then the gaseous sample passes through the detection chamber containing the sensing gels array (the array is composed by six sensing gels) and on figure 4.9. (Chapter4) is a schematic representation of the operation mode of this chamber. Regarding the response emitted by the sensors, these are received by the PhotoDiodes (PDs), which are semiconductors (or light detectors) that transmit a current proportional to the number of photons received, the photons that reached the optical active area of the sensors. This generated current is then converted into tension, through an amplifier of transimpedance in order that the signals emitted from the e-nose and received on the Arduino, might be understood and read.

The Arduino will act as the signal and command receiver, meaning the computer will give orders for the proper operation of the system and the Arduino receives and transmits these to the several components, such as the pumps and the LEDs, moreover it will act as well as the receiver of the signals emitted by the detection chamber [13]–[15]. It should be mentioned, that in the detection chamber all the components must be properly align, so that the light passes through the non-covered window on the sensing gels, thus, not dispersing, and reaching the PDs.

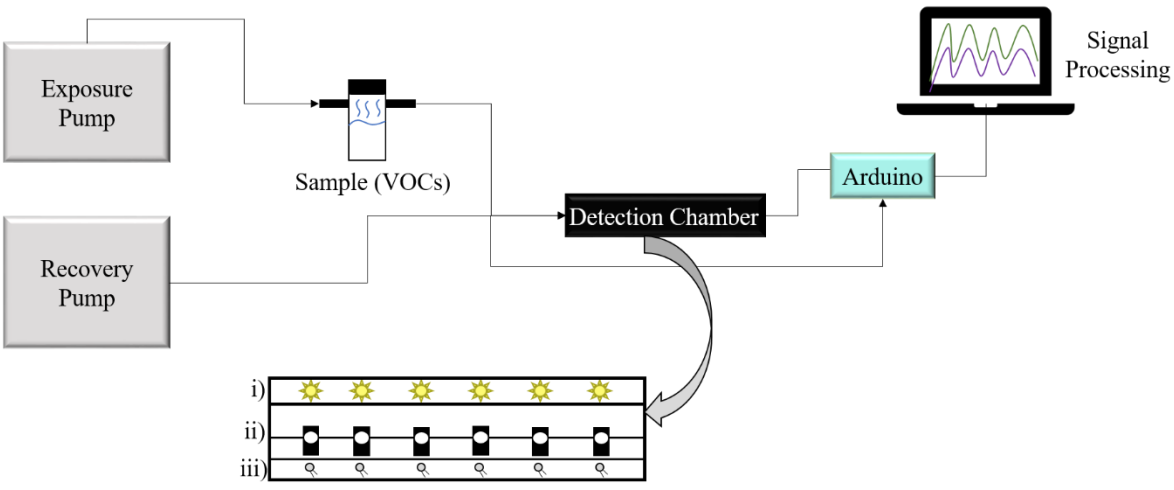

Figure 1.1 - Illustration of the e-nose system; i) LEDs that will emit the light when the system is working; ii) Array of glass slides containing the sensing gels; iii) Array of PDs

The search for newer and better technologies is always growing, particularly for some industries and sectors of the market this is a constant need, e.g. biomedical applications, food and beverages

industry, therefor it is important to have a realistic perspective of the market, where does the e-nose and its components are inserted [16].

According to the data published on the *Royal Society of Chemistry Advances* in 2015, which allowed the construction of graphic presented in figure 1.2., the gas sensing market revenue is estimated to be 6.3 billion USD with a growth rate of 10% for new technologies [16]. Observing the figure 1.2., it is verified that the e-nose belongs to the biggest share of the gas sensing market and according to the same literature, that is the sector with highest growth.

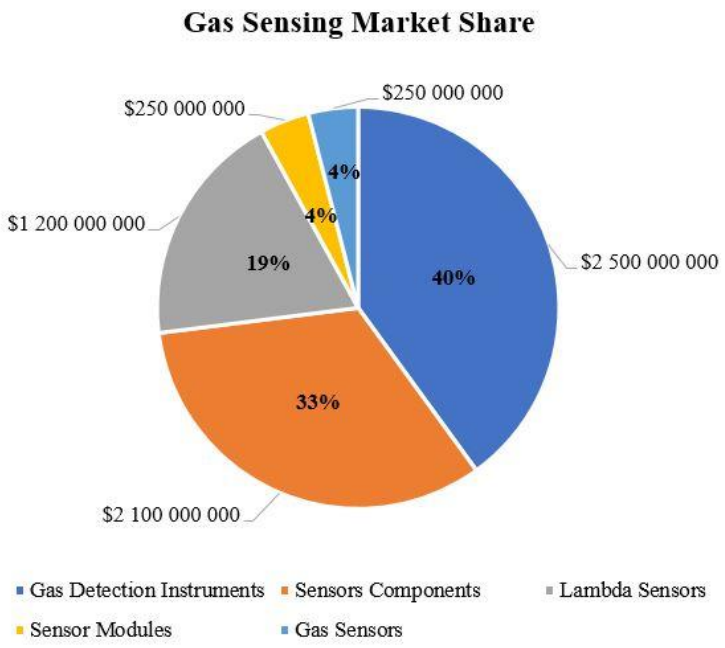

Figure 1.2. Global Share and Value of the different sectors regarding the gas sensing market

Regarding some more recent studies and published data, in 2017 the e-nose market was estimated to have a value of 17.7 million USD, with a 10.1 % forecast growth between 2018 and 2023 [17]–[19]. Nevertheless, other studies claim that between 2017 and 2025 the Compound Annual Rate Growth (CARG) will be of 42.7 % [20], meaning that this market is still growing with increasing rates, demonstrating the need of this new technology and device.

In terms of applications, the e-nose can be found in several field of interest due to its potential in the detection of gases and odours, such as Food and beverage industries, Agricultural industry, Pharmaceutical, Cosmetics, Biomedical, Environmental monitoring, among numerous others [2].

It is well known, that infectious diseases caused by bacteria that release VOCs as a form to interact, not only among themselves, but as well as a form to interact with the host [2], [11]. In this sense the e-nose reveals itself as a powerful device for early diagnostics application, since it can detect mixtures of bacterial VOCs.

1.2. New Gas Sensing Materials

In this work, the sensors employed on the e-nose system are sensing gels (optical sensors), that consist on four main components, the sensing material which in this case is a liquid crystal, the stabilizer, which is a surfactant, the immobilization agent and the medium, or solvent where the gels are produced. These sensing gels and the e-nose system adapted were recently developed [15], [21].

Regarding the sensing devices on the e-nose, these are composed by sensing gels applied on a glass slide.

Intrinsically these gels are emulsions, meaning they have two immiscible phases, an aqueous and an oil phase, being the latter the liquid crystal and in smaller proportion. Therefore, it will gain the ability to form colloids, in this case called droplets, if the right conditions are created, forming the metastability that is typically attributed to emulsions. Hence the need to add a surfactant, in another words, a tensioactive to reduce the interfacial tension between the interface of the liquid crystal with the aqueous medium, and thus increasing the stability, accordingly to the thermodynamic equation (1), that describes the stability of the system [22]:

$$\Delta G_{form} = \Delta A \gamma_{o,w} - T \Delta S_{conf} \quad (1)$$

In order to consider the system stable, meaning to form an emulsion spontaneously, ΔG_{form} must acquire a negative value. This can be achieved through one of two methods: a) increasing the value of ΔS_{conf} (configurational entropy change), or b) decreasing the value of $\Delta A \gamma_{o,w}$, that represents the interfacial tension, between the two phases (oil and water), usually this is the most used method. The purpose of increasing the stability of the droplets in the system is to avoid droplet coalescence, when this phenomenon takes place the droplets combine to become one [22].

1.2.1. Liquid Crystal Dropets

Considered as the fourth state of matter, liquid crystals combine both features from the crystalline and liquid state. In the case of crystals, the molecules demonstrate a high level of ordering, both positional and orientational, in the case of liquids however, the diffusion of molecules occurs randomly. Remarkably, liquid crystals (LC) are the only state in nature where both features can be found together, for their physical state appears to be as a liquid one, but their molecules are organized according to some ordering, thus, possessing unique features and considered to be crystalline mesophases [23]–[27].

Regarding the liquid crystals, distinct categories and classifications can be found, according to their arrangement and behaviour. Thus, considering the motivational factor for their organization transition, liquid crystals can be classified as thermotropic, meaning changes in the temperature are the main stimulus for their transition. Lyotropic is the other group of liquid crystals, where transitions are influenced by solvents, particularly the concentration of the LC in a specific solvent [28]. Nevertheless, these are considered as a more generic denomination, for LC have two major categories designated by calamitic ("rod-shape" molecules), which is the most common type where one of the axis is significantly longer than the others, and discotic ("disc-shape" molecules) where one molecular axis is considerably smaller than the others [28]–[31].

Nonetheless, more commonly LC, are classified according to their molecules' arrangement. Thus, LC can be called as Nematics, Cholesterics, Smectics or Columnar [32]. In figure 4.1. (Chapter 4), a schematic representation of each phase of the LC employed on this work can be seen. The isotropic phase, is a special phase where both positional and orientational order cease simultaneously [30].

Proceeding to the classification of LC according to their molecules' arrangement, most thermotropic LC are calamitic and can be sub-divided as nematic, cholesteric or smectic. Nematic LC are characterized as having a particular orientational order, on the center of mass of the molecules, but no positional one, and thus, they will possess a preferential director dictating the average orientation of the molecules. Cholesteric LCs are very similar to nematics since they also possess a director vector in terms of orientational order and likewise has no preferred positional order. However, it differs from the nematic arrangement, in the sense that the director vector may change its position throughout the medium. Hence, it is common to classify a nematic LC as a cholesteric as well, if considering the range of the director as infinite. Smectic LC oppositely, reveal not only an orientational ordering as well as some correlations in the positional ordering, this class of LC present stratifications and within this category three sub-divisions appear, namely smectic A, B and C, where the main difference between each other is the alignment of the

molecules towards the layers. In relation to the columnar arrangement, the molecules to be in cylindrical assemblies [28], [30], [32].

Concerning the application of Liquid Crystals, regardless of the class, one important factor to consider is the confinement of the LC, that will induce a specific configuration and alignment. In general terms there are two possible confinement: planar and non-planar, and for one which will depend on the boundary conditions, namely the strength of the anchoring which is correlated to the balance of external, elastic and surface forces. Hence, there are two major anchoring conditions or alignments designated by homeotropic and homogenous, accordingly. In figure 1.3. it can be found the most commonly stable configurations for homeotropic and planar anchoring [28], [29].

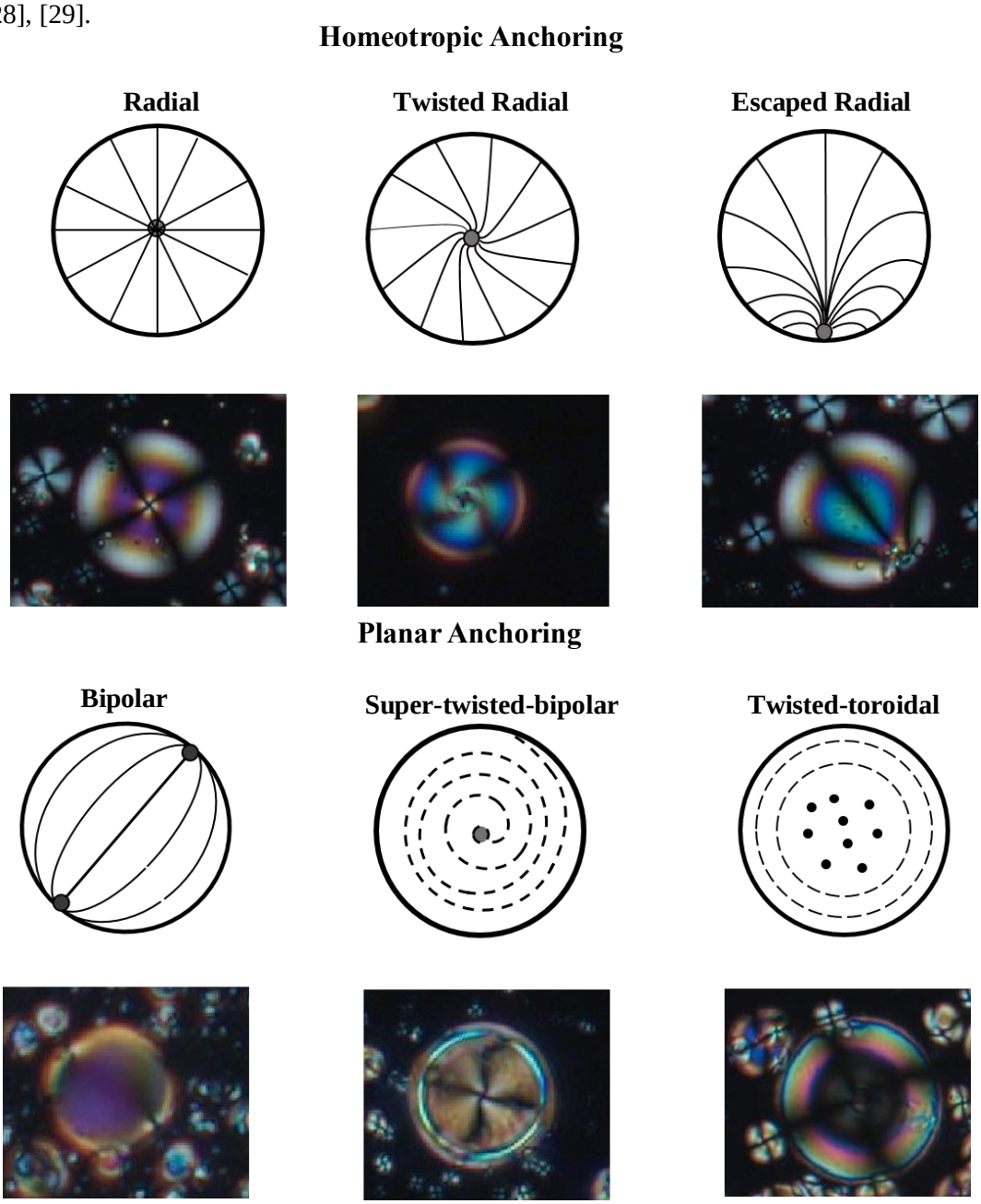

Figure 1.3. Examples of some possible configurations for homeotropic and planar anchoring. The darker points represent the defect points. Radial and bipolar configurations are stable, all the others are considered to be non-stable configurations

Regarding the applications, several fields took interest in the LC due to their versatile and unique properties, due mainly to their anisotropy, such as elastic, magnetic, dielectric, transport and optical properties [23], [29], [30]. Hence, Liquid Crystals have been used within numerous areas, such as, optical spectroscopy, organic compounds solvents, display technologies [26]. However, a new field relates where LCs applied in sensing, as real time detecting agents, such as sensing devices for biomedical applications in diagnostics, gas detection, biomolecules detection among others [21], [33]–[41].

Due to the optical anisotropy the LC possess different refractive indexes and directions, however, align liquid crystals possess the ability to control the polarization of the light and consequently these LC, if aligned in a uniaxial manner, the phenomenon of birefringence will occur. Hence, it is due to the fact that the light polarization velocity in the material is distinct, that the double refracting, or birefringence takes place [30].

Under crossed polarized light on the microscope, it is possible to observe the alignment or configuration of the LC, as it is presented in figure 1.3., moreover, in case of emulsions, the configuration on the LC might be strongly influenced upon the choice of the emulsifier. Considering the most common example, an aqueous solution with a common LC, which behaves like an oil in the presence of water, the molecules of the LC will tend to merge themselves, becoming a separated immiscible phase, with a particular alignment (depending on the environmental conditions of the experiment).

However, within the presence of a surfactant the alignment of the LC molecules can be turned according to the desired specifications. As mentioned before, if the concentration of the emulsifier is closer to its Critical Micellar Concentration (CMC), then micelles of LC and surfactant shall be formed in the medium. The hydrophobic tail of the surfactant tends to connect with the LC and the polar head will be turned into the hydrophilic medium, thus forming a micelle of LC-surfactant, trapping the LC inside and hence providing a specific configuration. In figure 1.4. it can be observed a schematic figure of the representation of the LC-surfactant micelle, it should be noted that most of the emulsifiers will tend to form a homeotropic align [22], [42], [43].

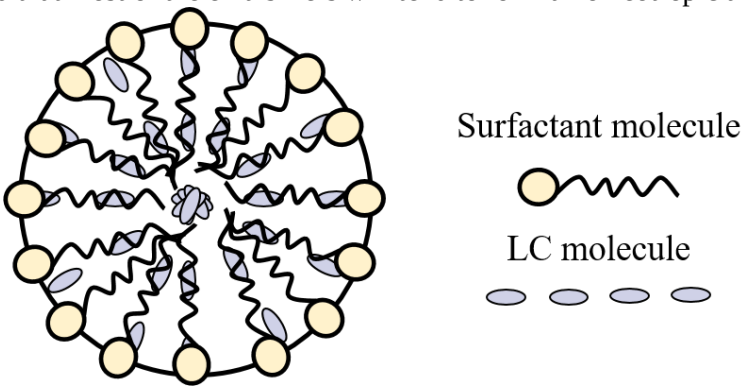

Figure 1.4. Induction of the radial configuration on a nematic liquid crystal with the presence of a surfactant

In order to produce liquid crystal droplets, several techniques become available, these include mechanical such as vortexing, homogenization, sonication among others, however these methods have no size control over the LC droplets and thus may lead to a vast size polydispersity. The major issue towards the size dispersion, is that according to the literature the droplet size affects the liquid crystal behaviour within, and thus if the droplets possess different sizes the LC droplet behaviour will be heterogeneous [44]–[46].

1.3. Changing the LC-Droplets Configuration

1.3.1 The Effect of Surfactants

Surfactants, also known as emulsifiers or tensioactives, are compounds capable of reduce the interfacial tension, or surface tension between two immiscible phases, regarding their state [22], [48]–[50].

These agents are considered to be amphiphilic compounds, meaning they will have a hydrophobic part, commonly being the "tail" of the surfactant, an aliphatic chain group and a hydrophilic part, being the latter the polar head, regardless of the classification of the surfactant (cationic, anionic, amphoteric, non-ionic, among others) [49], [51], [52].

One important factor to be considered is the CMC, since it is close to this value of surfactant concentration that micelles start being formed. Hence, in order to effectively reduce the value of the interfacial tension, the concentration of the emulsifier should be close to its CMC [22], [49], [51], [53].

In this thesis, ionic surfactants shall be the focus of attention, therefore some important concepts concerning this class of surfactants need to be approached, such as kosmotropic and chaotropic ions.

Kosmotrope and chaotropes agents are considered as stabilizers or destabilizers, respectively, of solvent structures, considering mainly water and its interactions with hydrophobic substances and proteins, among other macromolecules. However these definitions are a generic classification and apply both to non-ionic and ionic agent [54]–[56]. Thus, considering only the ionic agents and to know rather if it is in the kosmotropic category or chaotropic, the Hofmeister series reveals to be quite useful. For a given set of known ions, their ability to increase or decrease protein solubility in aqueous systems is considered. Thus, the Hofmeister series creates essentially a correlation between the electrostatic interactions of the protein present in the system with the ions from the added ionic agent. The structure of the water remains relatively the same, as a result ionic kosmotropes or chaotropes, could no longer be seen only as "water-stabilizers" or "water-breakers", for their activities take place at the electrostatic level [42], [57].

Nonetheless, some features are characteristic of the kosmotropic and of the chaotropic ions, such as high charge density, small and multiple charged ions are proper features of kosmotropic ions such as $(C_4H_9)_4N^+$, Al^{3+}, among others. In contrast chaotropic ions are larger and tend to be single charged molecules, with lower charge density such as SCN^- and I^-, among others[57]–[60].

Within the search of newer, better and greener surfactants, a relatively new class steps forward known as Ionic Liquids (IL) [61]–[63].

Fundamentally, Ionic Liquids are salts composed only of ions, possessing a negligible volatility, resulting in high thermal stability and nonflammability, low toxicity, possible recyclability and a melting temperature below 100 ºC. Hence normally they can be found liquid at room temperature and those characteristics made them to be considered as "green" solvents, henceforward one of the main purposes of the IL is to replace the "old" solvents that release hazardous VOCS into the atmosphere [64]–[68].

However, IL present considerably more interesting features, such as, high ionic conductivity, high ability to solubilize polymers, and unlimited possibilities of ion combination creating a wide possibility of different salts and IL with different properties, thus, IL are considered to be "designer solvents" [69], [70].

Concerning the surfactants, there is an additional possibility, denominated mixed surfactant system, it is particularly common to combine an IL with another ionic surfactant, or a cationic surfactant with an anionic one in order to achieve or enhance the desired properties [52], [71], [72].

On the subject of polymers, these are necessary with the intention of immobilization of the droplets, which in this case will contain the sensing probes. Thus, some particular features are desirable, such as stability, permeability towards VOCS, resistance to changes on the environment surrounding and solid at room temperature, so that the sensing probes remain immobilized. Table 1.3. exhibits some of the components used by other research groups in order to produce liquid crystal droplets.

Table 1.3. Table containing liquid crystal, surfactant, coating agent, LC configuration and particle size achieved by other research groups. PVP: Polyvinylpyrrolidone; PVA: poly(methacrylic acid); block Copolymer Paa-b-LCP: Poly(amide) with Liquid Crystal Polymer; PEI: polyethylenimine; PVDMA: poly(2- vinyl-4,4-dimethylazlactone)]; PVA: Polyvinyl alcohol; DTAB: Dodecyltrimethylammonium bromide; PFPE: perfluoropolyether; P(EO-PO): poly(ethylene oxide-co-propylene oxide); TPGDA: tripropyleneglycol diacrylate; RM257: 4-(3-acryloyloxypropyloxy)benzoic acid 2-methyl-1,4-phenylene ester; DMPAP: 2-Dimethoxy-2-phenyl acetophenone;

Ref.	Liquid Crystal	Surfactant	Coating	LC Configuration	Particle Size
[73]	5 CB	SDS	PVP and PMA	radial	44 +/- 1 µm
[74]	15CB and nematic mixture (RO-TN-403/015S)	none	PVP	-	-
[75]	5 CB	none	Paa-b-LCP	radial	-

[76]	E7	none	PEI and PVDMA	bipolar	6.7 +/- 0.3 µm
[76]	E7	SDS	PEI and PVDMA	radial	6.7 +/- 0.3 µm
[76]	E7	DTAB	PEI and PVDMA	radial	6.7 +/- 0.3 µm
[77]	15CB and nematic mixture (RO-TN-403/015S)	none	Mixture with glycerol and PVA	-	100 µm
[78]	CB15	SDS	Paa-b-LCP	non radial	-
[78]	CB15	PVA	Paa-b-LCP	radial	-
[27]	5 CB	PVA	none	-	200 µm
[79]	Cholesteric LC	PVA	-	-	
[80]	5 CB	SDS or DTAB	Paa-b-LCP	radial	-
[81]	5 CB	none	Paa-b-LCP	radial	variable
[82]	5 CB	SDS or PVA	-	transition from radial to isotropic alignment	100-150 µm
[83]	8 CB	PVA and Pluronics F127	-	planar alignment	100 µm
[84]	E7	none	optical glue (NOA61)	-	200 um average
[85]	Mixture with 15CB	SDS + Tween 80	Paa-b-LCP	homeotropic alignment	-
[85]	Mixture with 15CB	PVA	Paa-b-LCP	planar alignment	-
[86]	Cholesteric cellulose nanocrystals	PFPE and P(EO-PO)	-	radial	80-120 µm
[87]	5 CB	SDS	TPGDA	radial	20-200 µm
[88]	5 CB	SDS	PNIPAM-b-LCP	radial	35 +/- 1.3 µm
[89]	5 CB	SDS	-	radial	-
[90]	Mixture with 8CB	none	-	bipolar	120-150 µm
[91]	Mixture with: 5CB, RM257 and DMPAP	SDS	Glycerol	radial	10-15 µm

1.3.2. The Effect of pH on the Gelatine Matrix

Emulsions as oil in water, can be affected by several factors. The behaviour of the molecules in in suspension, may be influenced by temperature, pH, concentration of each component, electrical fields, among others [85], [105]–[110].

The change of pH in the medium where the droplets are formed will affect the charges of the molecules present on the system, thus possibly leading to changes on the droplets configuration, and consequently, e-nose responses.

It is important to know the alignment tendency of the molecules of liquid crystal, taking as an example one of the most common classes of LC, the nematic. In an oil in water emulsion the molecules of the liquid crystal will tend to have a planar anchoring, more specifically a bipolar configuration, or alignment, for the molecules tend to be in the most minimal energy stable form possible. In the case of the addition of a surfactant, however, in the right concentration, the LC alignment typically leans to a drastic change, from a planar anchoring towards the homeotropic anchoring and acquiring the radial configuration. Furthermore, in the case of immobilized LC droplets, the polymer surrounding them also plays an important part on their alignment, for the same medium and concentration the change of polymer may lead to a change in the LC anchoring and consequently the alignment.

Proceeding to the possible effects of changing the pH of the medium, these differ according to the several components present on the system, particularly in case of applying ionic surfactants and, or in case of coated droplets. Considering the coating of droplets, commonly used are the polyelectrolytes (PE). Polyelectrolytes are widely employed in LC droplet coating, especially acids, such as Polyacrylic acid (PAA) and Polystyrene sulfonate (PSS). These polymers will dissociate in polar solvents, such as water, and thus become charged, presenting similar properties to salts, electrolytes, which are the repeating unit, and polymers, meaning they are much more viscous. As such, the properties of these polymers are highly dependent on pH value, nonetheless, within the acid polyelectrolyte group, there can be a sub-division between weak and strong acid polyelectrolytes. For the weak acid PE to induce an alignment change on a LC droplet, it is necessary for a greater change in the pH. In contrast, strong acid PE will, *à priori*, induce an alignment modification without the need for major pH variations, this occurs due to the fact that strong PE will tend to fully dissociate in a polar solvent, meanwhile weak PE will only dissociate partially [81], [85], [111]–[113].

The pH effect on liquid crystal droplets alignment, can also occur in the case of a protein, or biopolymer. In these cases, one of the most important factors to have in consideration is the

isoelectric point (pI), which is the characteristic pH at which the electrical net charge is neutral, meaning the number of positive and negative groups is the same. Thus, above the pI, most proteins will present a negative net charge and, in contrast, at pH below the pI, the net charge becomes positive [114].

In the case of proteins and or mixtures of proteins (containing Collagen), such as gelatine, the value of pka of each amino acid residue should be taken in consideration. Comparing the behaviour of these mixtures and, or, proteins, with polyelectrolytes, it is reasonable to consider these as weak acid PE. As such it might be necessary a higher modification of the pH, in order to ensure that all pka values are below or above the pH, accordingly to the desirable outcome.

2. Aim of the Work

In this thesis, the focus of attention shall be on the optical properties, since the final purpose of this work is the application of sensing devices, employing liquid crystals, on the electronic nose for bacterial infection detection. Hence, this work aimed at: i) studying the effect of different surfactants molecules in the assembly of LC droplets and on the gas sensing abilities of such materials; ii) studying the effect of pH on the gelatine matrix embedding the LC droplets.

On the fourth Chapter it will be studied the effect of the variation of the surfactant employed to. cover the liquid crystal droplet. The surfactant surrounding the liquid crystal droplet induces a specific alignment of the liquid crystal molecules, thus, changing its morphology. This change of the droplet configuration might as well have implications on VOCs detection, consequently leading to the second subject to be approached, which will be the response of these different gels on the e-nose, to verify if the change of surfactant did lead to an enhanced selectivity.

Hence, five different surfactants and the particular case where no stabilizer is employed, were tested. The surfactants included three ionic liquids, two with short length and one with a long length of the tail chain, all three belonging to the [$Cnmim^{+}$] category; one strong anionic detergent; and a surfactant resulting from the mixture of the strong detergent with the ionic liquid with the same long length tail chain.

The fifth Chapter will be focusing on another study, which is the influence of the variation of the pH on the medium where the gels are produced. Since the immobilization agent, the matrix, employed on this work is a biopolymer, the alteration of the pH of the medium will lead to a change on the global charge of the matrix. Considering that the surfactants applied on this work are ionic, this will lead to new interactions between the matrix and the surfactant surrounding the sensing material of the gel, which might lead to changes on the morphology and on the e-nose responses.

3. Materials and Methods

3.1. Chemicals

Molecular Sieves ($Na_{12}[(AlO_2)_{12}(SiO_2)_{12}]\cdot xH_2O$, 4Å, beads 8-12 mesch) were purchased from Sigma Aldrich (Portugal).

Glycine (> 99,7%) was purchased from VWR chemicals (USA). Hydrochloric acid (HCl, 2mol/L) was purchased from Panreac AppliChem (Spain). Sodium hydroxide (NaOH) was purchased from VWR chemicals (USA).

The liquid crystal 4-Cyano-4'-pentylbiphenyl (5CB, > 98%) was purchased from TCI Europe (Belgium). The gelatine from bovine skin (gel strenght~225 Bloom, Type B) was purchased from Sigma-Aldrich (Portugal). The ionic liquids 1-Dodecyl-3-methylimidazolium chloride ($[C_{12}mim][Cl]$, > 98%), 1-Butyl-3-methylimidazolium chloride ([Bmim][Cl], > 98%) and 1-Butyl-3-methylimidazolium dicyanamide ([Bmim][DCA], > 98%) were purchased from LoliTec (Germany). The strong detergent Sodium Dodecyl Sulphate (micropellets) was purchased from NZYTTech (Portugal). All compounds were used as purchased.

The solvents N-Hexane (> 95%) and Heptane were purchased from VWR chemicals (USA). Ethyl Acetate, Chloroform and Methanol (> 99%) were purchased from Fisher Scientific (Portugal). Acetonitrile, Dichloromethane, Ethanol (> 96%) and Toluene were purchased from Panreac AppliChem (Spain). Diethyl Ether (> 99,7 %), Acetic Acid (> 99 %) and Ethanol (> 96 %) were purchased from Sigma Aldrich (Portugal). All solvents were employed as they were.

3.2. Synthesis of the surfactant $[C_{12}mim][DS]$

The method employed for the synthesis of this surfactant was reported elsewhere [47]. It involves the addition of 1 mol equivalent of both surfactants, $[C_{12}mim][Cl]$ and SDS, 1.1 g of each, on a roundbottom flask and stir (360 rpm) with 12 mL of Methanol overnight. As a result, the salt formed from this mixture, sodium chloride (NaCl) precipitated and the remaining mixture was then filtered, and the solvent was removed under reduced pressure. The residue was then dissolved in dried ethyl acetate, 5 mL, which was dehydrated with molecular sieves (2,78 g) on a closed flask overnight, and put on a centrifuge for an hour at 6000 rpm. The remaining excess of salt was then removed from the main solution, and the latter was put under reduced pressure to remove the solvent. The resulting liquid, the final surfactant, was then dried in vacuo for 24h at 70 ºC.

The characterization of this surfactant was performed using H^1-NMR technique (Advance III 400, from Bruker) using a QNP probe at 400mHz and 25 ºC. The solvent used was deuterated chloroform. Appendix I - A shows the graphic obtained for the characterization.

3.3. Buffer Preparation

The acidic and basic buffers were prepared according to the Henderson-Hasselbach equation (2). Regarding the Basic buffer, distilled water (200 mL) was added to a flask along with 0.938 g of glycine, 320 mg of NaOH, lastly 50 mL of distilled water were added to the solution. Five measurements of the pH were made, and the pH of this final solution was 9.41, in order to increase the strength of the buffer solution 635 mg of NaOH, thus, the final pH of the new solution was 11.11. Concerning the acidic buffer, 200 mL of distilled water were added along with the 1.88 g of Glycine, 2.5 mL of HCl and lastly 50 mL of distilled water. Five measurements of pH were performed to the final buffer solution, and the average pH value was 2.7. In order to increase the strength of the acid buffer solution 3 mL of HCl was added to the previous solution, and the final pH was 1.10.

$$pH = pKa + \log\frac{[A^-]}{[HA]} \qquad (2)$$

Hence the final buffer solutions and pH values were, Glycine-HCl (0.26M) with a final pH of 1.10 and Glycine-NaOH (0.05M) with a final pH of 11.11, for the acidic and basic buffers, respectively.

3.4. Sensing gel films

3.4.1. Preparation of the sensing gel films

Sensing gels were produced through the gelation of the viscous solutions containing the four main components of the gel, the liquid crystal, the surfactant, the biopolymer and the liquid medium, which in the case of the experiments performed in Chapter 4 is MilliQ water and in Chapter 5, two buffers are employed, an acid and a basic. The times and order of each components changes according to the surfactant employed, thus, tables 3.1. to 3.18. show the recipes for all the gels made. It should be noted that all gels were made at 38ºC, with the exception of [Bmim][Cl] that was made at 62ºC to melt the IL. Gels made within an aqueous medium employed on the experiments performed on Chapter 5, should use the same amount of water as the buffers and the same amount of gelatine. All the gels were made between 300-360 rpm. For all gels, 10-13 µL of

the resulting mixture were deposited on a non-treated glass slide and spread into a thin film of 30 nm thickness, with an automatic applicator possessing a quadrupole spacer sliding at 50 mm/s.

It should be mentioned that the original recipe, for the gels production, is the [Bmim][DCA] gel in aqueous medium. In order, to achieve these final recipes for all the other gels, particularly for the long tailed surfactants, several attempts were performed to reach the final optimization. In appendix II – A, are some of the trials performed for SDS gels in aqueous medium. Based on this experiments, and after verifying that [C_{12}mim][Cl] gels behaved very similarly, it was possibly to reach an optimum recipe for these long tailed surfactants.

In order to produce the sensing (gels) films, a thermal plate (VMS-C7, VWR Advanced) was used along with an automatic film applicator (TQC) to spread the gel as a thin film.

A) [Bmim][DCA]

Table 3.1. Recipe for [Bmim][DCA] gels in an aqueous medium

Aqueous Medium			
Component	**Amount**	**Order**	**Time (min)**
[Bmim][DCA]	150 µL	1	10
5CB	10 µL	2	10
Gelatine	50 mg	3	15
MilliQ water	50 µL	4	5

Final pH =5.4

Table 3.2. Recipe for [Bmim][DCA] gels in an acidic medium

Acidic Medium			
Component	**Amount**	**Order**	**Time (min)**
[Bmim][DCA] + Acidic Buffer	150 µL (IL) + 200 µL (Buffer)	1	10
5CB	10 µL	2	10
Gelatine	100 mg	3	15
Acidic Buffer	200 µL	4	5

Final pH =3.5

Table 3.3. Recipe for [Bmim][DCA] gels in a basic medium

Basic Medium			
Component	**Amount**	**Order**	**Time (min)**
[Bmim][DCA] + Basic Buffer	150 µL (IL) + 200 µL (Buffer)	1	10
5CB	10 µL	2	10
Gelatine	100 mg	3	15
Basic Buffer	200 µL	4	5

Final pH =9.5

B) [Bmim][Cl]

Table 3.4. Recipe for [Bmim][Cl] gels in an aqueous medium

Aqueous Medium			
Component	Amount	Order	Time (min)
[Bmim][Cl]	140 mg	1	10
5CB	10 µL	2	10
Gelatine	50 mg	3	15
MilliQ water	50 µL	4	5

Final pH =5.4

Table 3.5. Recipe for [Bmim][Cl] gels in an acidic medium

Acidic Medium			
Component	**Amount**	**Order**	**Time (min)**
[Bmim][DCA] + Acidic Buffer	150 µL (IL) + 200 µL (Buffer)	1	10
5CB	10 µL	2	10
Gelatine	100 mg	3	15
Acidic Buffer	200 µL	4	2
Basic Buffer	50 µL	5	3

Final pH =3.5

Table 3.6. Recipe for [Bmim][Cl] gels in a basic medium

Basic Medium			
Component	**Amount**	**Order**	**Time (min)**
[Bmim][Cl] + Basic Buffer	150 µL (IL) + 200 µL (Buffer)	1	10
5CB	10 µL	2	10
Gelatine	100 mg	3	15
Basic Buffer	250 µL	4	5

Final pH =9.4

C) [C_{12}mim][Cl]

Table 3.7. Recipe for [C_{12}mim][Cl] gels in an aqueous medium

Aqueous Medium			
Component	Amount	Order	Time (min)
[C_{12}mim][Cl] + MilliQ water	1.1 mg (IL) + 200 µL (H_2O)	1	10
MilliQ water	150 µL	2	3
Gelatine	100 mg	3	15
MilliQ water	150 µL	4	3
5CB	10 µL	5	7

Final pH =5.4

Table 3.8. Recipe for [C12mim][Cl] gels in an acidic medium

Acidic Medium			
Component	**Amount**	**Order**	**Time (min)**
[C_{12}mim][Cl] + Acidic Buffer	1.1 mg (IL) + 200 µL (Buffer)	1	10
Basic Buffer	100 µL	2	3
Gelatine	100 mg	3	15
Acidic Buffer	100 µL	4	2
Basic Buffer	100 µL	5	3
5CB	10 µL	6	7

Final pH =3.2

Table 3.9. Recipe for [C12mim][Cl] gels in a basic medium

Basic Medium			
Component	**Amount**	**Order**	**Time (min)**
$[C_{12}mim][Cl]$ + Basic Buffer	1.1 mg (IL) + 200 µL (Buffer)	1	10
Basic Buffer	150 µL	2	3
Gelatine	100 mg	3	15
Basic Buffer	150 µL	4	3
5CB	10 µL	5	7

Final pH =9.4

D) SDS

Table 3.10. Recipe for SDS gels in an aqueous medium

Aqueous Medium			
Component	Amount	Order	Time (min)
SDS + Milli Q water	1.1 mg (surf.) + 200 µL (H_2O)	1	10
MilliQ water	150 µL	2	3
Gelatine	100 mg	3	15
MilliQ water	150 µL	4	3
5CB	10 µL	5	7

Final pH= 5.2

Table 3.11. Recipe for SDS gels in an acidic medium

Acidic Medium			
Component	**Amount**	**Order**	**Time (min)**
SDS + Acidic Buffer	1.1 mg (surf.) + 200 µL (Buffer)	1	10
Basic Buffer	150 µL	2	3
Gelatine	100 mg	3	15
Acidic Buffer	100 µL	4	2
Basic Buffer	150 µL	5	3
5CB	10 µL	6	7

Final pH= 2.4

Table 3.12. Recipe for SDS gels in a basic medium

Basic Medium			
Component	**Amount**	**Order**	**Time (min)**
SDS + Basic Buffer	1.1 mg (surf.) + 200 µL (Buffer)	1	10
Basic Buffer	200 µL	2	3
Gelatine	100 mg	3	15
Basic Buffer	200 µL	4	3
5CB	10 µL	5	7

Final pH= 9.4

E) [C_{12}mim][DS]

Table 3.13. Recipe for [C12mim][Cl] gels in an aqueous medium

Aqueous Medium			
Component	Amount	Order	Time (min)
[C_{12}mim][DS] + MilliQ water	1.9 mg (surf.) + 200 µL (H_2O)	1	10
MilliQ water	100 µL	2	3
Gelatine	80 mg	3	15
MilliQ water	100 µL	4	3
5CB	10 µL	5	7

Final pH= 5.1

Table 3.14. Recipe for [C12mim][Cl] gels in an acidic medium

Acid Medium			
Component	**Amount**	**Order**	**Time (min)**
[C_{12}mim][DS] + Acidic Buffer	1.9 mg (surf.) + 200 µL (Buffer)	1	10
Acidic Buffer	100 µL	2	3
Gelatine	80 mg	3	15
Basic Buffer	50 µL	4	2
Acidic Buffer	50 µL	5	3
5CB	10 µL	6	7

Final pH= 3.5

Table 3.15. Recipe for [C12mim][Cl] gels in a basic medium

Basic Medium			
Component	**Amount**	**Order**	**Time (min)**
$[C_{12}mim][DS]$ + Basic Buffer	1.9 mg (surf.) + 200 µL (Buffer)	1	10
Basic Buffer	100 µL	2	3
Gelatine	80 mg	3	15
Basic Buffer	100 µL	4	3
5CB	10 µL	5	7

Final pH= 9.4

F) No Surfactant

Table 3.16. Recipe for gels with no surfactant in an aqueous medium

Aqueous Medium			
Component	Amount	Order	Time (min)
Milli Q water + 5CB	200 µL (H_2O) + 10 µL (LC)	1	10
Gelatine	50 mg	2	15

Final pH= 5

Table 3.17. Recipe for gels with no surfactant in an acidic Medium

Acidic Medium			
Component	Amount	Order	Time (min)
Acidic Buffer + 5CB	200 µL (Buffer) + 10 µL (LC)	1	10
Gelatine	50 mg	2	15

Final pH= 3.2

Table 3.18. Recipe for gels with no surfactant in a basic Medium

Basic Medium			
Component	Amount	Order	Time (min)
Basic Buffer + 5CB	200 µL (Buffer) + 10 µL (LC)	1	10
Gelatine	50 mg	2	15

Final pH= 8.8

3.4.2. Droplet Morphology Characterization and Analysis

To observe the droplets morphology of the sensing gels, a polarized optical microscope (Olympus CX41) with an incorporated camera (Olympus SC30) was utilized. Several replicates of each gel were observed and photographed at crossed polarizers (90º), and uncrossed polarizers, with the software programme Zeiss ZENPro, which allowed to obtain the images of the gels. The same equipment was used to make the gels movies to some VOCs exposure, with a small chamber adapted to the microscope. The movies were made with the total duration of 2 min, and the exposure and recovery time, alternate between 15 and 5 seconds, respectively.

To make the gels tiles, which are a panoramic image of the sensing area of the gel film the tool "Tiles" was employed, comprising 63 pictures, took automatically by the tool, thus, the final image of the sensing area can be obtained.

To measure the size of the droplets and the Mean Gray Value the programme *Immage J* (from Fiji.app) was employed. Six distinct "snap" images of each gel used on this work were utilized, for the measurements (Appendixes II-B and III-C). To measure the droplets size, the programme "Find Circles" must be installed, the image of the gel is opened, and the scale is defined with the tool "Analyse". With the plugin "Find Circles", the expected radius of the droplets is defined. At last, with the tool "Analyse Particles" the programme can deliver the number of particles analysed and their respective sizes. This process was applied to all six figures for each gel employed.

To obtain the Mean Gray Value, the same programme was used as well as the same six figures for each gel. With the option "Simulate colour blindness", the figure is turned to a gray scale of colours under the option "Total Monochromacy", afterwards with the tool "Analyse" and with the measurement of "Mean Gray Value" selected, this feature will be given as a result.

3.5. The E-nose system for gas detection

The e-nose used was an in-house built device equipped with a sensor array with six slots and a signal transductor. It was employed to obtain the optical response of the sensing gel films to the VOCs exposed. To contain the samples exposed to the sensors, a tailor-made glass vials with an approximate volume of 27 cm^3, with inlet and outlet channels with an external diameter of 6.45 mm. This container will be used to contain 15 mL of sample and to simplify the passage of the VOCs to the sensors chamber, with the assistance of an air pump. Two air pumps (Air 550R Plus, Sera Borsigstr, Germany), were applied to provide the gaseous sample to the sensor chamber,

intercalated with air for the recovery time. An Arduino Due was employed to command and control the pumps, the LEDs on the sensor chamber as well as to be the receptor of the signals. To connect the sensor chamber to the pumps, silicon tubes with 4 mm of internal diameter were used. The VOCs samples employed on this work, at room temperature are in the liquid form, thus, a thermal plate (VMS-C7, VWR Advanced) was used to heat the sample until 38 ºC, enough to volatilize part of the sample and to be carried to the array of sensors. The time of exposure and recovery will alternatively work between 5 and 10 seconds, respectively.

For the extraction of the features provided by the e-nose signals, a tailor-made python script (python 3.6) was applied, this script was developed by the Biomolecular Engineering Lab. Thus, two Machine Learning algorithms were employed: recursive feature selection method and Support Vector Machine classifier. These were employed to select the most appropriate features, to characterize the signals, and to distinguish the volatiles given to the device, respectively.

The features extracted from the analysis of the e-nose signals are: Morphological features and parameters of curve fitting models. However, it should be noted that since some of the signals presented unique characteristics that were not expected, the model employed might not be the most appropriate, and a new model should be developed for better fitting these results.

4. Effect of Surfactants on LC droplets

4.1. Results and Discussion

Regarding this Chapter the focus shall remain on the surfactants applied in this work and their influence on the probes, on the sensing droplets, mainly on their impact over the LC droplets morphology and functional purpose in the e-nose. Thus, five different surfactants were employed, namely three ionic liquids, 1-Butyl-3-methylimidazolium dicyanamide ([Bmim][DCA]), 1-Butyl-3-methylimidazolium chloride ([Bmim][Cl]) and 1-dodecyl-3-methylimidazolium chloride ([C_{12}mim][Cl]), one strong detergent, Sodium Dodecyl Sulphate (SDS) and lastly a synthesis of a mixture between the SDS and an ionic liquid with the same size chain (C_{12}mim][Cl]), was achieved and used as a surfactant as well. Table 4.1. consists on the representation of the structures of the several surfactants and liquid crystal, 4-Cyano-4'-pentylbiphenyl (5CB), employed on this work.

Regarding the chosen surfactants, the starting point for this work were the sensing gels made with self-assembly droplets using 5CB and [Bmim][DCA] as the main components of the probes [22], the protocol was adapted from the Biomolecular Engineering Lab.

Hence, a brief introduction to each of these surfactants and the liquid crystal employed, should firstly take place before proceeding to the obtained results. [Bmim][DCA] is an ionic liquid, with a short chain tail, containing four carbons, it is in the liquid state at room temperature and it has the ability to dissolve proteins, making it very easy to use with the purpose of producing gels with a gelatine based matrix [92], [93]. It is also considered to be a kosmotropic surfactant, this is actually the case for most imidazolium-based ionic liquids, regardless of the counter ion. The longer the size of the chain tail of these IL, the higher is the tendency to form structure-breakers, due to the increase of hydrophobicity of the alkyl chain, thus, leading to chaotropic surfactants [58], [94].

Afterwards and in order to verify the effect of the counter ion on the surfactant, [Bmim][Cl] was the second choice. This ionic liquid is very similar to [Bmim][DCA] since in its formulation it is equal in every aspect, except for the counter ion. Subsequently, and proceeding with the logic to observe the effect of gradual changes on the surfactant, the choice kept incising on the same category of tensioactives, the imidazolium-based ionic liquids, however the next step was to change the length size of the chain tail, keeping the same counter ion. Thus [C_{12}mim][Cl] was selected, since it has the same counter ion as the previous ionic liquid, though instead of a short size chain tail, the latter possess a much longer length of twelve carbons. This IL is a chaotropic surfactant as mentioned before since it belongs within the class of imidazolium-based IL, but has

much longer alkyl chain tail, and since, accordingly to the literature, the longer the size of the chain tail the more chaotropic the IL becomes [94]. Later it will be demonstrated that the impact of the size of the chain tail, will be considerably more significant than the effect of the counter ion.

Proceeding within the same approach and keeping the size chain tail consistent, instead of maintaining in the same class of surfactants, a transition was made towards a more common category of surfactants, the detergents. SDS is a strong detergent, which given its nature might be considered as a chaotropic agent [95]. The purpose with the last selection was to observe the effect of the nature of the surfactant, thus comparing two different categories of surfactants, but maintaining the same length of the alkyl chain.

Lastly, a synthesis of a mixture between SDS and the IL [C_{12}mim][Cl] was performed in order to verify the effect that a double chain surfactant could have on these LC-droplets. This mixture was made through the use of these two specific surfactants, due to the fact that mixtures between SDS and Il was already performed by other groups [47], [96]. It was advisable to mixture an IL with the same size chain tail, in order to obtain a more stable and enhanced surfactant, hence the combination of SDS and [C_{12}mim][Cl]. In order to verify if the mixture was successful, a H^1-NMR analysis was performed. On appendix I it is showed the spectrum obtained from the H^1-NMR analysis and comparing with the spectrum from the literature published by Brown *et al.* [47], which was the adapted protocol for this synthesis, it is possible to conclude that the mixture and the consequent resulted surfactant was successfully achieved, resulting in [C_{12}mim][DS].

Regarding the liquid crystal employed on this work, 5CB, this is a thermotropic nematic LC, and possess its temperature transition between 22,4 ºC to 34,5 ºC for the nematic phase [97], [98]. On figure 4.1. it can be seen a schematic figure for the molecules transition phases of this particular LC, based on the literature [98].

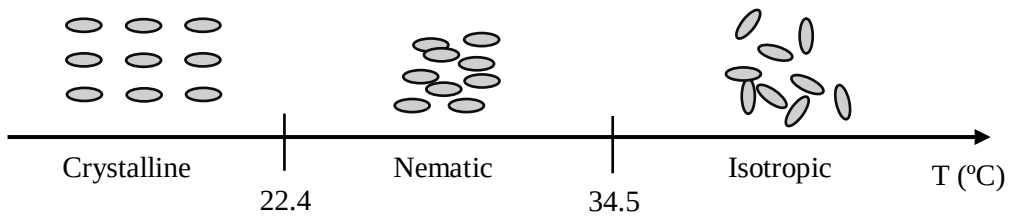

Figure 4.1 Liquid Crystal 5CB phase transitions temperature

Table 4.1. Schematic representation of the surfactant and 5CB structures

Surfactant	Liquid Crystal
[Bmim][DCA] 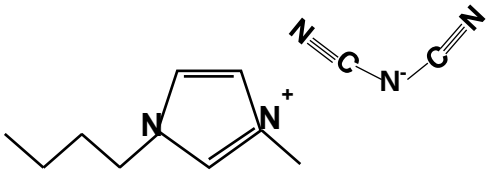	**5CB** 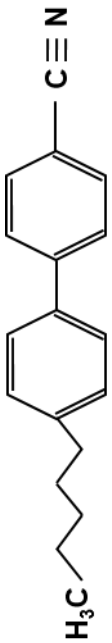
[Bmim][Cl] 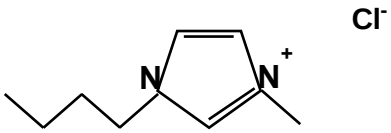	
[C_{12}mim][Cl] 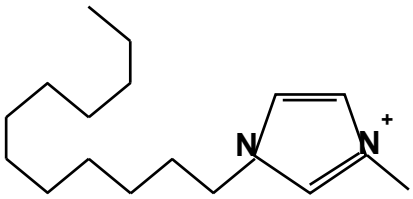	
SDS 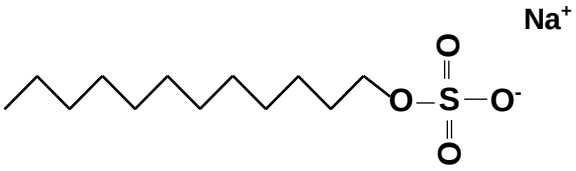	
[C12mim][DS] 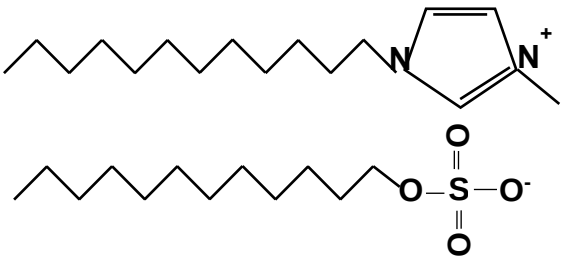	

4.1.1. Droplets Morphology

The morphology of the droplets is a fundamental feature to analyse, considering that different surfactants will induce different configurations on the droplets containing liquid crystal. The alignment of the droplets may also be an indicator of how the sensing gel will respond on the e-nose, in the sense that less stable droplets will be *à priori* easily disturbed than stable configurations, thus, although it is desired the stability of the droplet in the physical form, it is also desirable that this may be disturbed.

Figures 4.2., 4.3., and 4.4. show the configurations of 5CB droplets with the different surfactants tested, under crossed and uncrossed polarizers. Under crossed polarizers it is visible the configuration of the liquid crystal inside the droplets. In contrast, under uncrossed polarizers, the defect points of the droplets alignment becomes more clear as well as the limit, the droplet interface with the matrix and the shape that it takes reveals to be more evident.

Regarding the configuration obtained for the 5CB droplets with [Bmim][DCA] and [Bmim][Cl] as it is presented on figure 4.2., it is possible to verify under crossed polarizers that the configuration that the droplets assume is radial, and the anchoring of the liquid crystal is homeotropic. This suggests that these droplets will probably respond well on the e-nose, not merely their configuration is an indicative of this possible situation, but as well as from figure 4.2. that show the interface of the droplet with the matrix, demonstrating that the droplets are well immobilized and will not suffer from coalescence. Considering the surfactants employed in these gels, it is feasible to observe that the morphology between the droplets is very similar, possibly indicating that the counter ion of the surfactant is not a key factor on the droplet anchoring and consequent configuration.

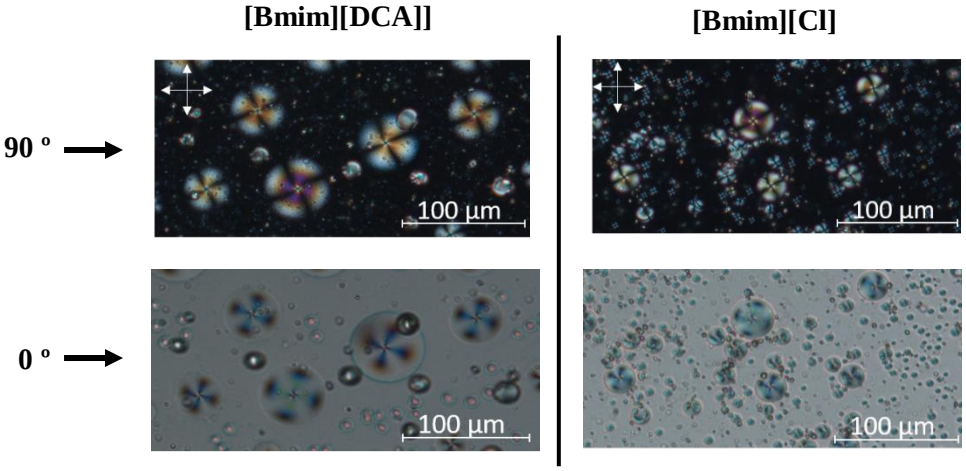

Figure 4.2. 5CB Droplets with ionic liquid, on a gelatine matrix, in an aqueous mean: ***Left:*** *[Bmim][DCA] (3.26M);* ***Right:*** *[Bmim][Cl] (3.26M)*

On figure 4.3. are the pictures for the gels of 5CB doped [C12mimCl] and SDS. Comparing these pictures with the ones presented on figure 4.2., a clear evidence of the significant effect of the size of the chain tail of the surfactant, in contrast with the effect of the counter ion. Analysing the droplet morphology between these two figures, and the pictures within, it is distinctive the similarities among the surfactants with the same size of the alkyl chain, regardless of the nature of the surfactant. Pictures on figures 4.2. (the [$Bmim^+$] gels) and 4.3. ([C12mimCl] and SDS), showed noticeable differences in their morphology. The size of the droplets, their colours and dispersion, were some of the features that differ the most, although these possessed the same counter ion, but different sizes on the chain tail.

To be noted that, in the case of longer tail chain surfactants ([C_{12}mim][Cl], SDS and [C_{12}mim][DS]) the time when the 5CB is added in the mixture while producing the droplets plays a very important role. If the liquid crystal is added in the beginning, along with the surfactant, and stays for more than fifteen minutes while the droplets are being formed in the gels, then the resulting droplets will be much smaller, all radial, much more compact and presenting a much higher level of stability. This might be due to the fact that, a longer length of the alkyl chain will probably lead to a higher anchoring energy and thus, originating to a poor response on the e-nose, since their configuration is so stable that is harder for the VOCS to disturb it. Moreover, these gels, with the current method of droplet production employed on this work, are very difficult to reproduce, concerning their accuracy. All these facts can be observed in Appendix II - A, that exhibits some of the several trials made in order to reach a compromise. Thus, the ideal time for the 5CB liquid crystal, to be in agitation with the other components of the mixture is between seven to ten minutes, for long tailed surfactants.

Hence, observing the pictures on figure 4.3., it is possible to verify the effect of a long length size chain tail surfactant on the 5CB droplets morphology, the pattern colours is broader, feasibly indicating a wider range of droplet sizes. Analysing these pictures it can be verified that different colours are associated with different sizes. Droplet size is also associated with droplet stability: smaller droplets will tend to be radial and very stable, meanwhile droplets possessing a bigger size will tend to deform, transitioning from radial configuration to a non-stable configuration such as escaped radial and a super-twisted bipolar, having the latter a planar anchoring and no longer homeotropic [99]. Another interesting aspect is the fact that they seem to be closer and with a tendency of overlapping, however from pictures on figure 4.3. at 0º, where the interfaces of each droplet are showed, it is clear that these are not coalescing, each one has its defined space on the gel.

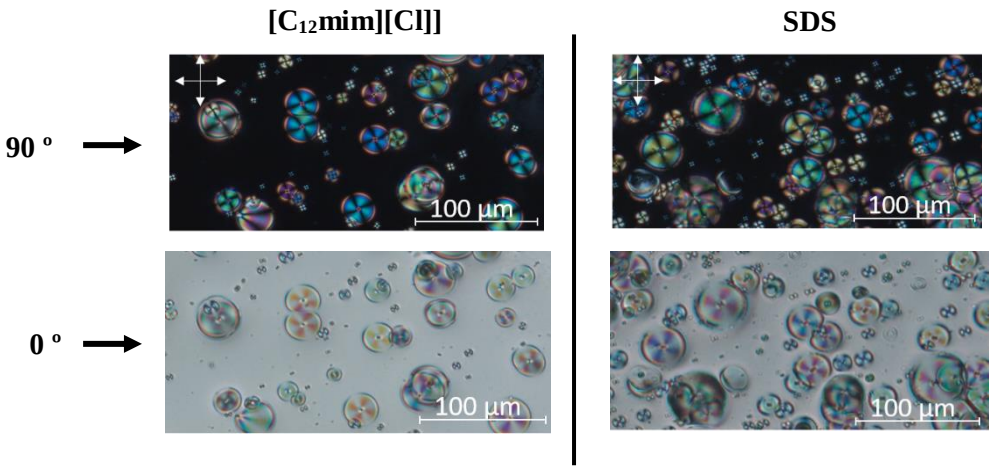

*Figure 4.3. 5CB Droplets with long-tailed surfactants, within a gelatine matrix: **Left**: ionic liquid [C12mim][Cl] (0.007M); **Right**: SDS (0.007M)*

Lastly on figure 4.4., the droplets configuration for the [C_{12}mim][DS] is presented as well as the case when no surfactant is employed. Figure 4.4. (on the left) that represent the configuration of 5CB droplets with the mixture surfactant, it is possible to verify that although their alignment seems to be homeotropic with a radial configuration, it is also visible another liquid crystal interface. This phenomenon might be caused by the two tailed surfactant, since the mixture between [C_{12}mim][Cl] and SDS, which are opposite ionic surfactants with the same alkyl chain tail. Interestingly this double LC interface may seem to lead to an increase of the droplet size and, as such, leading to non-stable configurations. In this case a mixture of configurations may seem to take place, since the droplets appear to possess a twisted-toroidal configuration, but at the same in the centre seems to have a twisted-bipolar, or a multi-defected structure [99]–[101].

Regarding the droplets with no surfactant, or with no orientation inducing agent, it is perceptible how the interface of the droplet with the matrix is no longer well defined and a clear tendency to coalescence emerge (Figure 4.4.). This confirms the role of the surfactant for the required stabilization and orientation. If no surfactant is applied, the anchoring will be planar with the propensity to form droplets with a multi-defect structure or a bipolar alignment, as it is represented. On figure 4.4. at 0º regarding the gel with no surfactant, the defect point is no longer on the centre of the droplet, instead has several defect points around the interface in some cases, designating a multi-defect configuration and some have two defect points on the edges, meaning it is a bipolar configuration for those cases [99], [102].

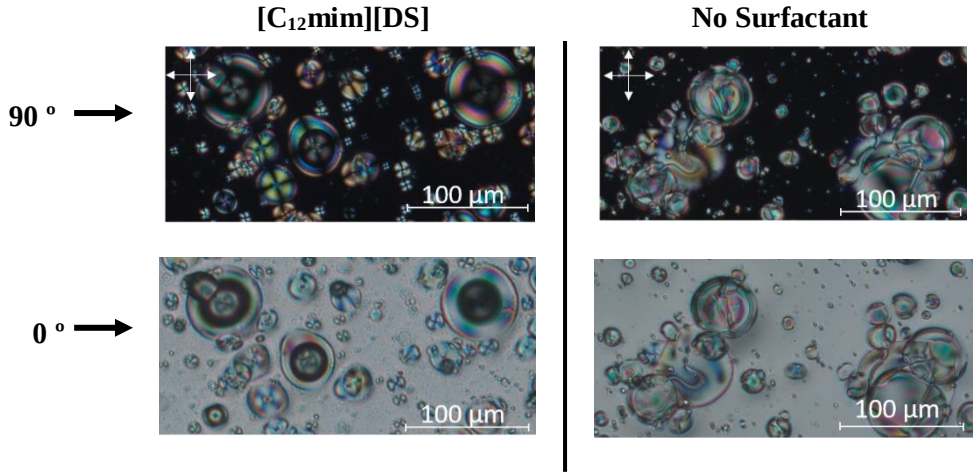

Figure 4.4. 5CB Droplets with the mixture surfactant and without surfactant, within a gelatine matrix: ***Left****: [C12mim][DS] (0.008M);* ***Right****: only 5CB on the gelatine matrix, with no surfactant*

As mentioned previously, the size of the droplets is an important feature. Using the software *ImageJ* an estimation of the droplet size was achieved for each surfactant, using six distinct figures for each gel [103]. Thus, figure 4.5. consists on an illustrative chart of the average droplet size, for each surfactant.

The chart reveals that the surfactant that induces a higher droplet size is [C_{12}mim][DS] ergo the previous analysis of the droplet morphology of the pictures on figure 4.4. proved to be accurate. Observing the graphic, the second surfactant with a higher average droplet size is the [C_{12}mim][Cl], possibly indicating that this is the responsible part, in the mixture of the [C_{12}mim][DS], to induce the additional liquid crystal interface. Regarding the ionic liquids from the [$Bmim^+$] family, these present very similar results demonstrating, once again, the minor influence of the counter ion on the droplet morphology. The detergent, SDS proved to be in between the short and the long tailed ionic liquids, without revealing any noticeable results, as well as the case for the droplets with no surfactant employed.

Another important feature is droplet size distribution, since it might be an indicator of the consistency and reproducibility of the gel. Figure 4.6. shows a box chart of the size distribution for the several cases mentioned so far. Analysing the chart attained, on a general approach all gels reveal a positive asymmetry, meaning that most values tend to be small, additionally there are no significant differences between the gels, however observing the graphic with a higher detail some differentiations arise. Hence, the best gel appears to be the one containing [C_{12}mim][DS] since it is the only surfactant that has no outliers, the value for the average size droplet is overlapping with the median and the interquartile range seems to be well positioned, close to centre in between the minimum and maximum values. Meaning that, only by considering these results, the most

consistent and easily reproducible gel would be the one with [C_{12}mim][DS]. On Appendix II-C are the tables with the average droplet size, for each gel employed.

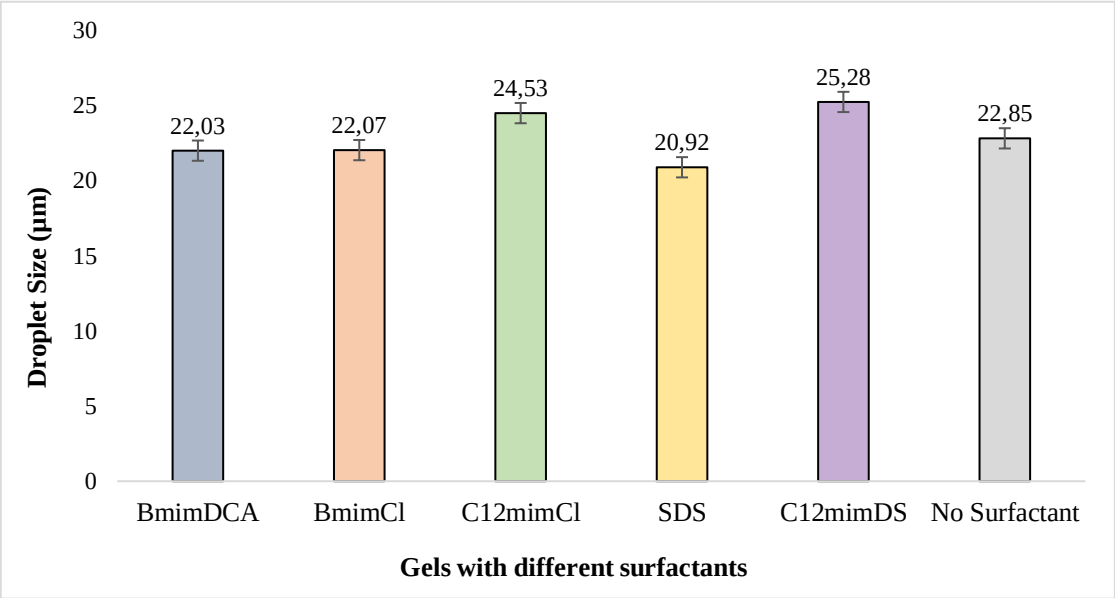

Figure 4.5. Graphic with the mean droplet size of the tested gels with different surfactants, made within an aqueous mean. The number of droplets count and analysed for each gel is: [Bmim][DCA] = 474; {Bmim][Cl] = 421; [C_{12}mim][Cl] = 229; SDS = 509; [C_{12}mim][DS] = 194; No surfactant = 328

Comparing the results achieved for the other surfactants, the one that is closer to the surfactant mentioned previously is the [C_{12}mim][Cl]. This outcome is coherent with what has been formerly mentioned, that this is the surfactant that appears to have a major influence on the droplets morphology of the mixture surfactant ([C_{12}mim][DS]). Considering that [C_{12}mim][Cl] barely has outliers, the distribution size of both surfactants is very similar and the mean value is closer to the median when compared to the SDS, thus making evidence to the closer similarities between the ionic liquid and the mixture surfactant.

Regarding the other ionic liquids and the case of no surfactant, both ionic liquids have similar behaviour, demonstrating, once more that the counter ion has no noticeable effect on the droplets. Nonetheless the gels made with [Bmim][Cl] have more outliers compared to [Bmim][DCA] thus, showing a greater inconsistency, however, the mean value is closer to the median and the inter-quartile range (box) is smaller, meaning the distribution of the sizes is more concentrated. Hence, in overall these two gels have very similar consistencies. Concerning the no surfactant case, it has outliers, the mean is relatively close to the median and the inter-quartile range is relatively small, implying (from this analysis) that the gels are relatively consistent.

On appendix II - F, is the statistical summary for the results presented in figure 4.6., in this table are presented several important values such as the median values, standard deviation among others, for all the cases given in figure 4.6.

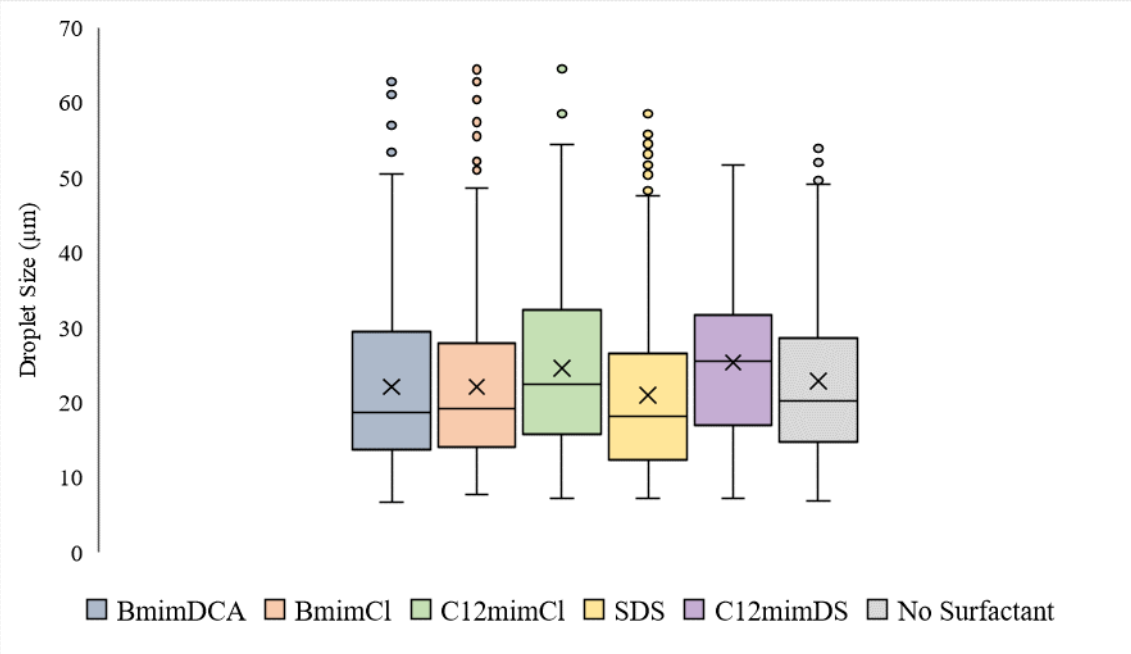

Figure 4.6. Box chart of droplet size distribution for the several gels made with the different surfactants, within an aqueous mean. The points above the charts represent the outliers, the line in each box is the median value and the cross is the average. The number of droplets count and analysed for each gel is: [Bmim][DCA] = 474; [Bmim][Cl] = 421; [C_{12}mim][Cl] = 229; SDS = 509; [C_{12}mim][DS] = 194; No surfactant = 328

An Additional feature regarding the droplets' morphology is their Mean Gray Value (MGV), which performs as an indicator of the available active optical surface area, suggesting the available area for VOCS detection. MGV scale is from 0 to 250, where 0 is total brightness and 250 is total darkness. In principle the higher the value of this parameter the better, revealing a greater area for detection, and thus, on the e-nose the baseline of the signals would appear to be lower for the sensors with a higher MGV, leaving available a higher range for the response amplitude. On figure 4.7. the Mean Gray Values for each situation formerly mentioned is represented. Typically, gels with smaller droplets would reveal a higher MGV, thus, analysing the chart, the surfactant that revealed a greater value was SDS ergo it should be the surfactant with smaller sized droplets, from figures 4.5. and 4.6. this proved to be the case. However for the [C_{12}mim][Cl] case there is an incongruity since it is presented as the second surfactant with the higher MGV. From the same figures mentioned previously this ionic liquid, was the second with higher sized droplets, this inconsistency is also observed with the [Bmim][Cl], considering that this gel should reveal a higher value for MGV. Hence, suggesting that the correlation between the droplet size and the MGV is not straightforward and the method production of the gels is not the

most adequate, since it reveals a succession of inconsistencies. Appendix II-D possess the table with the average MGV values for all gels employed.

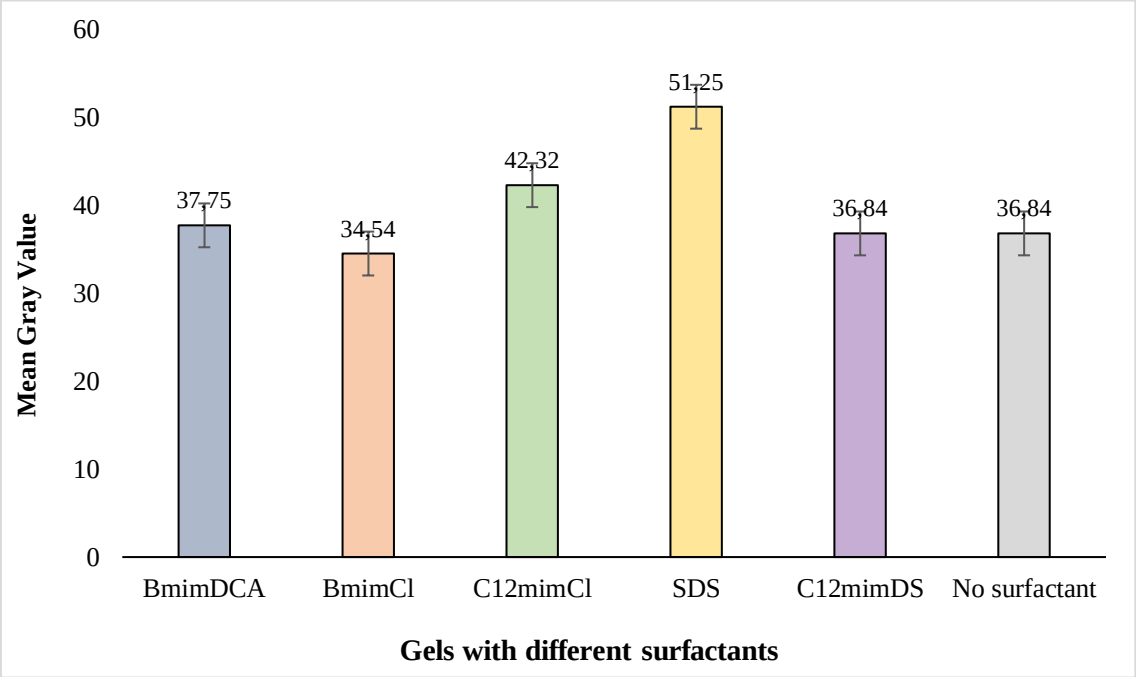

Figure 4.7. Mean gray value graphic for the several tested gels with different surfactants, within an aqueous mean. The minimum value is 0, representing total darkness and the maximum value is 250, representing total brightness. The number of droplets count and analysed for each gel is: [Bmim][DCA] = 474; {Bmim][Cl] = 421; [C_{12}mim][Cl] = 229; SDS = 509; [C_{12}mim][DS] = 194; No surfactant = 328

Considering the final purpose of these gels, applying them on as an array of sensors on an electronic device, the e-nose in order to detect the VOCS that will be exposed, some features are desirable for these sensors, such as stability, durability and consistency in their response. Figure 4.8. presens two examples of gels, focusing on a region with droplets before and after some time. It is only presented two examples since as previously demonstrated, some droplets of different gels behave very similarly, hence two distinguished surfactant gels were chosen for this particular purpose: [BmimDCA] and [C12mim][Cl], in order to observe the effect of time on the droplets morphology. Hence, it is evident the significant differences between these two LC droplets over time, both were under the same conditions, both were exposed to the same VOCS and stored in the same environment, however the effect of time was noticeably distinct on the two gels. Observing figure 4.8., after eleven days the droplets on the [Bmim][DCA] gel change their configuration from radial to an escaped radial, move their position, demonstrating a significant displacement and showed some coalescence effect [99]. Comparing with the LC [C_{12}mim][Cl] droplets before and after twenty two days, the droplets on this gel remain virtually the same, their position on the gel mainly persisted, and their configuration showed no shifting, reflecting the

higher durability and reusability of long chain tail surfactant contrasting with the shorted tail chain surfactant.

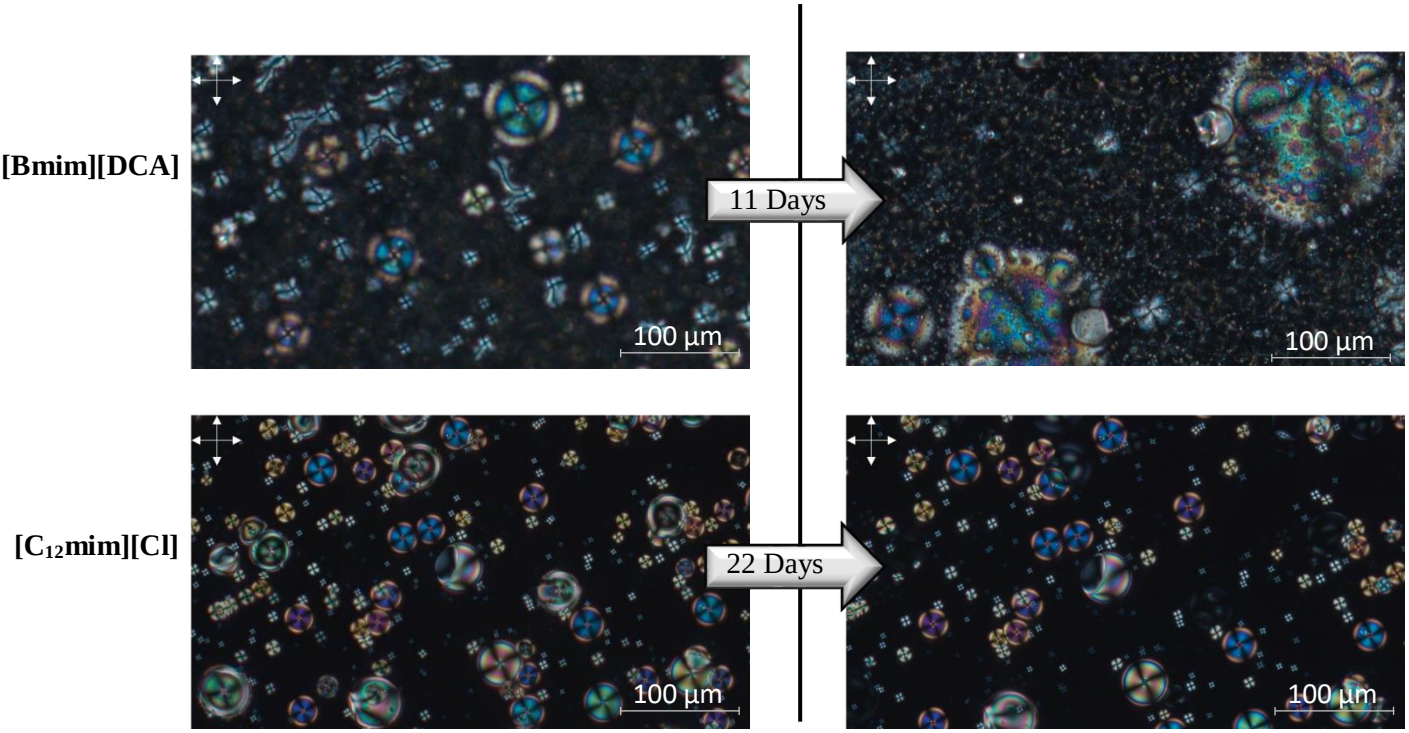

Figure 4.8. - Effect of time on 5CB droplet morphology: ***Above****: [Bmim][DCA] before and after 11 days;* ***Below****: [C_{12}mim][Cl] before and after 22 days*

4.1.2. Gels exposed to VOCs

The second subject of the Chapter concerns the exposure of sensing gels to VOCs using an e-nose device assembled in-house. The gels were exposed to twelve VOCS: Heptane, Hexane, Toluene, Chloroform, Dichloromethane, Diethyl Ether, Ethyl Acetate, Acetone, Acetonitrile, Ethanol, Methanol and Acetic Acid. The order was not necessarily this, since several orders were tested to verify if there was a correlation between the pattern of the signals and the order in which the VOCS were exposed. This specific order was the original one and the first to be experimented, and the logic behind was the polarity of the molecules. Considering that the matrix applied throughout this work was always gelatine type B, a hydrophilic mixture of proteins (containing Collagen), meaning it is a polar component. By firstly expose the sensing gels to the less polar VOCS, meaning the more hydrophobic ones, these will prefer to interact more with the liquid crystal than with the gelatine matrix, and thus, the structure of the gel would be more preserved. In theory the signals from these more apolar VOCS would be expected to be stronger, with a higher intensity, than the more polar ones, later this hypothesis will be proven, or not.

When the VOCs interact with the sensing gels, the LC-droplets turn isotropic in the presence of the VOCs and, should, return to their original conformation on the recovery. However, the way liquid crystal molecules transition to the isotropic state differs from VOC to VOC. For each gaseous sample, each VOC has its own specific imprinting, making possible to identify the components present in a sample.

Figure 4.9. illustrates the operating mode inside the sensor chamber, previously explained on the Introduction.

The signals received on the system are represented by scheme on figure 4.10. The orange line represents the signal emitted by the sensing gel with a certain pattern, the grey areas represent the moments when the VOCs are passing through the sensors (in this case the recovery time was 10 seconds and the exposure time was 5 seconds). The gels are considered to be saturated once they reach values between 2.5 and 3, as if none of the light is passing through, not imprinting any pattern, meaning the droplets of liquid crystal went isotropic and are not returning to their original conformation.

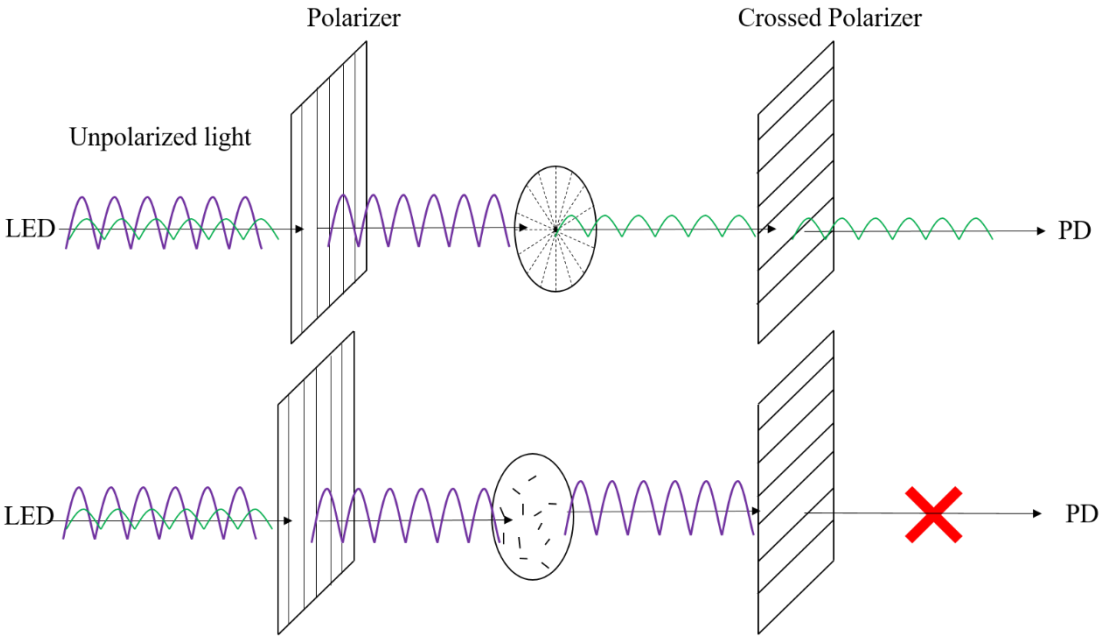

Figure 4.9. Illustration of the operating mode inside the detection chamber; a) When there is no disturbance of the sensing gel the light reaches, with the same intensity as it was emitted, to the PD; b) When the VOCs interacts with sensing gel causing a disturbance

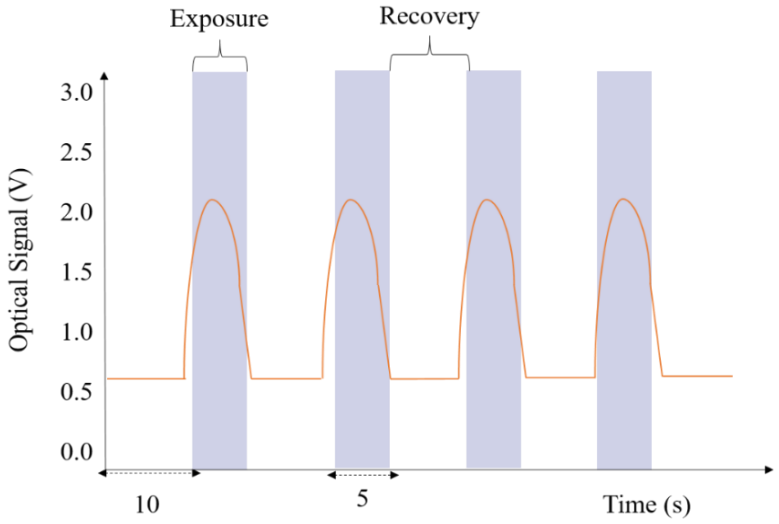

Figure 4.10. Scheme of an E-nose Signal

In this part of this Chapter, the e-nose signals and consequent responses of the different sensing gels will be analysed, in order to understand the influence and impact of the surfactant on the e-nose. Confusion matrices made from a machine-learning program, will also be presented, these are a simple form to represent the prediction results and the errors made by the machine learning. Meaning it gives the percentage of accuracy of the predicted answer with the actually correct one

as well as the type of error, meaning in this case which VOCs where confused and the accuracy for each right one [104].

Appendix II-F, contain all the signals obtained from two assays made to verify the e-nose responses to the different surfactants, thus, the gels made with [Bmim][DCA] were used as the "control" gels, since they were already optimized by the research group. Hence, considering the fact that the e-nose utilized had six entries, to compare the effect of each five different surfactant, two experiments were made. Usually these experiments are made with at least two gels from the same batch, in order to verify the accuracy between the signals obtained from the same gel type. In these experiments the VOCs order was the following: Hexane, Dichloromethane, Ethyl Acetate, Heptane, Acetonitrile, Toluene, Methanol, Chloroform, Acetone, Ethanol, Diethyl Ether and lastly Acetic Acid. This specific order had the purpose to mix the VOCs according to their polarity, so the responses would not create a dependency and to see if the signals were disturbed by the possible interaction of the polar VOCs with the gelatine matrix. Acetic Acid is always the last sample, since it affects the [$Bmim^+$] gels integrity. The first experiment was made using the three ionic liquids, [Bmim][DCA], [Bmim][Cl] and [C_{12}mim][Cl], and the second one was made with the remaining surfactants, SDS and [C_{12}mim][DS], with the repetition of [Bmim][DCA] (control gel).

Analysing the signals obtained on appendix II-F it is evident that the ionic liquids of the class of [$Bmim^+$], demonstrated to possess very similar responses implying once more that the counter ion has no significant effect on these sensing gels. Contrastingly, the [C_{12}mimCl][Cl], that possess the same counter ion and polar head as the [Bmim][Cl] with fourfold the size of the chain tail, revealed completely distinct responses to the same VOCs. Curiously, the responses of SDS gels did not coincided with the ionic liquid [C_{12}mim][Cl], demonstrating that even though the size of the alkyl chain has proven to be a crucial factor on droplet morphology, stability and durability, it is not the only factor that may affect the e-nose responses. The polar head seemed to redeem a very important role as well, as it may be verified by the e-nose signals.

Regarding the mixture surfactant, [C_{12}mim][DS] it responded to every VOC, however with a very low intensity and with no selectivity towards any VOC exposed.

It should be noted, that throughout these experiments, the baselines of the gels changed, immediately after the first sample being provided to the system. For most cases this change is not significantly different and it could be the result of a change in the alignment of the molecules, in the sense that in morphological terms, the configuration and size remain approximately the same. However, the molecules might not possess the exact same alignment as before the VOC exposure, thus, leading to an alteration of the baseline, particularly when exposed to Acetic Acid. Nevertheless, it could also be the result of the interaction of the VOC with the gelatine matrix

leading to a change in the droplets position, considering the fact that Acetic Acid will tend to interact strongly with the gelatine given its polarity. Evaluating the different gels tested, the surfactants that assured the less noticeable alteration on the baseline were [C_{12}mim][Cl] and [C_{12}mim][DS], followed by SDS, meaning that these long length chain tail may confer higher stability to the droplets.

Figure 4.11., shows three examples of e-nose responses, of three different VOCs, two of the same category (alcohols) Methanol and Ethanol, and Diethyl Ether. It is only showed a representative area of the complete chart, present on appendix II-F, in order to have a better understanding and analysis of the signals produced. Figure 4.11. shows the response of the three ionic liquids, employed on this experiment. As mentioned previously [C_{12}mim][Cl] presents very distinctive responses, contrasting with [Bmim][DCA] and [Bmim][Cl] signals, particularly analysing the e-nose signals for Methanol and Ethanol. It is interesting to verify that not only the amplitude of the signal is significantly different, as well as a curious phenomenon takes place, the [C_{12}mim][Cl] signal for Methanol is inverted, meaning the signal decreases to a value below the baseline when the VOC is being exposed to the sensors.

Comparing the response of [C_{12}mim][Cl] to Ethanol which is of the same family of VOCs than Methanol, it is noticeable that these are very distinct, the amplitude of the signal is significantly lower, and the signal exhibits a pattern that tends to be slightly higher than its baseline. A possible reason for this occurrence is the change of configuration of the IL-LC-droplets, meaning that instead of turning completely isotropic when the VOCs pass through, they might change their configuration without transitioning completely to the isotropic phase. Transition to another conformation with some specific VOCs, might occur, thus, possibly indicating selectivity, considering that this fact does not occur with all the twelve samples given. Concerning the other ionic liquids, these do not present such discrepancies between Methanol and Ethanol.

[C_{12}mim][Cl] also demonstrated an intriguing response to Diethyl Ether (figure 4.11.) for its behaviour is similar to the one showed to Methanol, the signals responded contrary to the other VOCs and gels. This type of responses, with particularities, revealing different patterns with different VOCs, are an evident form of selection, which, observing figures 4.11., 4.12 and Appendix II-F, seems to be present on the [C_{12}mim][Cl] surfactant.

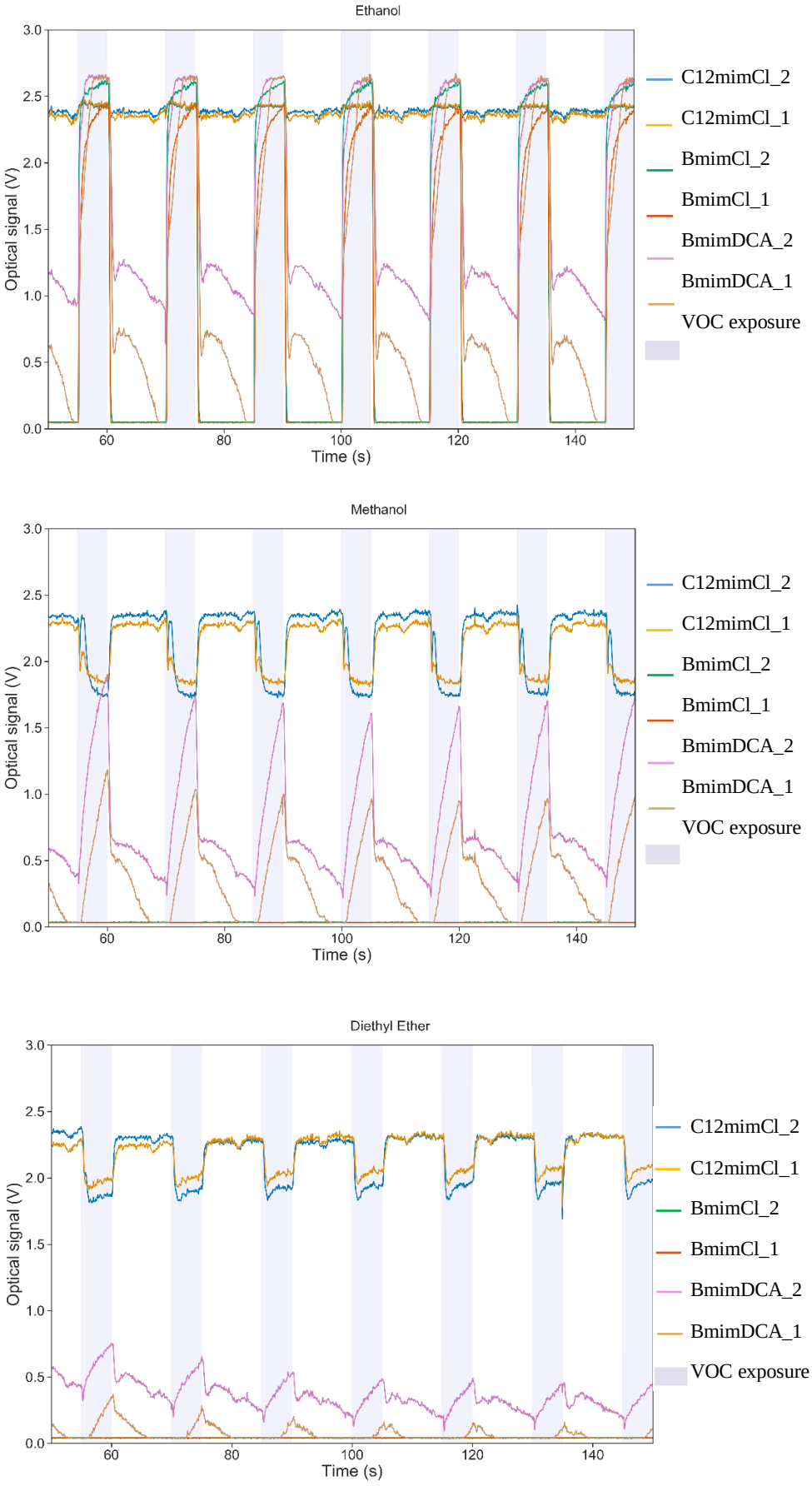

Figure 4.11. E-nose signals: Methanol, Ethanol and Diethyl Ether for the three ionic liquids

Figure 4.12. shows the e-nose responses of the second set of experiments to Ethanol, and the two set of assays to Acetic Acid.

[C_{12}mim][DS] shows a particular response to Ethanol. Observing figure 4.12., [C_{12}mim][DS] exhibits a contradictory response to this VOC. Observing the other e-nose responses of this surfactant to the other VOCs (Appendix II-F), all responses were coherent, meaning that the gel is consistent and that this is the only VOC and gel that possess this kind of response.

Regarding the Acetic Acid, which is considered to be a corrosive VOC for the [Bmim][DCA] gels, as it can be observed from figure 4.12., these gels tend to saturate over time, meaning the liquid crystal will not respond to this VOC, possibly due to the interaction of the Acetic Acid with the gelatine matrix instead of liquid crystal.

Nonetheless for the long length chain tail surfactants such as [C_{12}mim][Cl], SDS and [C_{12}mim]DS], this effect does not appear to take place, since these surfactants exhibit a clear response to this VOC, as it can be verified on figure 4.12.

Comparing the long-tailed surfactant behaviour to VOC exposure, Dichloromethane, Heptane, Ethanol and Methanol, were the VOCs that presented bigger differences on their response. [C_{12}mim][DS] and SDS, responded very similarly to all VOCs (except for Ethanol). Thus, the IL, [C_{12}mim][Cl], was the surfactant of this category, that revealed different responses to these VOCs, as it can be verified from pictures on appendix II-F.

Short-tailed surfactants ([$Bmim^+$]) and long-tailed surfactants ([C_{12}mim][DS], SDS and [C_{12}mim][Cl]) showed very distinctive responses to the VOCs exposed, and responded very similarly within these two categories of surfactants. Hence, revealing that the size of the chain of the surfactant is a more determinant factor on the e-nose response, than the counter ion. However, [C_{12}mim][Cl] was an exception, since it was the surfactant that possessed more distinctive responses to some VOCs, presenting different responses than the other long-tailed surfactants, thus, revealing to be the surfactant with greater selectivity.

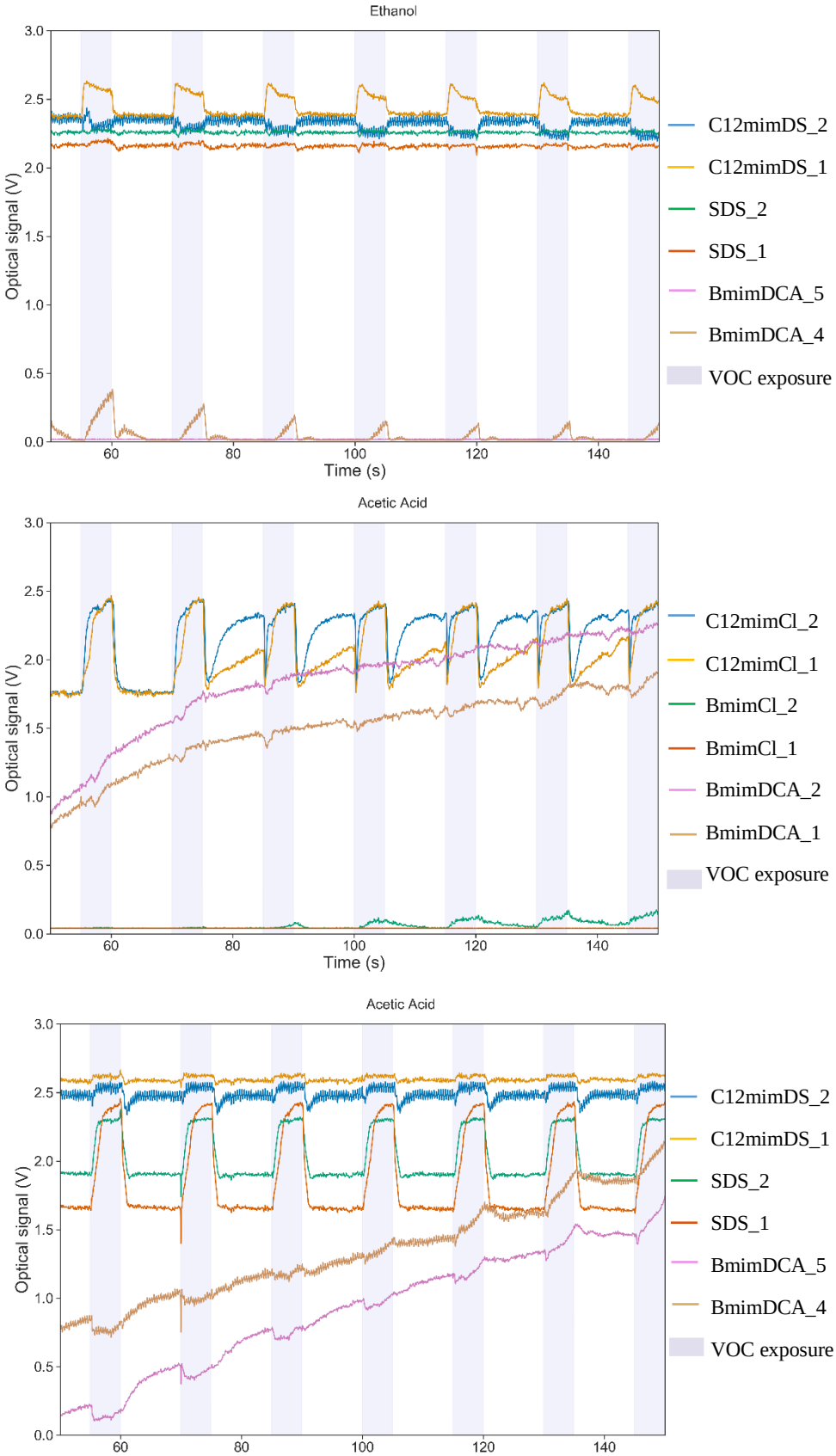

Figure 4.12. E-nose signals of the gels exposed to: Acetic Acid (two assays of experiments) and Ethanol (second set of experiments)

As previously stated, and observed on this Chapter, regarding the Droplets Morphology, the size of the surfactant will have a significant impact on the conformation of the droplets and their sizes. The main difference noted was that, long tailed surfactants will originate mixtures of configurations on the LC-droplets and their respectively sizes, namely they will create a miscellaneous of droplets with planar and homeotropic anchoring. The [$Bmim^+$]-LC-droplets only possess homeotropic anchored droplets, with radial configuration. Figure 4.13., shows seven frames throughout a video that demonstrated what happened when Acetic Acid was exposed to [Bmim][Cl] and to [C_{12}mim][Cl]. It is evident that the droplets doped with [Bmim][Cl] appear to have no signs of effect from this VOC, in contrast the other ionic liquid shows a bipolar droplet experiencing some changes when the VOC passes and then returning to its previous state, differing from the radial droplets presented on the same gel. Thus, the existence of these planar anchored droplets appears to be the crucial factor for these surfactants to emit a response to such VOC.

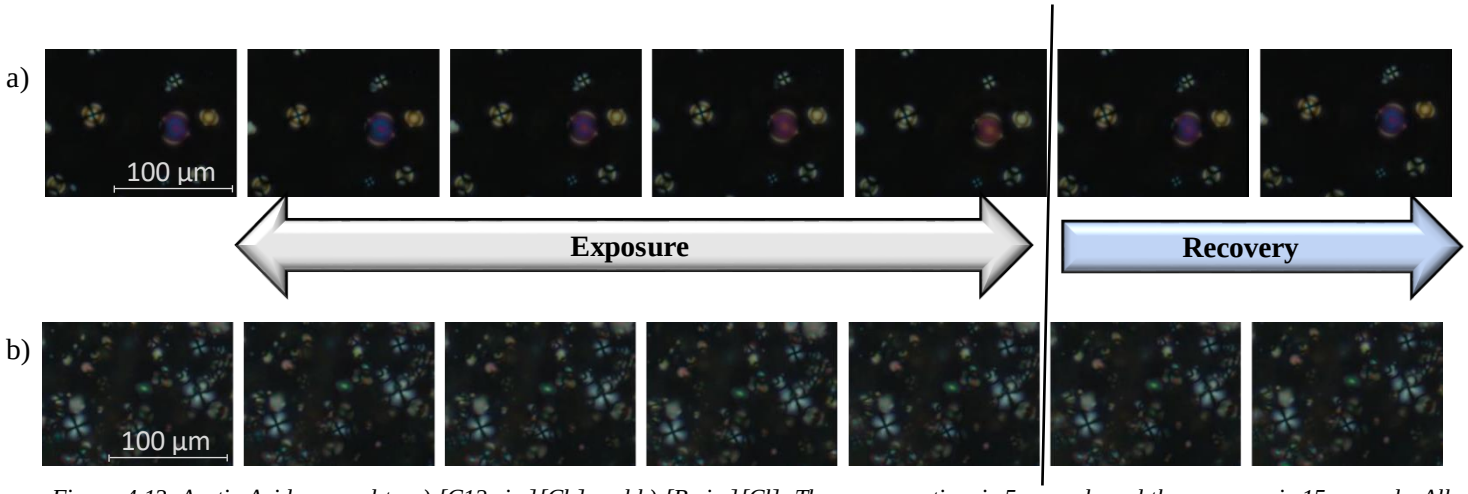

Figure 4.13. Acetic Acid exposed to a) [C12mim][Cl] and b) [Bmim][Cl]. The exposure time is 5 seconds and the recovery is 15 seconds. All images are in the same scale.

It should be noted that on Appendix II-G are the tiles for the "before and after" exposure to VOCs, for all the gels tested on this Chapter, the tiles are the aggregation of 63 photos that combine make the hole window through where the light passes on the sensors.

Proceeding to the confusion matrices, considering the diagonal of the matrix it is possible to calculate the total score for each gel, meaning the global accuracy of the gel towards the identification of the VOC sample. Figure 4.14., shows the confusion matrices for these two assays. It should be noted that for the first experience, Toluene is not included on the matrix, due to the fact, and as it can be verified on the e-nose response on appendix II-E, that the sensors did not respond to Toluene. This problem might be related to the electrical circuits of the e-nose and some problem may have occurred, such as the LED lights of the system shut down. It should also be

noted that, for the case of [Bmim][DCA], the final score is the mean of the two scores obtained from the confusion matrix of each experiment.

The algorithm that processes the data and produces these results, can only process the data of each VOC for each gel, it does not cross the information between the responses obtained for each VOC. Hence, these matrices allow to understand the consistency of the gel, however, it is not an indicator of selectivity, that feature can only be analysed through the observation of the e-nose signals pattern. Moreover, these results can be affected by several factors, such as disturbances on the e-nose itself, or the wrong choice of replicated gels (considering that the production method is not the most accurate).

Analysing the confusion matrices (figure 4.14.) and table 4.2., with the respective scores for each surfactant employed on these experiments, it is clear that [Bmim][DCA] is the surfactant with the highest score. This surfactant induces the higher accuracy between the predicted answer and the true obtained one. Followed by [C_{12}mim][DS] which was the second surfactant with the greatest score, although these are desirable results, none of these surfactants demonstrated the ability to possess selectivity (observing the e-nose signals on appendix II-F).

[Bmim][DCA] and [Bmim][Cl] presented similar results with confusions between the recognition of VOCs alike. Particularly for the Acetic Acid, both gels confused this VOC with Diethyl Ether, this might be due to the VOCs exposure order. Regardless, these two ([Bmim][DCA] and [Bmim][Cl]) were gels that presented the lowest score for the Acetic Acid as it can be seen on figures 4.14. and 4.15., this result might be due to these being the only surfactants that dissolve the gelatine, thus interacting more with it. Considering that Acetic Acid is the most polar VOC exposed, this will affect and interact more with the gelatine matrix than with the LC core. As it was observed on the e-nose signals (figure 4.11.) the responses will not be consistent, thus, the scores will not be as good.

Figure 4.15. shows the scores for the exposed VOCs and gels (with different surfactants) tested. From the error bars is possible to verify the consistency of the gels. [Bmim][DCA], SDS and [C_{12}mim][DS] were the gels that presented the best coherency, since these presented the smallest error bar for all VOCs. Contrastingly, [Bmim][Cl] and the gel with no surfactant, followed by [C_{12}mim][Cl], proven to be the gels with greatest inconsistencies, thus, being the gels with the lowest global scores.

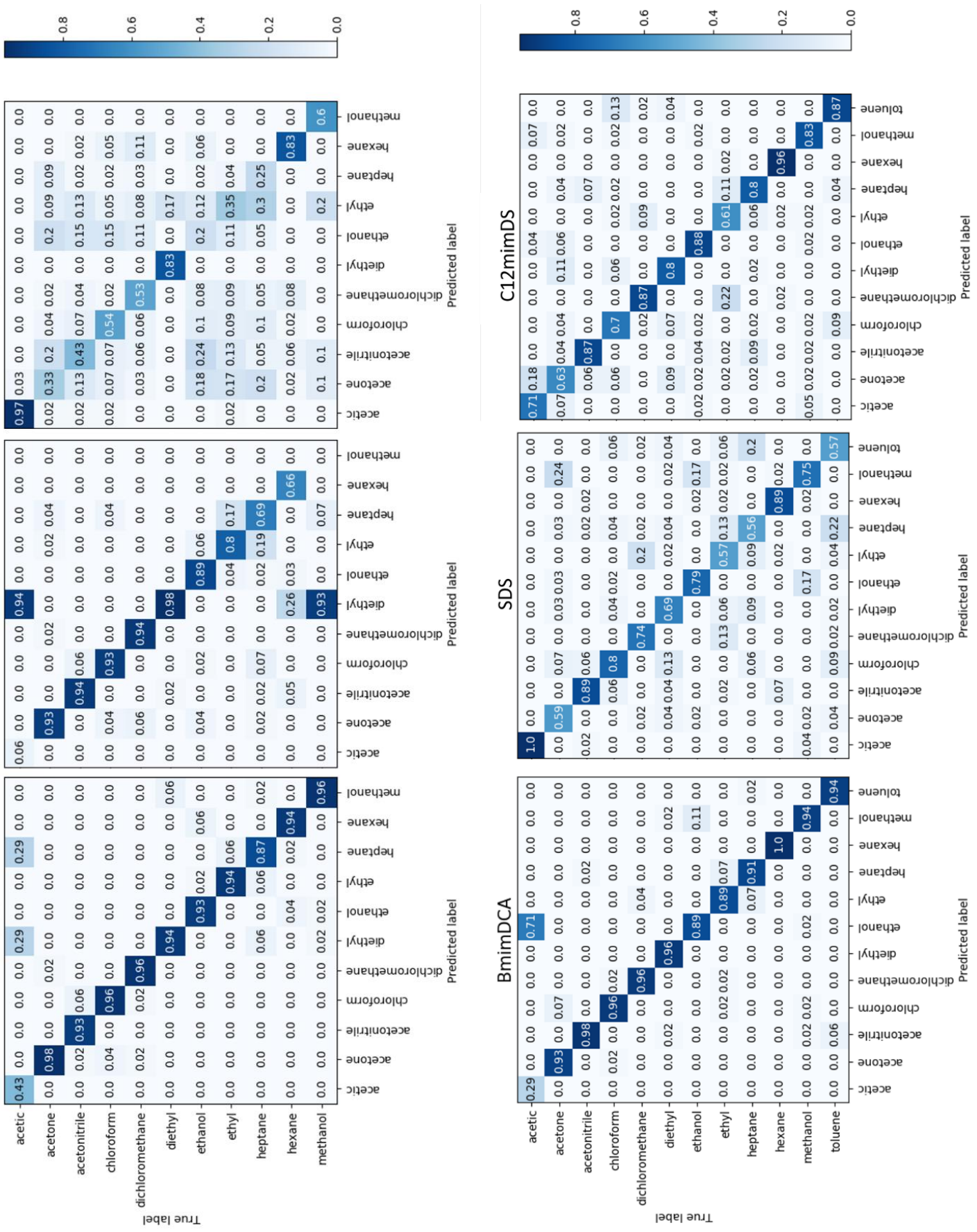

Figure 4.14. Confusion matrices for the different gels tested. These are regarding the experiments performed on this Chapter, with the purpose to compare the effect of different surfactants on the gel.

Table 4.2. Global Scores for all tested gels, with different surfactants, in aqueous Medium

Gel	Score
BmimDCA	**89.10%**
BmimCl	71.09%
C12mimCl	53.27%
SDS	73.67%
C12mimDS	79.42%

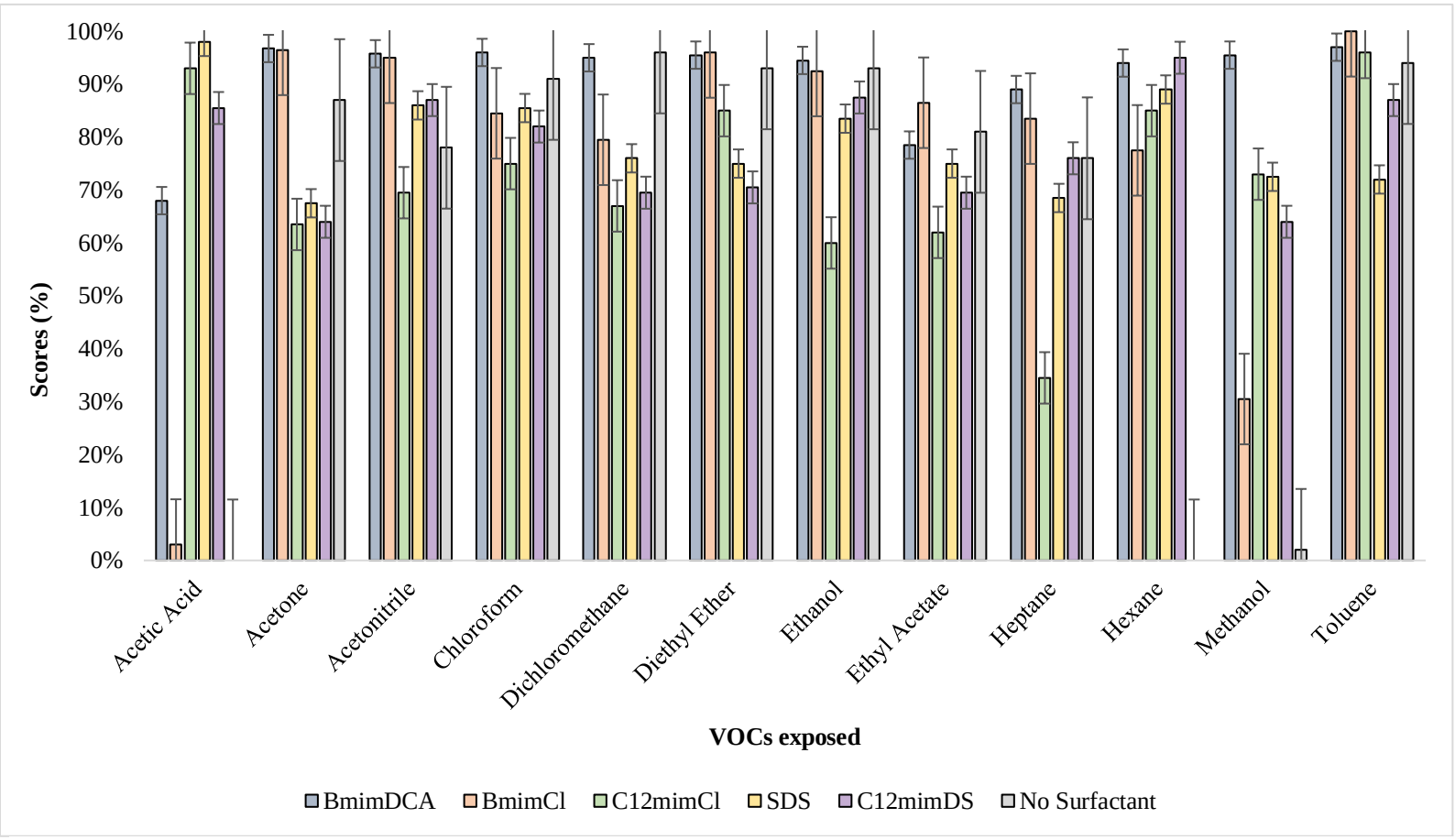

Figure 4.15. Average VOCs score, for all gels tested with different surfactants, in aqueous mean. The score is the average from all the assays performed. All surfactant have four replicas, except for [Bmim][DCA] that possess six and the gel with no surfactant has two replicas.

Tables 4.3. and 4.4, show the %(w/w) of each component for all gels made within an aqueous Medium, and some of the most relevant features, respectively, for all tested gels in an aqueous Medium. Analysing these two tables, it is evident the similarities among surfactants with the same size of the tail chain. The main difference on the composition of the gels is the amount of surfactant and solvent. Long-tailed surfactants ([C_{12}mim][Cl], SDS and [C_{12}mim][DS]) possessed much lower concentrations of surfactant and much higher concentrations of solvent, compared to the [$Bmim^+$] family surfactants. This is due to the fact, that these long-tailed surfactants

(considered to be chaotropic), possess a much higher tendency to form micelles than the short-tailed surfactants (considered kosmotropic), hence, need less amount of surfactant to cover the LC-droplets [42].

Table 4.3. %(w/w) of each component for all tested gels in aqueous Medium

Component/Gel	[Bmim][DCA] (%w/w)	[Bmim][Cl] (%w/w)	[C_{12}mim][Cl] (%w/w)	SDS (%w/w)	[C_{12}mim][DS] (%w/w)	No Surfactant (%w/w)
Surfactant	59.09%	55.98%	0.18%	0.18%	0.39%	-
5CB	3.75%	4.04%	1.65%	1.65%	2.05%	4%
Gelatine	18.58%	19.99%	16.36%	16.34%	16.26%	19%
MilliQ Water	18.58%	19.99%	81.81%	81.70%	81.30%	77%

*Table 4.4. Summary of some characteristics for all gels tested. * Stability refers to the consistency of the gels after VOCs exposure and storage for 10 days, compared to the original state of the gels.*

Characteristic/Gel	[Bmim][DCA]	[Bmim][Cl]	[C_{12}mim][Cl]	SDS	[C_{12}mim][DS]	No Surfactant
Droplets Morphology	Radial	Radial	Mixture: radial, escaped radial and super-twisted bipolar	Mixture: radial, escaped radial and super-twisted bipolar	Mixture: twisted-toroidal, twisted-bipolar and multi-defected	Mixture: Multi-defected and bipolar
Average Droplet Size (+/- 11 µm)	22.03	22.07	24.53	20.92	25.28	22.85
Selectivity to VOCs	None	None	Yes	None	None	None
Stability*	Low	Low	High	Medium	High	Very Low

4.2. Conclusions

Five different surfactants were tested in this chapter, in order to verify the effect of these on the droplets morphology and consequently the response on the e-nose.

Indeed, significant changes were observed on the droplets configurations, particularly when changing the size of the length of the alkyl tail, despite the counter ion. This fact occurred due to the fact that by increasing the size of the tail chain of the surfactant, the interactions with the water molecules and with the liquid crystal will be noticeably different. In this work, two short tailed surfactants belonging to the [$Bmim^+$] category of ionic liquids, two long tailed surfactants, [C_{12}mim][Cl] and SDS, and a long doubled chain tailed surfactant, [C_{12}mim][DS] were tested. The short tailed surfactants are considered to be kosmotropic, meaning they will dissociate into ions in the presence of water, since these are less hydrophobic than long tailed surfactants that are considered to be chaotropic, these, contrastingly will prefer to form micelles and to induce the radial configuration much faster than the kosmotropic. However, other factors should be considered as well, such as the concentration of the surfactant and the time of the each component interacting when making the sensing gels.

In fact, the interaction time of the Liquid Crystal with the other components when forming the gel, is dependent on the size of the tail of the surfactant and it will affect the droplet formation, consequently affecting the droplet morphology and e-nose response. For long-tailed surfactants no more than ten minutes should be the ideal time, and for shorted-tailed surfactants at least 30 minutes is the necessary time for the proper formation of the droplets.

Hence, surfactants with the same size of alkyl tail presented similar morphology and responses on the e-nose. Small tailed surfactants, form radial, more homogeneous, small droplets. In contrast, despite their different nature, long-tailed surfactants revealed similar morphology and e-nose behaviour, possessing a non-homogeneous mixture of droplets in the gels, revealing to be, in most cases, radial. Nevertheless possessing as well droplets with a planar anchoring, thus, having other configurations.

Regarding some of the purposes mentioned on the aims of this work, such as the stability and selectivity of these sensing gels, some were achieved with the use of longer tailed surfactants. [C_{12}mim][Cl] revealed to be a good droplet stabilizer, since it preserved with great efficiency, most of the droplets configuration after the e-nose experiments, for a longer period of time when compared to a short tailed ionic liquid, that revealed greater instability, due to the fact that the droplets gained a tendency to coalesce after a shorter period of time. This ionic liquid not only demonstrated to provide great stability for the droplets, as well as appeared to possess some sort

of selectivity to some VOCs on the e-nose, moreover the gels resisted the passage of Acetic Acid, contrasting to the [Bmim][DCA] gels that tended to saturated.

Hence, different surfactants, have significant effects on the 5CB-droplets, in terms of configurations and e-nose responses. It was also proved and verified that the length of the alkyl chain has a more noticeable impact than the counter ion.

5. Evaluation of the pH on the properties of the sensing gels

5.1. Results and Discussion

In this Chapter the focus will be incising on the pH effect on the interactions of the matrix with the surfactant, consequent effect on the droplets configuration and its response on the e-nose.

Throughout this work, gelatine from bovine skin (type B) was employed as the immobilization agent for the sensing gels. It is permeable to VOCS, dissolves in water and in some surfactants and it is solid at room temperature. Considering that gelatine is a mixture of proteins (containing Collagen), in order to study the pH effect on the gelatine matrix, it should be taken into attention the isoelectric point (IP) of the gelatine, which is between 4.7-5.4. Thus, by assuring that the buffer solutions are strong enough, there is no need to add much more solvent than the original gel recipe. On appendix III-A are all the amino acids present on the gelatine used to create the matrix of the gels, and their respective pKa and IP values [115], [116].

Hence, acidic and basic buffer solutions were prepared using glycine and hydrochloric acid, and sodium hydroxide, respectively. Glycine was selected to make the buffers since it has a large range of pka values, allowing to easily work with, since near those pH values it will not be charged, meaning the buffer solutions will not produce undesirable effects on the gels. Thus for the acidic and basic buffers, pH values of approximately 1 and 11, respectively, were used [117].

Figure 5.1. shows a possible illustration of the electrostatic interactions between the matrix and an ionic surfactant surrounding the LC droplet and their effects on the orientation alignment of the LC molecules. For the cationic surfactant, at low pH the gelatine becomes positively charged, thus, creating a repulsion between the surfactant molecules and the gelatine matrix, hence, supporting the homeotropic alignment and maintaining the radial configuration. At high pH the gelatine becomes negatively charged, and an attraction force is created between the surfactant and the matrix, thus, new interactions occur at the interface of the LC-droplet, as the surfactant molecules move and interact with the gelatine. Consequently, the molecules of the liquid crystal will also arrange in order to accommodate the surfactant molecules, hence, possibly a transition of anchoring and configuration may occur.

For anionic surfactants, the opposite effects should be noticed, for high pH media a repulsion between the surfactant molecules and matrix should occur, thus, maintaining the homeotropic anchoring. At low pH media, an attraction between the surfactant and the gelatine should take place, hence leading to transitions on the anchoring and configuration of the LC molecules.

It should be noted that for surfactants with shorter alkyl tail, the transition should be easier to occur, in the sense that due to the length of the tail of the surfactant it is easier for these to move,

to transit from one configuration to another. Long length tailed chain surfactants, however, possess higher difficulty in moving, hence, the smaller droplets formed with these surfactants are unlikely to change their configuration.

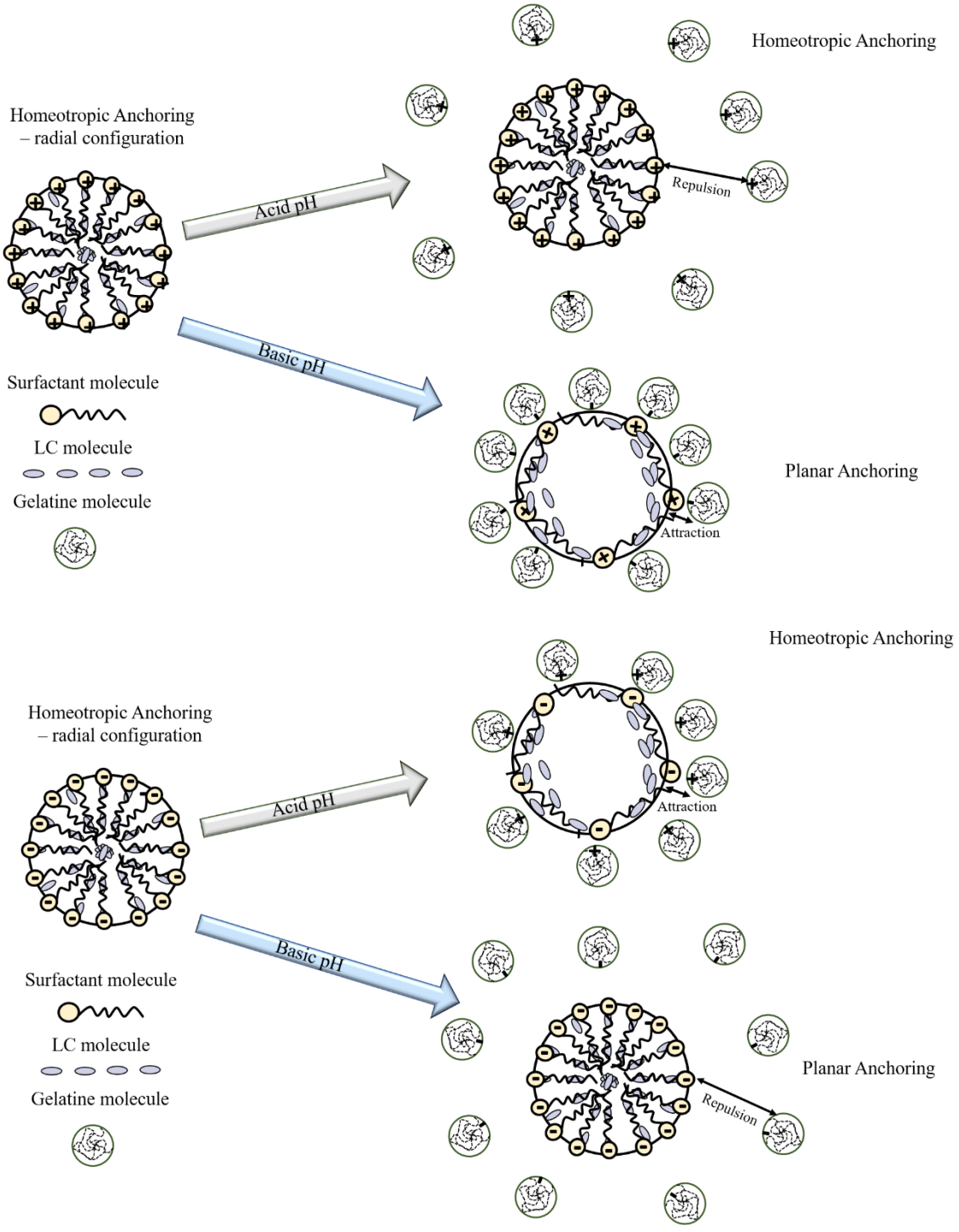

Figure 5.1. General illustration of the interactions between the charged gelatine matrix and an ionic surfactant

5.1.1. Droplet Morphology

As in the previous Chapter, the first subject of the Results will be dedicated to the analysis of the droplet morphology and its potential impact on the e-nose response. In this Chapter, however, the focus will be on the effect that changing the pH environment will cause on the configuration of the droplet as a consequence of new interactions between the matrix and the surfactant. Thus, for each surfactant, an analysis of the behaviour of the LC droplet within an aqueous, acidic and basic environment, is done, as well as a comparison between the effects observed for each class of surfactant.

Figure 5.2. shows the effect of pH on 5CB-[Bmim][DCA] droplets. It is evident that at basic pH the droplets change drastically their configuration, causing a serious disturbing on the alignment of the 5CB molecules, changing from a homeotropic anchoring with a stable radial configuration, to possibly a planar anchoring with a non-stable random director configuration, or a multi-defects structure. This significant change might as well lead to changes on the e-nose response, since this configuration is more unstable, thus, the sensitivity of these droplets on the device might be increased. Contrastingly, with the basic pH, the droplets on an acidic medium maintain their anchoring and orientation, not exhibiting a significant change on the configuration. However, a slight tilting on the orientation of the droplet is noticed, revealing a minor effect on the alignment of the LC molecules. Hence, it is not expected for these droplets to lead any significant changes on the e-nose response, when comparing with the original recipe, using only water as the medium.

On a more detailed observation, analysing figure 5.2. (Basic Medium at 0º) it is clear that these changes on the droplet only occurs at molecular level of the liquid crystal, considering that the interface of the LC with the matrix remains the same, a well-defined circle. Interestingly it noticed that some smaller droplets tend to surround the bigger droplets, this may occur due to the electrostatic interactions between the surfactant and the matrix, now charged.

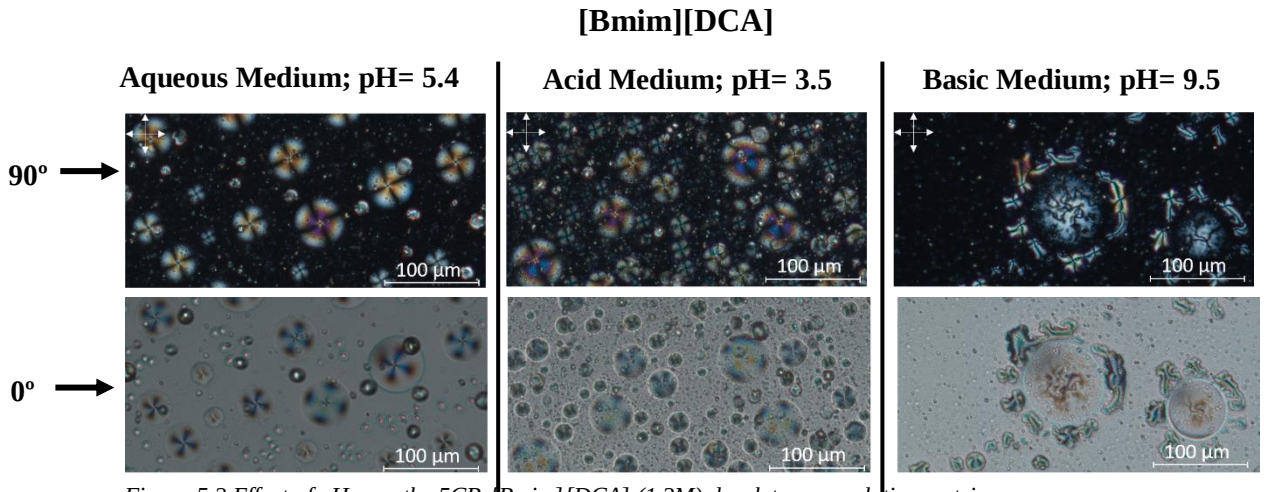

Figure 5.2 Effect of pH over the 5CB-[Bmim][DCA] (1.3M) droplets on a gelatine matrix

Regarding the other shorted tail chain surfactant, figure 5.3. exhibits the pH effect on the 5CB droplets decorated with [Bmim][Cl]. Observing the pictures presented, it is clear that similarly to the case of the [Bmim][DCA], the effect of the basic medium is significantly higher than the acidic buffer. Considering, that the basic buffer has a noticeable impact on the LC-droplet configuration, changing the homeotropic anchoring and consequent stable radial orientation to a random director configuration, or a multi-defects possibly with a planar anchoring, contrasting with the effect of the acidic buffer that seemed to have no noticeable impact on the droplet morphology. However, these effects were expected according to figure 5.1. as an attempt to explain the molecular interactions that occur on the gels, and the purpose of replacing the water for an acidic, or basic, buffer.

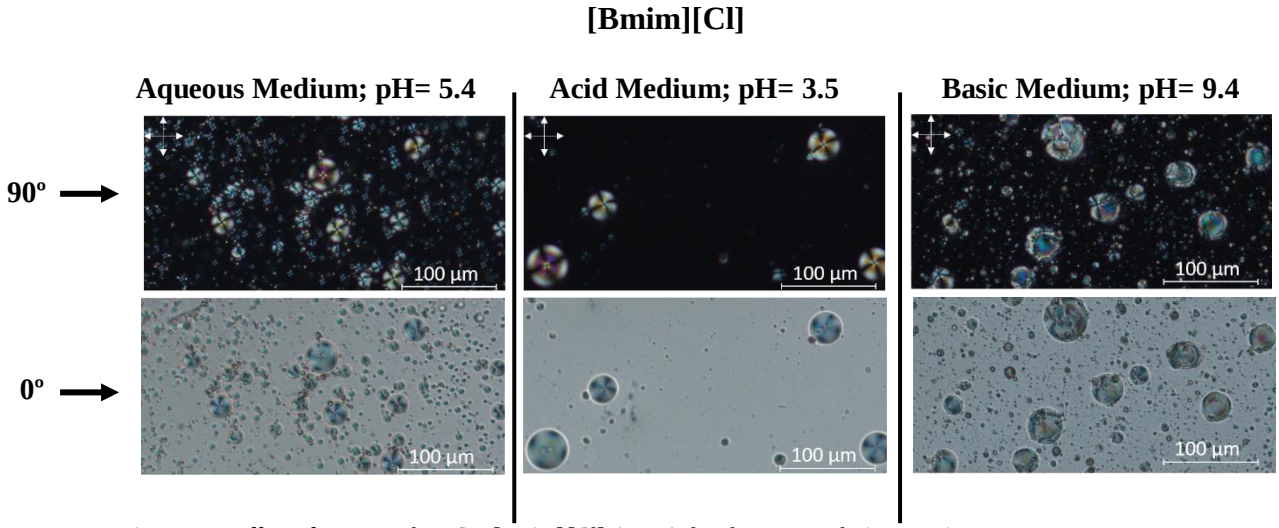

Figure 5.3. Effect of pH over the 5CB-[Bmim][Cl] (1.2M) droplets on a gelatine matrix

Concerning the longer tailed chain surfactant and starting with the ionic liquid ([C_{12}mimCl]), figure 5.4. demonstrates that due to the length of the alkyl tail, the change of pH in the medium does not have a significant impact on the droplet configuration. Pictures from the aqueous medium exhibit the mixture of configurations, already mentioned on the previous Chapter for the long-tailed chain surfactants, such as twisted-bipolar and radial configurations, notwithstanding both cases (acidic and basic media) exhibit some sort of configurational change. For the acidic case, pictures show a higher tendency to stabilize the radial orientation which supports what has been previously supposed and represented on figure 5.1., where the repulsion between the positively charged matrix and the cationic surfactant molecules stabilizes the radial configuration. In this case, a higher force imposing the surfactant molecules to turn to the 5CB droplet appear, thus, increasing the tendency to an homeotropic anchoring and consequent radial configuration. The gels made within the basic medium exhibit a change of configuration, to super-twisted-bipolar and twisted-toroidal.

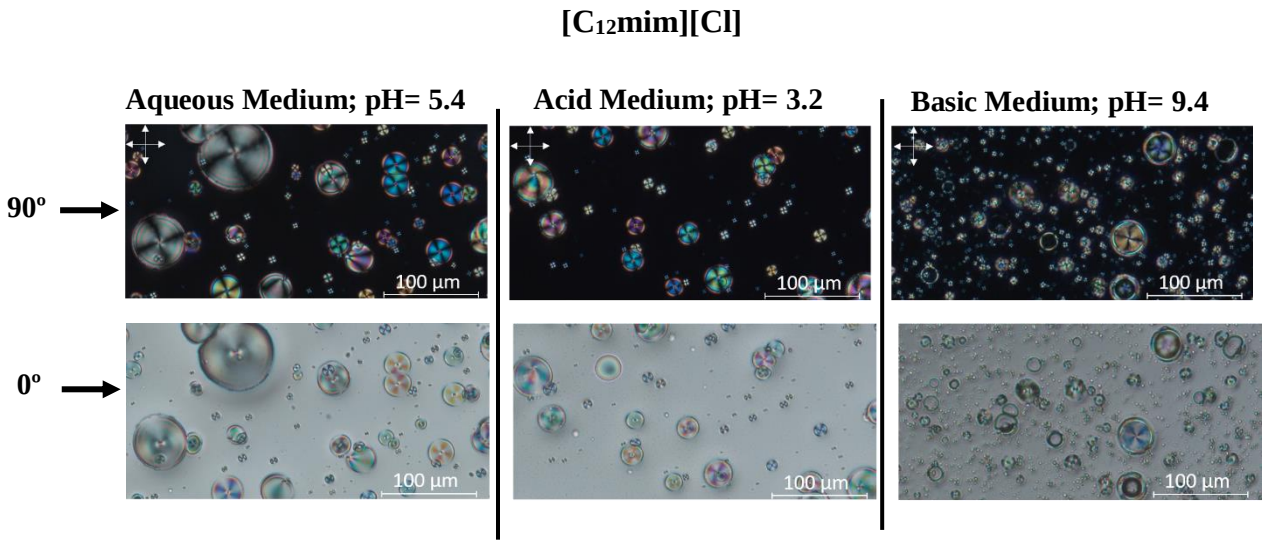

Figure 5.4. Effect of pH over the 5CB-[C_{12}mim][Cl] (0.007M) droplets on a gelatine matrix

Regarding the strong detergent surfactant, the SDS, it should cause changes on the LC-droplet configuration upon the acidic medium, due to the attraction of the negatively charged molecules of the SDS surfactant and the positively charged gelatine matrix. This would cause the molecules of the surfactant to align in a parallel form to the interface since they would not be so repelled to be inside the droplet. However, it was observed that the changes occurred not only in the acidic medium, but also in the basic medium (Figure 5.5.). For the acidic case it is observed a change of the LC configuration from radial, escaped-radial and bipolar, to increase the tendency to form twisted-bipolar configuration, maintaining, nonetheless some radial droplets, showing that the effect of the change of pH is not as significant as for the case of the ionic liquids [$Bmim^+$]. Considering the basic medium, it is noted a predisposition to form a twisted-toroidal, but at the same time it appears to possess a crystalline centre and twisted-bipolar structure, exhibiting in an evident that for both changes of pH, the structures formed are non-stable ones.

Thus, these figures (5.1. – 5.5) prove once more what has been stated previously on the previous Chapter, that independently of the counter ion, the size of the surfactant is the most important feature in the case of the liquid crystal molecules alignment and consequent configuration of the droplet.

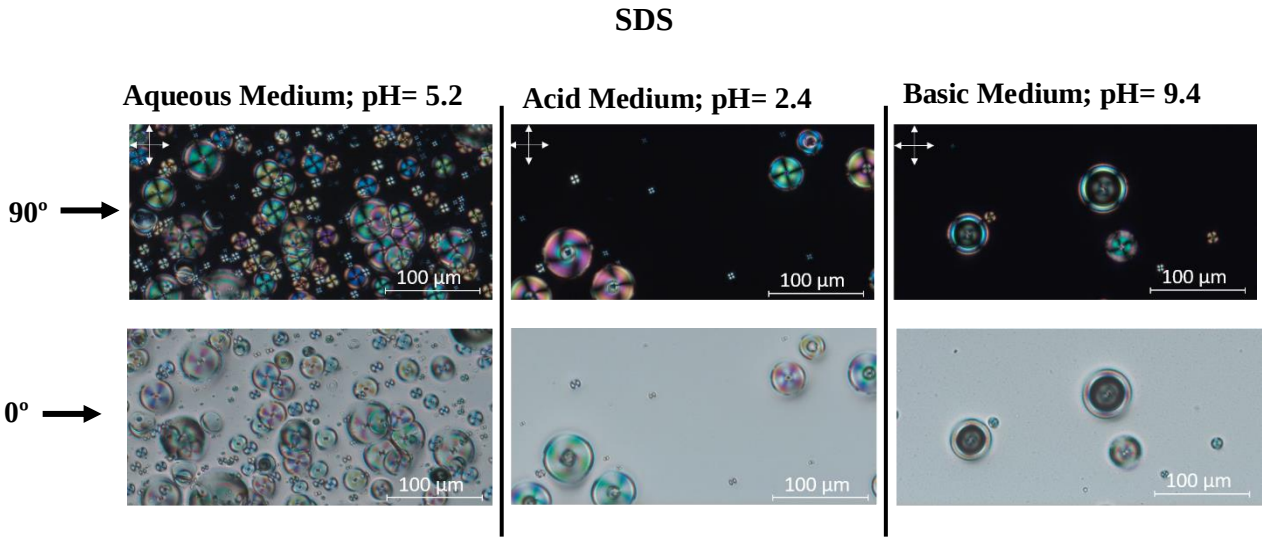

Figure 5.5. Effect of pH over 5CB-SDS (0.006M) droplets on a gelatine matrix

Regarding the [C_{12}mim][DS] surfactant, from pictures on figure 5.6. (Aqueous medium) it is noticeable a mixture of conformations, between radial for the smaller sized droplets, super twisted-bipolar for the middle sized ones and what appears to be a combination of twisted-toroidal structures with a twisted-radial for the larger droplets. This mixture is relatively similar to the one presented for the [C_{12}mim][Cl], possibly indicating that the mixture surfactant will have a similar behaviour to the ionic liquid part that formed when compared to the SDS [99], [118]. Considering the effects of the pH changes on the medium, in this case there is no expectable transition, or formation of configuration, since in this particular case the polar head consists on opposite charged molecules which will both attract and repel the charged matrix, and some sort of "game of forces" takes place.

Thus, starting with the acid, the matrix is positively charged, and an evident transition of configuration occurs to form a more homogeneous mixture of twisted-bipolar droplets leading as well to what appears to be a decrease of sizing. This phenomenon might have implications later, on the Mean Gray Value, and the behaviour of the droplets when exposed to the VOCS. However, focusing on what might be occurring on a molecular level, no more homeotropic anchoring and radial configurations are observed, meaning that there is an attraction of the surfactant towards the matrix surrounding. This might be due to the presence of the SDS part, which has an anionic head [69].

Regarding the basic medium effect, a change of configuration is also noted. All droplets seem to present a planar anchoring, with a tendency to form a super-twisted-bipolar configuration for the case of larger droplets and an inclination to form toroidal, or bipolar, structures for the smaller sized droplets, producing a new mixture of droplet configurations [99]. These phenomena are due to the influence of both anionic and cationic surfactants that form this resultant surfactant, revealing that both acidic and basic media have influence on these droplet conformations.

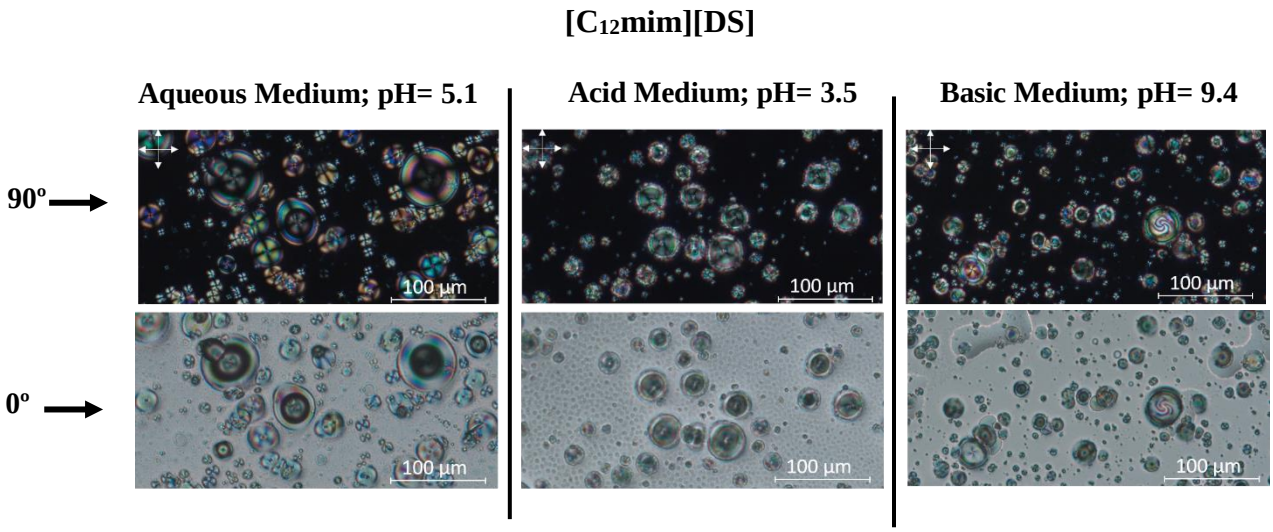

Figure 5.6. Effect of pH over 5CB-[C12mim][DS] (0.008M) droplets on a gelatine matrix

Lastly considering the case where no surfactant is employed, no changes on the configuration are expected considering that there is no ionic surfactant covering the liquid crystal droplet. Hence, regardless of the matrix being charged, or not, the interaction of the latter with the LC-droplet should remain the same. Figure 5.7. exhibits the effect, or in this case the ineffectiveness of the change of the pH, proving what has been mentioned before. Observing the four pictures on figure 5.7., it is clear that no significant effect is noted, the droplets remain with a planar anchoring with a tendency to align in a bipolar conformation. Perhaps a slight change on the droplet size is noted, upon the basic surfactant, which seemed to form a monopolar configuration and tend to become smaller. Thus, this figure demonstrates the fact that without any ionic surfactant to interact with the charged matrix, there can be no noticeable effects on the configuration of the 5CB droplets.

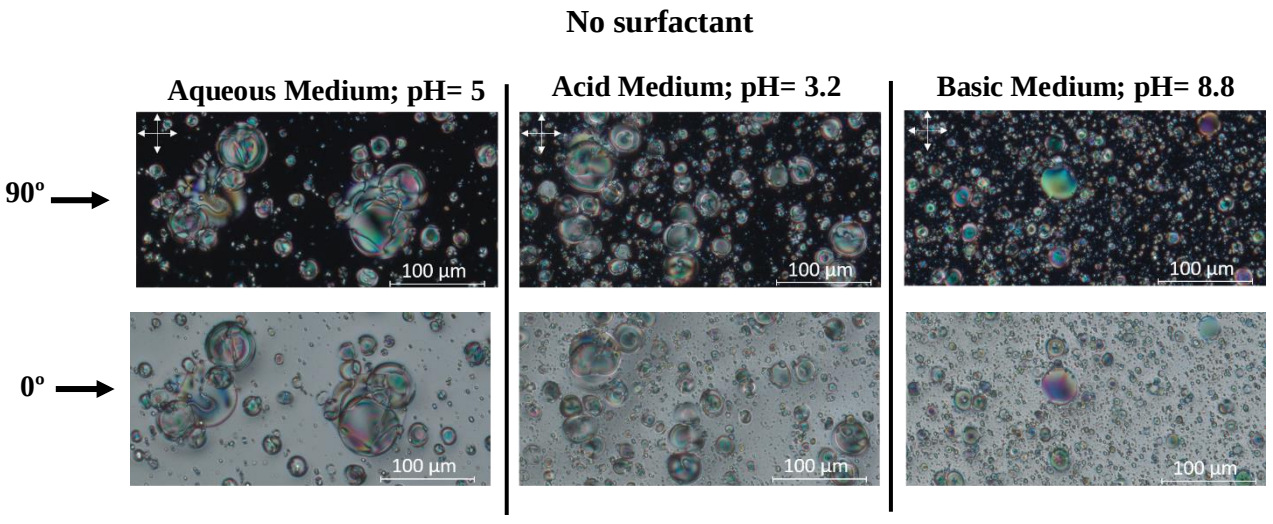

Figure 5.7. Effect of pH over 5CB droplets with no surfactant on a gelatine matrix

Concerning the analysis of the mean droplet size, now comparing not only between the different surfactants, but as well as the effect of the change pH of the medium within the same surfactant. Figure 5.8. shows the average size of the droplets for the several media, aqueous, acidic and basic buffer, for each surfactant employed. Firstly, it is noted that no major alterations on the size occurred when comparing using water as the medium, or using an acidic, or a basic buffer.

Analysing the chart in more detail, the most homogeneous gel was the one with [Bmim][DCA], followed by the case where no surfactant was employed. Regarding the case where no surfactant was used it makes sense since no effect were excepted, and as previously demonstrated no noticeable effects were registered. However, considering the case for [Bmim][DCA], it would be excepted an increase on the size for the basic buffer, considering that in the pictures showed before (figure 5.2.) a significant disturbance on the configuration of the droplets was verified, leading to what appeared to be larger droplets with a non-stable configuration. Nevertheless, it was also noticed that a substantial number of smaller droplets emerged and surrounded the larger droplets, meaning since this chart only considers the average size, the result might be balanced.

Regarding the other [$Bmim^+$], [Bmim][Cl] registers an expected result, since as it was explained previously on this Chapter, for the cationic surfactants, in the acidic buffer the droplets will tend to become smaller and more stable due to the repulsion between the surfactant and the positively charged matrix. About the basic medium, as similar to the case of [Bmim][DCA], despite the fact that larger droplets were formed, smaller ones also appeared equilibrating this final and average result for the mean size of the droplets. Nonetheless, a small increment was registered as it can be verified on Appendix III-C.

The long chain tail surfactants, [C_{12}mim][Cl] and SDS, do not reveal any significant discrepancies between the droplet sizes for the acidic and basic buffers. For the ionic liquid ([C_{12}mim][Cl]), this situation might have a similar explanation to the [$Bmim^+$] cases, since it also is considered as a cationic surfactant, thus, the acidic buffer will result in a stabilization of the radial configuration and the droplets tend to be smaller. A decrement of the mean size for the acidic medium can be verify on figure 5.8., and the tables present on Appendix III-D.

Concerning the basic buffer as the medium (for [C_{12}mim][Cl]), a balanced situation might be taking place, as previously explained on this Chapter, when a mixture of droplets with heterogeneous sizes are present. Nonetheless, comparing with the value achieved for the case where water is used as the medium, both buffers reveal to result in smaller droplets.

Regarding the SDS the opposite outcome takes place, both buffers originate larger droplets, not showing a great discrepancy between them, this may be due to the fact that in both cases, the droplets produced possess non-stable structures and barely any stable small radial droplets, thus leading to an increase of size.

Lastly concerning the C_{12}mimDS surfactant, the most significant effect is with the acidic buffer as the medium leads to a decrease of size. However, in this case it would be expected that for both buffers the size would remain relatively the same, the reason why this does not occur, may be due to the fact that the method of production leads to several heterogeneous areas on the gel.

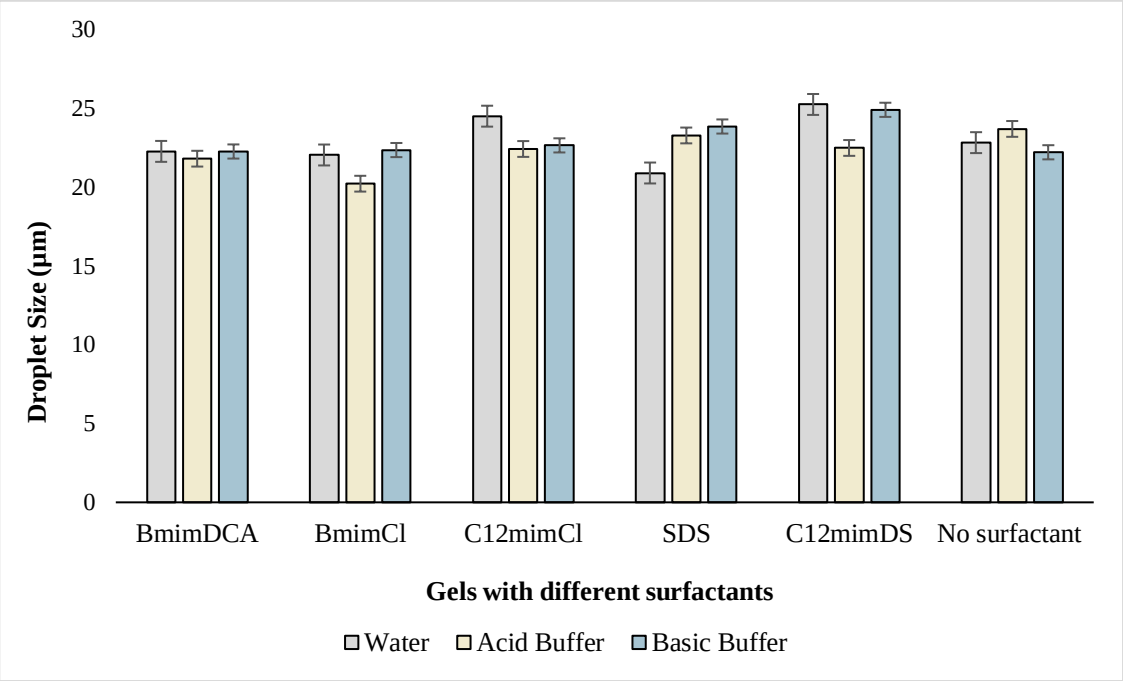

Figure 5.8. Average droplet size for the several pH means and gels tested with different surfactants. The number of droplets count and analysed for each gel is: ***Aqueous Mean:*** *[Bmim][DCA] = 474; {Bmim][Cl] = 421; [C_{12}mim][Cl] = 229; SDS = 509; [C_{12}mim][DS] = 194; No surfactant = 328;* ***Acid Mean:*** *[Bmim][DCA] = 327; {Bmim][Cl] =290; [C_{12}mim][Cl] = 275; SDS = 72; [C_{12}mim][DS] = 248; No surfactant =259;* ***Basic Mean:*** *[Bmim][DCA] = 481; {Bmim][Cl] = 457; [C_{12}mim][Cl] = 239; SDS = 267; [C_{12}mim][DS] = 282; No surfactant = 364*

Observing figure 5.9., which is a box chart representing the droplet size distribution for the acidic buffer as the medium, the best case belongs to the SDS, since it is the surfactant that demonstrates the smallest dispersion, meaning the gel is, in terms of droplets size, relatively homogeneous and barely possess outliers. Following is the [C_{12}mim][DS] that also has practically no outliers, and the mean value is very close to the median, however, it shows a greater dispersion when compared to the others surfactants, revealing possibly a more heterogeneous gel. Interestingly the mode was the smallest value compared to the other cases, and the one that revealed a greater discrepancy relatively to the mean value, thus, explaining the decrease of mean value of the average size of droplets. All these values can be obtained from, Appendix III-D.

Comparing the ionic liquids, [Bmim][DCA] was the one that presented greater dispersion and more outliers, that caused the mean value to increase significantly, considering the fact that the mode value was lower than 20 µm. [Bmim][Cl] and [C_{12}mim][Cl], both presented relatively the same amount of outliers. Regarding the short tail ionic liquid ([Bmim][Cl]), its results correspond to what was expected. However, the same phenomenon is observed, due to the outliers, the mean

value did not present the anticipated decrease of size. Nonetheless, the mode value was approximately 15µm, revealing a discrepancy between the latter and the mean value. Concerning [C_{12}mim][Cl] the same fact, that occurred with the others ionic liquids, is observed, the mean value is greatly influenced by the outliers and the mode value tends to drive further from the average size of the droplet.

Lastly, considering the case of no surfactant, the results show no significant outcomes beyond of what would be expected.

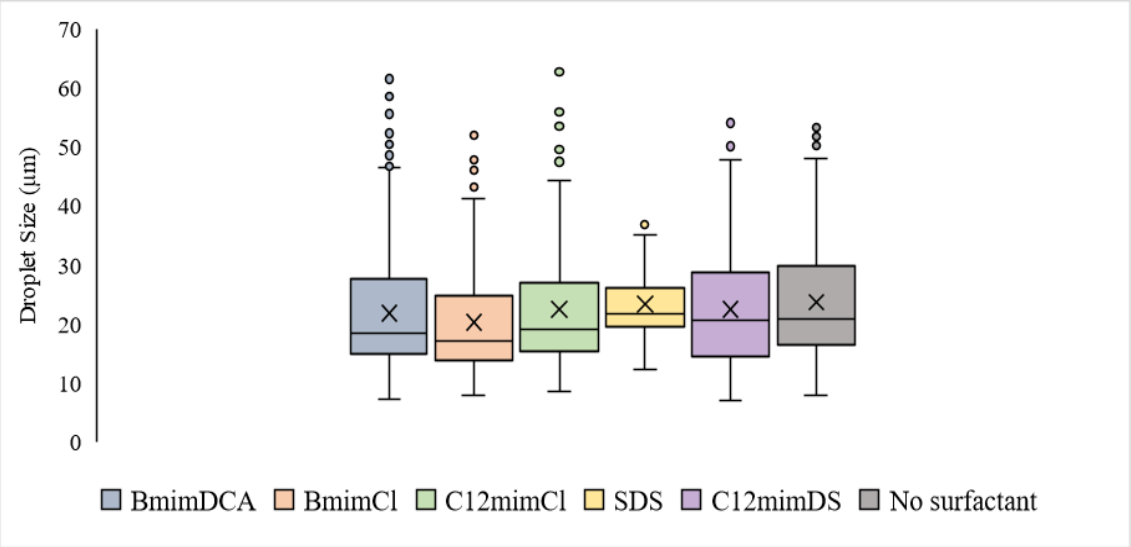

Figure 5.9. Acid Mean Droplet size distribution for the tested gels with different surfactants within a gelatine matrix. The points above the charts represent the outliers, the line in each box is the median value and the cross is the average. The number of droplets count and analysed for each gel is: [Bmim][DCA] = 327; {Bmim][Cl] =290; [C_{12}mim][Cl] = 275; SDS = 72; [C_{12}mim][DS] = 248; No surfactant =259;

Respecting the basic medium, figure 5.10. (respective table with values on appendix III-D), shows the box graphic for the droplet size distribution. Starting with [Bmim][DCA], this is the surfactant that showed a greater number of outliers. However, in this case, these outliers are probably due to the formation of those larger droplets observed on figure 5.2., meaning that although they are in less quantity and seemed to be anomalies are actually a consequence of the interactions of the charged matrix with the cationic ionic liquid. This might also be the case for the [Bmim][Cl], that revealed similar effects with its gel.

[C_{12}mim][Cl], contrastingly barely has outliers, the dispersion of the droplets size is smaller and the mean value is very close to the median. All these factors are indicators that the gels are relatively homogeneous, at least when compared to the others, made with different surfactants.

[C_{12}mim][DS] presented a greater dispersion but barely possess outliers. In this particular case, the results tend to be closer to the ones registered by the SDS, with a closer dispersion and average size value. However, considering the mode value, which is noticeably closer to the mode value

for [C_{12}mim][Cl], thus, the majority of droplets revealed to possess a much similar size to the droplets of this ionic liquid, consequently this might be an indicator that the influence of the [C_{12}mim][Cl] could be stronger than the SDS influence.

The no surfactant case demonstrated be slightly influenced by the basic buffer, where a small decrease of size is registered. Nonetheless, a great number of outliers is also noted, thus, the average size remains approximately the same for all the media employed. Appendix III-F shows the statistical summaries for the results presented on figures 5.9. and 5.10.

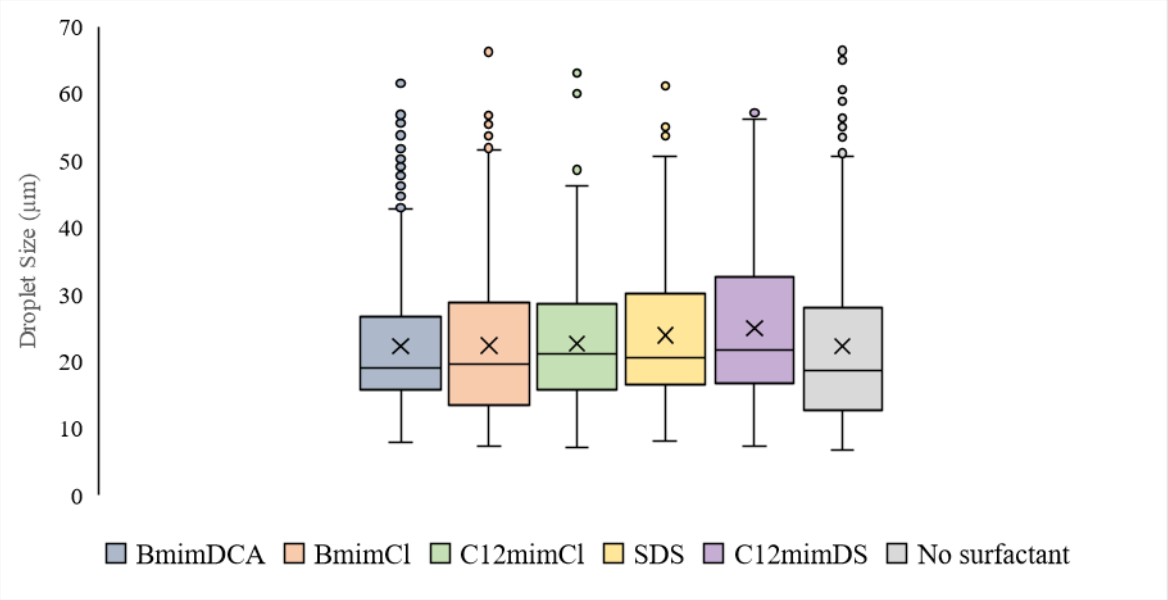

Figure 5.10. Basic mean droplets size distribution the tested gels with different surfactants within a gelatine matrix. The points above the charts represent the outliers, the line in each box is the median value and the cross is the average. The number of droplets count and analysed for each gel is:. [Bmim][DCA] = 481; {Bmim][Cl] = 457; [C_{12}mim][Cl] = 239; SDS = 267; [C_{12}mim][DS] = 282; No surfactant = 364

Regarding the Mean Gray Value, this feature demonstrates, as well, the impact of changing the pH of the medium, since some significant discrepancies between the same surfactant are registered and observed on figure 5.11.

Hence, starting with the one that seemed to possess a greater discrepancy between the aqueous medium and the buffers, SDS, it was stated on the previous Chapter, that smaller droplets would lead to higher values of active optical area available (higher values of MGV). SDS presented previously on figure 5.8., lower values for the droplets size on aqueous medium, and virtually the same mean values for the buffers. Figure 5.11. shows a significant difference between the MGV for the aqueous medium, that is considerably higher than the MGV for the buffers, that are essentially the same as anticipated.

For the [C_{12}mim][Cl] similar results were foreseen, yet these were not achieved, the droplets within the buffers as medium presented inferior MGV compared to the droplets in aqueous medium, and accordingly it should be the inverse.

[C_{12}mim][DS] reveals some expected results, such as the droplets of the acidic medium possessing the higher MGV, but as well as some unforeseen results, such as the discrepancy between the MGV for the basic buffer and the aqueous medium, which according to figure 5.11. should be, essentially, the same. These factors may be an indicator that this correlation, might be not so straightforward, as already noticed on the previous Chapter. Considering the cases for the [Bmim+] these also demonstrate results that were not the expected.

Thus, briefly revealing what should be anticipated on the e-nose regarding the baselines of each surfactant for each pH medium. Starting with [Bmim][DCA], the gels made with a basic buffer should present the lower baseline contrasting with the one produced within an acidic buffer, that should present the highest one. Similar results would be expected from [C_{12}mim][DS].

For [Bmim][Cl] and [C_{12}mim][Cl] these should demonstrate the inverse situation, where the droplets produced within an acidic buffer should present the highest baseline, meanwhile the gels made with a basic buffer should reveal he lowest baseline.

For SDS, the lowest baseline should occur with the droplets made within an aqueous medium, as for the buffers both baselines should remain very similar. Lastly the case of no surfactant employed, the highest baseline should be on the gels made from water as medium, and the lowest should be on the case of the basic buffer.

Hence, observing this figure (5.11.), it is clear that the results, in general terms, do not correspond to the previously obtained for the droplets size, meaning that the program used to estimate the MGV (mentioned on the previous Chapter) might not be most appropriate, since it creates incoherencies between the results. Appendix III-E shows the average MGV for all tested gels.

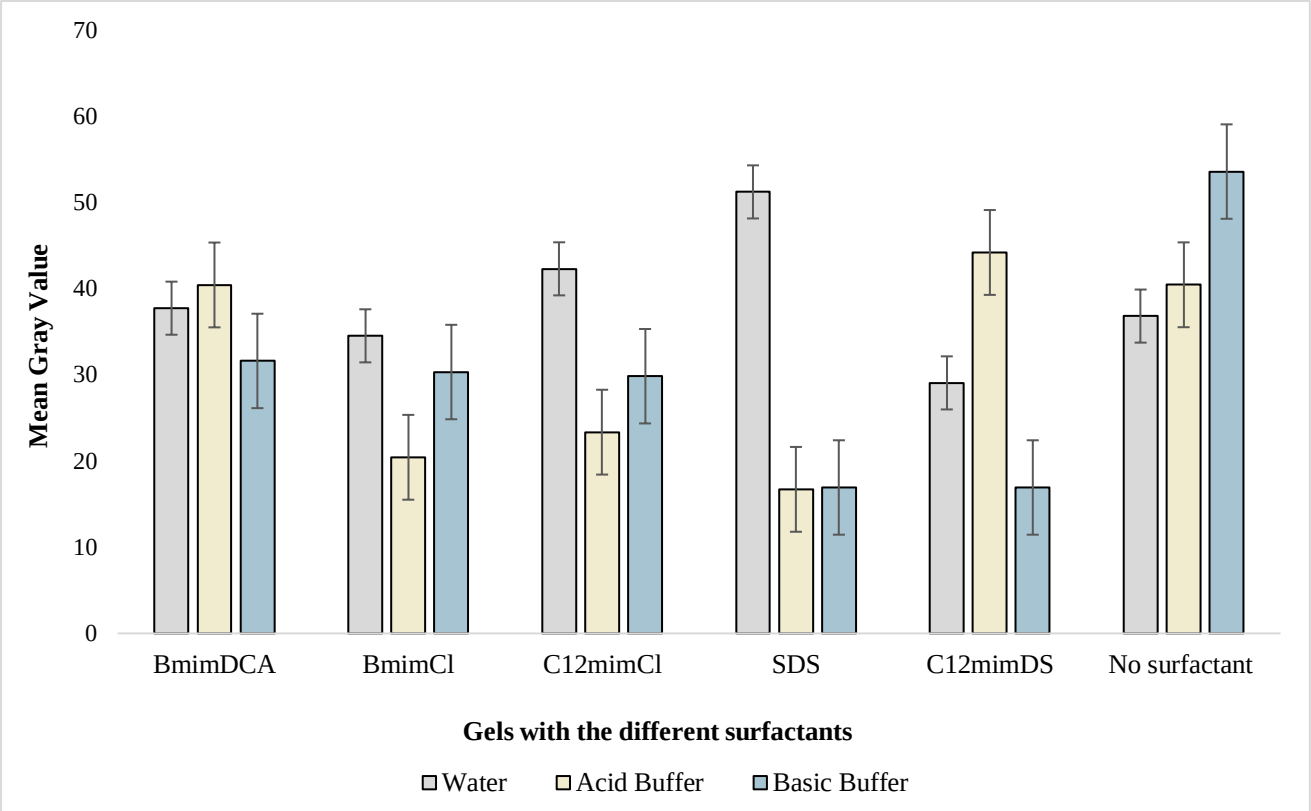

Figure 5.11. Mean Gray Value for the several pH means and the tested gels with different surfactants within a gelatine matrix. The minimum value of MGV is 0, that represents total darkness, and the maximum value is 250, representing total brightness. The number of droplets count and analysed for each gel is: ***Aqueous Mean:*** *[Bmim][DCA] = 474; {Bmim][Cl] = 421; [C_{12}mim][Cl] = 229; SDS = 509; [C_{12}mim][DS] = 194; No surfactant = 328;* ***Acid Mean:*** *[Bmim][DCA] = 327; {Bmim][Cl] =290; [C_{12}mim][Cl] = 275; SDS = 72; [C_{12}mim][DS] = 248; No surfactant =259;* ***Basic Mean:*** *[Bmim][DCA] = 481; {Bmim][Cl] = 457; [C_{12}mim][Cl] = 239; SDS = 267; [C_{12}mim][DS] = 282; No surfactant = 364*

5.1.2. Gels exposed to VOCs

Proceeding to the analysis of the functionalization of the gels, indicating how the LC-droplets doped with surfactant response to the twelve VOCs exposed. Similarly, to the discussion that has been formerly performed on the previous Chapter concerning the same subject. In this chapter an analysis to the VOCs response will be performed, however the pH variations and effects will be taken into consideration.

As previously demonstrated, the variation of pH in the medium where the droplets are formed has a significant influence and effect on the arrangement of the liquid crystal molecules. This might be due to the electrostatic interactions of the surfactant, since all the surfactants employed on this work are ionic, and the, now charged, gelatine. Henceforth, it is expected that the response on the e-nose will also be affected by the change of the medium and consequent transformation of the LC-droplets configuration.

Thus, six different experiments were performed, five with the different surfactants and the corresponding three media, and one with no surfactant, merely the LC-droplet on the gelatine matrix within the respective medium.

In these six experiments the VOCs order was shifted in order to verify the independency of the signals, thus, on appendix III-G, are the VOCs order for each surfactant experiment. On the same appendix, are the respective e-nose signals for the twelve VOCs tested, the VOCs scores on the corresponding tables and charts, as well as the confusion matrices for all the situations mentioned above. It should be noted on the label of the e-nose signals, where appears the name “Normal”, it corresponds to the gels made within an aqueous medium.

Comparing the results obtained from the previous chapter, it can be verified from figures presented on appendix III-G 4) and 5), that the signals for the two shorted tail ionic liquids [$Bmim^+$], are different from the ones previously obtained.

Considering that the protocol followed for the fabrication of these gels was the same, these results are not the anticipated ones, proving that the method production of these sensors is not the most adequate. Moreover, other factors may influence the gels production, such as the surrounding environment, temperature and humidity are some of the factors that have great influence over these surfactants. Thus, if the preservation conditions for these surfactants is not controlled, then not only the production method will have impact on the formation and consequent response to the VOCs, as well as the surrounding environment. Taking [Bmim][Cl] as an example, this is a very hygroscopic ionic liquid, meaning that if not properly stored, with a higher level of humidity, the properties and droplet formation on the gel will be completely different than the same ionic liquid isolated from these exterior factors [119].

Figure 5.12. exhibits the response of different gels with different surfactants made within the three media (Aqueous, Acidic, Basic). [C_{12}mim][Cl] gels to Ethanol, SDS and [C_{12}mim][DS] gels to Acetic Acid.

Regarding the [C_{12}mim][Cl] response to Ethanol, it is clear that comparing to the response presented on the previous Chapter, all gels made with this surfactant responded contrarily to the previous results. In this case the signals went brighter when exposed to the VOC, meaning that probability a change of configuration must have occurred, instead of turning the initial droplets isotropic. No differences on the signals, regarding the different media of gels production, were noted.

The response of SDS gels to Acetic Acid differs according to the medium and its effect on the gelatine matrix and LC-droplets. Particularly for the gels made within an aqueous medium, that responded oppositely to the gels made within the other media. Regardless, all gels (made within different media) seemed to possess their unique characteristic pattern on the signals, predominantly the acidic gels, which seem to have a unique pattern.

[C_{12}mim][DS] gels responded similarly to the Acetic Acid, with the exception of the gels made within a basic medium, which seemed to possess some slight differences on the pattern, when compared to the gels made with the other media. This could indicate some selectivity.

Figure 5.13. shows the responses of [Bmim][Cl] gels to Acetone, [Bmim][DCA] gels to Hexane and the gels with no surfactant to Ethanol. The VOCs chosen for both figures (5.12. and 5.13.) were the most peculiar responses, since to the other VOCs, none of the gels revealed significant differences on their responses.

[Bmim][Cl] gels made within an aqueous medium, tend to saturate over time in response to Acetone exposure, meaning the droplets tend to go isotropic without returning to their original configuration. However, for the gels made within an acidic and basic media the gels respond consistently, demonstrated that for this gel ([Bmim][Cl]) and this VOC particularly, changing the pH of the medium where the droplets are produced, leaded to an enhanced response on the e-nose.

Regarding the response of [Bmim][DCA] to Hexane, a slight difference on the basic gels pattern is noticeable. Nonetheless, no significant differences were noted on the e-nose responses to all tested VOCs, for all gels made with [Bmim][DCA] as surfactant.

Gels made with no surfactant showed inconsistent responses to Ethanol. None of the gels made within an aqueous medium responded to this VOC, only one of the replicas of the acidic and the basic medium gels exhibit responses. These were very similar, as predicted, considering that the pH does not affect these gels, since there is no surfactant to interact with the charged gelatine matrix.

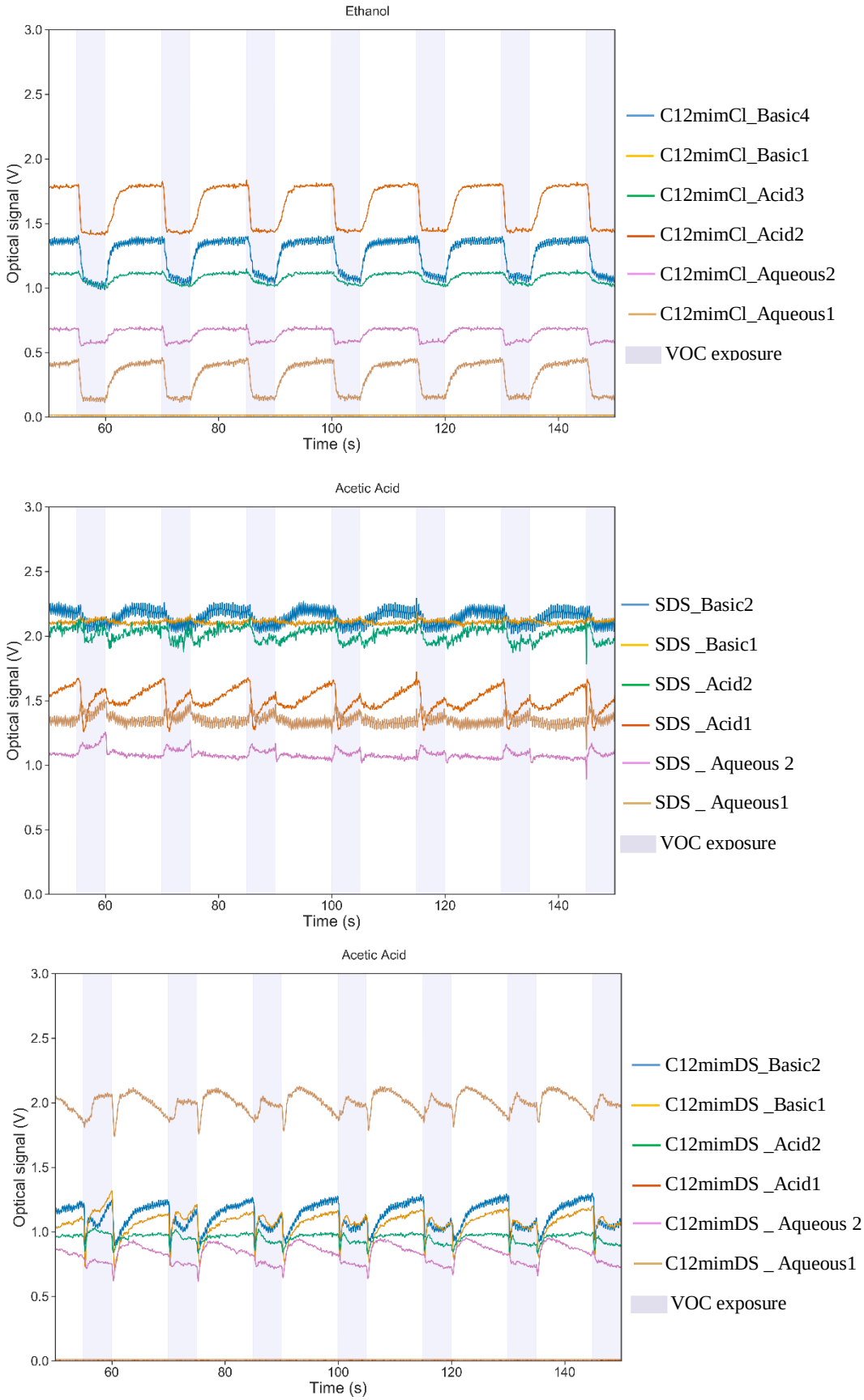

Figure 5.12. E-nose signals of Ethanol for gels with [C_{12}mim][Cl] and Acetic Acid, for gels with [C_{12}mim][DS] and SDS as surfactants

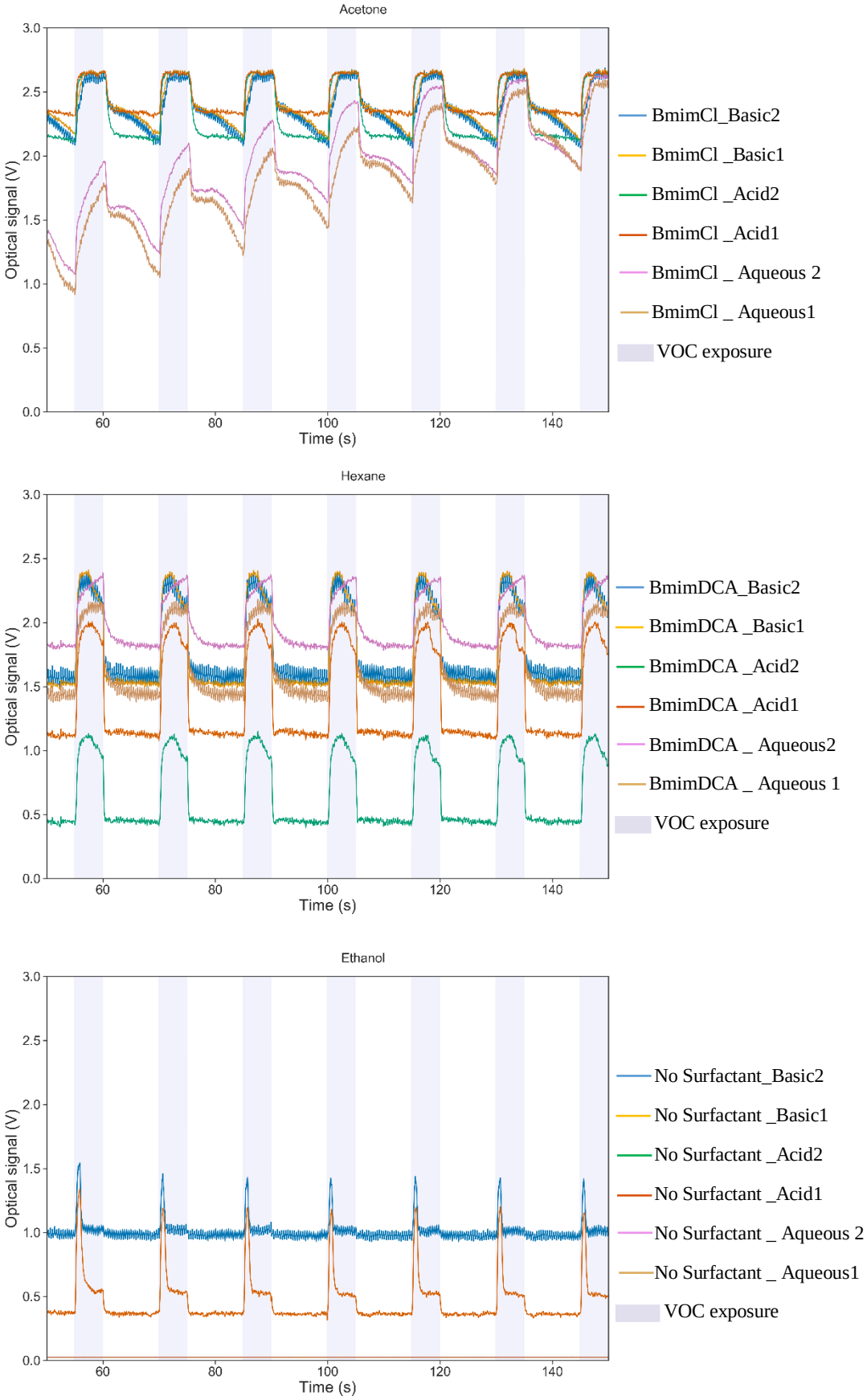

Figure 5.13. E-nose signals of Acetone for gels with [Bmim][Cl], Hexane for gels with [Bmim][DCA] and Ethanol for gels with no surfactant

Hence, observing the VOCs scores chart presented on appendix III – H 4) and 5)., it is evident that the [Bmim$^+$] ionic liquids, did not possess the same behaviour, as expected and previously exhibited on the previous Chapter, indicating incoherencies on the production method or not proper storage. Particularly for the [Bmim][Cl] surfactant, that exhibited more discrepancies with the former and with the current results presented on figure 5.13. and appendix III-G 4) and 5), for [Bmim][DCA], regardless of the morphological similarities. The basic buffer was the medium that demonstrated to have a greater influence and impact on the [Bmim$^+$]-LC-droplets, in fact figure 5.14. reveals the behaviour of the [Bmim][Cl]-LC-droplets, to Acetonitrile exposure, made within a basic medium, opposing the droplets of the same surfactant made within an aqueous medium in different days.

Observing the seven frames that illustrate the droplets behaviour to Acetonitrile exposure, it can be verified that the droplets made within a basic medium, are the only ones that transition completely into an isotropic state, revealing a greater instability in its configuration. Comparing pictures **ii)** and **iii)**, it is evident that the same protocol, with the same surfactant, may produce droplets, that although possess the same configuration, the size and behaviour might change. Nevertheless, on both cases, not all droplets transit to an isotropic state, in fact droplets on picture **iii)** do not turn isotropic at the same time, meaning there could be different layers where the droplets are positioned. This might have effects on the e-nose response, considering that the diffusion of light will not be the same throughout the entire gel.

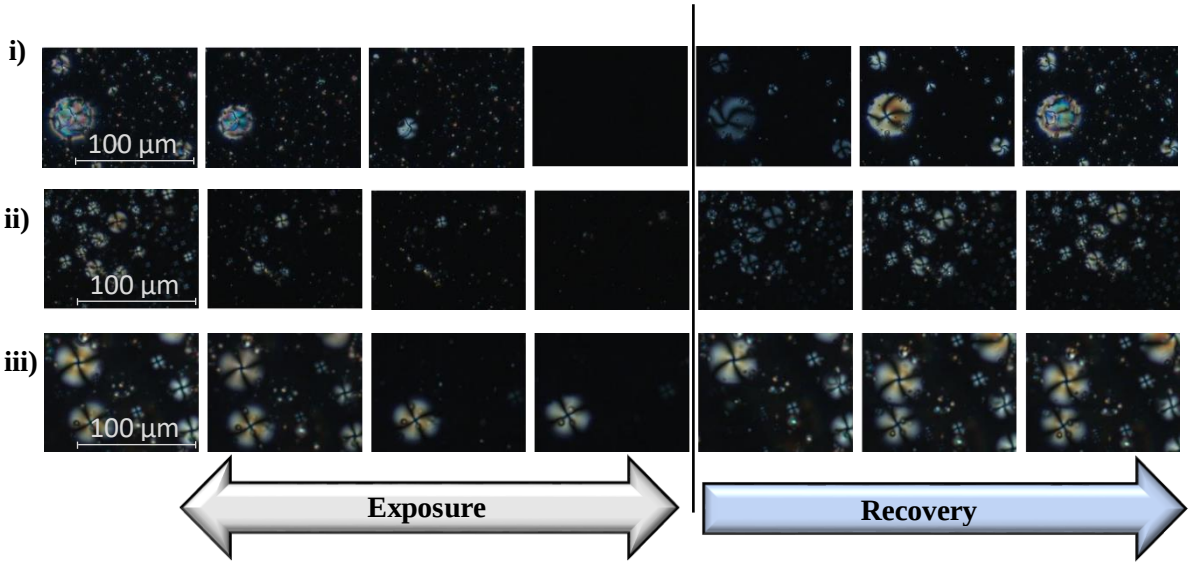

Figure 5.14. Behaviour of [Bmim][Cl]-LC-droplets, within a gelatine matrix, to Acetonitrile exposure: i) droplets formed within a Basic mean; ii) droplets formed on the same day as the droplets on i), within aqueous mean; iii) droplets formed within an aqueous mean, produced previously for the set of experiments performed on the previous Chapter. The exposure time is 5 seconds and the recovery time is 15 seconds. All images are in the same scale.

Notwithstanding, in all the presented cases the droplets return to their original configuration, not leaving the position where they are found.

Concerning the confusion matrices and the respective scores for the six cases tested, table 5.1., reveals the global scores obtained for each case. It is clear that the use of surfactants enhances the score of the sensors, particularly [Bmim][DCA], which was the surfactant with the highest score for all three production media, however, this was the only fully optimized gel.

Considering the best score for each surfactant, [Bmim][DCA] is followed by [C_{12}mim][Cl], SDS and [C_{12}mim][DS], that presented a best score above 80% and lastly is the [Bmim][Cl] with the best result being 80.67%. Regarding the no surfactant case, all the scores are similar, as it would be expected, since the pH showed no significant influence on the droplets and consequent behaviour on the e-nose.

Considering the pH effects on the global scores for each surfactant and starting with the [Bmim][DCA], the best result was achieved with the basic buffer, reaching the value of 95.33%. This could be the result of the change on the droplet configuration which could enhance the score result, however, the values obtained for the other production media are not significantly different, thus, it is not clear that this was the cause for the basic buffer being the best result.

Relatively to the [C_{12}mim][Cl], clearly the droplets produced within the aqueous medium, achieved a noticeable better score than the other media. Nonetheless, comparing this result with the score obtained on the previous Chapter, this is considerably a much superior value, thus implying that this discrepancy might be due to the production method.

[C_{12}mim][DS] and SDS revealed very similar results, although for different media, while SDS revealed a better score for aqueous medium and not a significant discrepancy for the other media, the [C_{12}mim][DS] demonstrated that the best result relies on the basic buffer as the medium.

Lastly for [Bmim][Cl] two media presented very similar results, the aqueous and the basic ones, it would be expected that the basic medium would reveal a superior result, from the droplet morphology analysis. It should be noted that, the enhanced score for [Bmim][DCA] might be the result from the droplet change of configuration with the pH, that was also observed on the [Bmim][Cl] droplets. Considering the similarities between these [$Bmim^+$] ionic liquids and the results obtained, if these experiments were replicated, there is a high probability for the basic medium to be the best result be for [Bmim][Cl]. Appendix III-H shows all the confusion matrices and scores, for all tested gels.

Table 5.1. Global Scores for all the gels with different surfactants and their respective media

Scores						
Medium/Surfactant	**[Bmim][Cl]**	**[Bmim][DCA]**	**[C_{12}mim][Cl]**	**[C_{12}mim][DS]**	**SDS**	**No Surfactant**
Acidic Buffer	73.42%	93.50%	70.58%	40.58%	72.17%	**79.70%**
Water	**80.67%**	93.25%	**87.08%**	76.83%	**84.42%**	79.10%
Basic Buffer	80.17%	**95.33%**	62.42%	**83.58%**	81.42%	68.00%

Figure 5.15. shows the tiles of before and after the exposure to the twelve VOCs tested, for [C_{12}mim][Cl] gels made within an aqueous medium and [Bmim][DCA] gels made within basic medium. These two gels were chosen due to the fact that the [C_{12}mim][Cl] gels were the ones that preserve most of their droplets configuration, position and size, thus, revealing high stability. Contrastingly, [Bmim][DCA] gels made within a basic medium, were the gels that revealed greater differences after VOCs exposure. Droplets changed their position, size and configuration. This reveals the low stability of the gels, due to the size of the surfactant and the effect of the pH, that induces non-table configurations. Appendix III-I shows the (before and after VOCs exposure) tiles for all tested gels.

[C_{12}mim][Cl] in Aqueous Mean

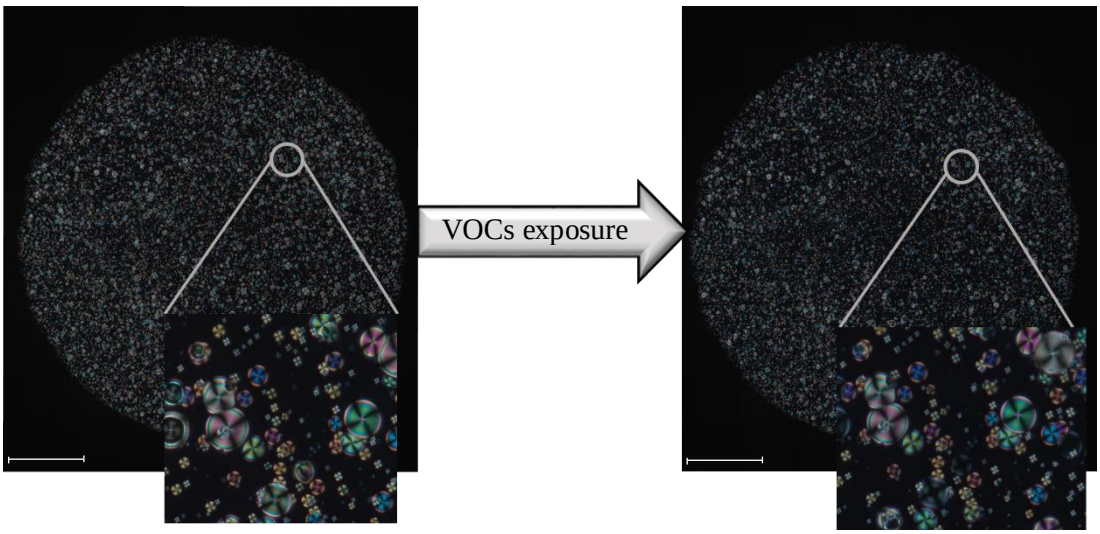

[Bmim][DCA] in Basic Mean

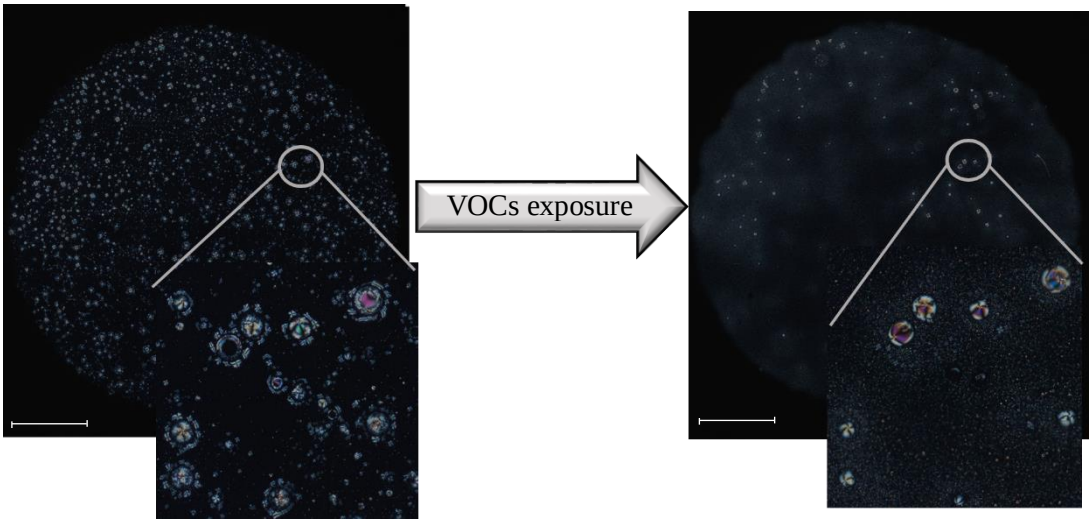

Figure 5.15. Tiles of [C12mim][Cl] and [Bmim][DCA] gels, before and after VOCs exposure. The scale bar represents 500 µm

Table 5.2. presents a summary of the most relevant features for all the tested gels (with different surfactants and pH media). Analysing the table (5.2.), it is possible to verify that, the pH effect is more noticeable on the morphology of the droplets. The most promising gels, appeared to be the [C_{12}mim][Cl] made within an aqueous or basic medium, since these presented greater stability and selectivity to VOCs exposure.

*Table 5.2. Relevant features for all gels tested with different surfactants and media, on a gelatine matrix. *Stability refers to the consistency of the gels after VOCs exposure and storage for 10 days, compared to the original state of the gels.*

Gel/Characteristic	Droplets Morphology	Droplet Size (+/- 11 µm)	Selectivety to VOCs	Stability*
[Bmim][DCA]				
Aqueous Medium	Radial	22.30	None	Low
Acidic Medium	Radial	21.83	None	Low
Basic Medium	Multi-defected structure	22.29	None	Low
[Bmim][Cl]				
Aqueous Medium	Radial	22.07	None	Low
Acidic Medium	Radial	20.24	None	Low
Basic Medium	Multi-defected structure	22.38	None	Low
[C_{12}mim][Cl]				
Aqueous Medium	Twisted-bipolar and radial	24.53	Yes	High
Acidic Medium	Radial	22.45	Yes	made Medium
Basic Medium	Super-twisted-bipolar and twisted-toroidal	22.68	Yes	High
SDS				
Aqueous Medium	Twisted-bipolar, radial and escaped radial	20.92	None	Medium
Acidic Medium	Escaped radial and bipolar	23.31	Yes	Medium
Basic Medium	Twisted-toroidal	23.88	Yes	Medium
[C_{12}mim][DS]				
Aqueous Medium	Twisted-toroidal and radial	25.28	Yes	Medium
Acidic Medium	Twisted-bipolar	22.51	Yes	Medium
Basic Medium	Super-twisted-bipolar, toroidal and bipolar	24.94	Yes	Medium
No Surfactant				
Aqueous Medium	Bipolar	22.85	None	Low
Acidic Medium	Bipolar	23.72	None	Low
Basic Medium	Bipolar	22.24	None	Low

5.2. Conclusions

On this Chapter, the effects of the variation of pH in the medium where the gels are produced were studied. The behaviour of some gels went according to the expectable, as discussed throughout this Chapter, however this was not the case for every gel, some revealed some inconsistencies and not expected behaviours, such as SDS within the basic buffer, among others.

Regarding the droplets morphology, all the gels were affected and thus, changed their configuration dependently on the pH of the medium where were produced, however the impact on the configuration variations was not the same in all the gels. [$Bmim^+$] ionic liquids, demonstrated to possess very similar behaviours, considering that they only differ on the counter ion, and as previously concluded on the previous Chapter, the counter ion does not appear to influence with significant impact the liquid crystal configuration and response on the sensing device. These surfactants demonstrated to be the most affected in terms of droplet configuration, presenting a drastic change from homeotropic anchoring with a radial configuration, to a planar anchoring with a multi-defected, or random director, configuration, increasing the instability of the droplets. However, considering the VOCs scores, appendix III – H, the most significant changes on the e-nose response are not attributed to these surfactants.

In general terms, the droplets produced within basic or acidic buffers, appear to possess more unstable configurations, which in some surfactants might be the cause for the increase of the global scores. Demonstrating that the pH will change the global charge of the gelatine matrix, thus, increasing the electrostatic interactions between the ionic surfactant surrounding the LC-droplet and the matrix, which will consequently, lead to variations on the droplets configurations and behaviour on the e-nose responses.

6. Final Remarks and Further Work

On this work two main studies regarding sensing gels made with liquid crystal droplets covered with a surfactant and immobilized on a biopolymeric matrix, were carried through. One of the studies concerned the effect of changing the surfactant itself, and the other study focused on the effect of the variation of the pH on the medium where the gels (where the droplets were produced). Within these studies, two subjects were approached, the morphology of the droplets and the gels response on a gas sensing device (e-nose).

The main conclusions of the work were the following: changing the surfactant that covers the LC-droplet possess a highly significant effect and impact on the droplet configuration, including increasing the stability and leading to noticeable changes on the sensors response, enhancing the selectivity of longer chained tail surfactants. Concerning the pH effect, in terms of droplet configuration, this was more noticeable on shorted tailed surfactants, contrasting with the effects on the e-nose response that were more perceptible on longer tailed surfactants. Nonetheless, in all the surfactants, effects were noted both regarding the morphology of the droplets and the e-nose responses, however the effect on the droplet configuration was more evident.

Throughout this work, some inconsistencies on surfactants response were noted, regarding the morphology of the droplets as well as the e-nose responses. These might be due to several factors, such as the environmental conditions, e-nose electrical issues, inappropriate models employed to analyse the e-nose signals. However, the main problem remains on the inaccurate production method, that leads to numerous inconsistencies and incoherencies on the final result of the gels.

A method that can help solving this imminent problem is called microfluidics. Focusing on the droplet production, microfluidics consists on the manipulation of every component present in the LC droplet within the micro channels, that are designed accordingly to the pretended purpose, in which the droplets are produced. It should be mentioned that this is a continuous process and the droplets production is achieved through laminar flow, thus the size of the droplets can be controlled and design accordingly. Hence, microfluidics presents new possibilities of control, manipulation and monitoring over the concentrations, the environmental changes, the location and time where components combine with each other [84], [120]–[123].

Thus, microfluidics should be explored and applied, in order to increase the accuracy of the droplets production.

Hence, some microfluidics masks were designed with the help of the software Autodesk *AutoCad* 2019 and can be observed on figure 6.1. Focusing on picture a) it can be seen on a closer detail, the flow focusing part of the mask, on this section of the mask, the droplets are formed and

separated from each other acquiring the proper shape of droplets, due to the suddenly increase of size of the channel leading to a disruption on the previous mixture. Picture b) exhibits a closer image of the serpentine, this allows the droplets to pass slower throughout the channel, thus avoiding coalescence and allowing a better observation of the process under the microscope.

As future work, optimization of the long length alkyl chain surfactants and the implementation of the microfluidics technique should be the priority, in order to proper compare the response of the gels and analyse the results without so many inconsistencies.

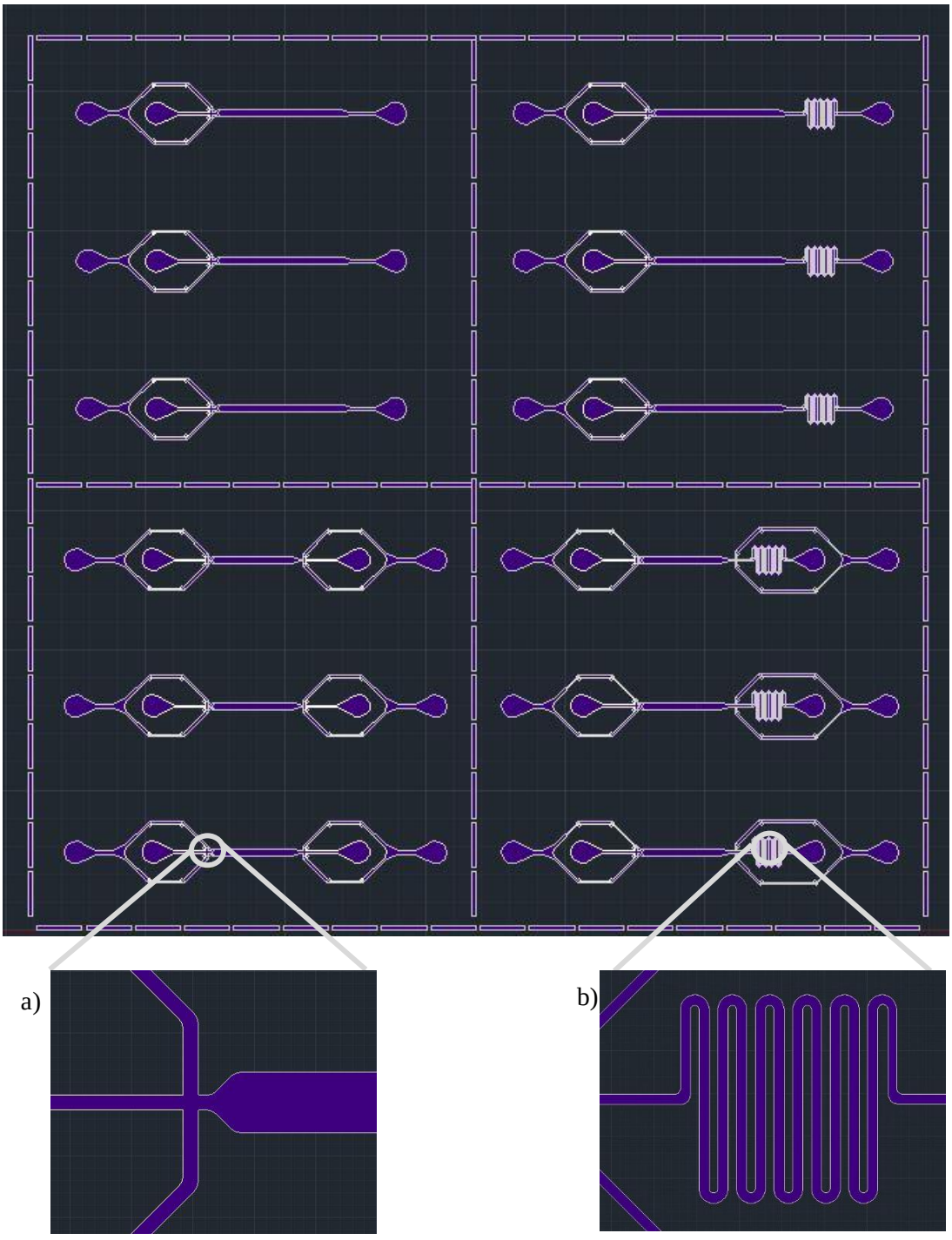

Figure 6.1. Microfluidics Masks; a) with zoom on the flow focusing part; b) zoom on the serpentine

7. Bibliography

[1] T. C. Pearce, S. S. Shiffman, H. T. Nagel, and J. W. Gardner, *Handbook of Machine Olfaction*. WILEY-VCH Verlag GmbH & Co. KGaA, 2003.

[2] H. K. Patel, R. H. Austin, and J. Barber, *The Electronic Nose: Artificial Olfaction Technology*. 2014.

[3] F. Röck, N. Barsan, and U. Weimar, "Electronic nose: Current status and future trends," *Chem. Rev.*, vol. 108, no. 2, pp. 705–725, 2008.

[4] J. E. Fitzgerald, E. T. H. Bui, N. M. Simon, and H. Fenniri, "Artificial Nose Technology: Status and Prospects in Diagnostics," *Trends Biotechnol.*, vol. 35, no. 1, pp. 33–42, 2017.

[5] A. D. Wilson and M. Baietto, "Applications and Advances in Electronic-Nose Technologies," *Sensors*, vol. 9, no. 7, pp. 5099–5148, 2009.

[6] K. Arshak, E. Moore, G. M. Lyons, J. Harris, and S. Clifford, *A review of gas sensors employed in electronic nose applications*, vol. 24, no. 2. 2004.

[7] E. A. Baldwin, J. Bai, A. Plotto, and S. Dea, "Electronic noses and tongues: Applications for the food and pharmaceutical industries," *Sensors*, vol. 11, no. 5, pp. 4744–4766, 2011.

[8] D. Hodgins, "The 'Electronic Nose' Using Conducting Polymer Sensors," *Sens. Rev.*, vol. 14, no. 4, pp. 28–31, 1994.

[9] "No Title." [Online]. Available: https://www.epa.gov/. [Accessed: 01-Mar-2019].

[10] X. Fu, "Indoor Microbial Volatile Organic Compound (MVOC) Levels and Associations with Repiratory Health, Sick Building Syndrome (SBS), and Allergy," in *Environmental Mycology in Public Health*, Academic Press, 2016, pp. 387–395.

[11] A. D. Wilson, "Application of electronic-nose technologies and VOC-biomarkers for the noninvasive early diagnosis of gastrointestinal diseases," *Sensors (Switzerland)*, vol. 18, no. 8, 2018.

[12] A. Amann and D. Smith, *Volatile Biomarkers: Non-Invasive Diagnosis in Physiology and Medicine*. Elsevier, 2013.

[13] H. Costa, "Sensing humidity with multicomponent hybrid gel films and characterization of an optimized gas delivery system," Faculdade de Ciências e Tecnologias da

Universidade Nova de Lisboa, 2018.

[14] C. Alves, “Signal processing and automatic classification tools in the development of a new opto-electronic nose,” Faculdade de Ciências e Tecnologias da Universidade Nova de Lisboa, 2018.

[15] A. C. Roque, H. Gamboa, A. Carolina Pádua, J. Gruber, and S. Palma, “Design and Evolution of an Opto-electronic Device for VOCs Detection,” vol. 1, no. Biostec, pp. 48–55, 2018.

[16] A. Rehman and X. Zeng, “Methods and approaches of utilizing ionic liquids as gas sensing materials,” *RSC Adv.*, vol. 5, no. 72, pp. 58371–58392, 2015.

[17] “Global Electronic Nose Market Research and Forecast 2018-2023.” [Online]. Available: https://www.omrglobal.com/industry-reports/electronic-nose-market/. [Accessed: 26-Oct-2018].

[18] “Global Electrnic Nose Market Research and Forecast 2018-2023,” 2018. [Online]. Available: https://www.researchandmarkets.com/reports/4585997/global-electronic-nose-market-research-and. [Accessed: 26-Oct-2018].

[19] “Global Electronic Nose Market Research and Forecast 2018-2023,” 2018. [Online]. Available: https://www.wiseguyreports.com/reports/3271386-global-electronic-nose-market-research-and-forecast-2018-2023.

[20] “Global Electronic Nose (E-Nose) Market to Surpass US$ 42.7 Million by 2025 - Coherent Market Insights,” 2018. [Online]. Available: https://globenewswire.com/news-release/2018/06/11/1519708/0/en/Global-Electronic-Nose-E-Nose-Market-to-Surpass-US-42-7-Million-by-2025-Coherent-Market-Insights.html. [Accessed: 26-Oct-2018].

[21] A. Hussain *et al.*, “Tunable Gas Sensing Gels by Cooperative Assembly,” *Adv. Funct. Mater.*, vol. 27, no. 27, pp. 1–9, 2017.

[22] T. Cosgrove, *Colloid Science Principles , Methods and Applications*, Second Ed. Bristol, UK: Wiley, 2010.

[23] P. J. Collings and M. Hird, *Introduction to Liquid Crystals*. Taylor & Francis, 2009.

[24] D. Andrienko, “Introduction to liquid crystals,” *J. Mol. Liq.*, vol. 267, pp. 520–541, 2018.

[25] S. Singh, *Liquid crystals: Fundamentals*. World Scientific Publishing Co. Pte. Ltd., 2002.

[26] S. Verlag and G. Meier, *Applications of Liquid Crystals*. 1975.

[27] Y. Dogishi, S. Endo, W. Y. Sohn, and K. Katayama, "Formation of photo-responsive liquid crystalline emulsion by using microfluidics device," *Entropy*, vol. 19, no. 12, pp. 1–8, 2017.

[28] S. J. Woltman, G. P. Crawford, and G. D. Jay, *Liquid Crystals: Frontiers in Biomedical Applications*. World Scientific Publishing Co. Pte. Ltd., 2007.

[29] D. Demus, J. Goodby, G. W. Gray, H. W. Spiess, and V. Vill, *Handbook of Liquid Crystals*. WILEY-VCH Verlag GmbH, 1998.

[30] S. Singh, *Liquid crystals: Fundamentals*. World Scientific Publishing Co. Pte. Ltd., 2002.

[31] X. Wang, "Phases of Liquid Crystals."

[32] D. Andrienko, "Introduction to liquid crystals," *J. Mol. Liq.*, vol. 267, pp. 520–541, 2018.

[33] Y.-C. Hsiao, Y.-C. Sung, M.-J. Lee, and W. Lee, "Highly sensitive color-indicating and quantitative biosensor based on cholesteric liquid crystal," *Biomed. Opt. Express*, vol. 6, no. 12, p. 5033, 2015.

[34] T. T. Nguyen, G. R. Han, C. H. Jang, and H. Ju, "Optical birefringence of liquid crystals for label-free optical biosensing diagnosis," *Int. J. Nanomedicine*, vol. 10, pp. 25–32, 2015.

[35] L. Zhou, Q. Kang, O. Hu, and L. Yu, "Ultrasensitive detection of glutathione based on liquid crystals in the presence of γ-glutamyl transpeptidase," *Anal. Chim. Acta*, pp. 1–9, 2018.

[36] Z. Hussain, F. Qazi, M. I. Ahmed, A. Usman, A. Riaz, and A. D. Abbasi, "Liquid crystals based sensing platform-technological aspects," *Biosens. Bioelectron.*, vol. 85, pp. 110–127, 2016.

[37] S. J. Woltman, G. D. Jay, and G. P. Crawford, "Liquid-crystal materials find a new order in biomedical applications," *Nat. Mater.*, vol. 6, no. 12, pp. 929–938, 2007.

[38] K. J. Kek, J. J. Z. Lee, Y. Otono, and S. Ishihara, "Chemical gas sensors using chiral nematic liquid crystals and its applications," *J. Soc. Inf. Disp.*, vol. 25, no. 6, pp. 366–373, 2017.

[39] H. J. Kim, J. Rim, and C.-H. Jang, "Liquid-Crystal-Based Immunosensor for Diagnosis

of Tuberculosis in Clinical Specimens," *ACS Appl. Mater. Interfaces*, vol. 9, no. 25, pp. 21209–21215, 2017.

[40] P. V. Shibaev, M. Wenzlick, J. Murray, A. Tantillo, and J. Howard-Jennings, "Rebirth of liquid crystals for sensoric applications: Environmental and gas sensors," *Adv. Condens. Matter Phys.*, vol. 2015, 2015.

[41] R. J. Carlton *et al.*, "Chemical and biological sensing using liquid crystals," *Liq. Cryst. Rev.*, vol. 1, no. 1, pp. 29–51, 2013.

[42] F. He, H. Liu, X. Xiong, and S. Zhai, "Nematic Liquid Crystal Reorientation at Aqueous-LC Interface for Monitoring Biochemical Interactions by Specific Ions Effects," vol. 1, no. 1, pp. 35–51, 2018.

[43] N. A. Smirnova, A. A. Vanin, E. A. Safonova, I. B. Pukinsky, Y. A. Anufrikov, and A. L. Makarov, "Self-assembly in aqueous solutions of imidazolium ionic liquids and their mixtures with an anionic surfactant," *J. Colloid Interface Sci.*, vol. 336, no. 2, pp. 793–802, 2009.

[44] H. Ono, H. Shimokawa, A. Emoto, and N. Kawatsuki, "Effects of droplet size on photorefractive properties of polymer dispersed liquid crystals," *Polymer (Guildf).*, vol. 44, no. 26, pp. 7971–7978, 2003.

[45] M. Radian-Guenebaud and P. Sixou, "Droplet Size Effects in Polymer Dispersed Nematic Chiral Liquid Crystal Materials," *Mol. Cryst. Liq. Cryst. Sci. Technol. Sect. A. Mol. Cryst. Liq. Cryst.*, vol. 220, no. 1, pp. 53–62, 1992.

[46] X. Wang, E. Bukusoglu, and N. L. Abbott, "A practical guide to the preparation of liquid crystal-templated microparticles," *Chem. Mater.*, vol. 29, no. 1, pp. 53–61, 2017.

[47] P. Brown *et al.*, "Anionic surfactant ionic liquids with 1-Butyl-3-methyl-imidazolium cations: Characterization and application," *Langmuir*, vol. 28, no. 5, pp. 2502–2509, 2012.

[48] I. Instabilities, *Polymers, Liquids and Colloids in Electric Fields: Interfacial Instabilites, Orientation and Phase Transitions*. World Scientific Publishing Co. Pte. Ltd., 2009.

[49] D. Myers, *SURFACTANT SCIENCE AND TECHNOLOGY SURFACTANT SCIENCE*, Third. Wiley, John, 2006.

[50] T. Chakraborty, I. Chakraborty, and S. Ghosh, "The methods of determination of critical micellar concentrations of the amphiphilic systems in aqueous medium," *Arab. J. Chem.*, vol. 4, no. 3, pp. 265–270, 2011.

[51] I. D. Robb, *Specialist Surfactants*. Blackie Academic & Professional, 1997.

[52] B. Kronberg, "Surfactant mixtures," *Curr. Opin. Colloid Interface Sci.*, vol. 2, no. 5, pp. 456–463, 1997.

[53] "Critical micelle concentration (CMC) and surfactant concentration." [Online]. Available: https://www.kruss-scientific.com/services/education-theory/glossary/critical-micelle-concentration-cmc-and-surfactant-concentration/. [Accessed: 23-Oct-2018].

[54] M. Chaplin, "Water Structure and Science." [Online]. Available: http://www1.lsbu.ac.uk/water/kosmotropes_chaotropes.html. [Accessed: 08-Feb-2019].

[55] A. Pal and S. Chaudhary, "Ionic liquids effect on critical micelle concentration of SDS: Conductivity, fluorescence and NMR studies," *Fluid Phase Equilib.*, vol. 372, pp. 100–104, 2014.

[56] P. Ball and J. E. Hallsworth, "Water structure and chaotropicity: their uses, abuses and biological implications," *Phys. Chem. Chem. Phys.*, vol. 17, pp. 8297–8305, 2015.

[57] Y. Marcus, "Effect of Ions on the Structure of Water : Structure Making and Breaking," pp. 1346–1370, 2009.

[58] H. Zhao, "Are ionic liquids kosmotropic or chaotropic ? An evaluation of available thermodynamic parameters for quantifying the ion kosmotropicity of ionic liquids," vol. 891, no. August 2005, pp. 877–891, 2006.

[59] A. Cryst, "Charge Densities of Selected Ions," pp. 13–15, 1976.

[60] M. Chaplin, "Water Structure and Science." .

[61] S. Zhang and J. Wang, *Structures and Interactions of Ionic Liquids*, vol. 151. 2014.

[62] S. T. Handy, *IONIC LIQUIDS – CLASSES AND PROPERTIES*. IntechOpen, 2011.

[63] H. Ohno, *Electrochemical Aspects of Ionic Liquids*. Wiley, John, 2005.

[64] N. A. Smirnova and E. A. Safonova, "Ionic Liquids as Surfactants 1," vol. 84, no. 10, pp. 1695–1704, 2010.

[65] V. B. A. De Meijere, K. N. H. H. Kessler, J. L. S. V Ley, M. O. S. Schreiber, B. M. T. P. Vogel, and F. V. H. Wong, *Topics in Current Chemistry*. 2010.

[66] S. Zhang, X. Lu, Q. Zhou, X. Li, X. Zhang, and S. Li, *Ionic Liquids: Physicochemical Properties*, First. Elsevier, 2009.

[67] Z. Q. Tan, J. F. Liu, and L. Pang, "Advances in analytical chemistry using the unique

properties of ionic liquids," *TrAC - Trends Anal. Chem.*, vol. 39, pp. 218–227, 2012.

[68] P. Brown *et al.*, "Anionic Surfactants and Surfactant Ionic Liquids with Quaternary Ammonium Counterions," *Langmuir*, vol. 27, pp. 4563–4571, 2011.

[69] E. Andrzejewska, A. Marcinkowska, and A. Zgrzeba, "Ionogels – materials containing immobilized ionic liquids *)," no. 5, pp. 344–352, 2017.

[70] K. S. Rao, P. Bharmoria, and T. J. Trivedi, "Self - Assembly of Surface - Active Ionic Liquids in Aqueous Medium," 2015.

[71] L. C. Peng, C. H. Liu, C. C. Kwan, and K. F. Huang, "Optimization of water-in-oil nanoemulsions by mixed surfactants," *Colloids Surfaces A Physicochem. Eng. Asp.*, vol. 370, no. 1–3, pp. 136–142, 2010.

[72] R. Nagarajan, "Mixed Surfactant Systems," *ACS Symp. Ser.*, vol. 501, pp. 54–95, 1992.

[73] C. Priest, A. Quinn, A. Postma, A. N. Zelikin, J. Ralston, and F. Caruso, "Microfluidic polymer multilayer adsorption on liquid crystal droplets for microcapsule synthesis," *Lab Chip*, vol. 8, no. 12, pp. 2182–2187, 2008.

[74] E. Enz and J. Lagerwall, "Electrospun microfibres with temperature sensitive iridescence from encapsulated cholesteric liquid crystal," *J. Mater. Chem.*, vol. 20, no. 33, pp. 6866–6872, 2010.

[75] J. Kim, M. Khan, and S. Y. Park, "Glucose sensor using liquid-crystal droplets made by microfluidics," *ACS Appl. Mater. Interfaces*, vol. 5, no. 24, pp. 13135–13139, 2013.

[76] D. M. Lynn, N. L. Abbott, Y. M. Zayas-Gonzalez, U. Manna, and R. J. Carlton, "Surfactant-Induced Ordering and Wetting Transitions of Droplets of Thermotropic Liquid Crystals 'Caged' Inside Partially Filled Polymeric Capsules," *Langmuir*, vol. 30, no. 49, pp. 14944–14953, 2014.

[77] Y. Geng, J. Noh, I. Drevensek-Olenik, R. Rupp, G. Lenzini, and J. P. F. Lagerwall, "High-fidelity spherical cholesteric liquid crystal Bragg reflectors generating unclonable patterns for secure authentication," *Sci. Rep.*, vol. 6, no. May, pp. 2–10, 2016.

[78] H. G. Lee, S. Munir, and S. Y. Park, "Cholesteric Liquid Crystal Droplets for Biosensors," *ACS Appl. Mater. Interfaces*, vol. 8, no. 39, pp. 26407–26417, 2016.

[79] S. S. Lee, H. J. Seo, Y. H. Kim, and S. H. Kim, "Structural Color Palettes of Core–Shell Photonic Ink Capsules Containing Cholesteric Liquid Crystals," *Adv. Mater.*, vol. 29, no. 23, pp. 1–8, 2017.

[80] L. Yang, M. Khan, and S. Y. Park, “Liquid crystal droplets functionalized with charged surfactant and polyelectrolyte for non-specific protein detection,” *RSC Adv.*, vol. 5, no. 118, pp. 97264–97271, 2015.

[81] W. Khan, J. H. Choi, G. M. Kim, and S. Y. Park, “Microfluidic formation of pH responsive 5CB droplets decorated with PAA-b-LCP,” *Lab Chip*, vol. 11, no. 20, pp. 3493–3498, 2011.

[82] J. H. Noh, K. Reguengo De Sousa, and J. P. F. Lagerwall, “Influence of interface stabilisers and surrounding aqueous phases on nematic liquid crystal shells,” *Soft Matter*, vol. 12, no. 2, pp. 367–372, 2015.

[83] H. L. Liang, S. Schymura, P. Rudquist, and J. Lagerwall, “Nematic-smectic transition under confinement in liquid crystalline colloidal shells,” *Phys. Rev. Lett.*, vol. 106, no. 24, pp. 1–4, 2011.

[84] D. E. Lucchetta, F. Simoni, P. Pagliusi, and G. Cipparrone, “Polymer stabilized Monodispersed Liquid Crystal Droplets: Microfluidics Generation and Optical Analysis,” *Opt. Data Process. Storage*, vol. 1, no. 1, pp. 16–21, 2015.

[85] J. H. Jang and S. Y. Park, “pH-responsive cholesteric liquid crystal double emulsion droplets prepared by microfluidics,” *Sensors Actuators, B Chem.*, vol. 241, pp. 636–643, 2017.

[86] Y. Li *et al.*, “Colloidal cholesteric liquid crystal in spherical confinement,” *Nat. Commun.*, vol. 7, 2016.

[87] S. Xu *et al.*, “Generation of monodisperse particles by using microfluidics: Control over size, shape, and composition,” *Angew. Chemie - Int. Ed.*, vol. 44, no. 5, pp. 724–728, 2005.

[88] Y. D. Jung, M. Khan, and S. Y. Park, “Fabrication of temperature- and pH-sensitive liquid-crystal droplets with PNIPAM-b-LCP and SDS coatings by microfluidics,” *J. Mater. Chem. B*, vol. 2, no. 30, pp. 4922–4928, 2014.

[89] L. Mei *et al.*, “A Simple Capillary-based Open Microfluidic Device for Size On-demand High-throughput Droplet/Bubble/Microcapsule Generation,” *Lab Chip*, pp. 2806–2815, 2018.

[90] J. Noh, B. Henx, and J. P. F. Lagerwall, “Taming Liquid Crystal Self-Assembly: The Multifaceted Response of Nematic and Smectic Shells to Polymerization,” *Adv. Mater.*, vol. 28, no. 46, pp. 10170–10174, 2016.

[91] X. Wang *et al.*, "Patterned surface anchoring of nematic droplets at miscible liquid-liquid interfaces," *Soft Matter*, vol. 13, no. 34, pp. 5714–5723, 2017.

[92] C. Schröder, "Proteins in Ionic Liquids: Current Status of Experiments and Simulations," *Top. Curr. Chem.*, vol. 375, no. 2, 2017.

[93] S. M. Murray, T. K. Zimlich, A. Mirjafari, R. A. O'Brien, J. H. Davis, and K. N. West, "Thermophysical properties of imidazolium-based lipidic ionic liquids," *J. Chem. Eng. Data*, vol. 58, no. 6, pp. 1516–1522, 2013.

[94] J. C. Thermodynamics, T. Singh, and A. Kumar, "Thermodynamics of dilute aqueous solutions of imidazolium based ionic liquids," *J. Chem. Thermodyn.*, vol. 43, no. 6, pp. 958–965, 2011.

[95] M. Fountoulakis and B. Takács, "Effect of strong detergents and chaotropes on the detection of proteins in two-dimensional gels," *Electrophoresis*, vol. 22, no. 9, pp. 1593–1602, 2001.

[96] M. Blesic, M. H. Marques, N. V. Plechkova, K. R. Seddon, L. P. N. Rebelo, and A. Lopes, "Self-aggregation of ionic liquids: Micelle formation in aqueous solution," *Green Chem.*, vol. 9, no. 5, pp. 481–490, 2007.

[97] G. Toquer, G. Porte, M. Nobili, J. Appell, and C. Blanc, "Lyotropic structures in a thermotropic liquid crystal," *Langmuir*, vol. 23, no. 7, pp. 4081–4087, 2007.

[98] X. Zhang, Y. Meng, Y. Tian, Y. Guo, X. Qiao, and S. Yang, "Boundary layer viscosity of CNT-doped liquid crystals: effects of phase behavior," *Rheol. Acta*, vol. 52, no. 10–12, pp. 939–947, 2013.

[99] O. O. Prishchepa, V. Y. Zyryanov, A. P. Gardymova, and V. F. Shabanov, "Optical textures and orientational structures of nematic and cholesteric droplets with heterogeneous boundary conditions," *Mol. Cryst. Liq. Cryst.*, vol. 489, no. September 2014, 2008.

[100] B. C. van Zuiden *et al.*, "Stable nematic droplets with handles," *Proc. Natl. Acad. Sci.*, vol. 110, no. 23, pp. 9295–9300, 2013.

[101] A. Fernández-Nieves, D. R. Link, M. Márquez, and D. A. Weitz, "Topological changes in bipolar nematic droplets under flow," *Phys. Rev. Lett.*, vol. 98, no. 8, 2007.

[102] O. O. Prishchepa, A. V. Shabanov, and V. Y. Zyryanov, "Director configurations in nematic droplets with inhomogeneous boundary conditions," *Phys. Rev. E - Stat. Nonlinear, Soft Matter Phys.*, vol. 72, no. 3, 2005.

[103] W. Rasband, “ImageJ version 1.52i.” National Institutes of Health, USA, 2018.

[104] J. Brownlee, “What is a Confusion Matrix in Machine Learning.” [Online]. Available: https://machinelearningmastery.com/confusion-matrix-machine-learning/. [Accessed: 20-Feb-2019].

[105] M. Obi, S. Morino, and K. Ichimura, “Factors affecting photoalignment of liquid crystals induced by polymethacrylates with coumarin side chains,” *Chem. Mater.*, vol. 11, no. 3, pp. 656–664, 1999.

[106] R. Kaur, G. K. Bhullar, N. V. S. Rao, and K. K. Raina, “Effect of pH on the control of molecular orientation in monolayer of bent-core liquid crystal materials by Langmuir–Blodgett method,” *Liq. Cryst.*, vol. 42, no. 1, pp. 8–17, 2015.

[107] H. F. Gleeson, R. J. Miller, L. Tian, V. Görtz, and J. W. Goodby, “Liquid crystal blue phases: stability, field effects and alignment,” *Liq. Cryst.*, vol. 42, no. 5–6, pp. 760–771, 2015.

[108] H. C. Lin, C. H. Wang, J. K. Wang, and S. F. Tsai, “Fast response and spontaneous alignment in liquid crystals doped with 12-hydroxystearic acid gelators,” *Materials (Basel).*, vol. 11, no. 5, 2018.

[109] D. S. Miller and N. L. Abbott, “Influence of droplet size, pH and ionic strength on endotoxin-triggered ordering transitions in liquid crystalline droplets,” *Soft Matter*, vol. 9, no. 2, pp. 374–382, 2013.

[110] B. Zeeb, A. H. Saberi, J. Weissa, and D. J. McClements, “Retention and release of oil-in-water emulsions from filled hydrogel beads composed of calcium alginate: impact of emulsifier type and pH,” *Soft*, vol. 11, p. 18, 2015.

[111] “Polyelectrolytes.” [Online]. Available: https://polymerdatabase.com/polymer classes/Polyelectrolyte type.html. [Accessed: 13-Feb-2019].

[112] L. Yang, M. Khan, and S. Y. Park, “Liquid crystal droplets functionalized with charged surfactant and polyelectrolyte for non-specific protein detection,” *RSC Adv.*, vol. 5, no. 118, pp. 97264–97271, 2015.

[113] D. Wang, S. Y. Park, and I. K. Kang, “Liquid crystals: Emerging materials for use in real-time detection applications,” *J. Mater. Chem. C*, vol. 3, no. 35, pp. 9038–9047, 2015.

[114] S. C. Moldoveanu and V. David, *Essentials in Modern HPLC Separations*. Elsevier, 2013.

[115] C. Blei, C. Farrugia, J. Mifsud, A. Pharma, and E. Sinagra, “Potentiometric Studies on Gelatin Solutions and Gelatin Nanoparticles Dispersions,” no. January 2014, 2004.

[116] (Members of the GMIA), *Gelatin Handbook*. Gelatin Manufacturers Istitute of America (GMIA), 2012.

[117] “Isoelectric Point.” [Online]. Available: https://www.revolvy.com/page/Isoelectric point. [Accessed: 15-Jan-2019].

[118] D. S. Miller, X. Wang, J. Buchen, O. D. Lavrentovich, and N. L. Abbott, “Analysis of the internal configurations of droplets of liquid crystal using flow cytometry,” *Anal. Chem.*, vol. 85, no. 21, pp. 10296–10303, 2013.

[119] “Chemical Book,” 2016. [Online]. Available: https://www.chemicalbook.com/ChemicalProductProperty_EN_CB5114025.htm. [Accessed: 02-Feb-2019].

[120] G. M. Whitesides, “The origins and the future of microfluidics,” *Nature*, vol. 442, no. 7101, pp. 368–373, 2006.

[121] D. T. Chiu *et al.*, “Small but Perfectly Formed? Successes, Challenges, and Opportunities for Microfluidics in the Chemical and Biological Sciences,” *Chem*, vol. 2, no. 2, pp. 201–223, 2017.

[122] L. Shang, Y. Cheng, and Y. Zhao, “Emerging Droplet Microfluidics,” *Chem. Rev.*, vol. 117, no. 12, pp. 7964–8040, 2017.

[123] G. F. Christopher and S. L. Anna, “Microfluidic methods for generating continuous droplet streams,” *J. Phys. D. Appl. Phys.*, vol. 40, no. 19, 2007.

Appendixes

Appendix I

A - Results from H^1-NMR for the synthesis of $[C_{12}mim][DS]$

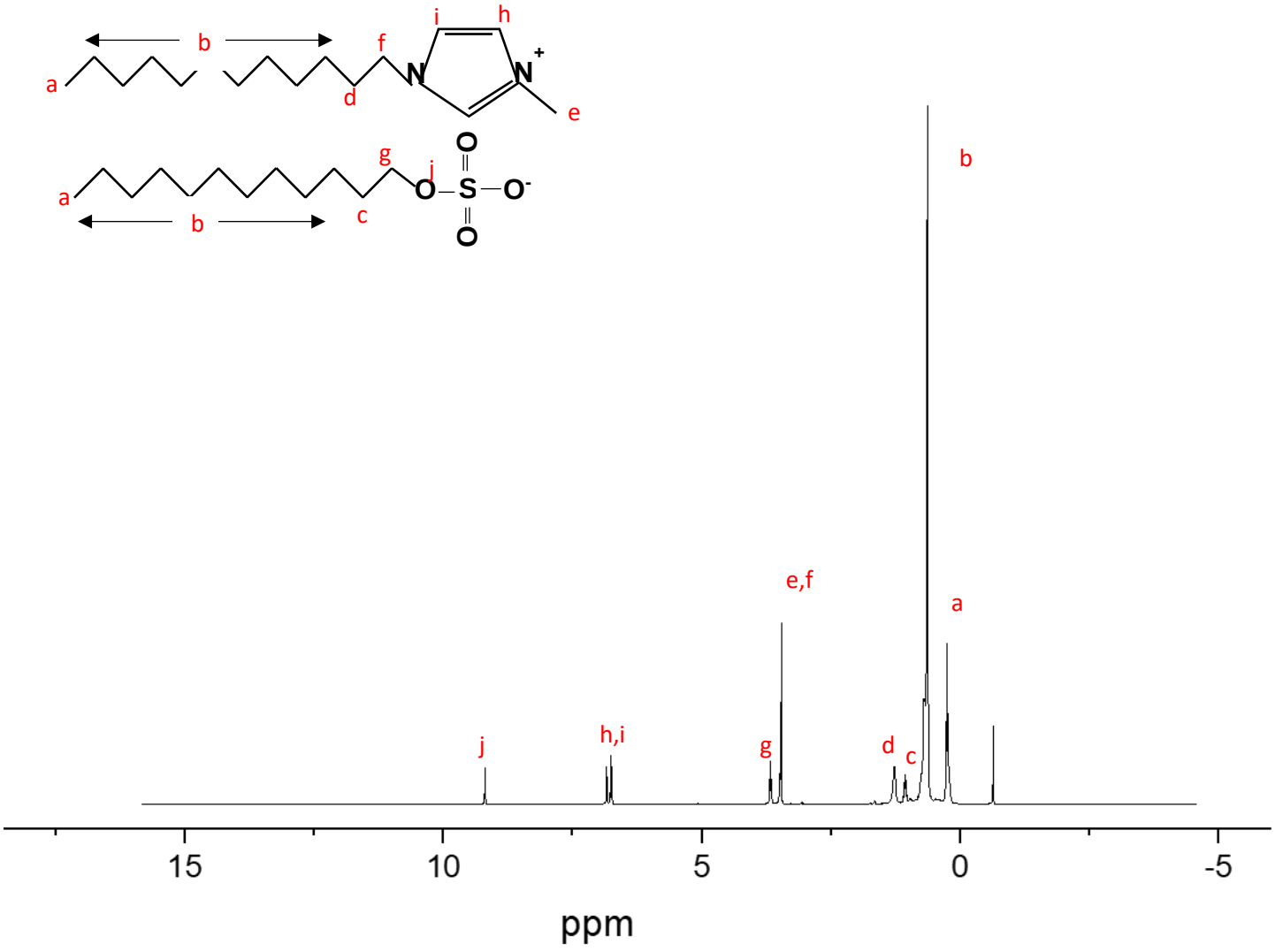

Figure 0.1. H^1-NMR Spectrum of the synthesis of $[C_{12}mim][DS]$

Appendix II – Chapter 4

A - SDS experimental trials

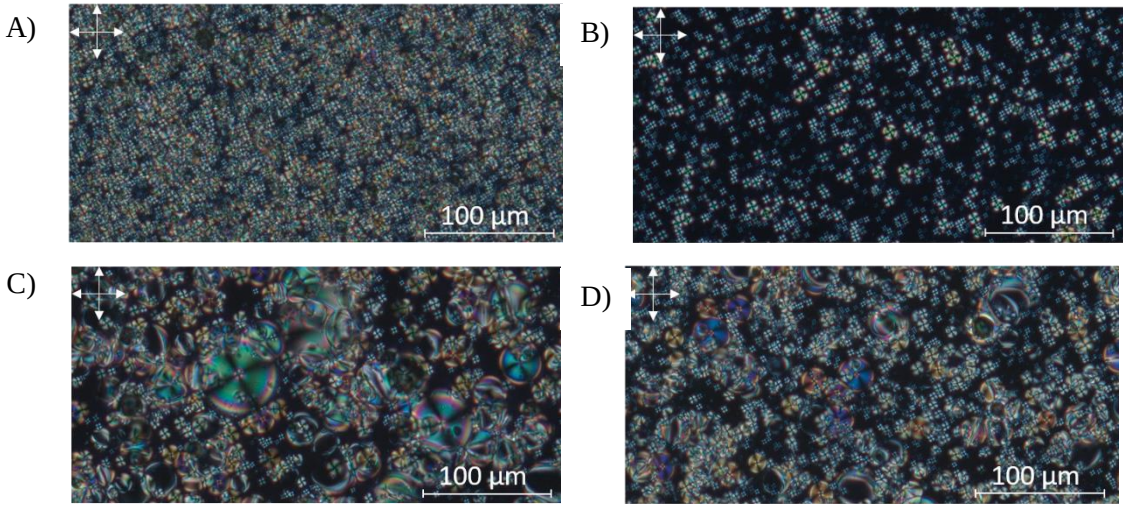

Figure 0.2. Experimental trials with the addition of 5CB to create 5CB-SDS droplets with water as mean: A) 500uL of water and 5CB stayed 30 min in agitation with the mixture; B) 400uL of water and 5CB stayed for 30 min in agitation with the mixture; C) 350uL of Water and 5CB stayed 12 min in agitation with the mixture; D) 300uL of water and 5CB stayed 15 min in agitation with the mixture

B – Gel Figures to the analysis of the droplet size and Mean Gray Value

1) [C_{12}mim][Cl]

Aqueous Medium

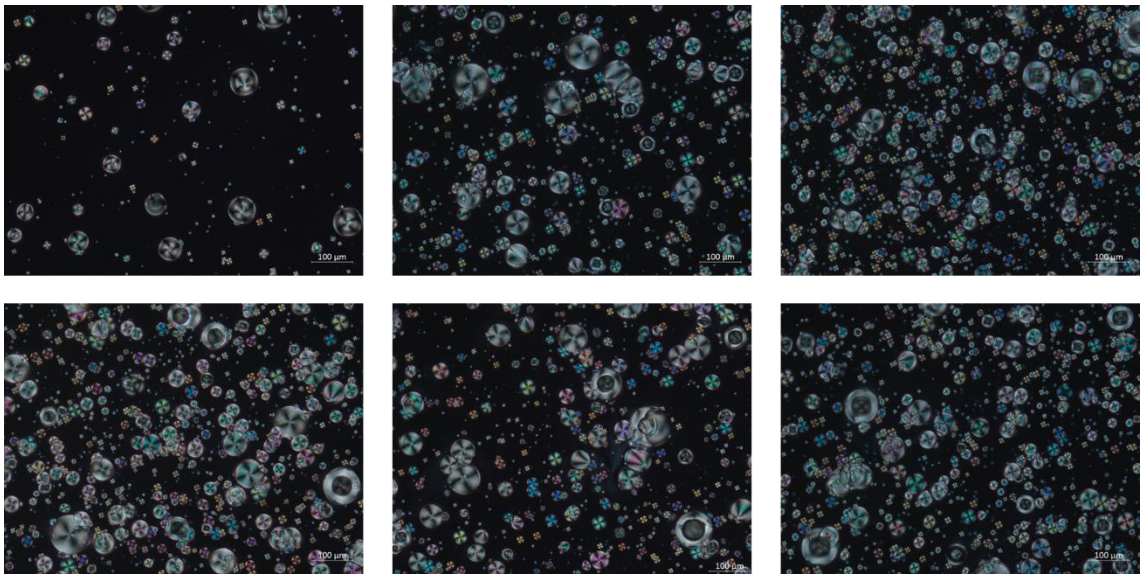

2) SDS

Aqueous Medium

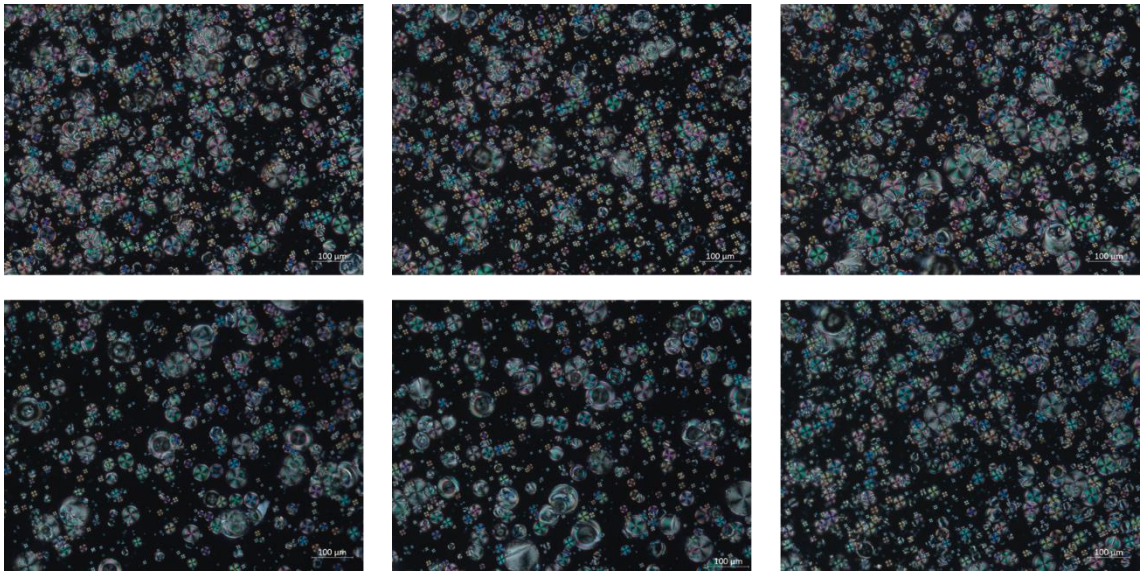

3) [C_{12}mim][DS]

Aqueous Medium

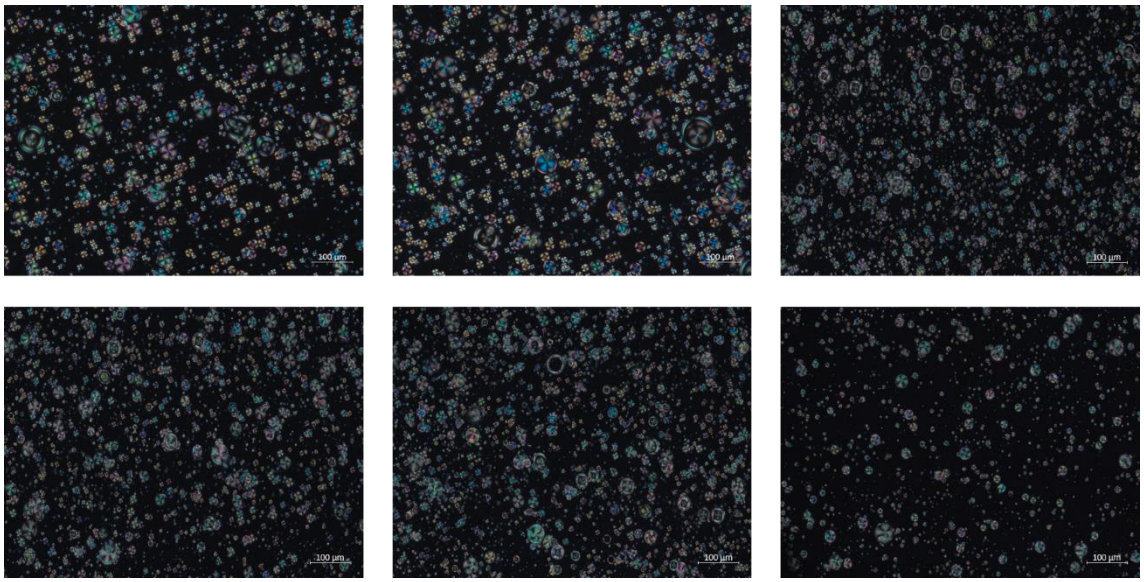

4) [Bmim][Cl]

Aqueous Medium

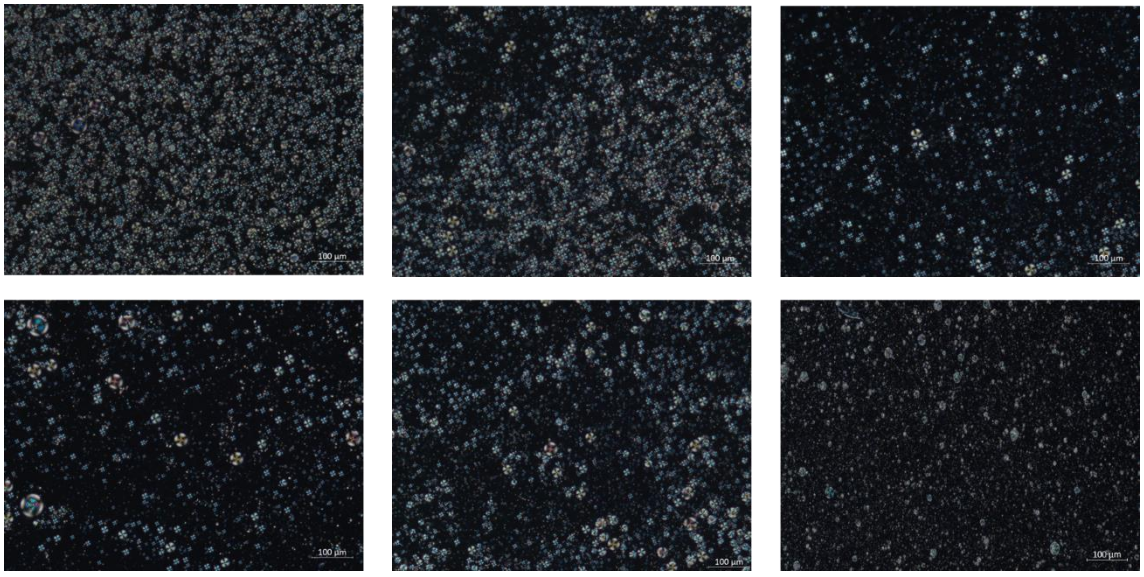

5) [Bmim][DCA]

Aqueous Medium

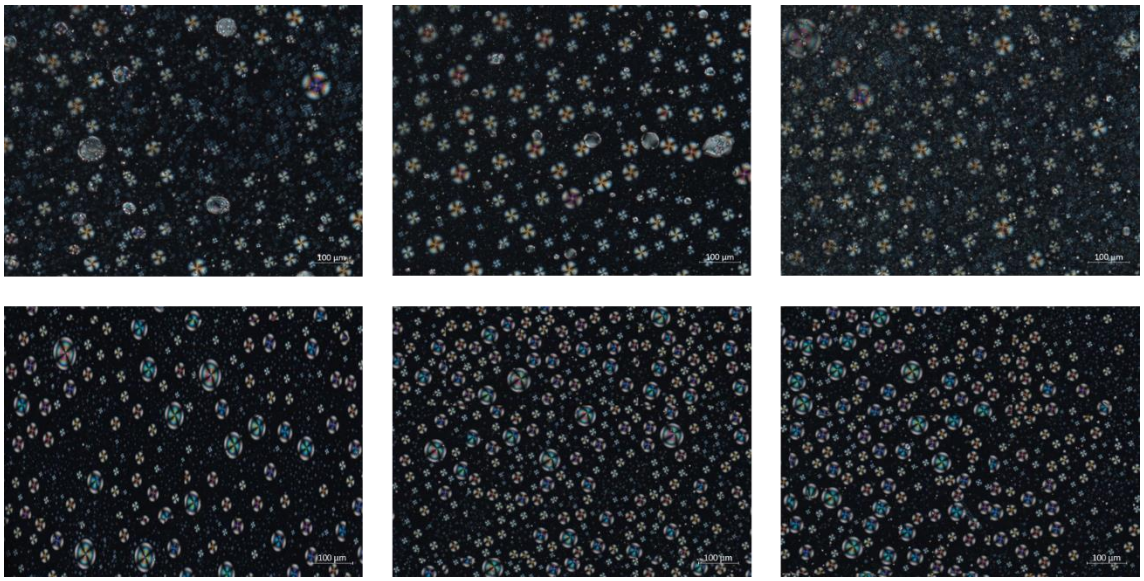

6) No Surfactant

Aqueous Medium

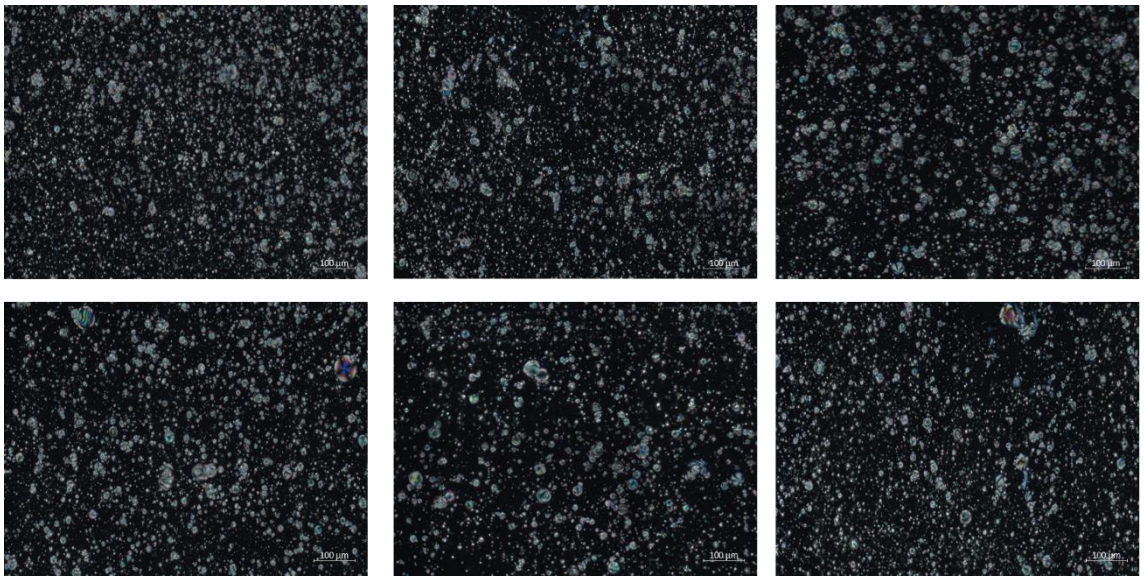

C – Mean Size of the Droplets

Table 0.1. Average Droplet Size for all the surfactants

Surfactant	Mean Size
BmimDCA	22.03
BmimCl	22.07
C_{12}mimCl	24.53
SDS	20.92
C_{12}mimDS	25.28
No Surfactant	22.85

D – Mean Gray Value

Table 0.2. Average Mean Gray Value for all the surfactants

Surfactant	Mean Gray Value
BmimDCA	37.75
BmimCl	34.54
C_{12}mimCl	42.32
SDS	51.25
C_{12}mimDS	36.84
No surfactant	36.84

E - Statistical Summary for Droplet Sizes Distribution

Table 1.1. 1 - Statistical summary for droplet size distribution

Parameter	*BmimDCA*	*BmimCl*	*C_{12}mimCl*	*SDS*	*C_{12}mimDS*	*No Surfactant*
Mean	22.03	22.07	24.53	20.92	25.28	22.85
Standard Error	0.50	0.53	0.76	0.48	0.73	0.58
Median	18.59	19.08	22.40	18.21	25.45	20.13
Mode	9.85	9.00	21.55	7.39	38.13	14.60
Standard deviation	10.87	10.89	11.47	10.77	10.13	10.48
Sample variance	118.07	118.61	131.45	115.96	102.56	109.83
Curtose	0.08	1.58	0.25	0.54	-0.46	0.08
Asymmetry	0.85	1.24	0.74	1.03	0.16	0.89
Range	56.00	57.34	57.31	51.39	44.29	47.43
Minimum	6.71	7.67	7.11	7.14	7.28	6.78
Maximum	62.70	65.01	64.42	58.53	51.56	54.22
Sum	10442.35	9289.97	5618.00	10649.60	4903.72	7495.11
Score	474.00	421.00	229.00	509.00	194.00	328.00
Major (1)	62.70	65.01	64.42	58.53	51.56	54.22
Minor (1)	6.71	7.67	7.11	7.14	7.28	6.78
Confidence Interval (95.0%)	0.98	1.04	1.49	0.94	1.43	1.14

F – E-nose Signals for all tested VOCs and gels with different surfactants within an aqueous medium

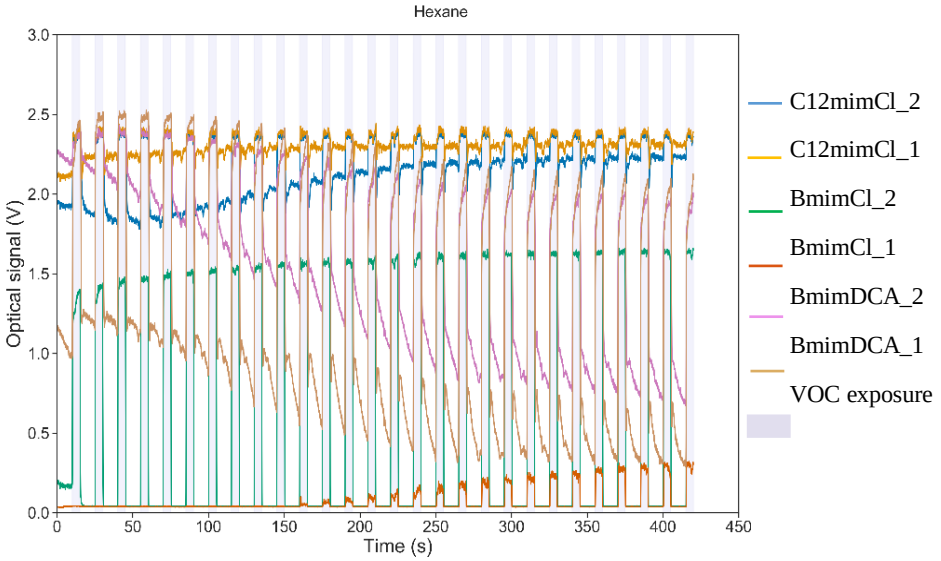

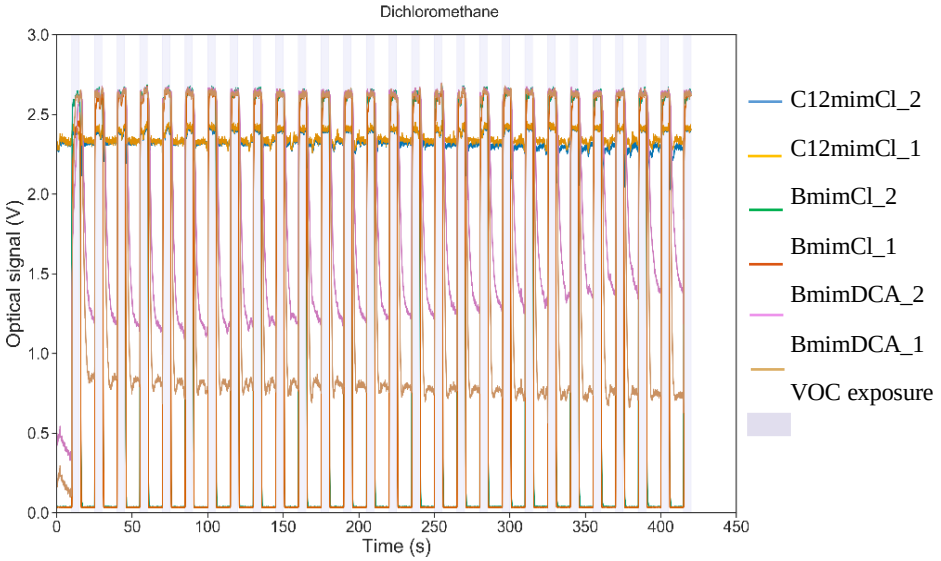

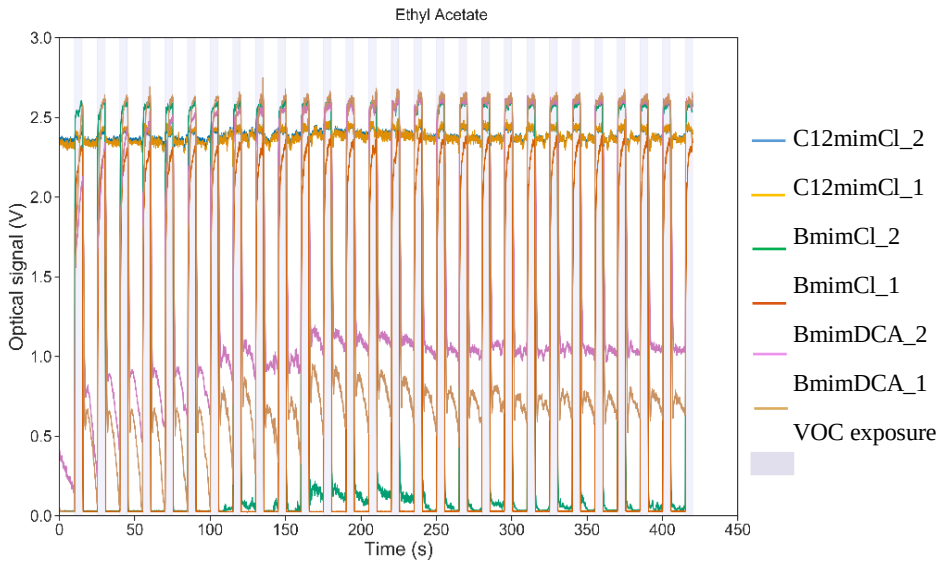

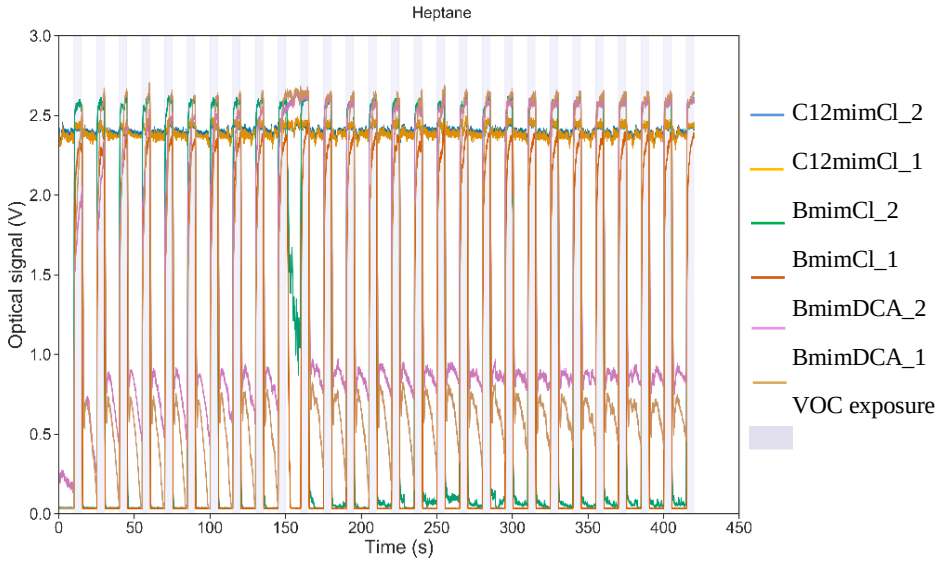
Heptane
Optical signal (V)
Time (s)
C12mimCl_2
C12mimCl_1
BmimCl_2
BmimCl_1
BmimDCA_2
BmimDCA_1
VOC exposure

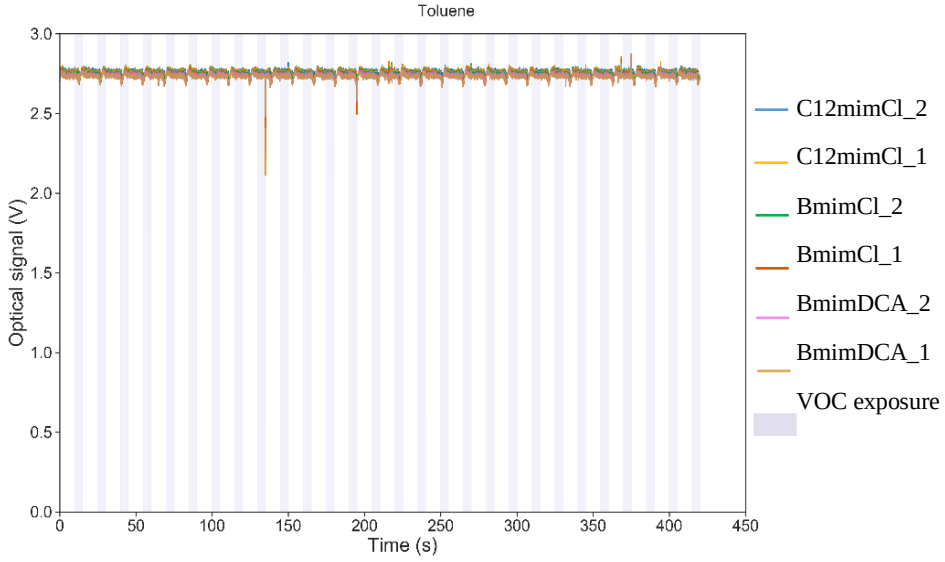
Toluene
Optical signal (V)
Time (s)
C12mimCl_2
C12mimCl_1
BmimCl_2
BmimCl_1
BmimDCA_2
BmimDCA_1
VOC exposure

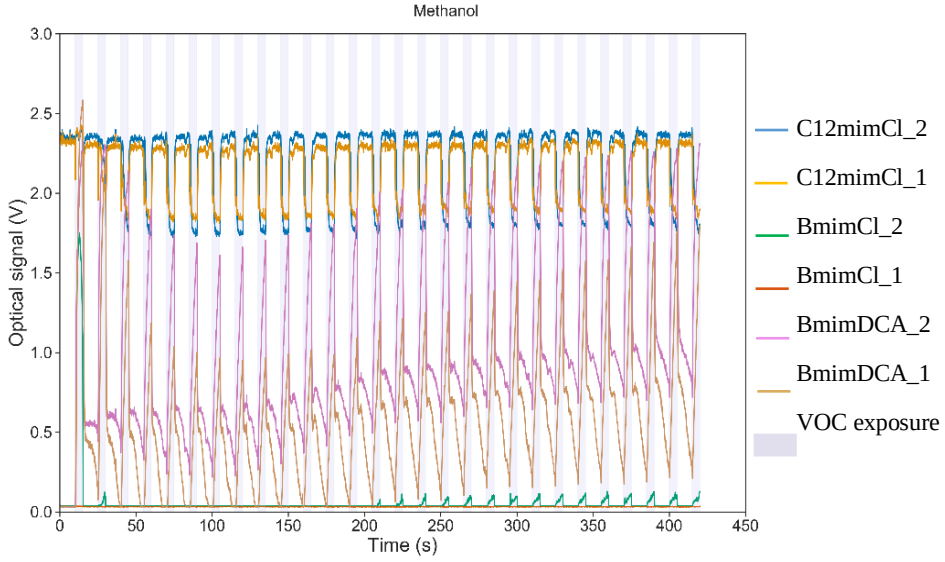
Methanol
Optical signal (V)
Time (s)
C12mimCl_2
C12mimCl_1
BmimCl_2
BmimCl_1
BmimDCA_2
BmimDCA_1
VOC exposure

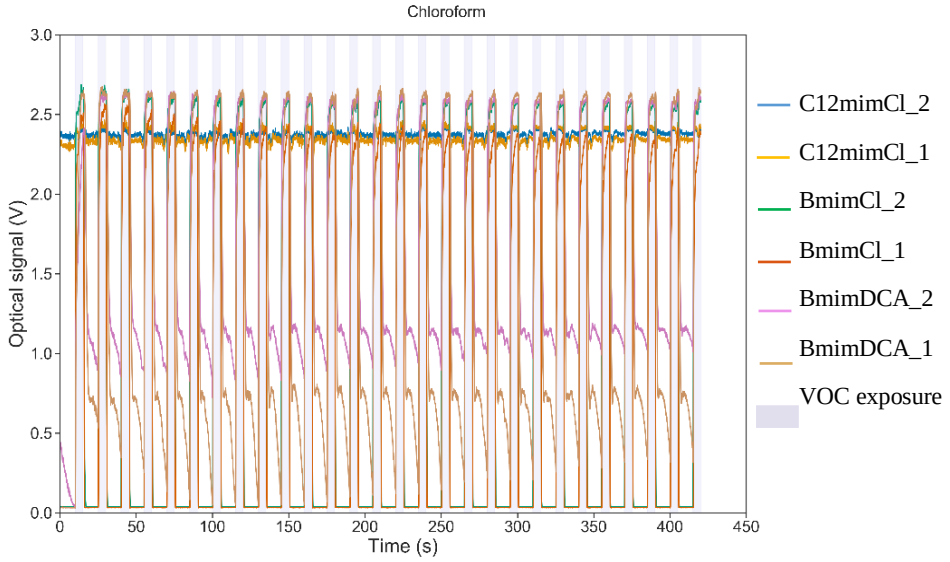
Chloroform
Optical signal (V)
Time (s)
C12mimCl_2
C12mimCl_1
BmimCl_2
BmimCl_1
BmimDCA_2
BmimDCA_1
VOC exposure

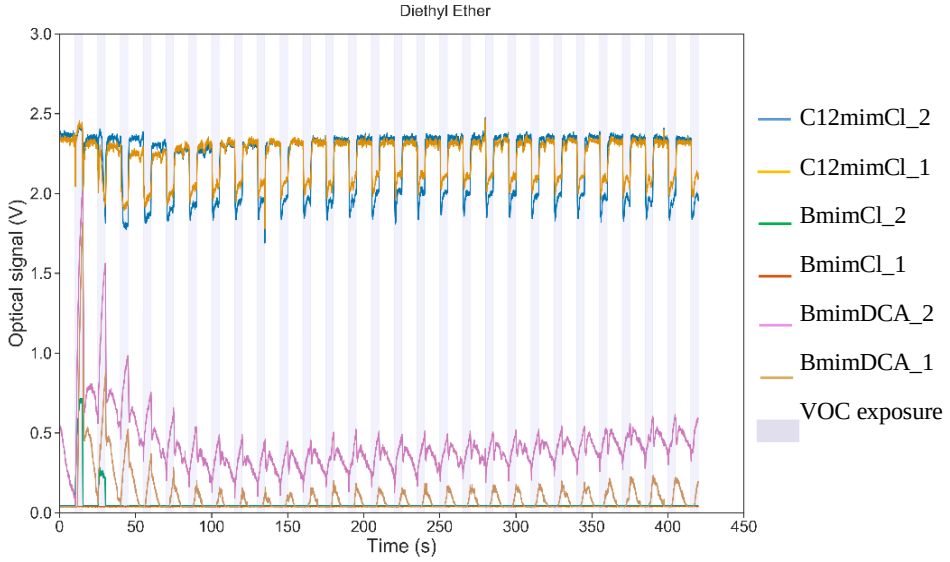
Diethyl Ether
Optical signal (V)
Time (s)
C12mimCl_2
C12mimCl_1
BmimCl_2
BmimCl_1
BmimDCA_2
BmimDCA_1
VOC exposure

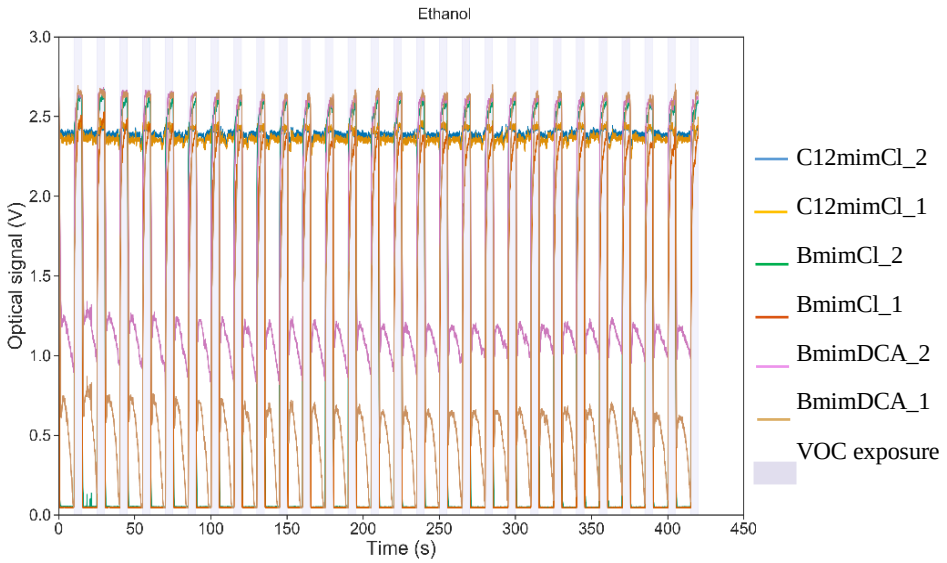
Ethanol
Optical signal (V)
Time (s)
C12mimCl_2
C12mimCl_1
BmimCl_2
BmimCl_1
BmimDCA_2
BmimDCA_1
VOC exposure

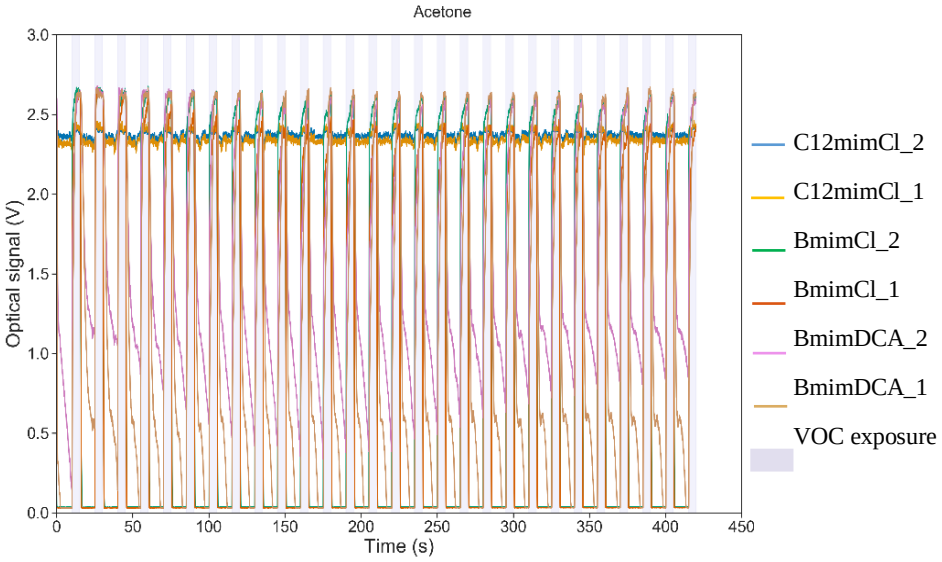
Acetone
Optical signal (V)
Time (s)
C12mimCl_2
C12mimCl_1
BmimCl_2
BmimCl_1
BmimDCA_2
BmimDCA_1
VOC exposure

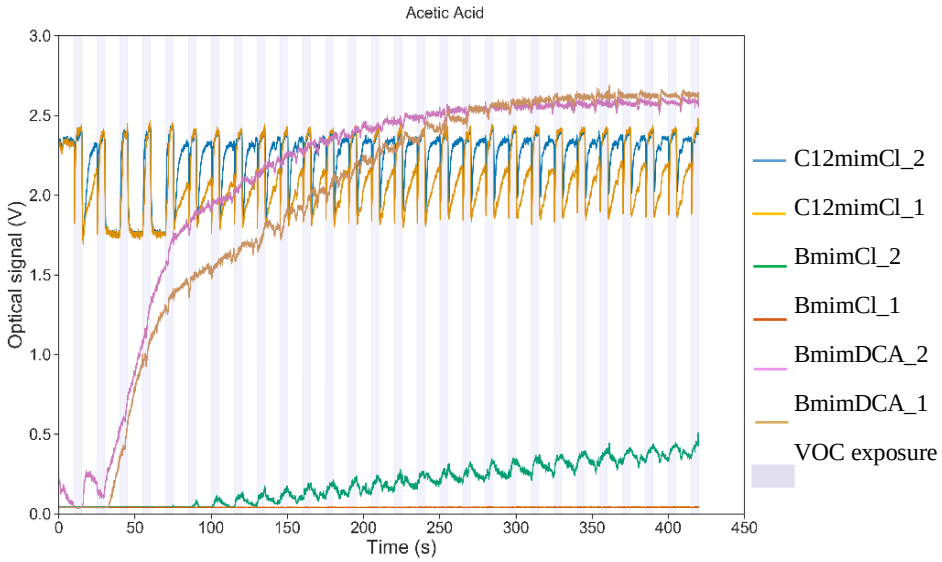
Acetic Acid
Optical signal (V)
Time (s)
C12mimCl_2
C12mimCl_1
BmimCl_2
BmimCl_1
BmimDCA_2
BmimDCA_1
VOC exposure

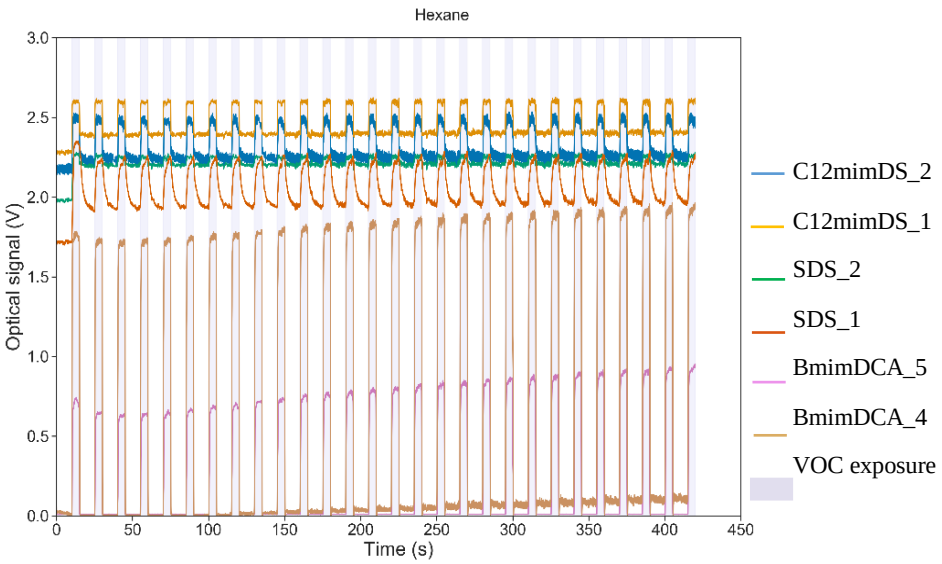
Hexane
Optical signal (V)
Time (s)
C12mimDS_2
C12mimDS_1
SDS_2
SDS_1
BmimDCA_5
BmimDCA_4
VOC exposure

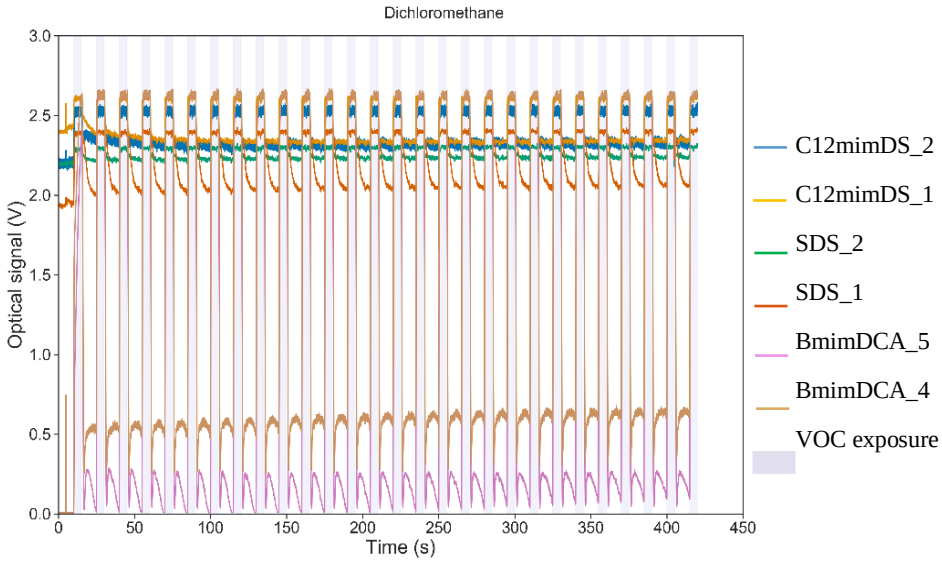
Dichloromethane
Optical signal (V)
Time (s)
C12mimDS_2
C12mimDS_1
SDS_2
SDS_1
BmimDCA_5
BmimDCA_4
VOC exposure

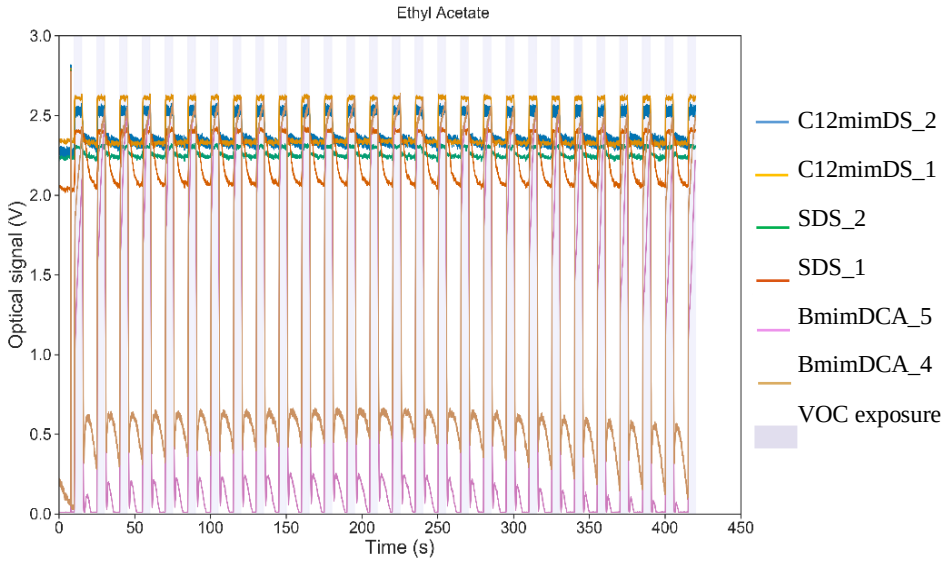
Ethyl Acetate
Optical signal (V)
Time (s)
C12mimDS_2
C12mimDS_1
SDS_2
SDS_1
BmimDCA_5
BmimDCA_4
VOC exposure

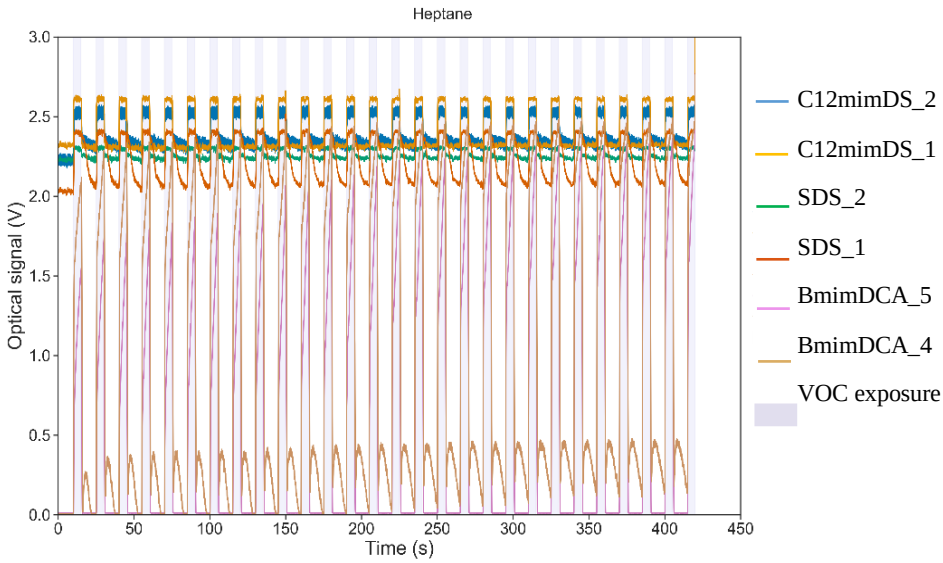
Heptane
Optical signal (V)
Time (s)
C12mimDS_2
C12mimDS_1
SDS_2
SDS_1
BmimDCA_5
BmimDCA_4
VOC exposure

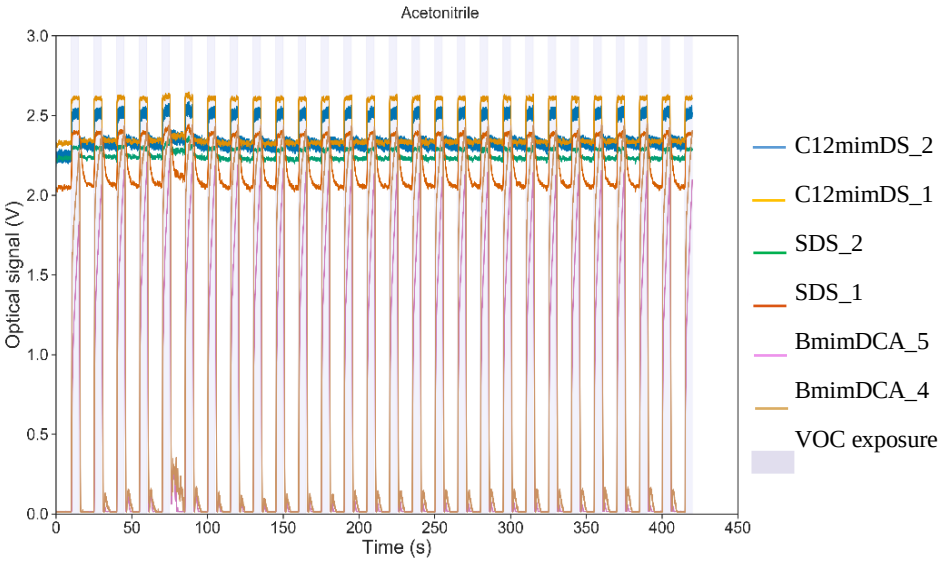
Acetonitrile
Optical signal (V)
Time (s)
C12mimDS_2
C12mimDS_1
SDS_2
SDS_1
BmimDCA_5
BmimDCA_4
VOC exposure

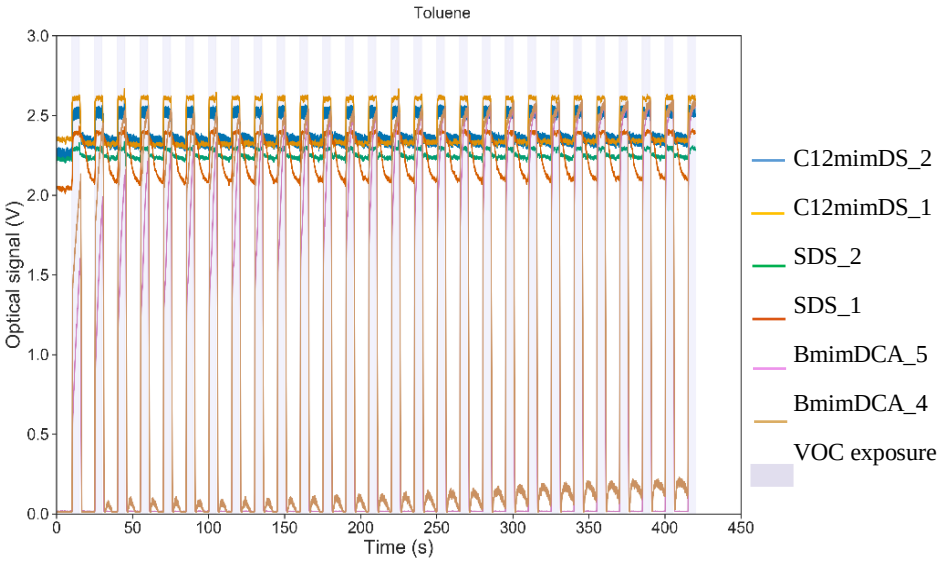
Toluene
Optical signal (V)
Time (s)
C12mimDS_2
C12mimDS_1
SDS_2
SDS_1
BmimDCA_5
BmimDCA_4
VOC exposure

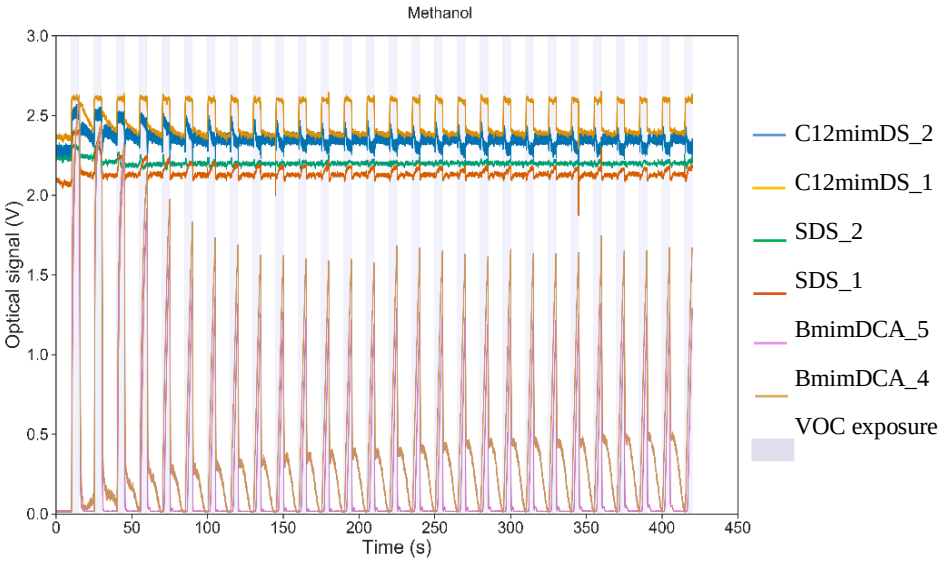
Methanol
Optical signal (V)
Time (s)
C12mimDS_2
C12mimDS_1
SDS_2
SDS_1
BmimDCA_5
BmimDCA_4
VOC exposure

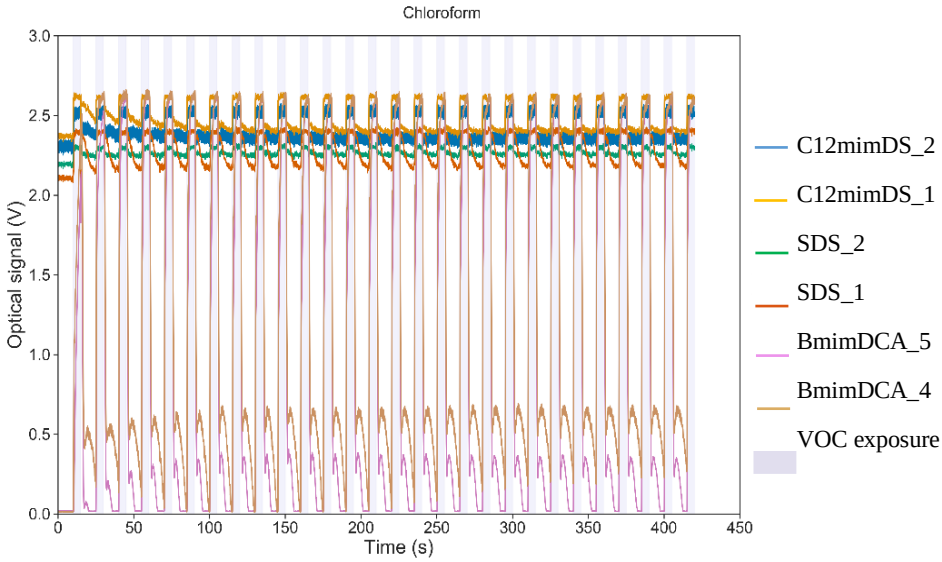
Chloroform
Optical signal (V)
Time (s)
C12mimDS_2
C12mimDS_1
SDS_2
SDS_1
BmimDCA_5
BmimDCA_4
VOC exposure

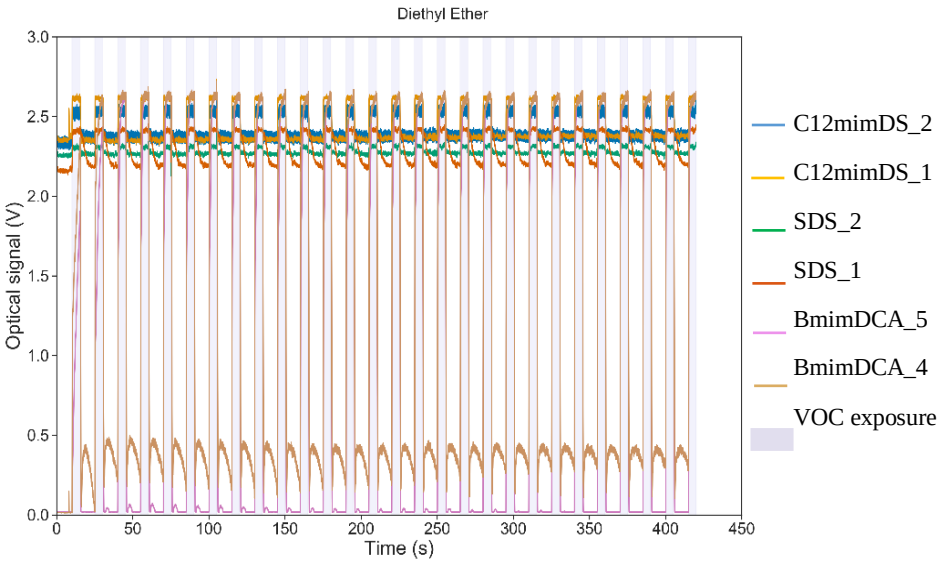
Diethyl Ether
Optical signal (V)
Time (s)
C12mimDS_2
C12mimDS_1
SDS_2
SDS_1
BmimDCA_5
BmimDCA_4
VOC exposure

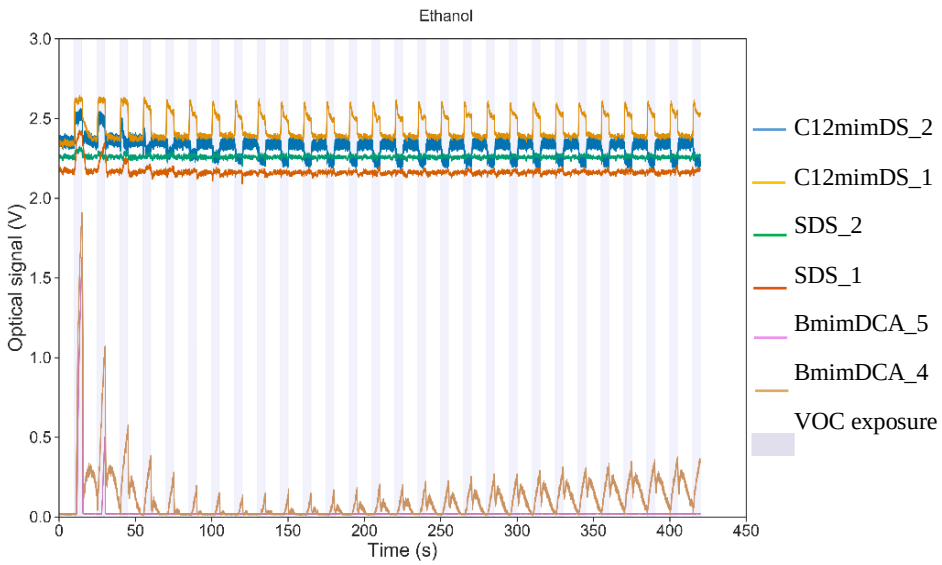
Ethanol
Optical signal (V)
Time (s)
C12mimDS_2
C12mimDS_1
SDS_2
SDS_1
BmimDCA_5
BmimDCA_4
VOC exposure

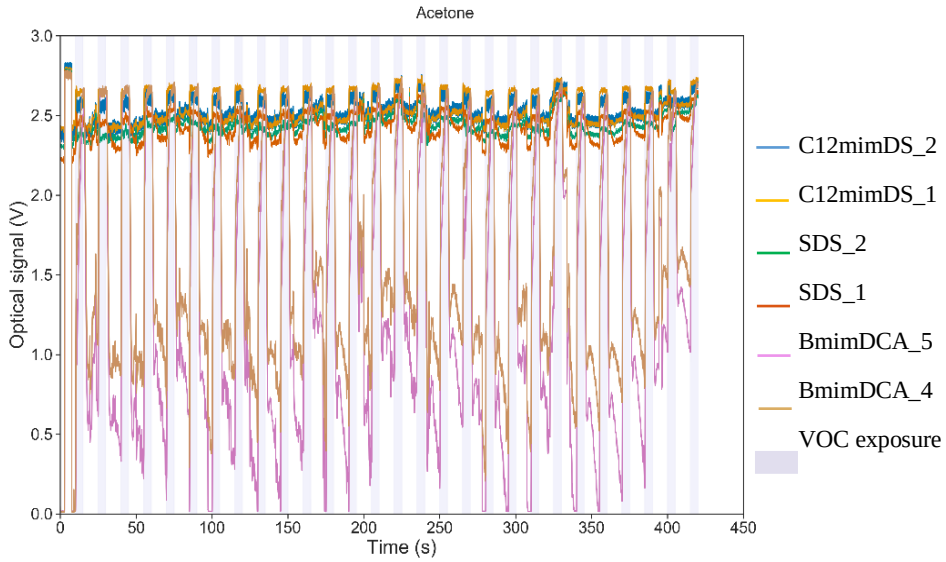
Acetone
Optical signal (V)
Time (s)
C12mimDS_2
C12mimDS_1
SDS_2
SDS_1
BmimDCA_5
BmimDCA_4
VOC exposure

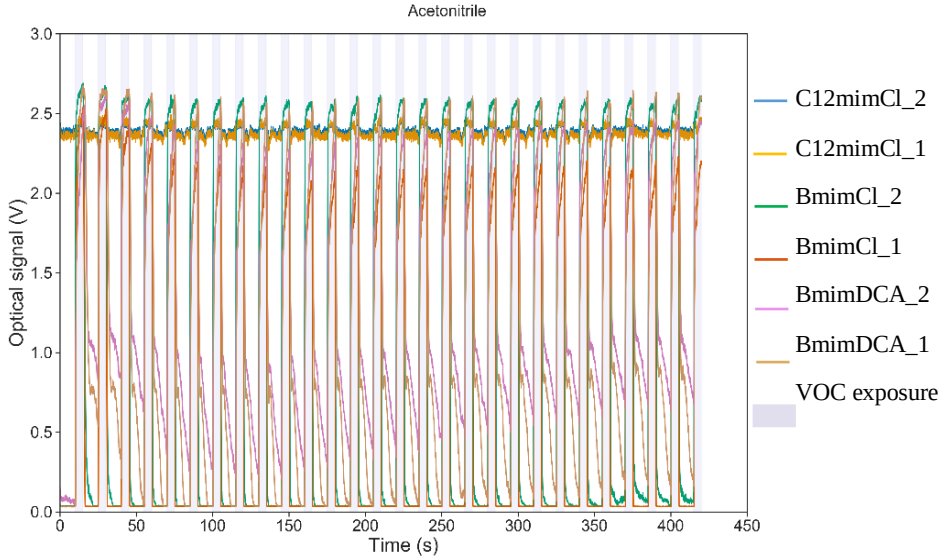
Acetonitrile
Optical signal (V)
Time (s)
C12mimCl_2
C12mimCl_1
BmimCl_2
BmimCl_1
BmimDCA_2
BmimDCA_1
VOC exposure

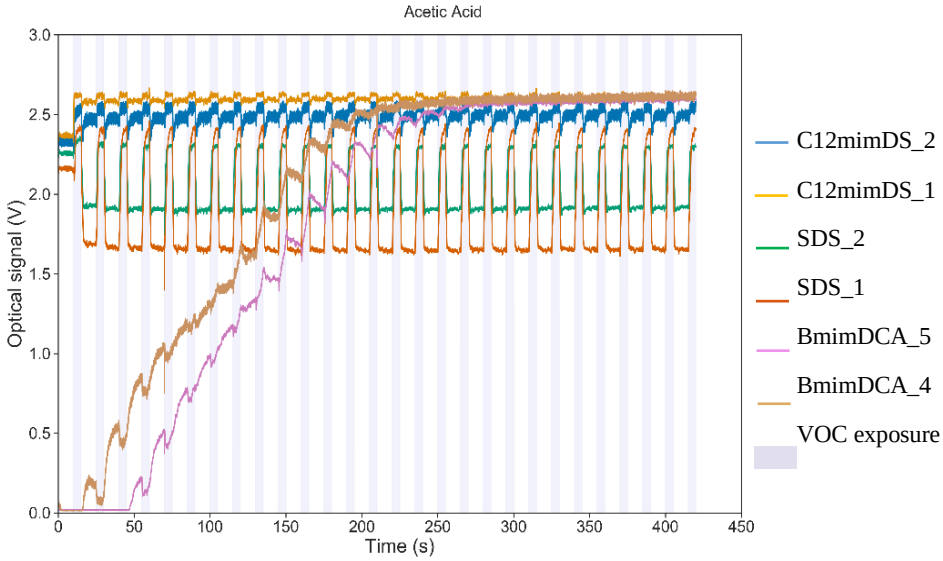
Acetic Acid
Optical signal (V)
Time (s)
C12mimDS_2
C12mimDS_1
SDS_2
SDS_1
BmimDCA_5
BmimDCA_4
VOC exposure

Table 0.3. Individual Scores for all the VOCs and gels tested

VOC/Gel	**[Bmim][DCA]**	**[Bmim][Cl]**	**[C_{12}mim][Cl]**	**SDS**	**[C_{12}mim][DS]**
Acetic Acid	36%	6%	97%	**100%**	71%
Acetone	**96%**	93%	33%	59%	63%
Acetonitrile	**96%**	94%	43%	89%	87%
Chloroform	**96%**	93%	54%	80%	70%
Dichloromethane	**96%**	94%	53%	74%	87%
Diethyl Ether	95%	**98%**	83%	69%	80%
Ethanol	**91%**	89%	20%	79%	88%
Ethyl Acetate	**92%**	80%	35%	57%	61%
Heptane	**89%**	69%	25%	56%	80%
Hexane	**97%**	66%	83%	89%	96%
Methanol	**95%**	0%	60%	75%	83%
Toluene	**94%**	-	-	57%	87%

G – E-nose Sensors Tiles

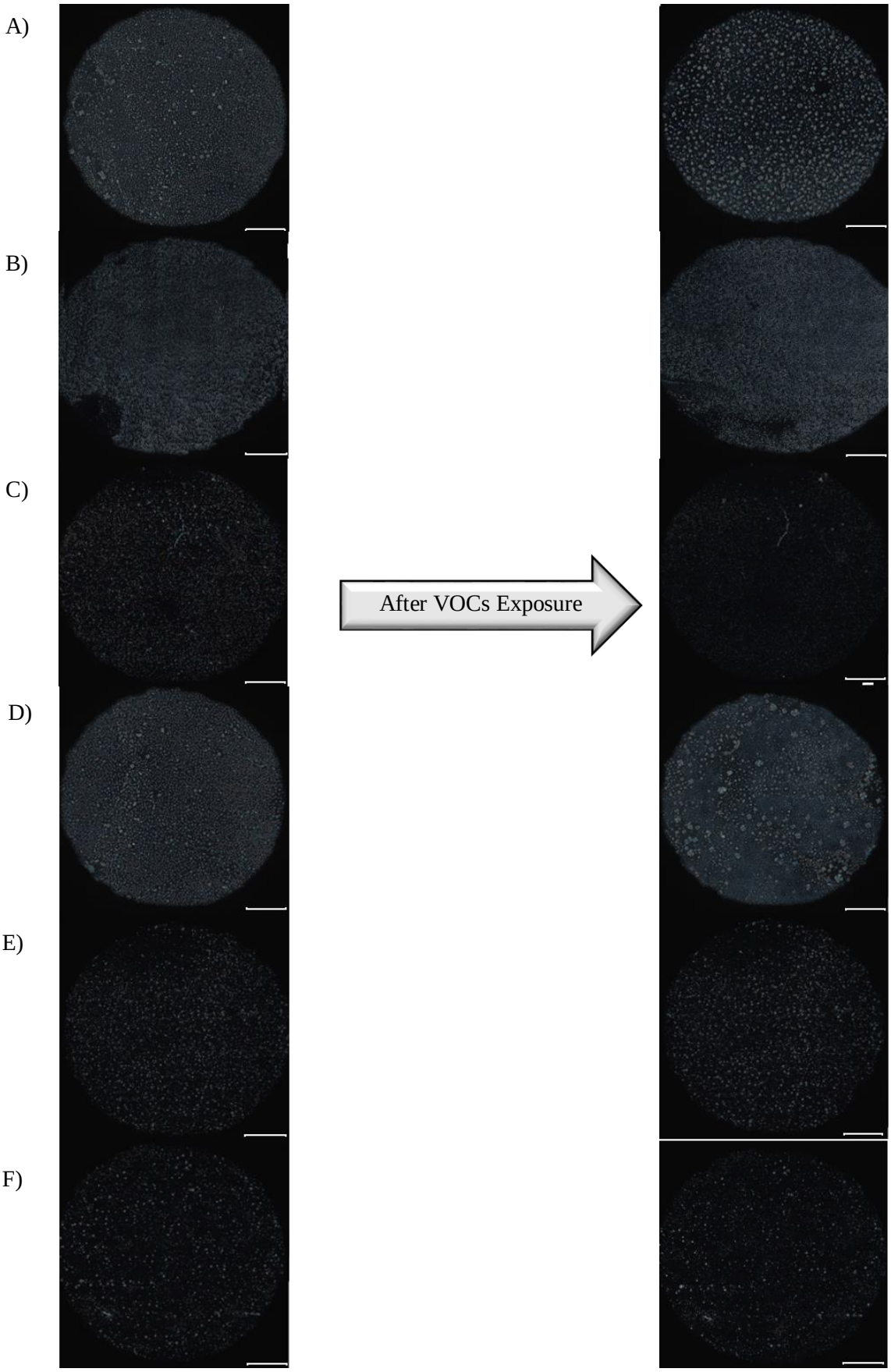

Figure 0.3. Tiles of all the surfactants before and after the VOCs exposure; A) [Bmim][DCA] from the first set of experiments; B) [Bmim][Cl]; C) [C_{12}mim][Cl]; D) [Bmim][DCA] for the second set of experiment; E) SDS; F) [C_{12}mim][DS]

Appendix III – Chapter 5

A – pKa and IP values for all the amino acids present on the gelatine

Table 0.4. pka and PI values for the amino acids residues present on the gelatine from bovine skin (type B). The amount in % of each amino acid is also presented. The amino acids that possess greater influence on the IP of the gelatine are highlighted (Glutamic acid and Arginine). pka1 refers to the carboxyl group, pka2 to ammonium group and lastly, pka3 refers to the side chain group.

Amino Acid	pKa1	pka2	pka3	IP	amount %
Nonpolar Hydrophobic					
Alanine	2.34	9.69	-	6.00	3.30
Valine	2.32	9.62	-	5.96	1.00
Leucine	2.36	9.60	-	5.98	1.20
Isoleucine	2.36	9.60	-	6.02	0.70
Phenylalanine	1.38	9.13	-	5.48	1.00
Methionine	2.28	9.21	-	5.74	0.40
Proline	1.99	10.60	-	6.30	6.30
Polar uncharged					
Glycine	2.34	9.60	-	5.97	10.80
Serine	2.21	9.15	-	5.68	1.50
Threonine	2.09	9.10	-	5.60	1.00
Tyrosine	2.20	9.11	-	5.66	0.20
Polar acidic					
Aspartic acid	1.88	9.60	3.65	2.77	1.70
Glutamic acid	2.19	9.67	4.25	3.22	3.40
Polar basic					
Lysine	2.18	8.95	10.53	9.74	1.10
Arginine	2.17	9.04	12.48	10.76	4.70
Histidine	1.82	9.17	6.00	7.59	-

B – SDS Experiments E-nose Signals

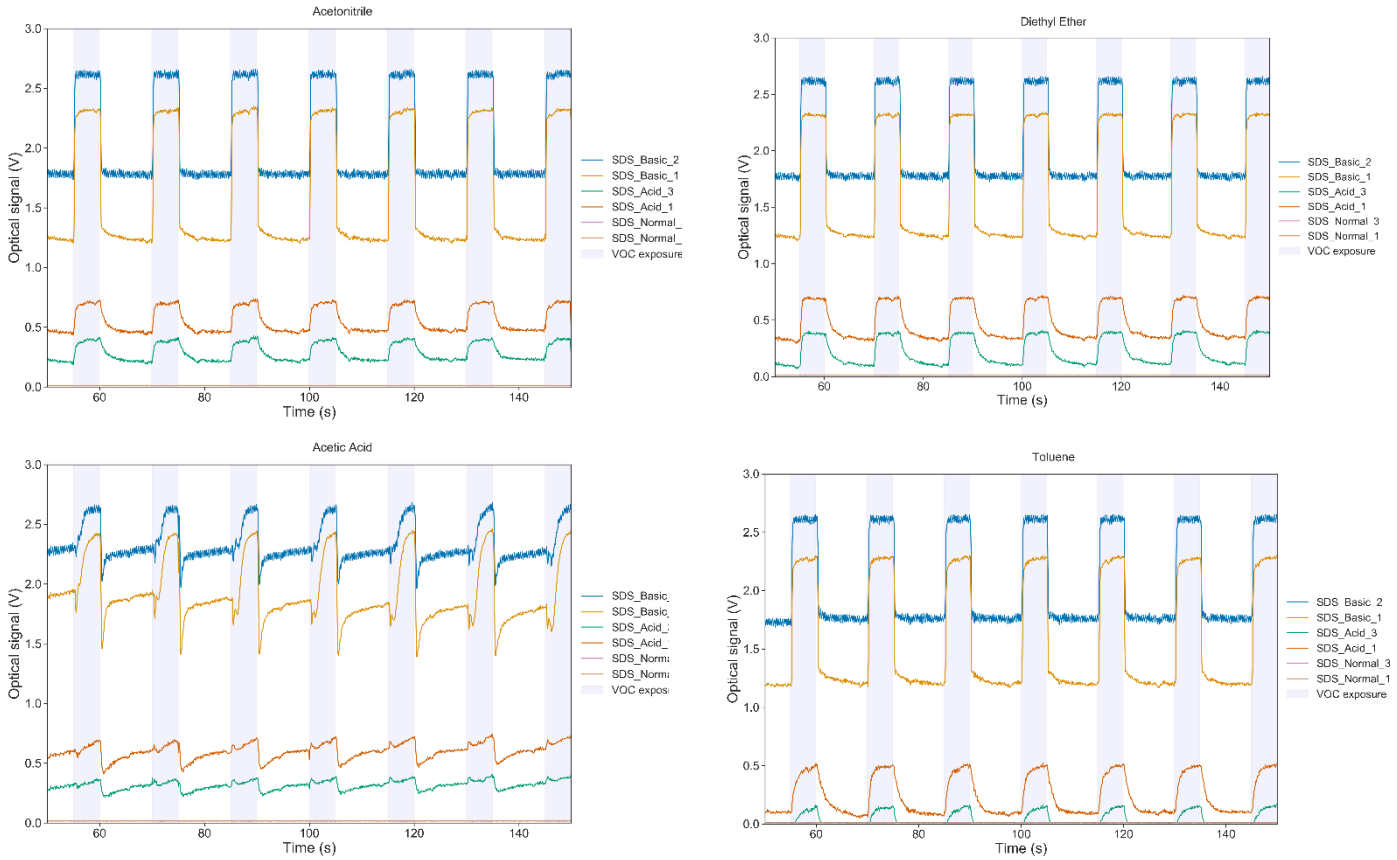

Table 0.5.Example of Signals obtained with the first experiments with SDS surfactant; The droplets made with aqueous mean did not respond to any VOC tested

VOCs Order:

Heptane

Hexane

Toluene

Chloroform

Dichloromethane

Diethyl Ether

Ethyl Acetate

Acetone

Acetonitrile

Ethanol

Methanol

Acetic Acid

C – Gel Figures to the analysis of the droplet size and Mean Gray Value

1) [C_{12}mim][Cl]

Acid Medium

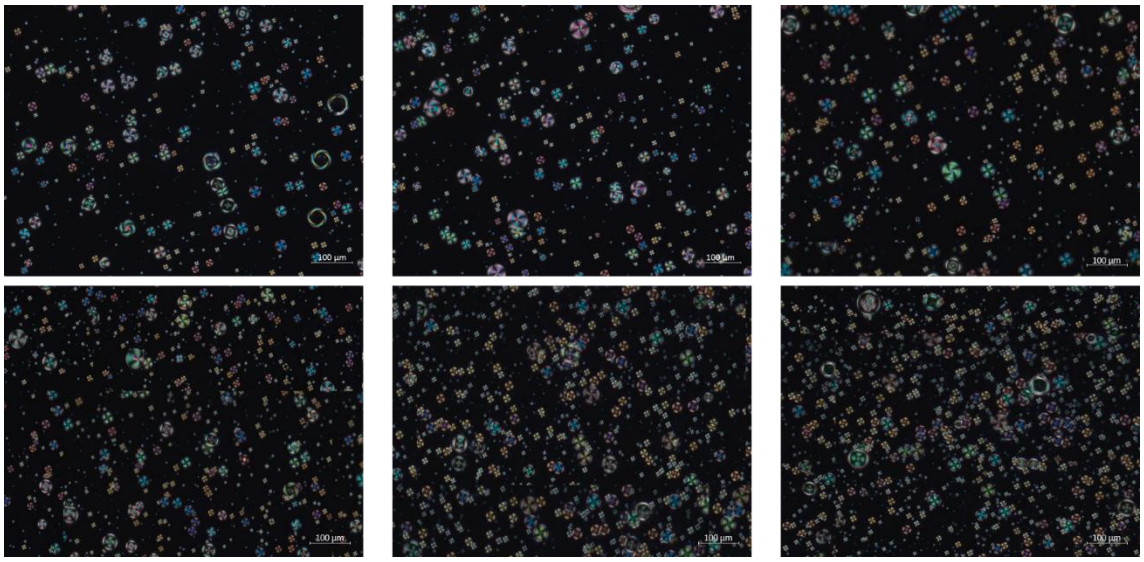

Basic Medium

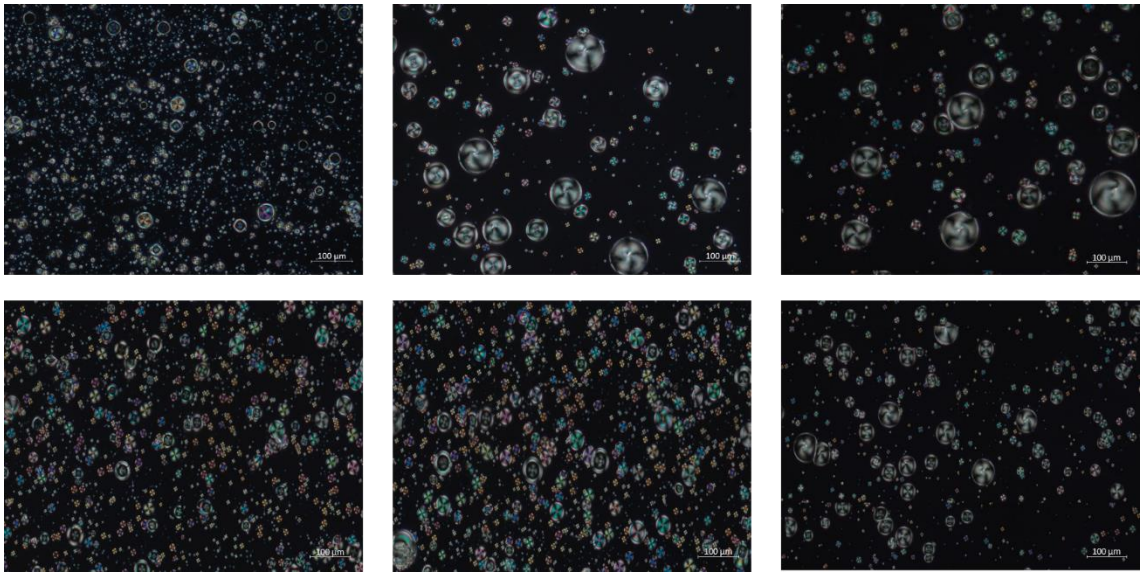

2) SDS

Acid Medium

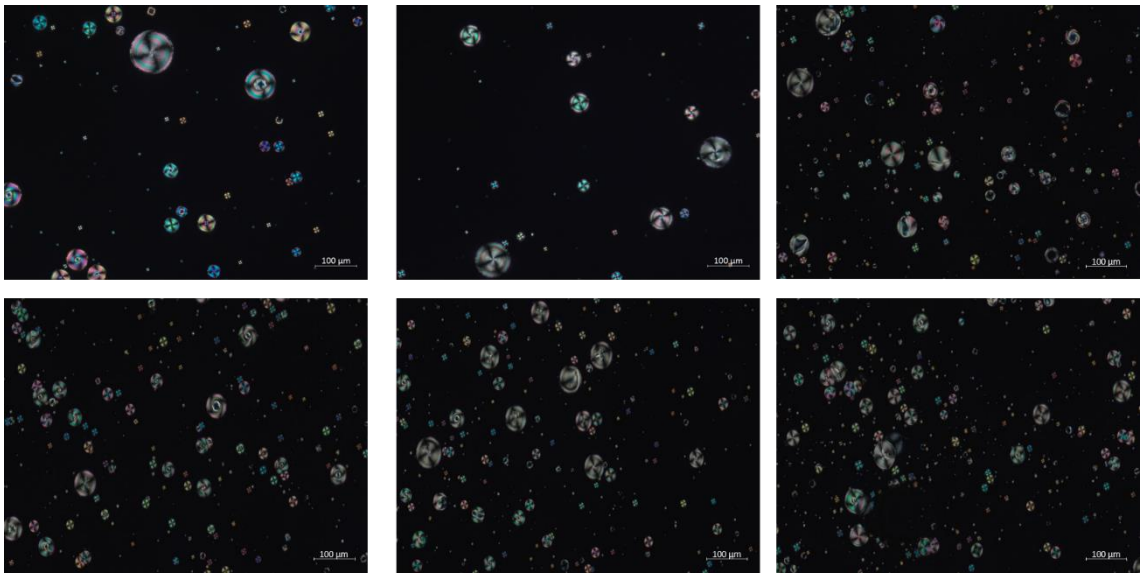

Basic Medium

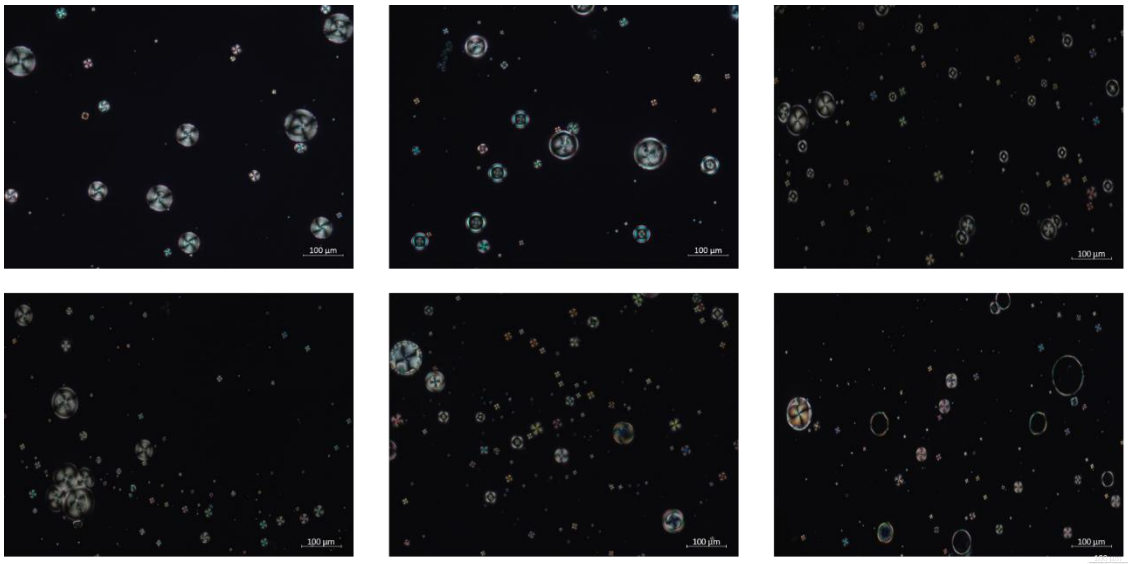

3) [C_{12}mim][DS]

Acid Medium

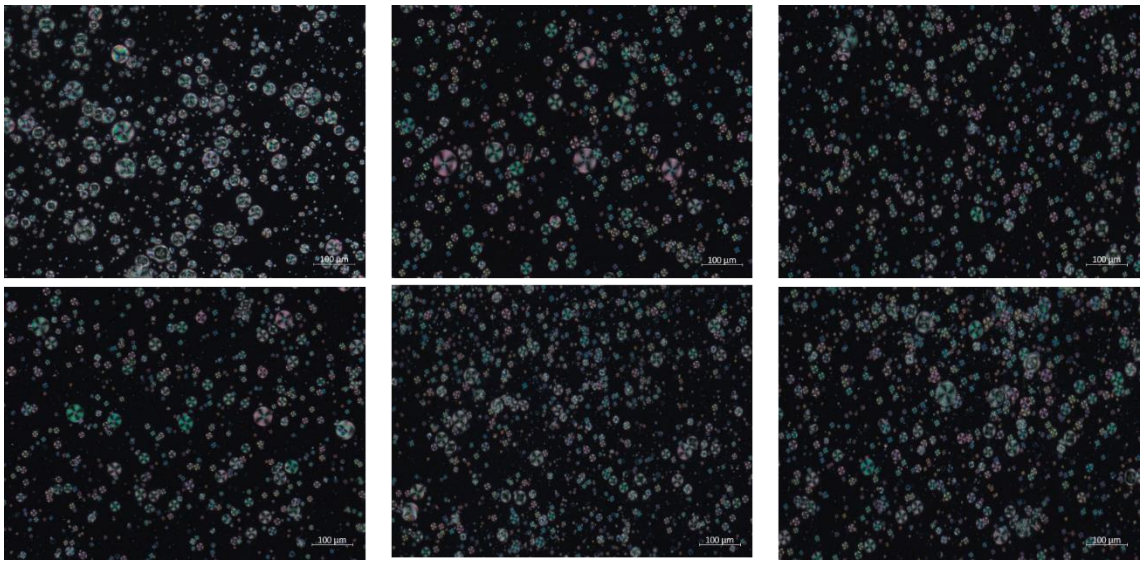

Basic Medium

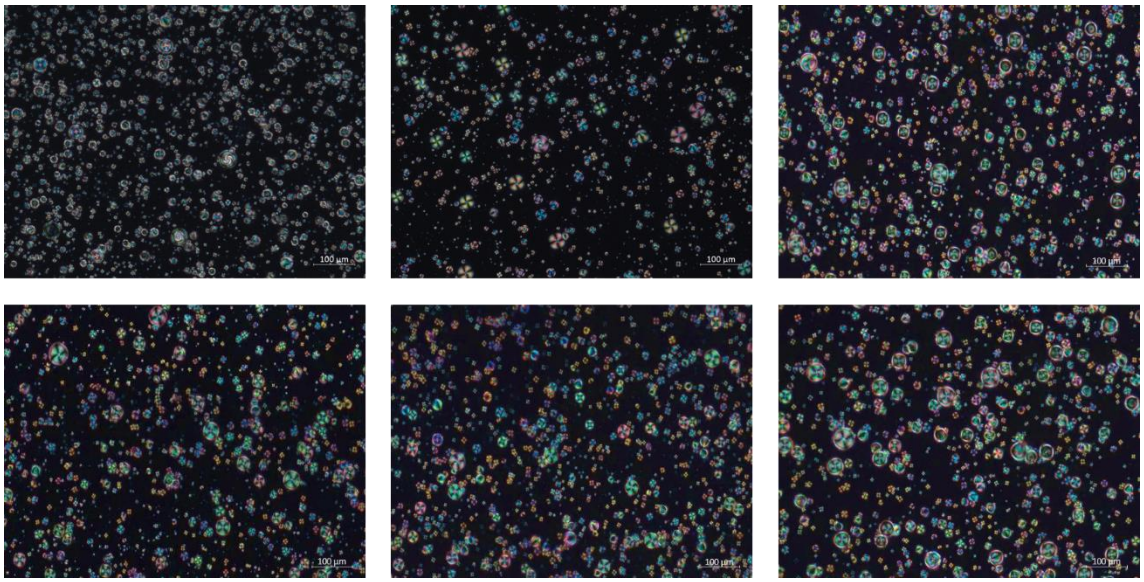

4) [Bmim][Cl]

Acid Medium

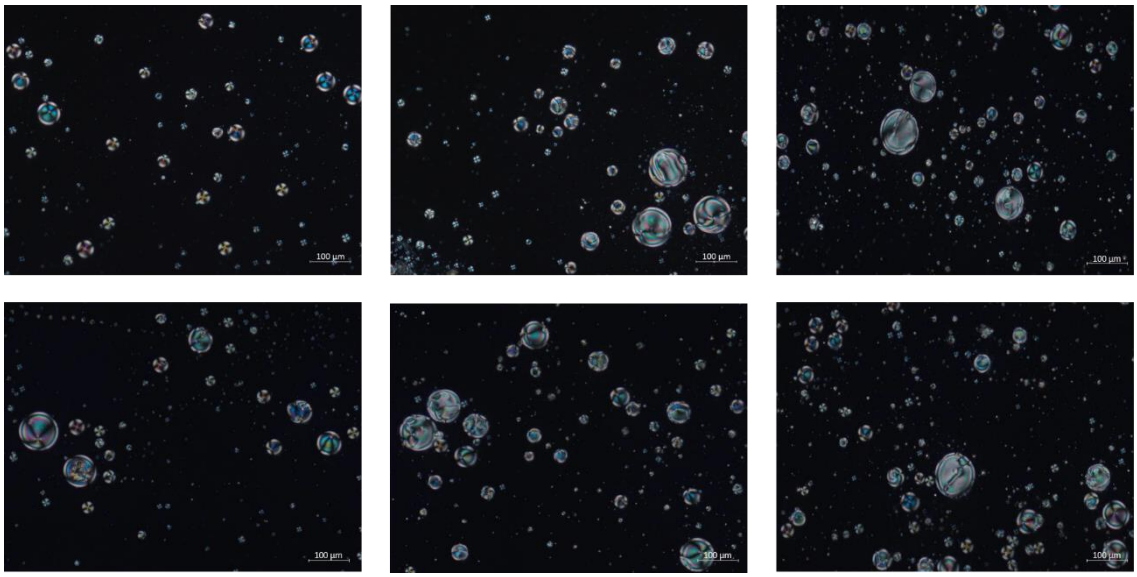

Basic Medium

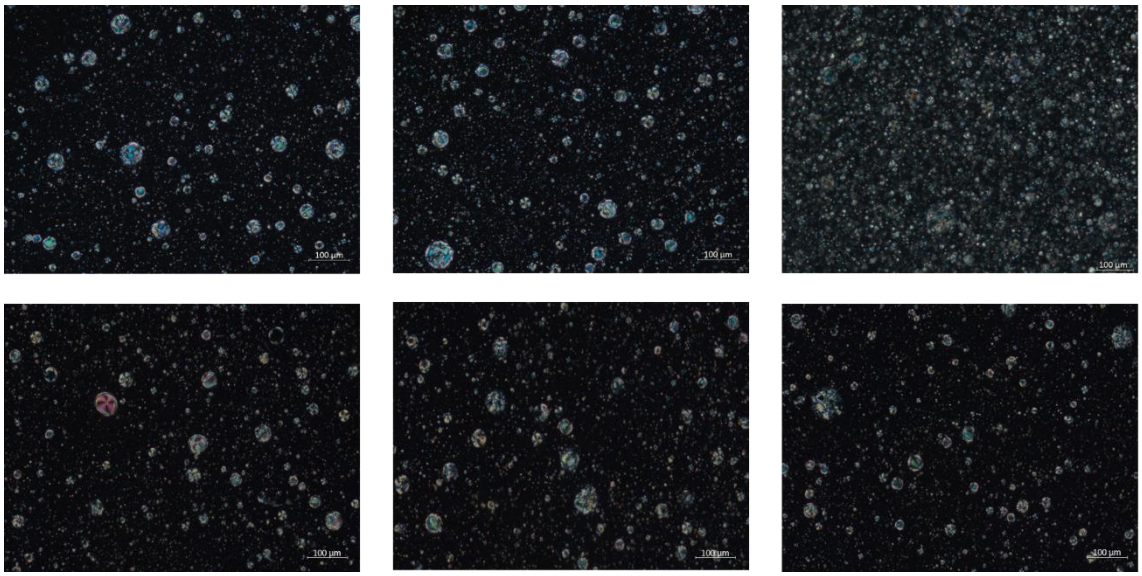

5) [Bmim][DCA]

Acid Medium

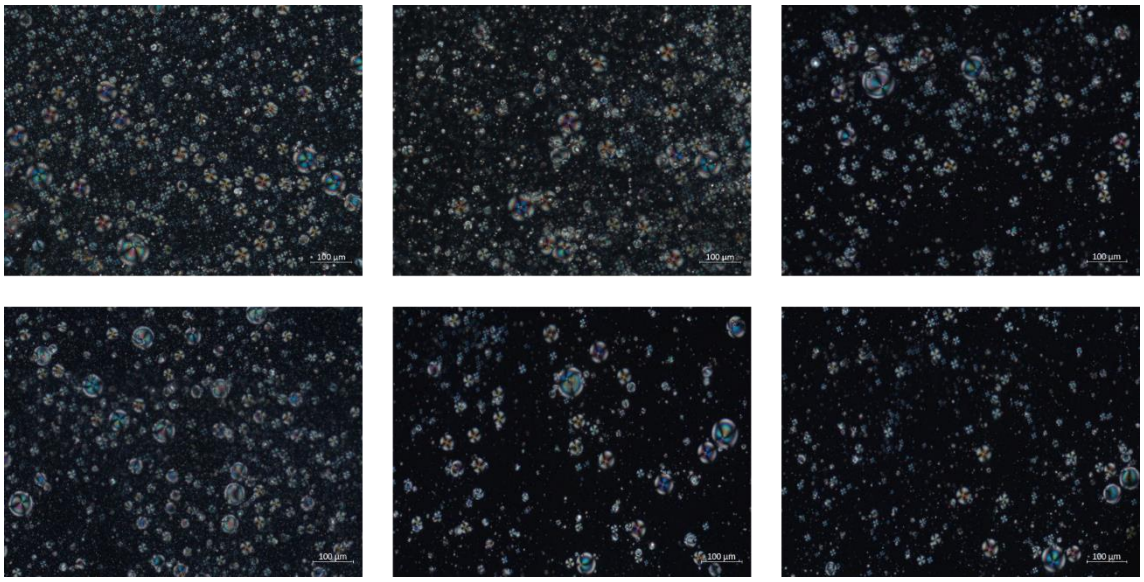

Basic Medium

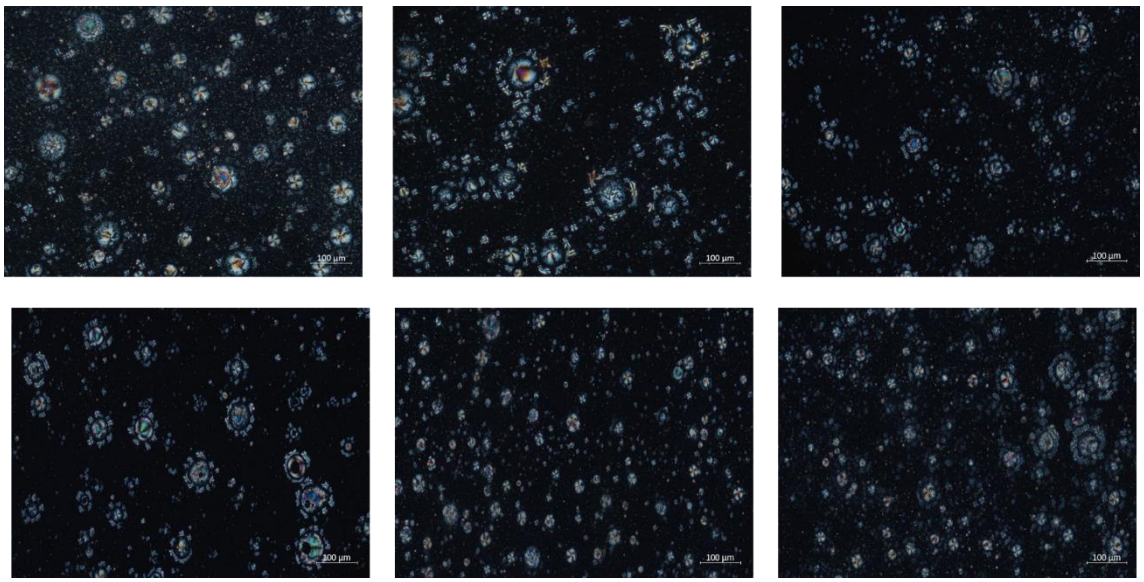

6) No Surfactant

Acid Medium

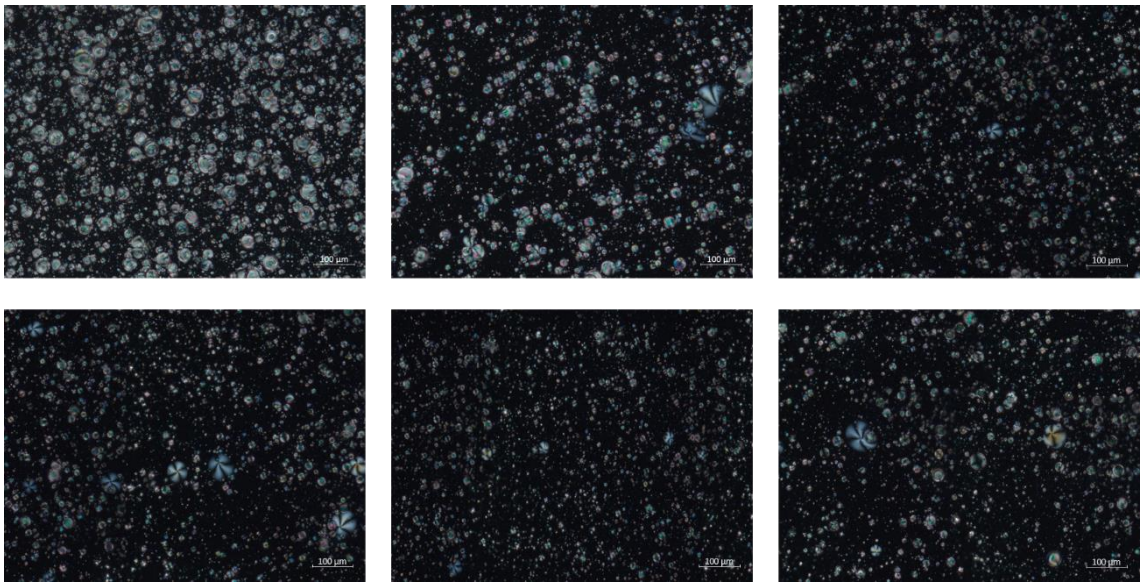

Basic Medium

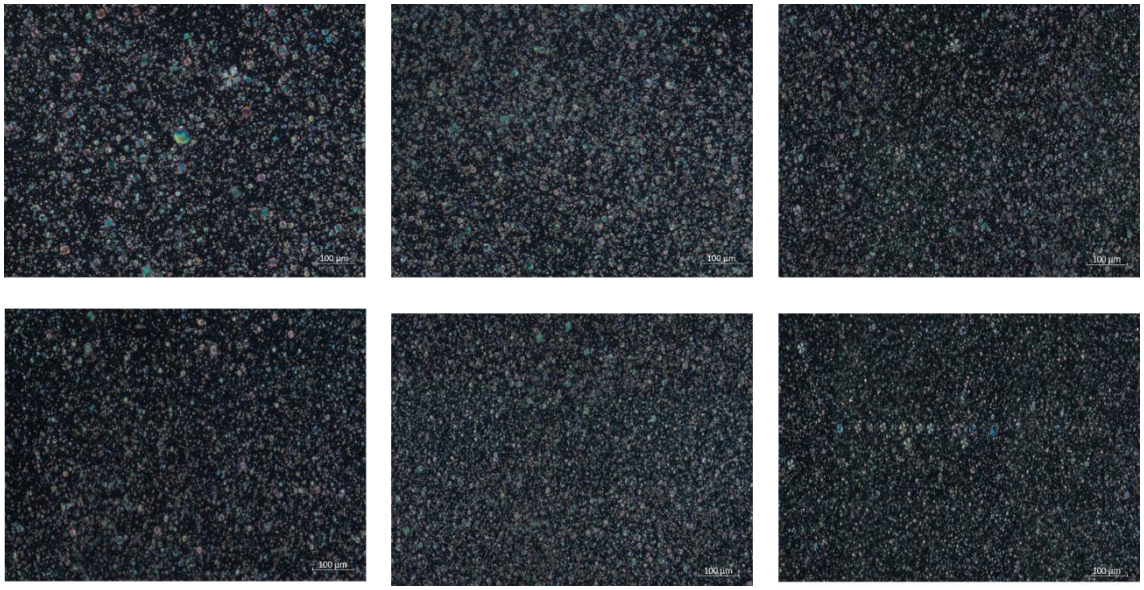

D – Mean Size of the Droplets

Table 0.6. Average Droplet Size for all the surfactants and cases, for the different pH media tested.

Surfactant/ Medium	Average Droplet Size (+/- 0.1µm)
BmimDCA	
Aqueous	22.30
Acid Buffer	21.83
Basic Buffer	22.29
BmimCl	
Aqueous	22.07
Acid Buffer	20.24
Basic Buffer	22.38
C_{12}mimCl	
Aqueous	24.53
Acid Buffer	22.45
Basic Buffer	22.68
SDS	
Aqueous	20.92
Acid Buffer	23.31
Basic Buffer	23.88
C_{12}mimDS	
Aqueous	25.28
Acid Buffer	22.51
Basic Buffer	24.94
No surfactant	
Aqueous	22.85
Acid Buffer	23.72
Basic Buffer	22.24

E – Mean Gray Value

Table 0.7. Average Mean Gray Value for all the surfactants and cases, for the different pH media

Surfactant/Medium	Mean Gray Value
BmimDCA	
Aqueous	37.75
Basic	31.63
Acid	40.45
BmimCl	
Aqueous	34.54
Basic	30.34
Acid	20.45
C_{12}mimCl	
Aqueous	42.32
Basic	29.85
Acid	23.36
SDS	
Aqueous	51.25
Basic	16.94
Acid	16.72
C_{12}mimDS	
Aqueous	29.08
Basic	16.94
Acid	44.22
No surfactant	
Aqueous	36.84
Basic	53.61
Acid	40.47

F – Statistical Summaries for Droplet Sizes Distribution

Table 1.1. 2 - Statistical Summary for the Droplet Sizes Distribution for the Acid Buffer as the medium

Parameter	*BmimDCA*	*BmimCl*	*C_{12}mimCl*	*SDS*	*C_{12}mimDS*	*No Surfactant*
Mean	21.83	20.24	22.45	23.31	22.51	23.72
Standard Error	0.34	0.51	0.57	0.67	0.66	0.63
Median	18.41	17.11	19.07	21.66	20.56	20.90
Mode	17.09	15.74	19.74	22.11	14.84	18.52
Standard deviation	9.67	8.72	9.41	5.65	10.45	10.17
Sample variance	93.59	76.01	88.55	31.88	109.22	103.40
Curtose	0.73	0.64	1.37	0.05	0.22	-0.21
Asymmetry	1.10	1.16	1.25	0.89	0.86	0.70
Range	54.13	43.97	53.97	24.70	47.36	45.25
Minimum	7.35	7.92	8.65	12.24	7.10	8.00
Maximum	61.48	51.89	62.62	36.93	54.46	53.25
Sum	17509.62	5870.67	6173.19	1678.18	5583.51	6144.18
Score	802.00	290.00	275.00	72.00	248.00	259.00
Major (1)	61.48	51.89	62.62	36.93	54.46	53.25
Minor (1)	7.35	7.92	8.65	12.24	7.10	8.00
Confidence Interval (95.0%)	0.67	1.01	1.12	1.33	1.31	1.24

Table 1.1. 3 - Statistical Summary for the Droplet Sizes Distribution for the Basic Buffer as the medium

Parameter	*BmimDCA*	*BmimCl*	*C_{12}mimCl*	*SDS*	*C_{12}mimDS*	*No Surfactant*
Mean	22.29	22.38	22.68	23.88	24.94	22.24
Standard Error	0.35	0.45	0.62	0.62	0.64	0.54
Median	19.02	19.55	21.07	20.59	21.74	18.73
Mode	17.15	17.71	15.64	19.27	15.24	9.42
Standard deviation	9.77	11.42	9.55	10.11	10.67	12.12
Sample variance	95.36	130.43	91.29	102.16	113.76	146.82
Curtose	1.24	0.37	1.47	0.58	-0.04	0.67
Asymmetry	1.28	1.01	0.95	1.02	0.80	1.10
Range	53.54	58.85	55.78	53.06	49.69	59.70
Minimum	8.00	7.35	7.22	8.12	7.35	6.71
Maximum	61.54	66.21	63.00	61.19	57.04	66.41
Sum	17162.53	14681.63	5419.87	6375.16	7032.23	11008.34
Score	770.00	656.00	239.00	267.00	282.00	495.00
Major (1)	61.54	66.21	63.00	61.19	57.04	66.41
Minor (1)	8.00	7.35	7.22	8.12	7.35	6.71
Confidence Interval (95.0%)	0.69	0.88	1.22	1.22	1.25	1.07

G – E-nose Signals for all tested VOCs and gels, with different surfactants and media (Aqueous, Acid and Basic)

Table 0.8. VOCs order for the different experiments performed on Chapter 5

Surfactant	Heptane	Hexane	DCM	Diethyl Ether	Ethyl Acetate	Chloroform	Toluene	Methanol	Ethanol	Acetonitrile	Acetone	Acet Aci
[C_{12}mim][Cl]	1	2	4	5	6	3	11	9	10	8	7	12
SDS	1	2	8	3	4	7	11	9	10	6	5	12
[C_{12}mim][DS]	7	1	3	2	6	10	5	9	11	4	8	12
[Bmim][Cl]	4	1	2	10	3	7	6	9	11	5	8	12
[Bmim][DCA]	4	1	2	11	3	8	6	7	10	5	9	12
No Surfactant	4	1	2	10	3	8	6	7	11	5	9	12

1) [C_{12}mim][Cl]

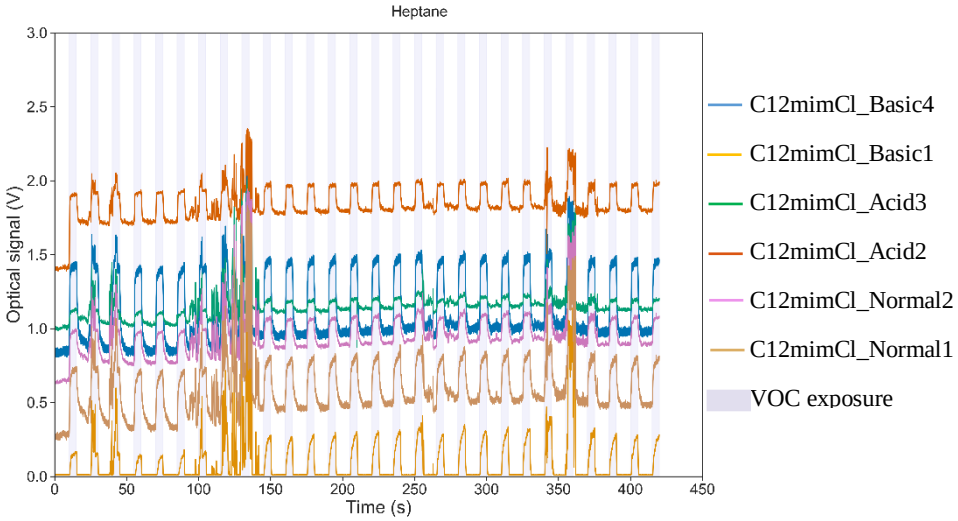
Heptane
Optical signal (V)
Time (s)
C12mimCl_Basic4
C12mimCl_Basic1
C12mimCl_Acid3
C12mimCl_Acid2
C12mimCl_Normal2
C12mimCl_Normal1
VOC exposure

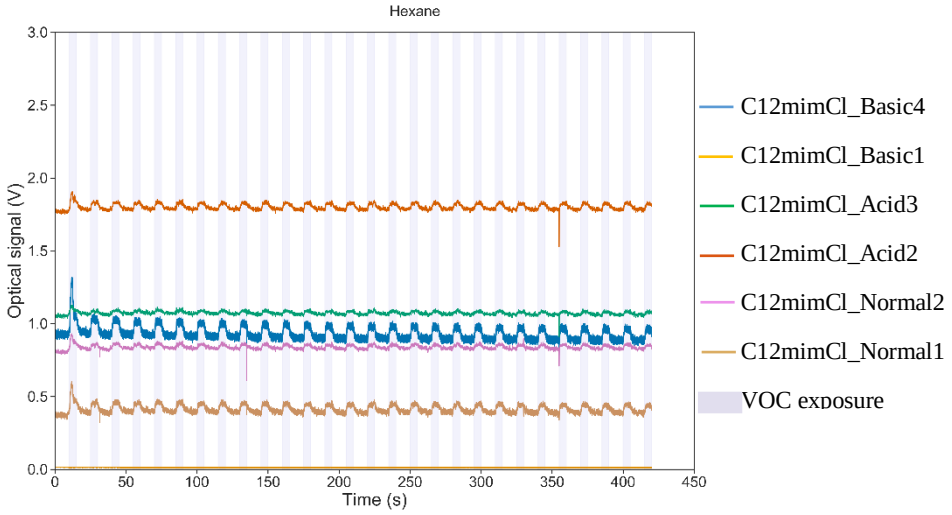
Hexane
Optical signal (V)
Time (s)
C12mimCl_Basic4
C12mimCl_Basic1
C12mimCl_Acid3
C12mimCl_Acid2
C12mimCl_Normal2
C12mimCl_Normal1
VOC exposure

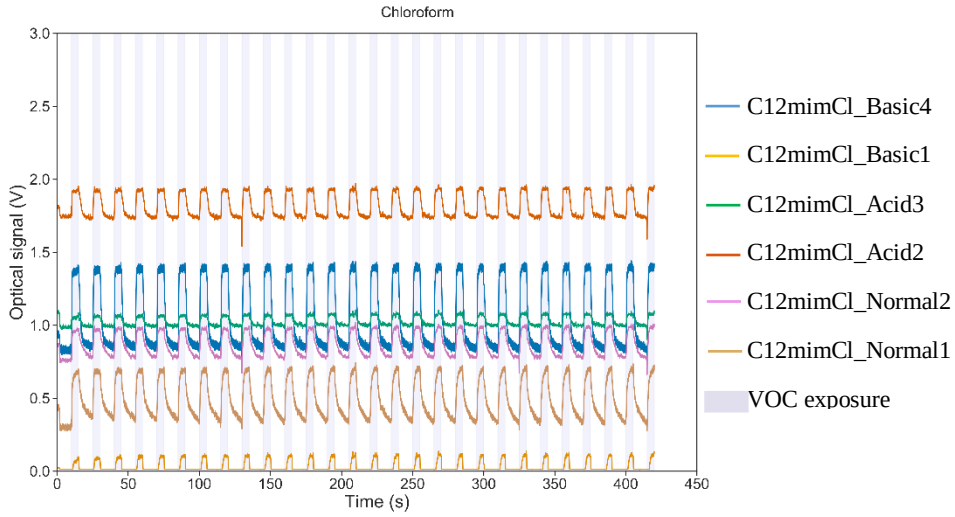
Chloroform
Optical signal (V)
Time (s)
C12mimCl_Basic4
C12mimCl_Basic1
C12mimCl_Acid3
C12mimCl_Acid2
C12mimCl_Normal2
C12mimCl_Normal1
VOC exposure

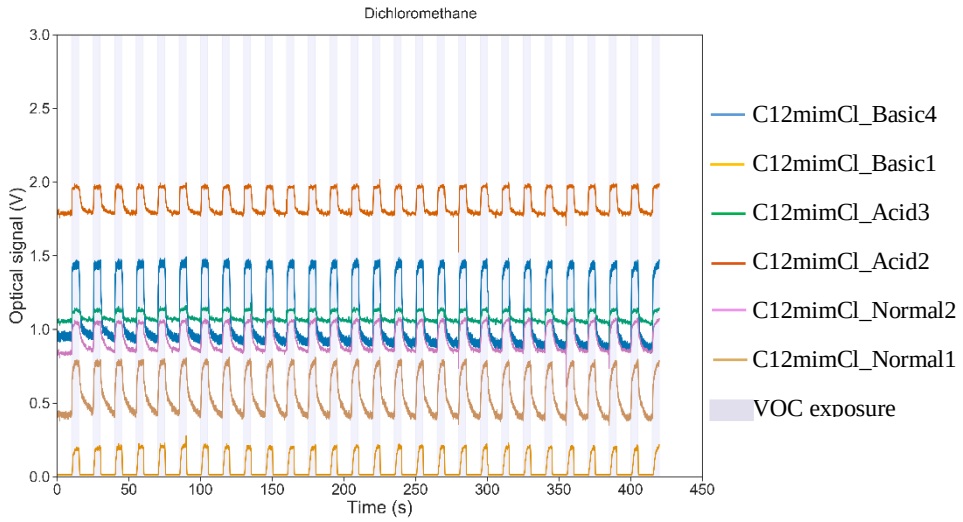
Dichloromethane
Optical signal (V)
Time (s)
C12mimCl_Basic4
C12mimCl_Basic1
C12mimCl_Acid3
C12mimCl_Acid2
C12mimCl_Normal2
C12mimCl_Normal1
VOC exposure

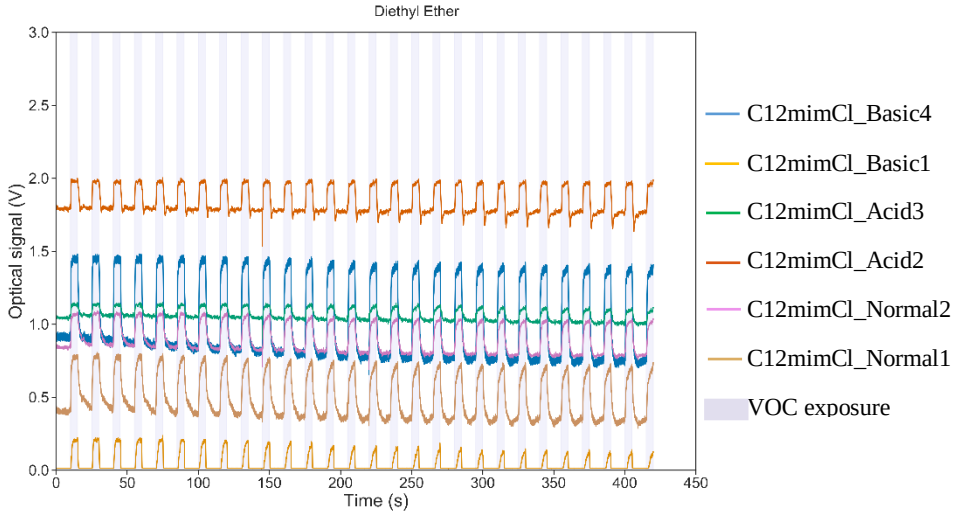
Diethyl Ether
Optical signal (V)
Time (s)
C12mimCl_Basic4
C12mimCl_Basic1
C12mimCl_Acid3
C12mimCl_Acid2
C12mimCl_Normal2
C12mimCl_Normal1
VOC exposure

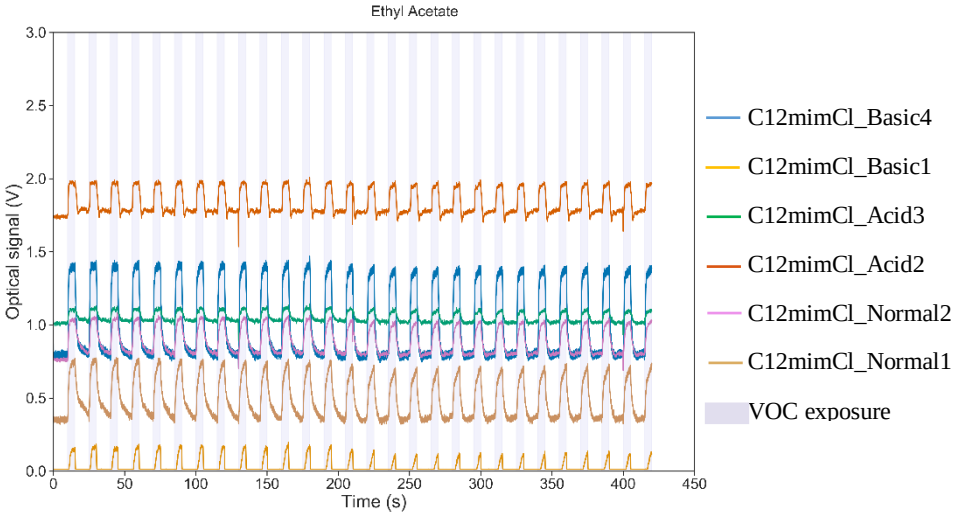
Ethyl Acetate
Optical signal (V)
Time (s)
C12mimCl_Basic4
C12mimCl_Basic1
C12mimCl_Acid3
C12mimCl_Acid2
C12mimCl_Normal2
C12mimCl_Normal1
VOC exposure

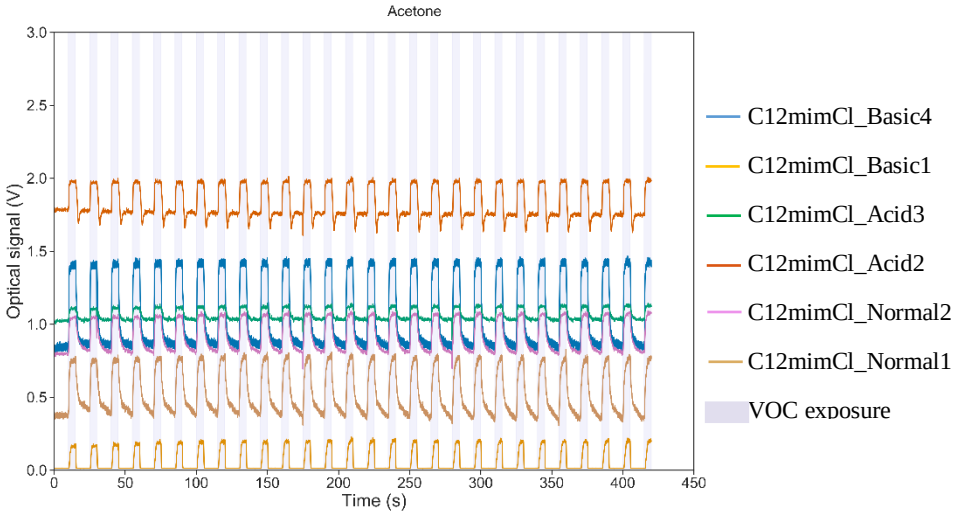
Acetone
Optical signal (V)
Time (s)
C12mimCl_Basic4
C12mimCl_Basic1
C12mimCl_Acid3
C12mimCl_Acid2
C12mimCl_Normal2
C12mimCl_Normal1
VOC exposure

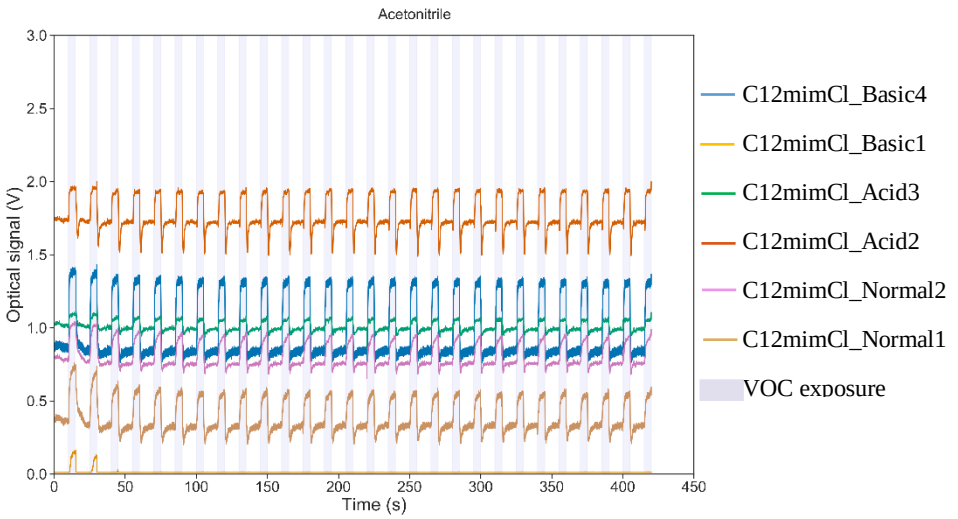
Acetonitrile
Optical signal (V)
Time (s)
C12mimCl_Basic4
C12mimCl_Basic1
C12mimCl_Acid3
C12mimCl_Acid2
C12mimCl_Normal2
C12mimCl_Normal1
VOC exposure

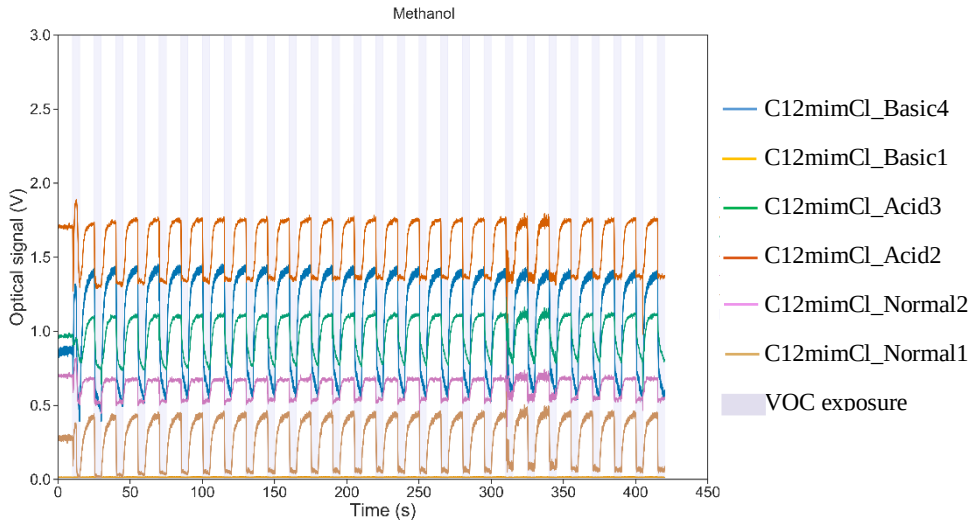
Methanol
Optical signal (V)
Time (s)
C12mimCl_Basic4
C12mimCl_Basic1
C12mimCl_Acid3
C12mimCl_Acid2
C12mimCl_Normal2
C12mimCl_Normal1
VOC exposure

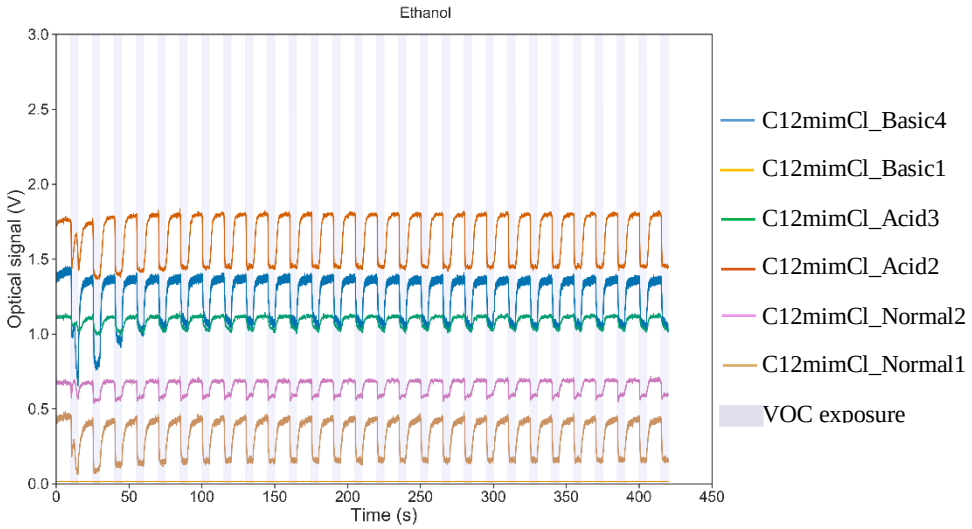
Ethanol
Optical signal (V)
Time (s)
C12mimCl_Basic4
C12mimCl_Basic1
C12mimCl_Acid3
C12mimCl_Acid2
C12mimCl_Normal2
C12mimCl_Normal1
VOC exposure

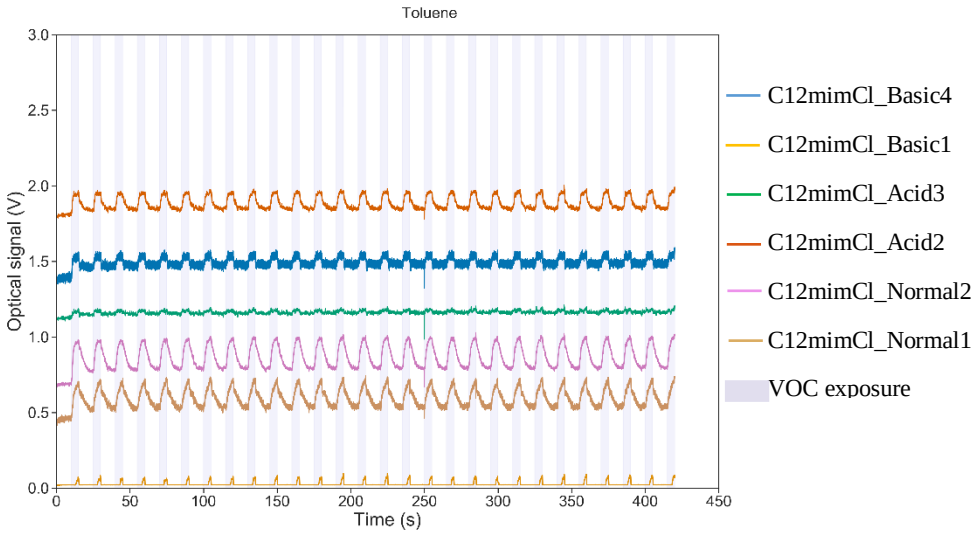
Toluene
Optical signal (V)
Time (s)
C12mimCl_Basic4
C12mimCl_Basic1
C12mimCl_Acid3
C12mimCl_Acid2
C12mimCl_Normal2
C12mimCl_Normal1
VOC exposure

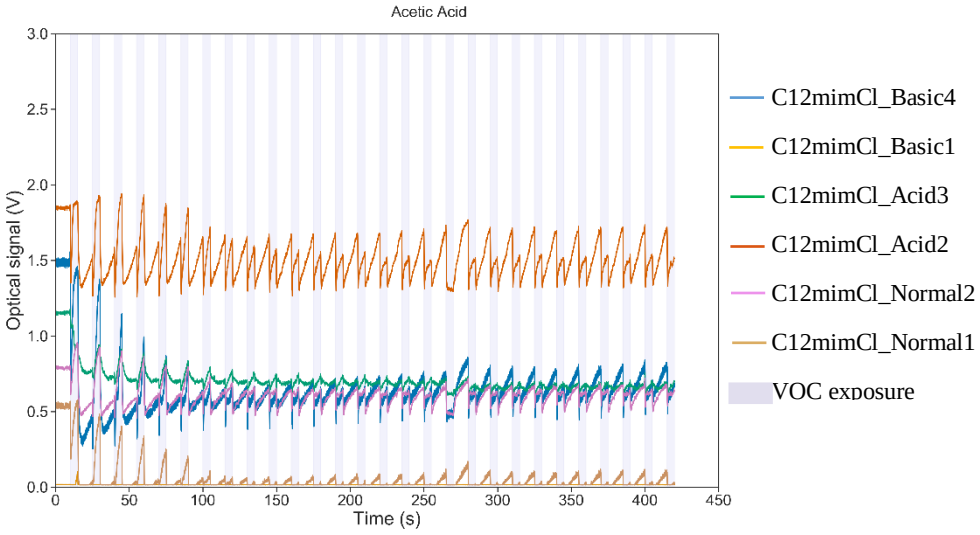
Acetic Acid
Optical signal (V)
Time (s)
C12mimCl_Basic4
C12mimCl_Basic1
C12mimCl_Acid3
C12mimCl_Acid2
C12mimCl_Normal2
C12mimCl_Normal1
VOC exposure

2) SDS

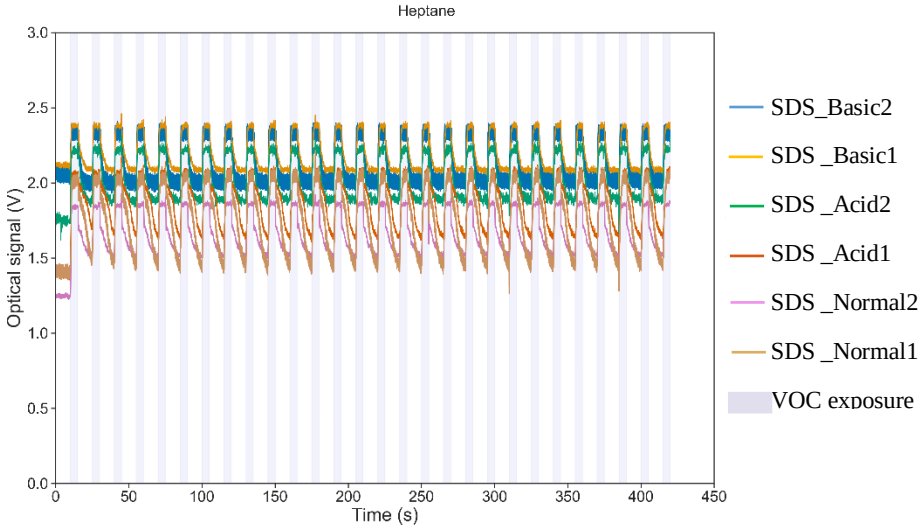
Heptane
Optical signal (V)
Time (s)
SDS_Basic2
SDS _Basic1
SDS _Acid2
SDS _Acid1
SDS _Normal2
SDS _Normal1
VOC exposure

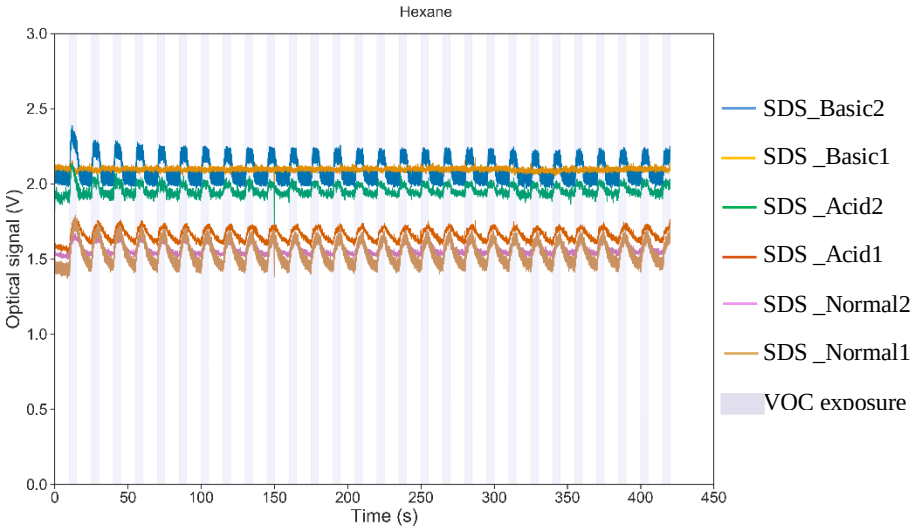
Hexane
Optical signal (V)
Time (s)
SDS_Basic2
SDS _Basic1
SDS _Acid2
SDS _Acid1
SDS _Normal2
SDS _Normal1
VOC exposure

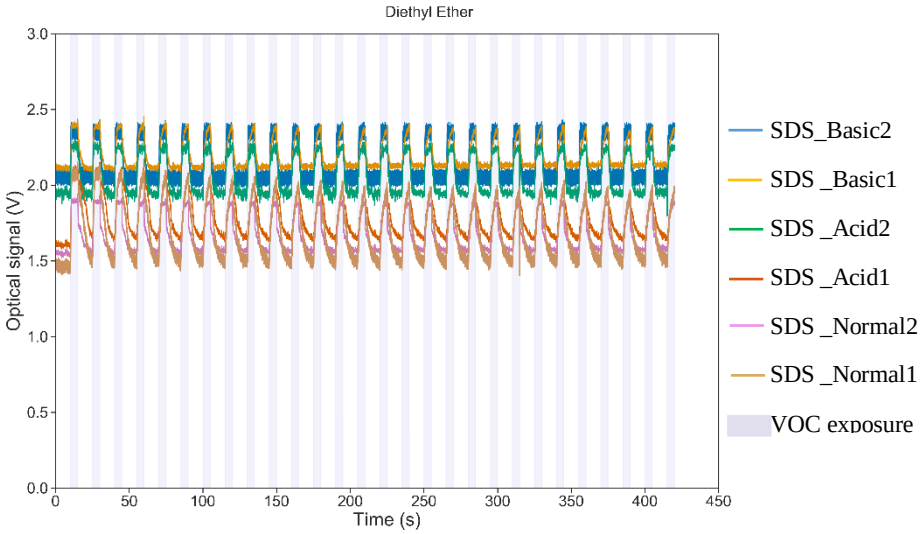
Diethyl Ether
Optical signal (V)
Time (s)
SDS_Basic2
SDS _Basic1
SDS _Acid2
SDS _Acid1
SDS _Normal2
SDS _Normal1
VOC exposure

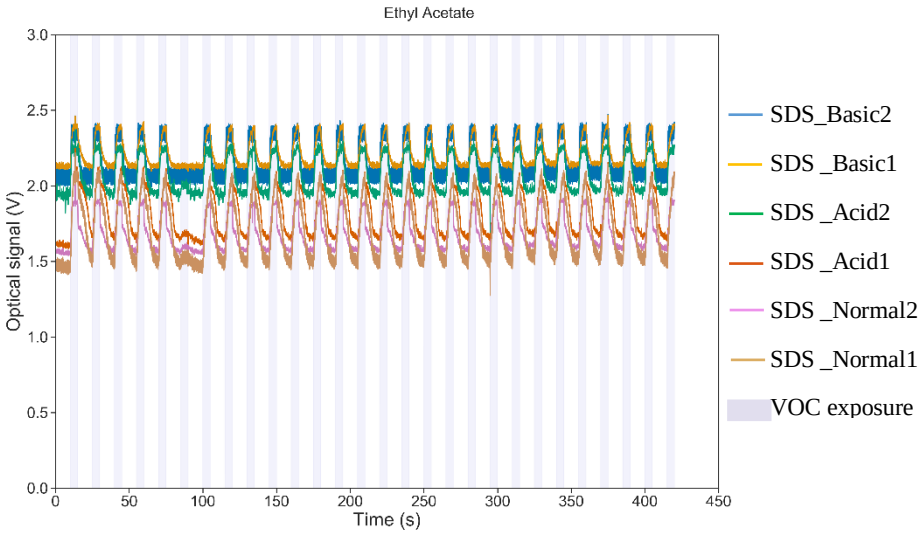
Ethyl Acetate
Optical signal (V)
Time (s)
SDS_Basic2
SDS _Basic1
SDS _Acid2
SDS _Acid1
SDS _Normal2
SDS _Normal1
VOC exposure

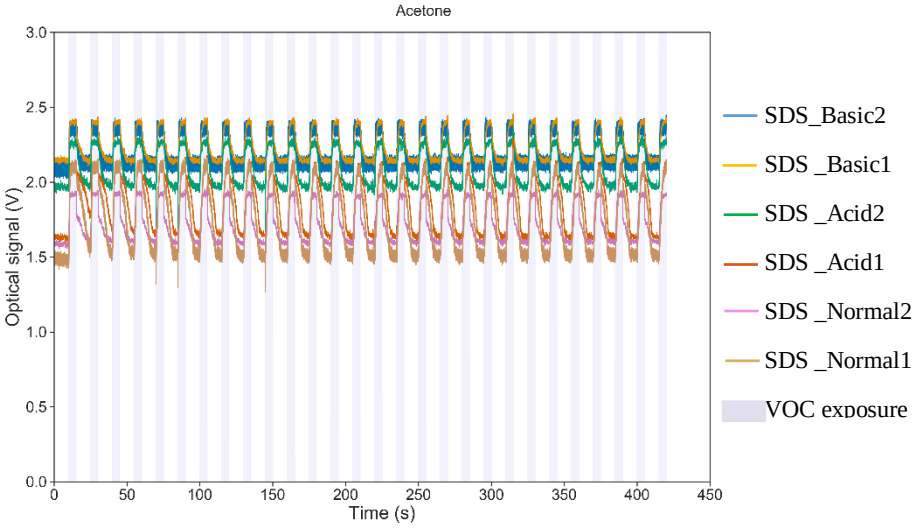
Acetone
Optical signal (V)
Time (s)
SDS_Basic2
SDS _Basic1
SDS _Acid2
SDS _Acid1
SDS _Normal2
SDS _Normal1
VOC exposure

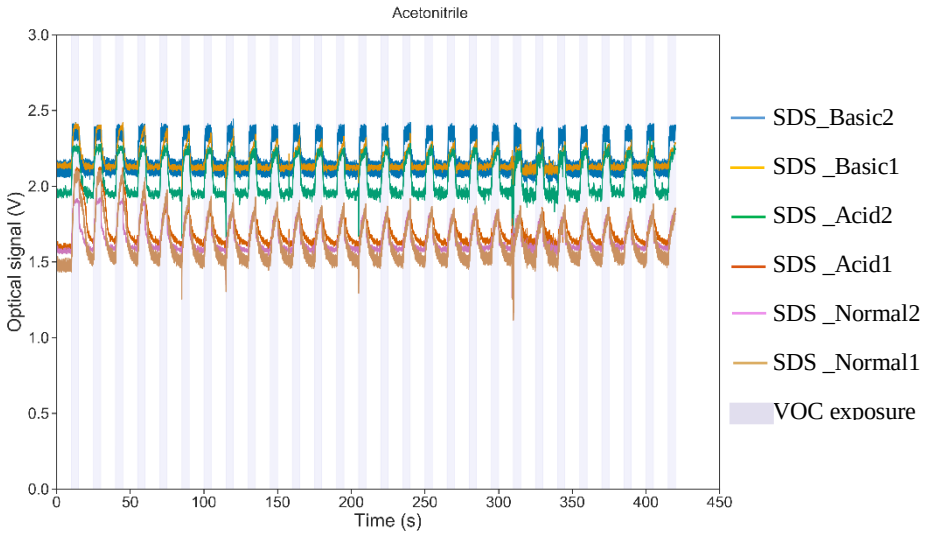
Acetonitrile
Optical signal (V)
Time (s)
SDS_Basic2
SDS _Basic1
SDS _Acid2
SDS _Acid1
SDS _Normal2
SDS _Normal1
VOC exposure

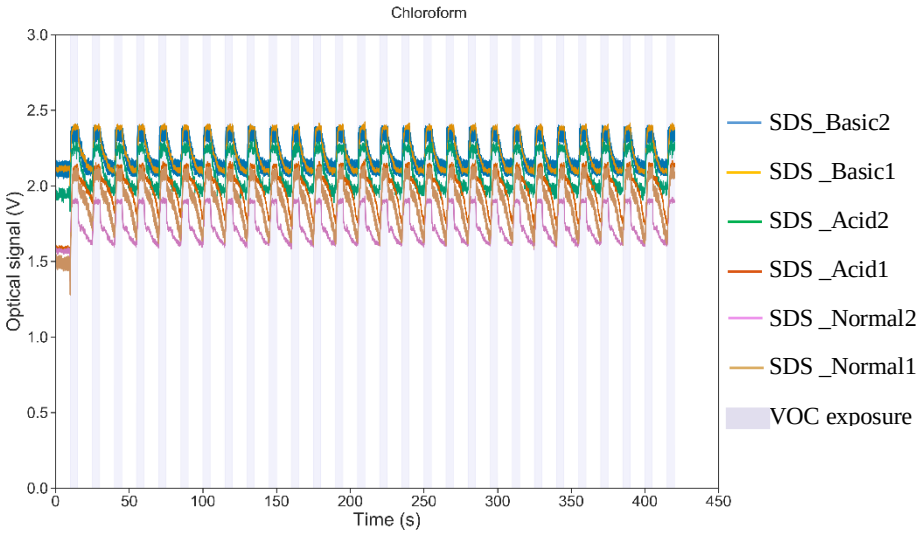
Chloroform
Optical signal (V)
Time (s)
SDS_Basic2
SDS _Basic1
SDS _Acid2
SDS _Acid1
SDS _Normal2
SDS _Normal1
VOC exposure

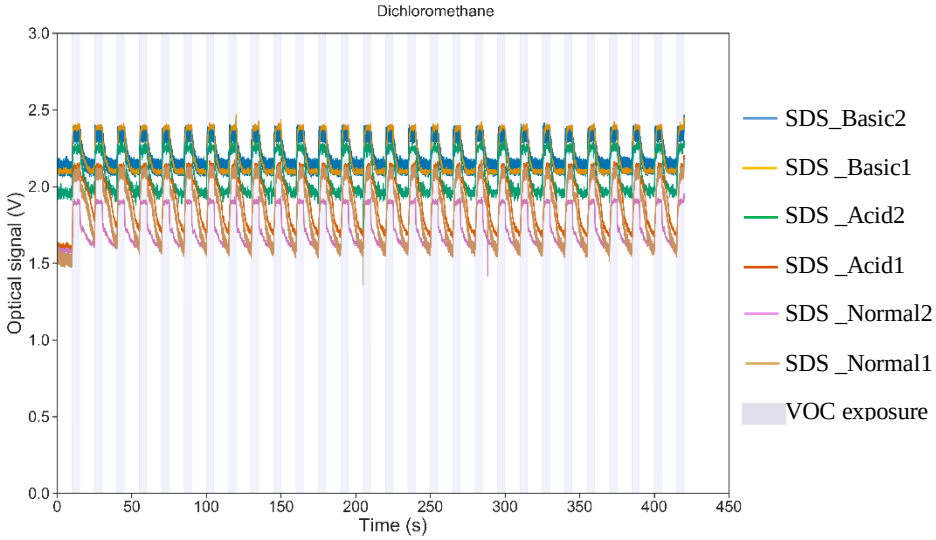
Dichloromethane
Optical signal (V)
Time (s)
SDS_Basic2
SDS _Basic1
SDS _Acid2
SDS _Acid1
SDS _Normal2
SDS _Normal1
VOC exposure

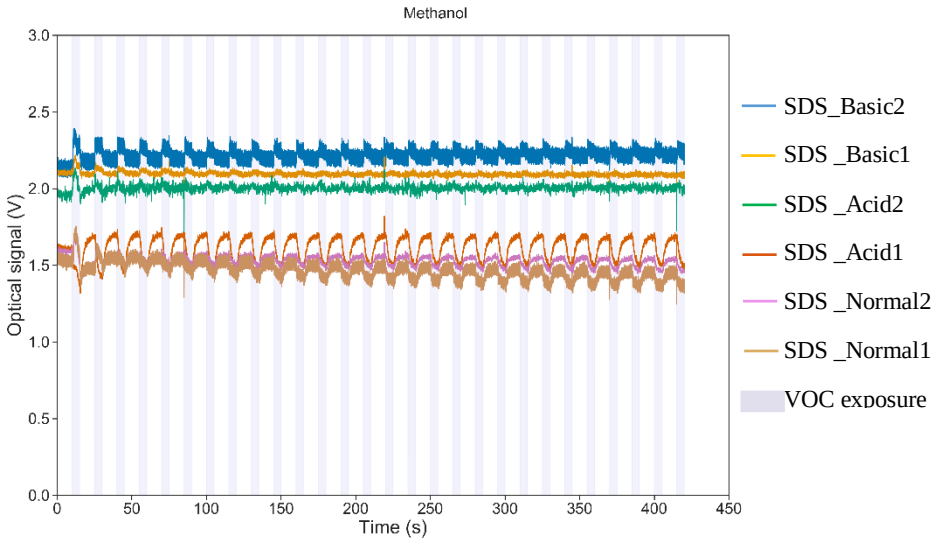
Methanol
Optical signal (V)
Time (s)
SDS_Basic2
SDS _Basic1
SDS _Acid2
SDS _Acid1
SDS _Normal2
SDS _Normal1
VOC exposure

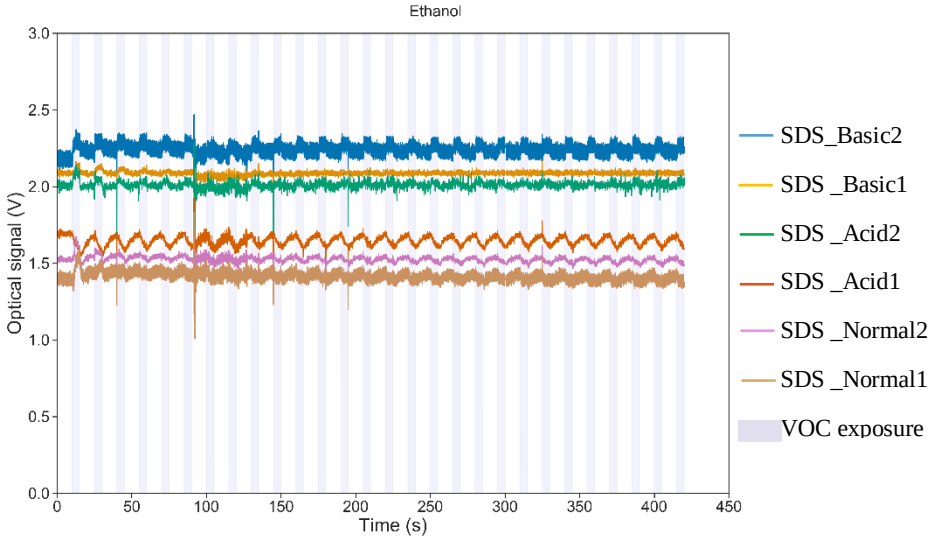
Ethanol
Optical signal (V)
Time (s)
SDS_Basic2
SDS _Basic1
SDS _Acid2
SDS _Acid1
SDS _Normal2
SDS _Normal1
VOC exposure

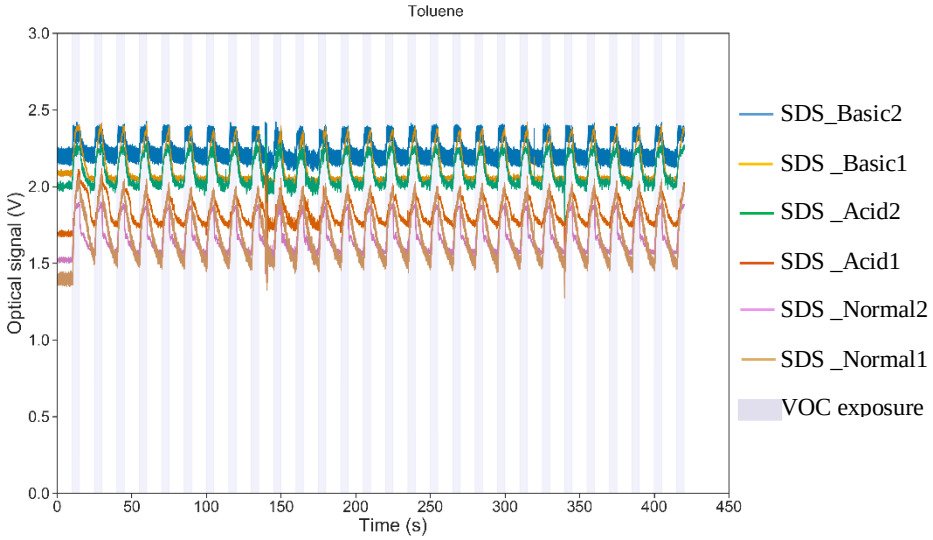
Toluene
Optical signal (V)
Time (s)
SDS_Basic2
SDS _Basic1
SDS _Acid2
SDS _Acid1
SDS _Normal2
SDS _Normal1
VOC exposure

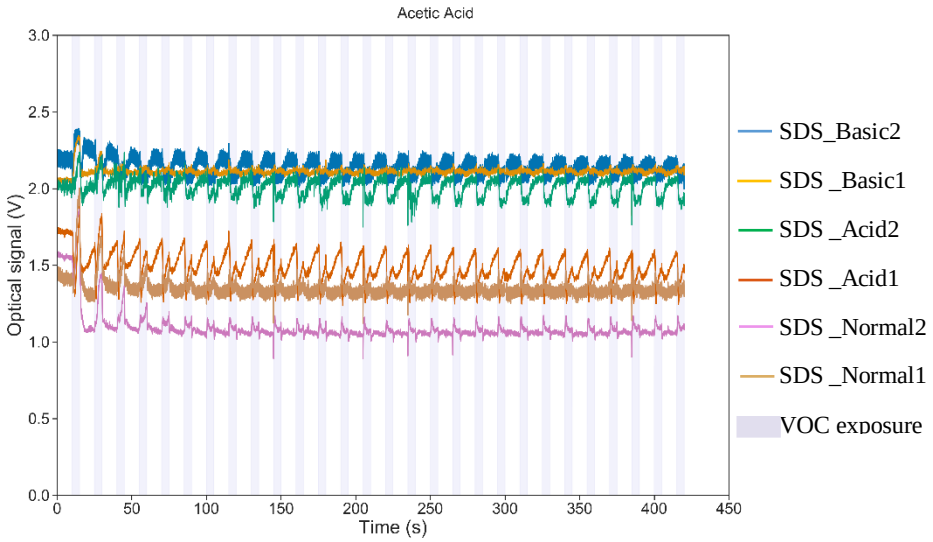
Acetic Acid
Optical signal (V)
Time (s)
SDS_Basic2
SDS _Basic1
SDS _Acid2
SDS _Acid1
SDS _Normal2
SDS _Normal1
VOC exposure

3) [C_{12}mim][DS]

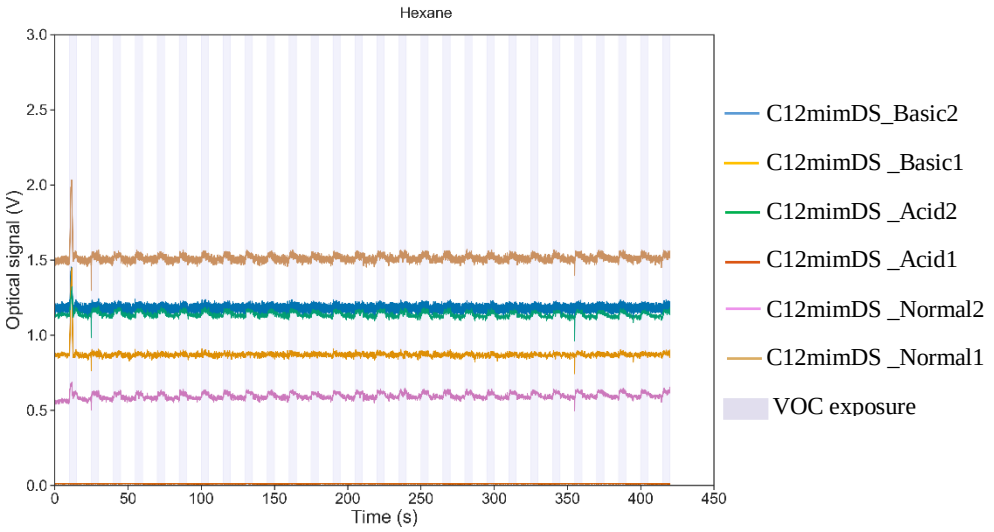
Hexane
Optical signal (V)
Time (s)
C12mimDS_Basic2
C12mimDS _Basic1
C12mimDS _Acid2
C12mimDS _Acid1
C12mimDS _Normal2
C12mimDS _Normal1
VOC exposure

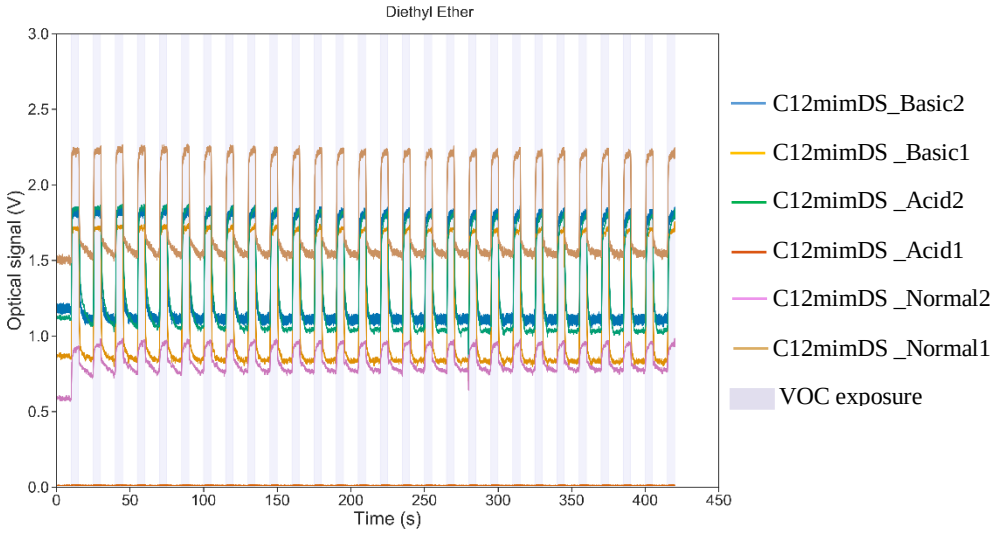
Diethyl Ether
Optical signal (V)
Time (s)
C12mimDS_Basic2
C12mimDS _Basic1
C12mimDS _Acid2
C12mimDS _Acid1
C12mimDS _Normal2
C12mimDS _Normal1
VOC exposure

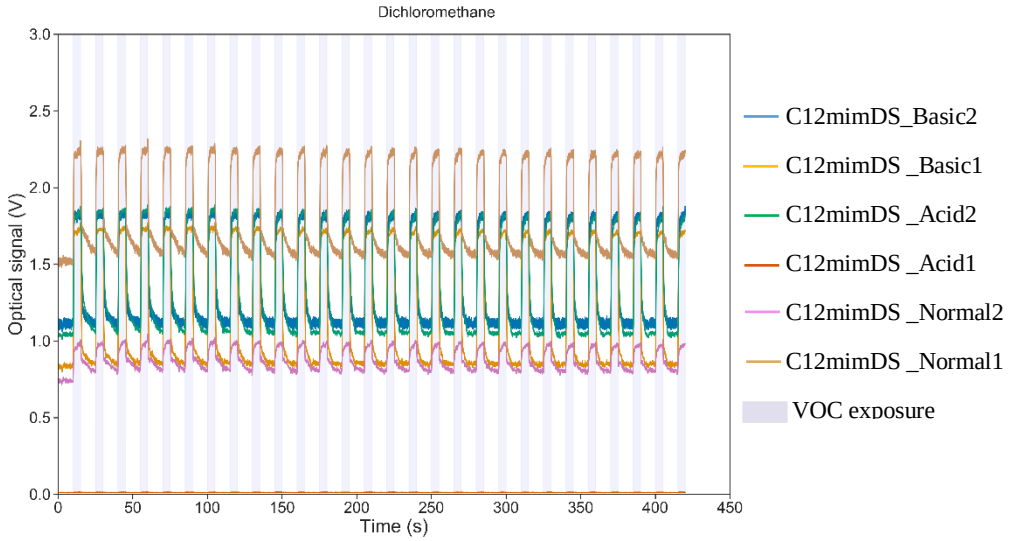
Dichloromethane
Optical signal (V)
Time (s)
C12mimDS_Basic2
C12mimDS _Basic1
C12mimDS _Acid2
C12mimDS _Acid1
C12mimDS _Normal2
C12mimDS _Normal1
VOC exposure

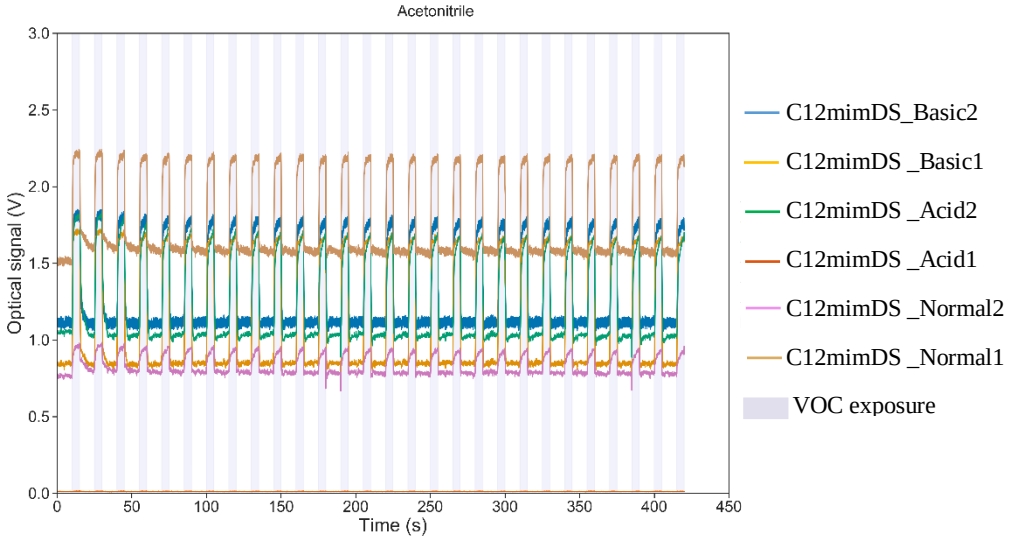
Acetonitrile
Optical signal (V)
Time (s)
C12mimDS_Basic2
C12mimDS _Basic1
C12mimDS _Acid2
C12mimDS _Acid1
C12mimDS _Normal2
C12mimDS _Normal1
VOC exposure

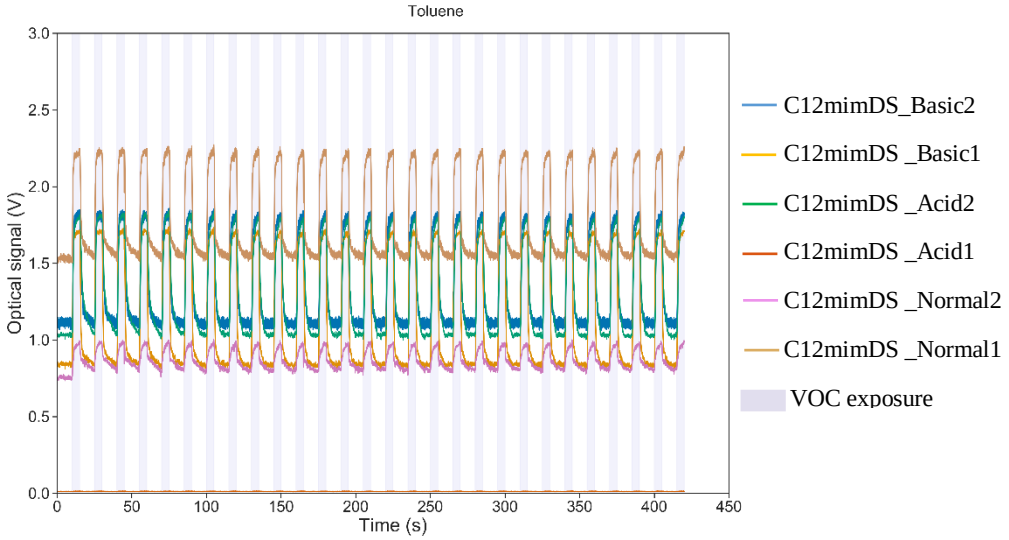
Toluene
Optical signal (V)
Time (s)
C12mimDS_Basic2
C12mimDS _Basic1
C12mimDS _Acid2
C12mimDS _Acid1
C12mimDS _Normal2
C12mimDS _Normal1
VOC exposure

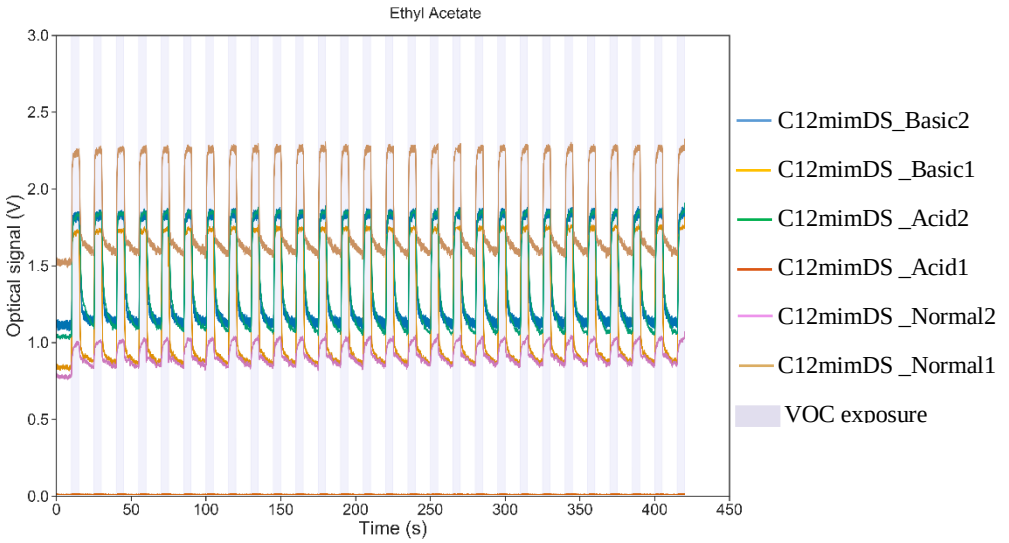
Ethyl Acetate
Optical signal (V)
Time (s)
C12mimDS_Basic2
C12mimDS _Basic1
C12mimDS _Acid2
C12mimDS _Acid1
C12mimDS _Normal2
C12mimDS _Normal1
VOC exposure

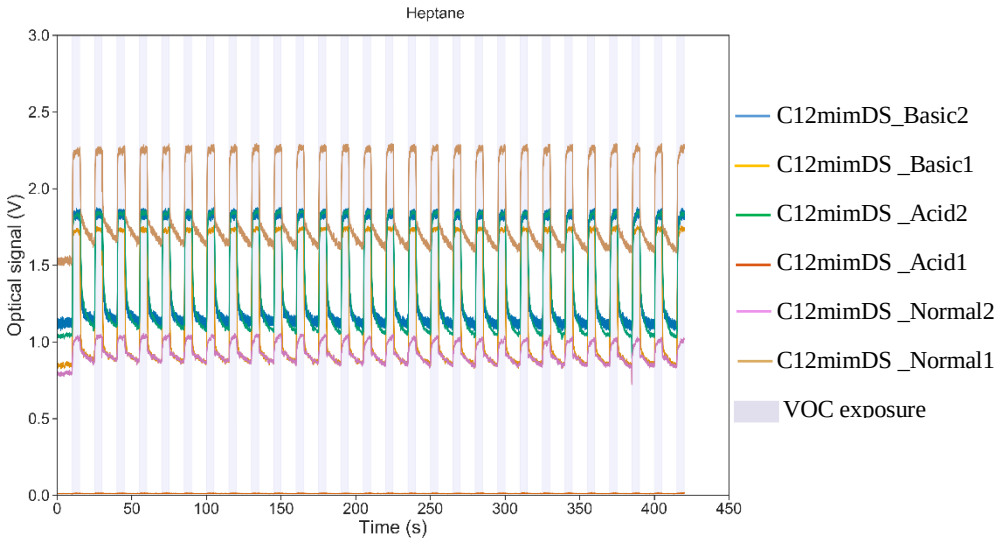
Heptane
Optical signal (V)
Time (s)
C12mimDS_Basic2
C12mimDS _Basic1
C12mimDS _Acid2
C12mimDS _Acid1
C12mimDS _Normal2
C12mimDS _Normal1
VOC exposure

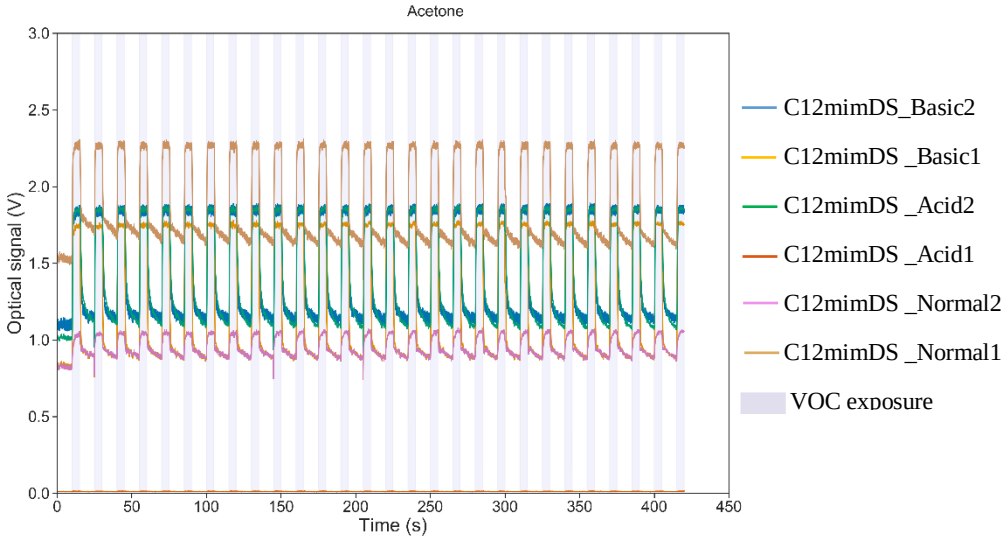
Acetone
Optical signal (V)
Time (s)
C12mimDS_Basic2
C12mimDS _Basic1
C12mimDS _Acid2
C12mimDS _Acid1
C12mimDS _Normal2
C12mimDS _Normal1
VOC exposure

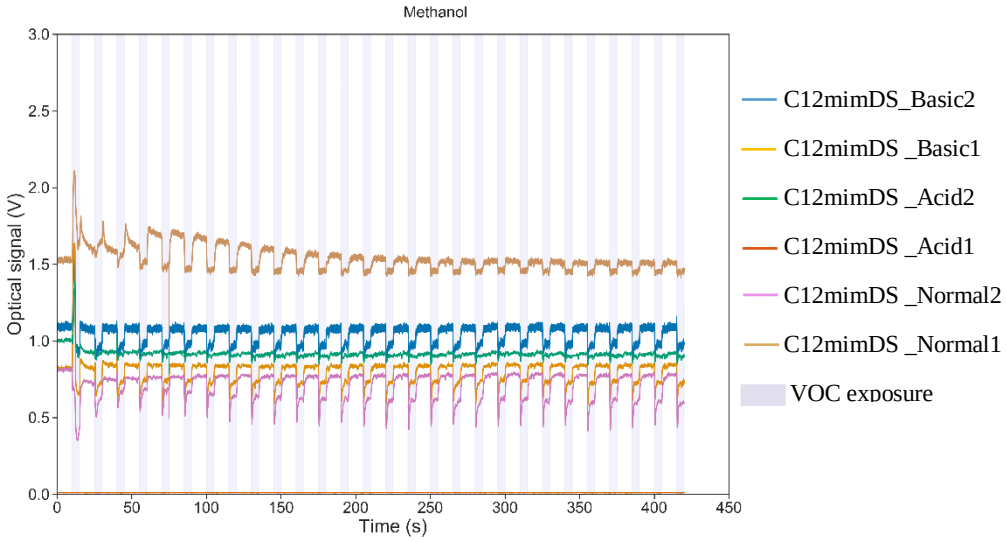
Methanol
Optical signal (V)
Time (s)
C12mimDS_Basic2
C12mimDS _Basic1
C12mimDS _Acid2
C12mimDS _Acid1
C12mimDS _Normal2
C12mimDS _Normal1
VOC exposure

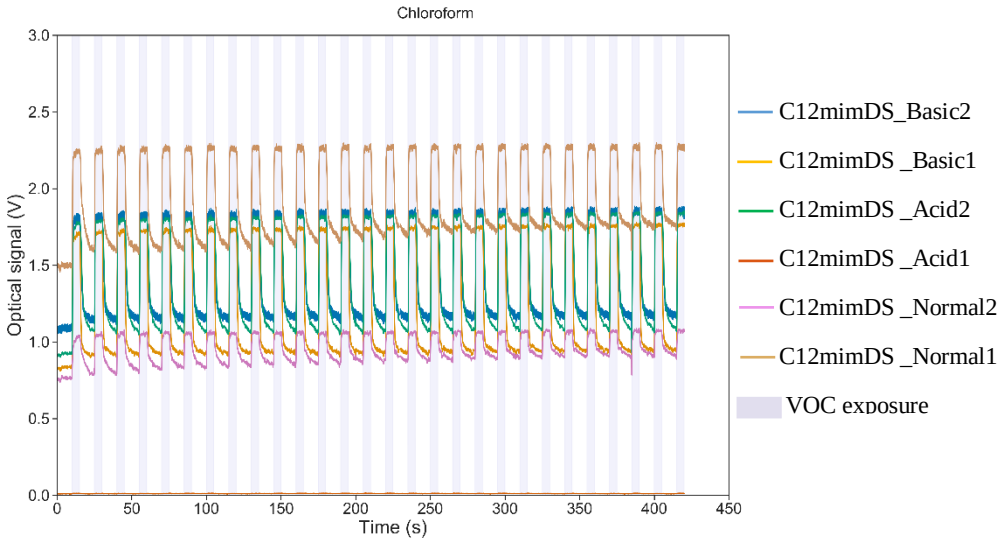
Chloroform
Optical signal (V)
Time (s)
C12mimDS_Basic2
C12mimDS _Basic1
C12mimDS _Acid2
C12mimDS _Acid1
C12mimDS _Normal2
C12mimDS _Normal1
VOC exposure

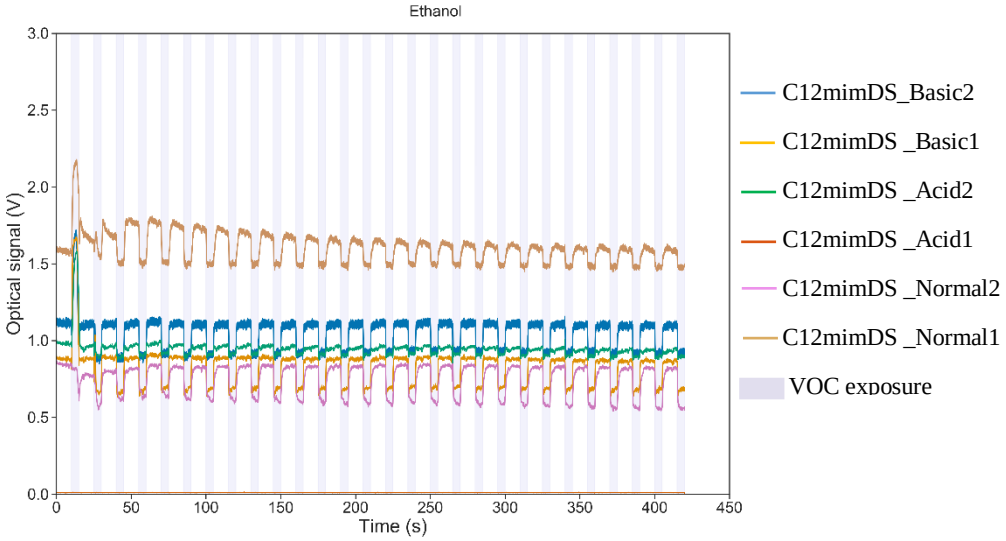
Ethanol
Optical signal (V)
Time (s)
C12mimDS_Basic2
C12mimDS _Basic1
C12mimDS _Acid2
C12mimDS _Acid1
C12mimDS _Normal2
C12mimDS _Normal1
VOC exposure

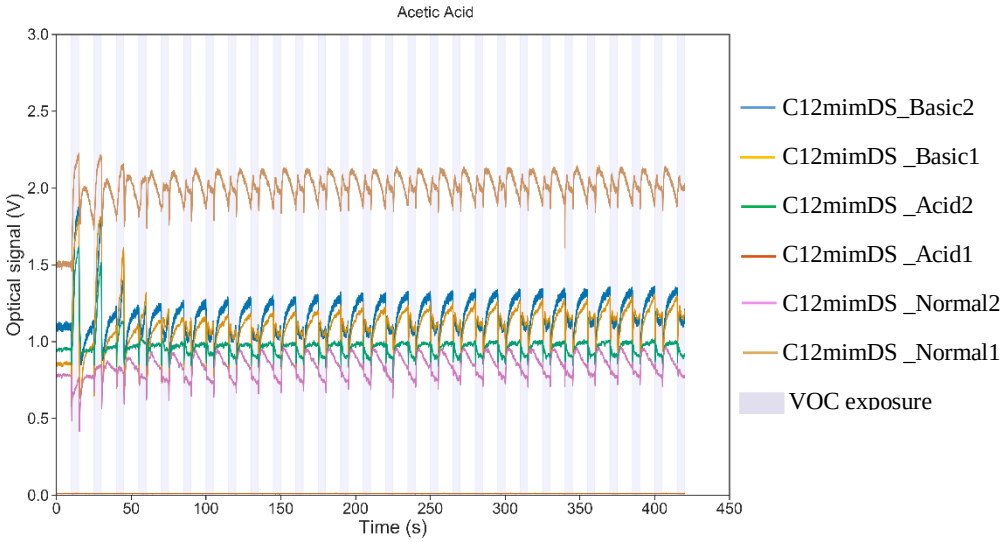
Acetic Acid
Optical signal (V)
Time (s)
C12mimDS_Basic2
C12mimDS _Basic1
C12mimDS _Acid2
C12mimDS _Acid1
C12mimDS _Normal2
C12mimDS _Normal1
VOC exposure

4) [Bmim][Cl]

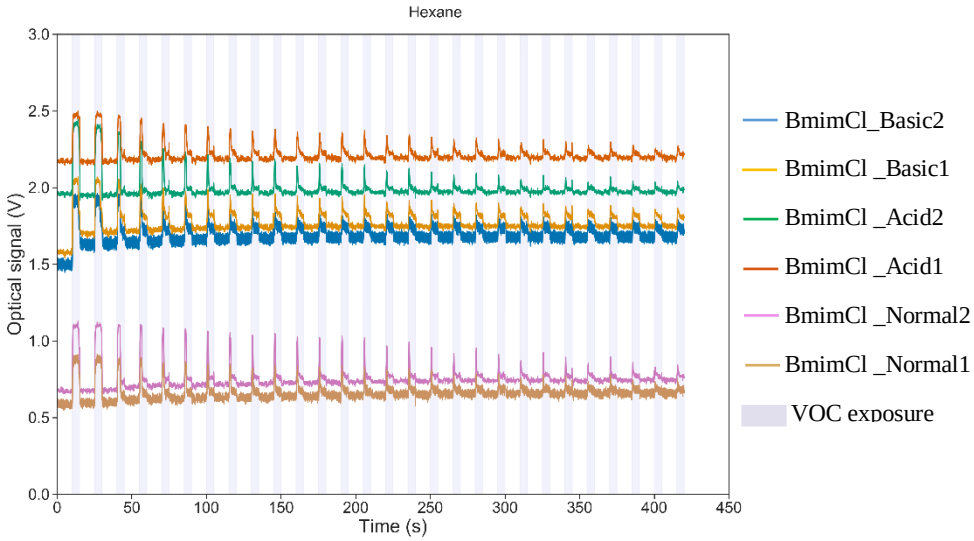
Hexane
Optical signal (V)
Time (s)
BmimCl_Basic2
BmimCl _Basic1
BmimCl _Acid2
BmimCl _Acid1
BmimCl _Normal2
BmimCl _Normal1
VOC exposure

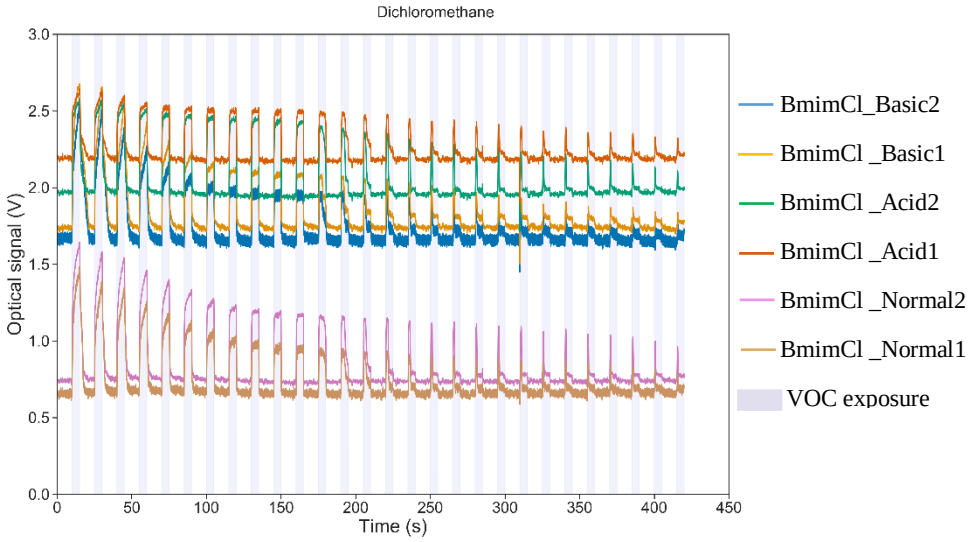
Dichloromethane
Optical signal (V)
Time (s)
BmimCl_Basic2
BmimCl _Basic1
BmimCl _Acid2
BmimCl _Acid1
BmimCl _Normal2
BmimCl _Normal1
VOC exposure

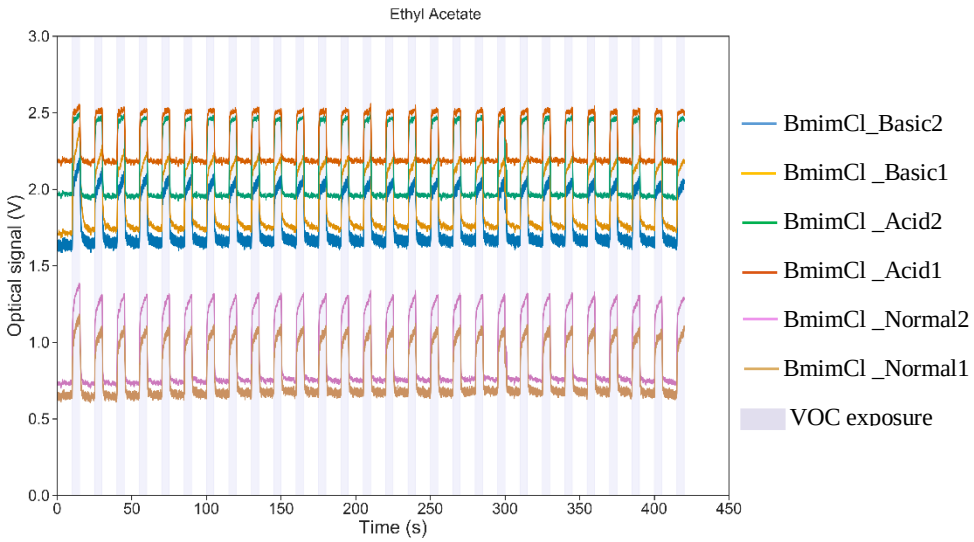
Ethyl Acetate
Optical signal (V)
Time (s)
BmimCl_Basic2
BmimCl _Basic1
BmimCl _Acid2
BmimCl _Acid1
BmimCl _Normal2
BmimCl _Normal1
VOC exposure

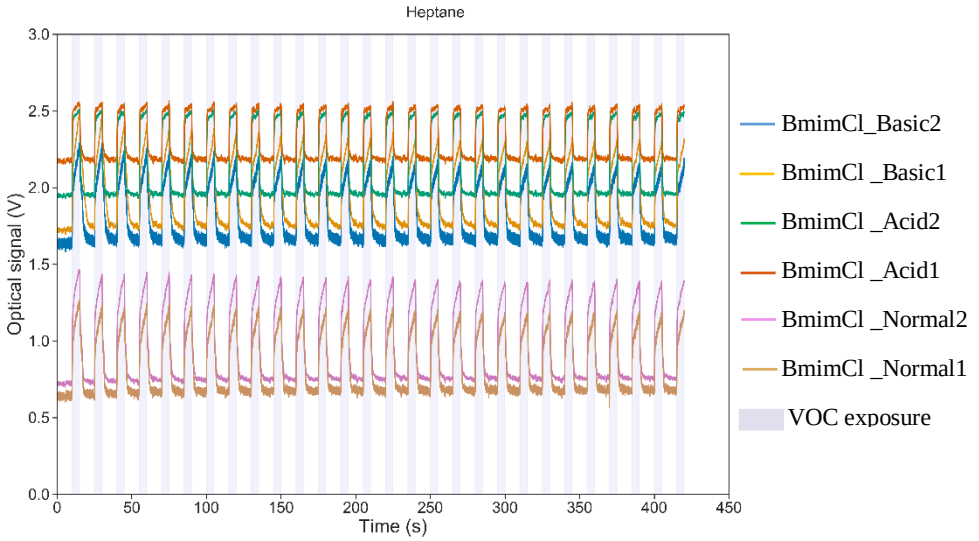
Heptane
Optical signal (V)
Time (s)
BmimCl_Basic2
BmimCl _Basic1
BmimCl _Acid2
BmimCl _Acid1
BmimCl _Normal2
BmimCl _Normal1
VOC exposure

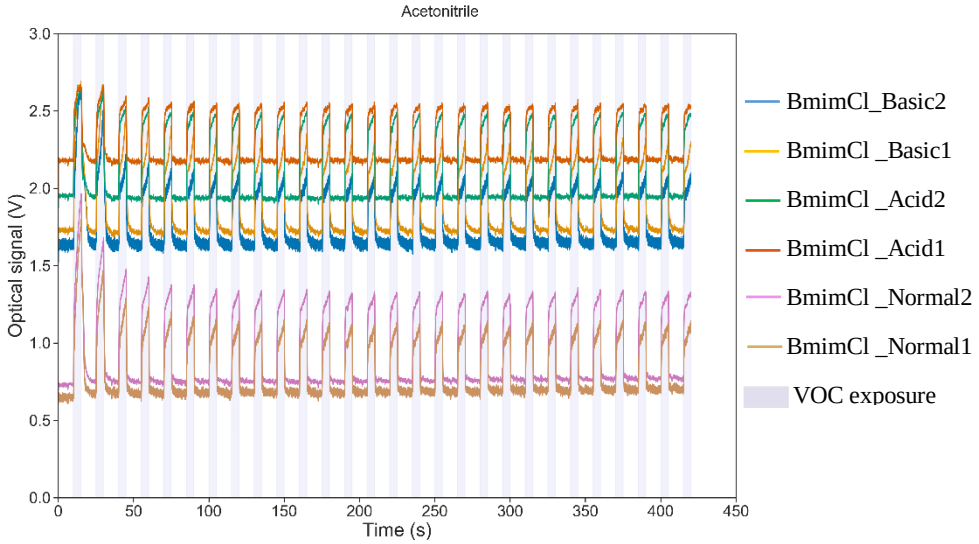
Acetonitrile
Optical signal (V)
Time (s)
BmimCl_Basic2
BmimCl _Basic1
BmimCl _Acid2
BmimCl _Acid1
BmimCl _Normal2
BmimCl _Normal1
VOC exposure

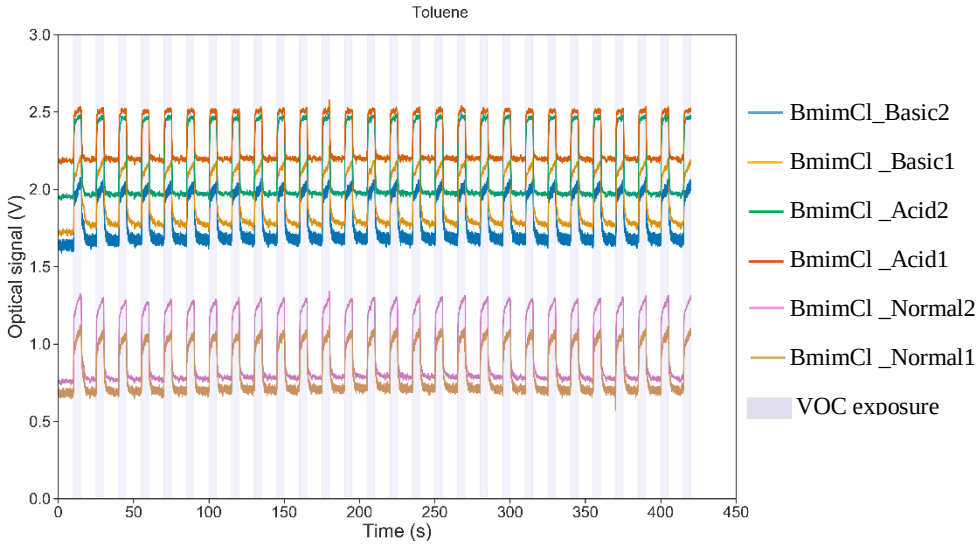
Toluene
Optical signal (V)
Time (s)
BmimCl_Basic2
BmimCl _Basic1
BmimCl _Acid2
BmimCl _Acid1
BmimCl _Normal2
BmimCl _Normal1
VOC exposure

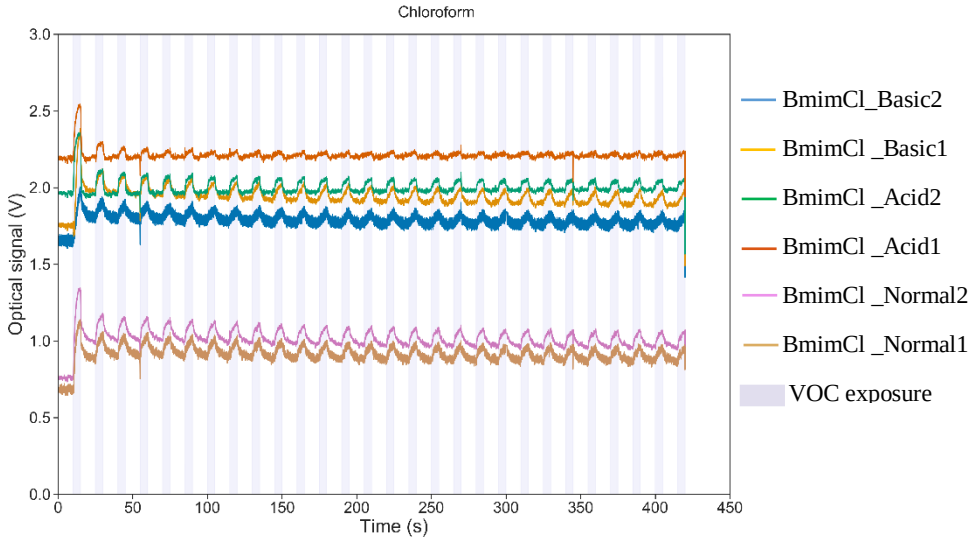
Chloroform
Optical signal (V)
Time (s)
BmimCl_Basic2
BmimCl _Basic1
BmimCl _Acid2
BmimCl _Acid1
BmimCl _Normal2
BmimCl _Normal1
VOC exposure

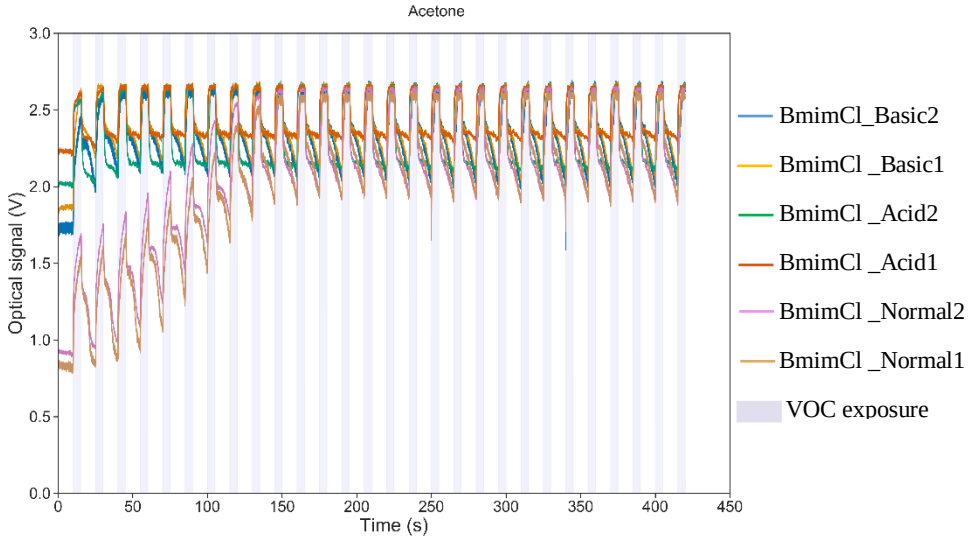
Acetone
Optical signal (V)
Time (s)
BmimCl_Basic2
BmimCl _Basic1
BmimCl _Acid2
BmimCl _Acid1
BmimCl _Normal2
BmimCl _Normal1
VOC exposure

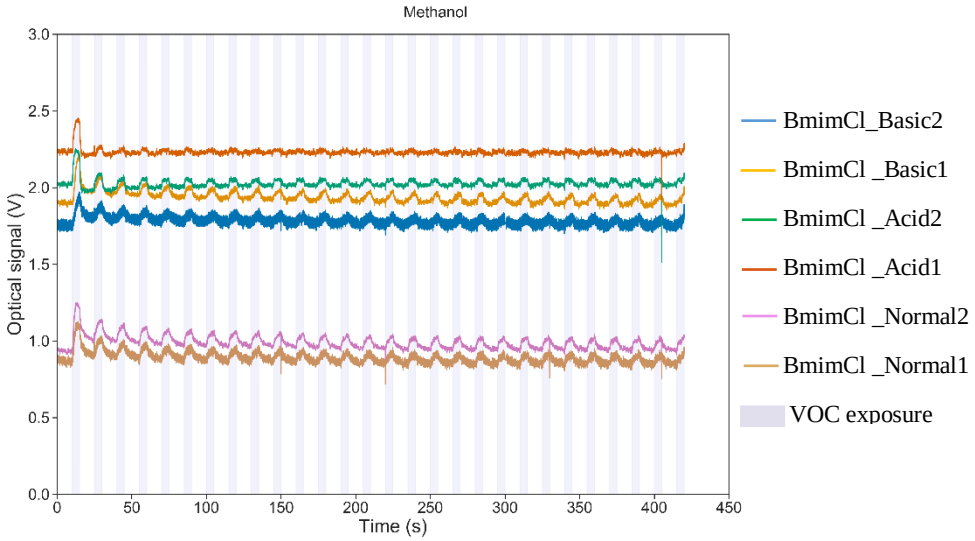
Methanol
Optical signal (V)
Time (s)
BmimCl_Basic2
BmimCl _Basic1
BmimCl _Acid2
BmimCl _Acid1
BmimCl _Normal2
BmimCl _Normal1
VOC exposure

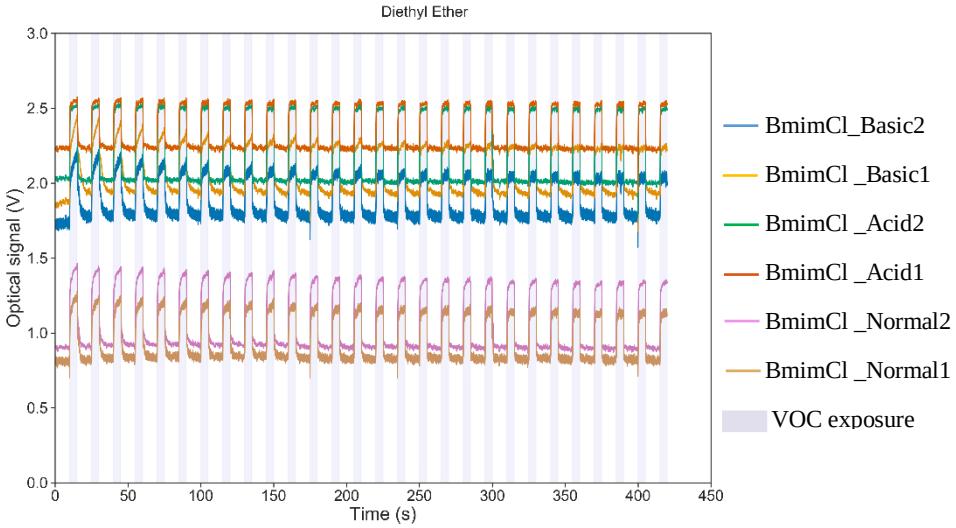
Diethyl Ether
Optical signal (V)
Time (s)
BmimCl_Basic2
BmimCl _Basic1
BmimCl _Acid2
BmimCl _Acid1
BmimCl _Normal2
BmimCl _Normal1
VOC exposure

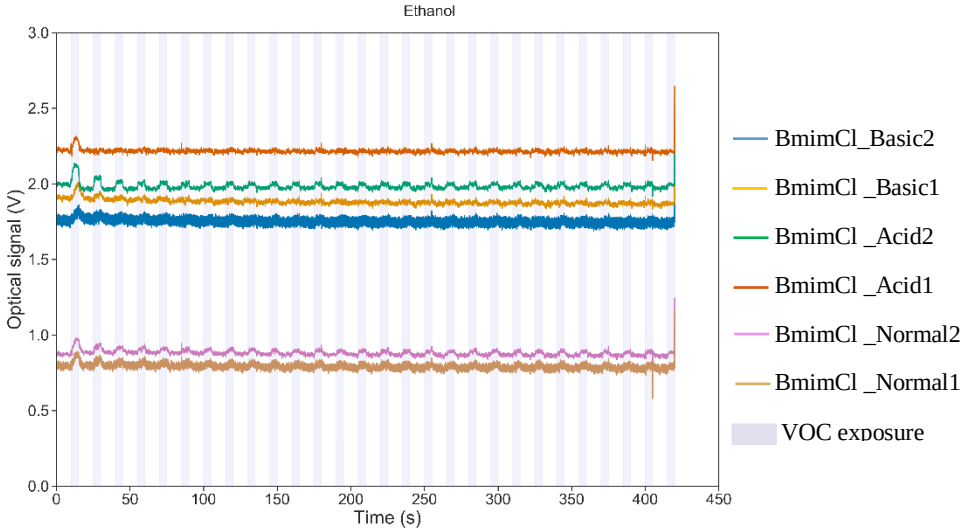
Ethanol
Optical signal (V)
Time (s)
BmimCl_Basic2
BmimCl _Basic1
BmimCl _Acid2
BmimCl _Acid1
BmimCl _Normal2
BmimCl _Normal1
VOC exposure

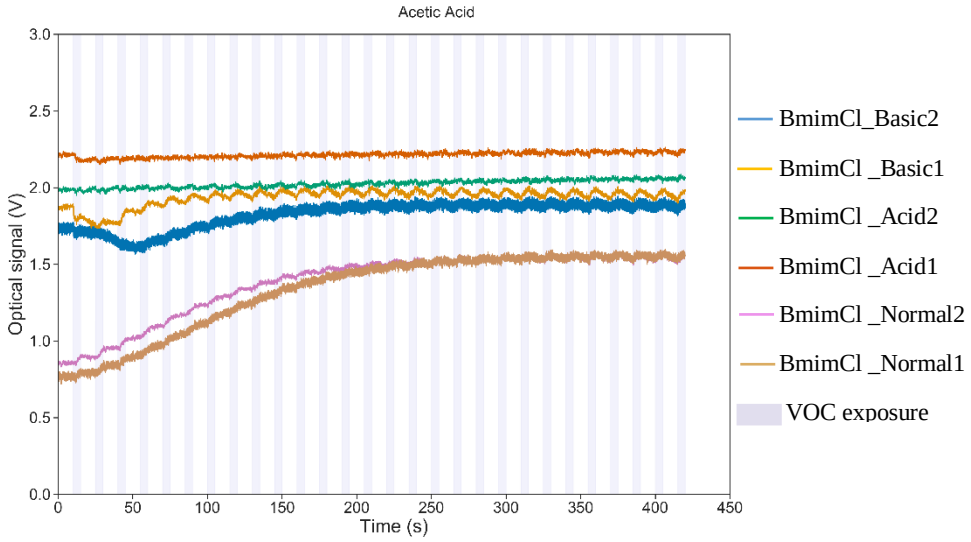
Acetic Acid
Optical signal (V)
Time (s)
BmimCl_Basic2
BmimCl _Basic1
BmimCl _Acid2
BmimCl _Acid1
BmimCl _Normal2
BmimCl _Normal1
VOC exposure

5) [Bmim][DCA]

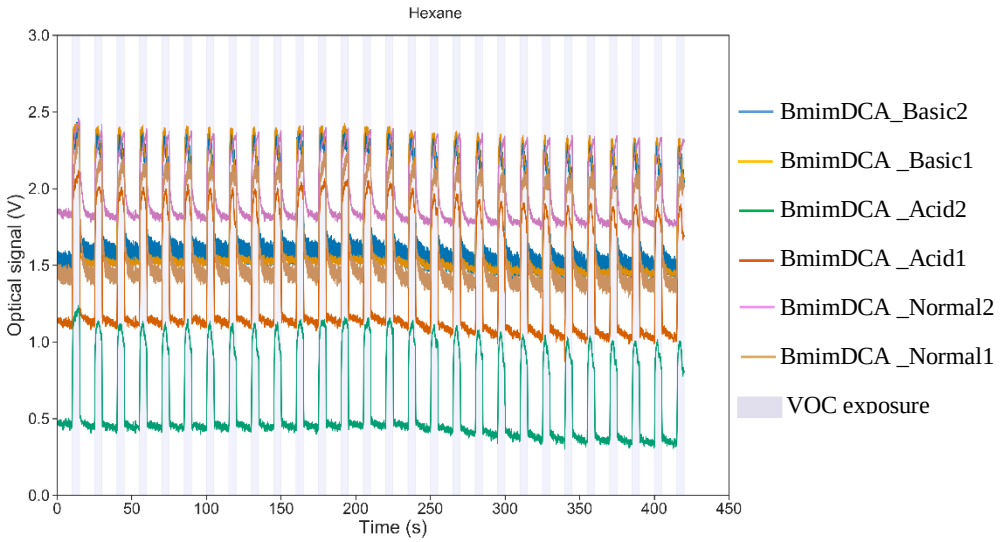
Hexane
Optical signal (V)
Time (s)
BmimDCA_Basic2
BmimDCA _Basic1
BmimDCA _Acid2
BmimDCA _Acid1
BmimDCA _Normal2
BmimDCA _Normal1
VOC exposure

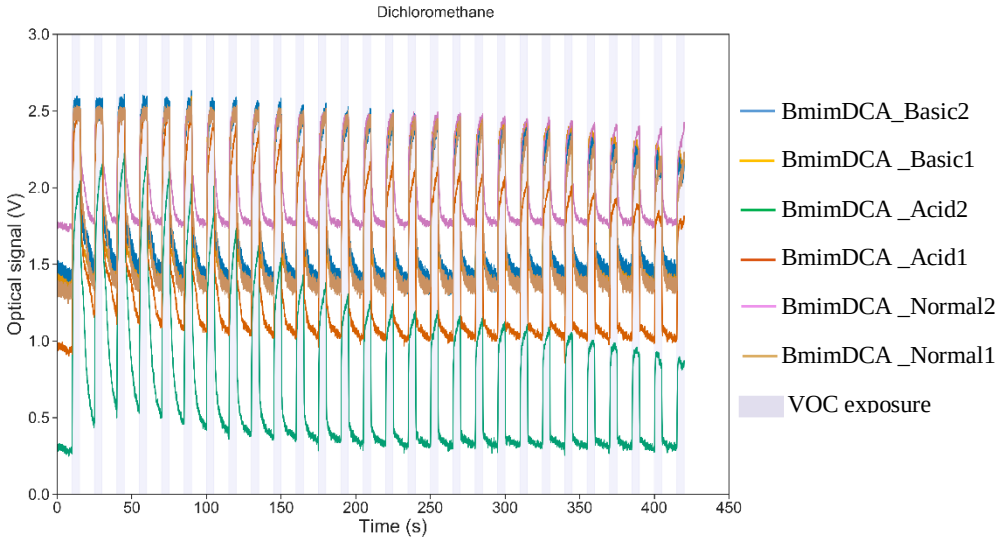
Dichloromethane
Optical signal (V)
Time (s)
BmimDCA_Basic2
BmimDCA _Basic1
BmimDCA _Acid2
BmimDCA _Acid1
BmimDCA _Normal2
BmimDCA _Normal1
VOC exposure

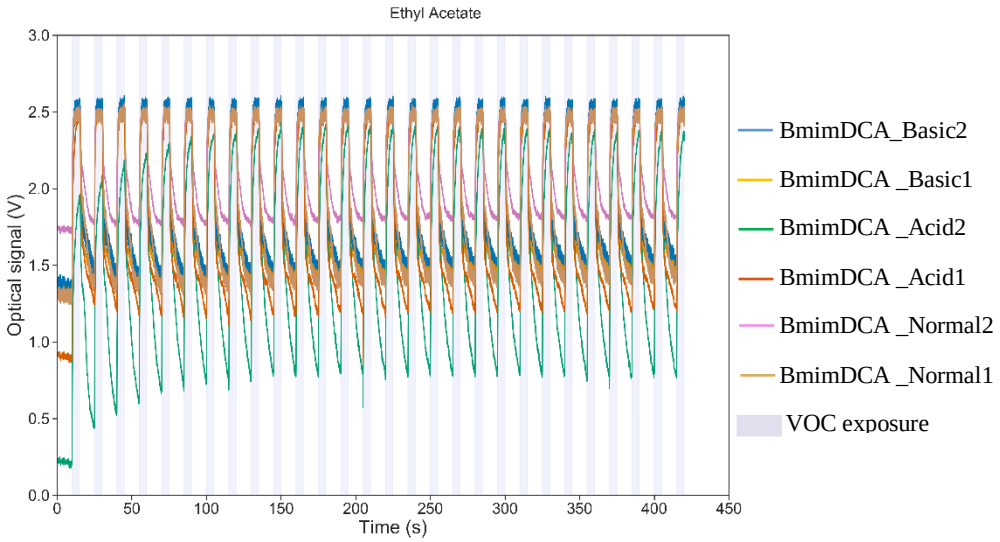
Ethyl Acetate
Optical signal (V)
Time (s)
BmimDCA_Basic2
BmimDCA _Basic1
BmimDCA _Acid2
BmimDCA _Acid1
BmimDCA _Normal2
BmimDCA _Normal1
VOC exposure

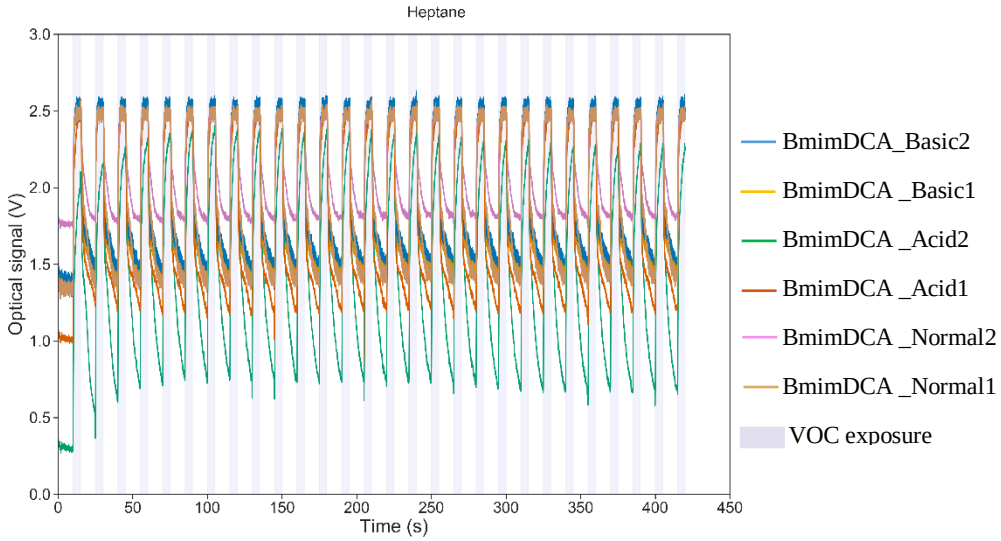
Heptane
Optical signal (V)
Time (s)
BmimDCA_Basic2
BmimDCA _Basic1
BmimDCA _Acid2
BmimDCA _Acid1
BmimDCA _Normal2
BmimDCA _Normal1
VOC exposure

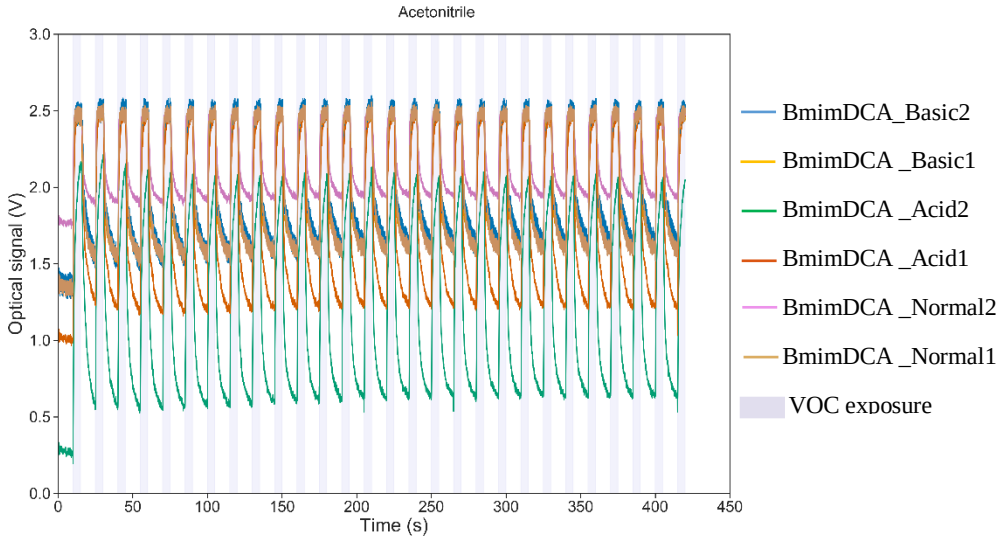
Acetonitrile
Optical signal (V)
Time (s)
BmimDCA_Basic2
BmimDCA _Basic1
BmimDCA _Acid2
BmimDCA _Acid1
BmimDCA _Normal2
BmimDCA _Normal1
VOC exposure

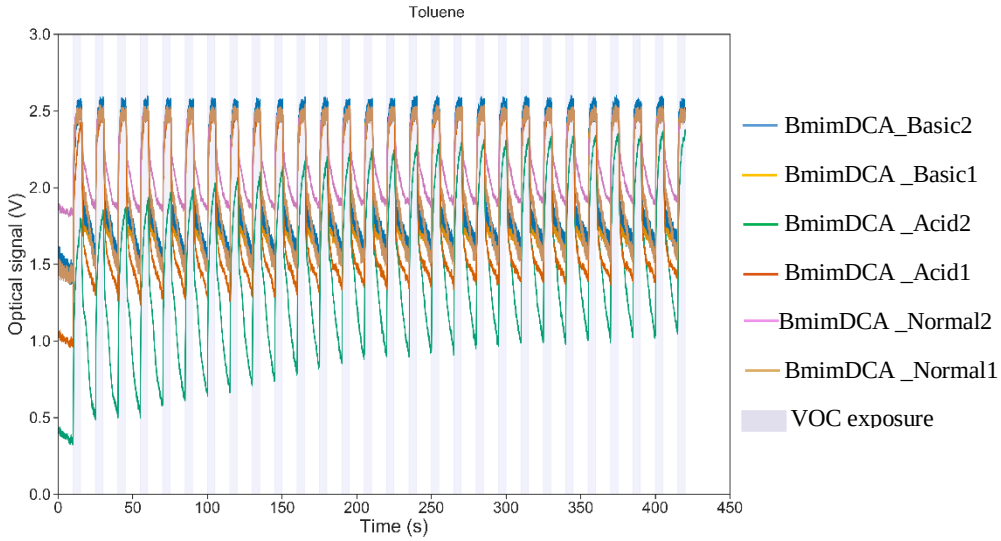
Toluene
Optical signal (V)
Time (s)
BmimDCA_Basic2
BmimDCA _Basic1
BmimDCA _Acid2
BmimDCA _Acid1
BmimDCA _Normal2
BmimDCA _Normal1
VOC exposure

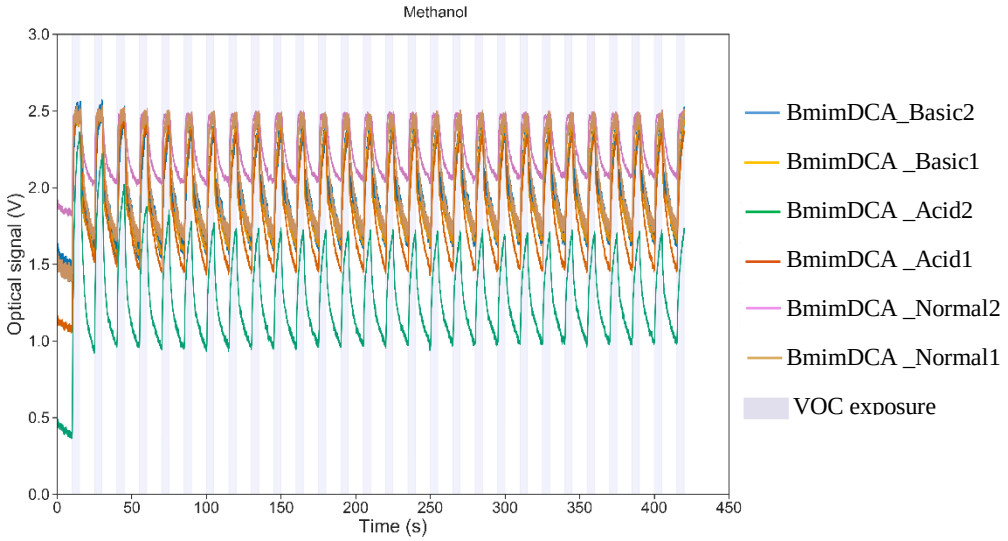
Methanol
Optical signal (V)
Time (s)
BmimDCA_Basic2
BmimDCA _Basic1
BmimDCA _Acid2
BmimDCA _Acid1
BmimDCA _Normal2
BmimDCA _Normal1
VOC exposure

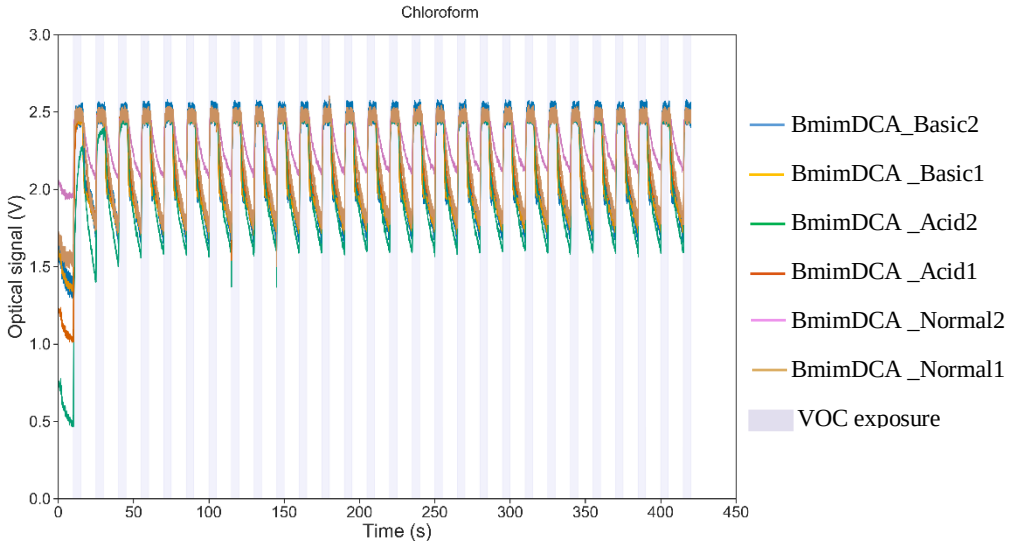
Chloroform
Optical signal (V)
Time (s)
BmimDCA_Basic2
BmimDCA _Basic1
BmimDCA _Acid2
BmimDCA _Acid1
BmimDCA _Normal2
BmimDCA _Normal1
VOC exposure

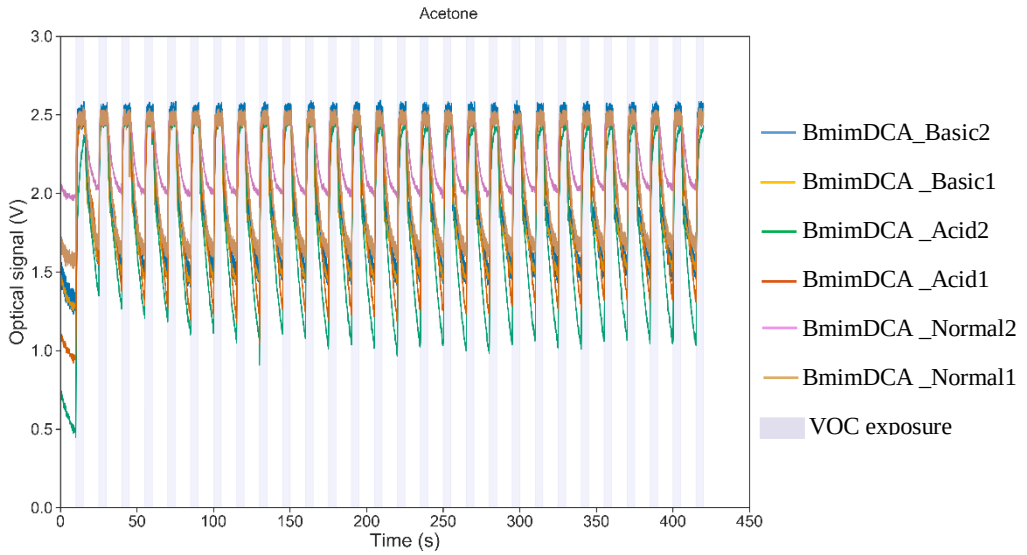
Acetone
Optical signal (V)
Time (s)
BmimDCA_Basic2
BmimDCA _Basic1
BmimDCA _Acid2
BmimDCA _Acid1
BmimDCA _Normal2
BmimDCA _Normal1
VOC exposure

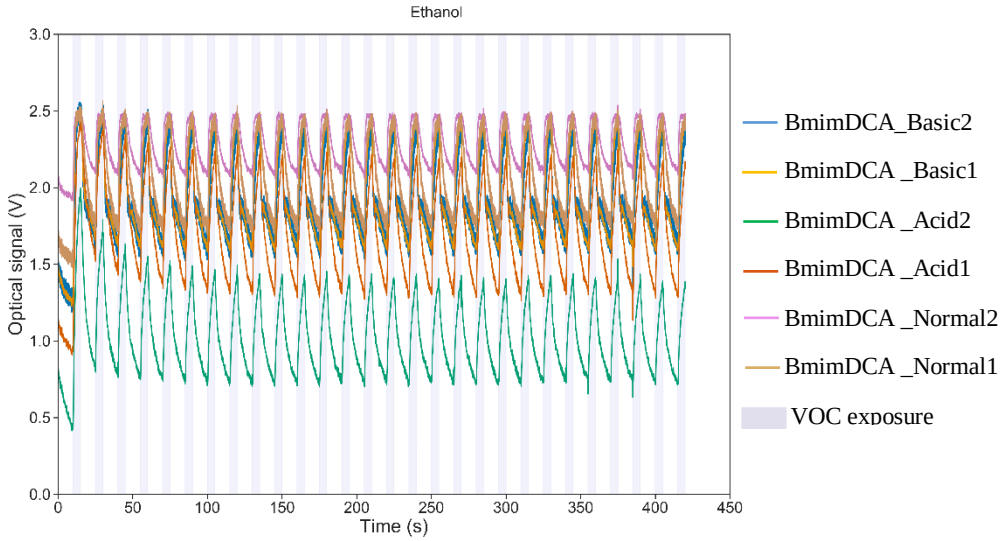
Ethanol
Optical signal (V)
Time (s)
BmimDCA_Basic2
BmimDCA _Basic1
BmimDCA _Acid2
BmimDCA _Acid1
BmimDCA _Normal2
BmimDCA _Normal1
VOC exposure

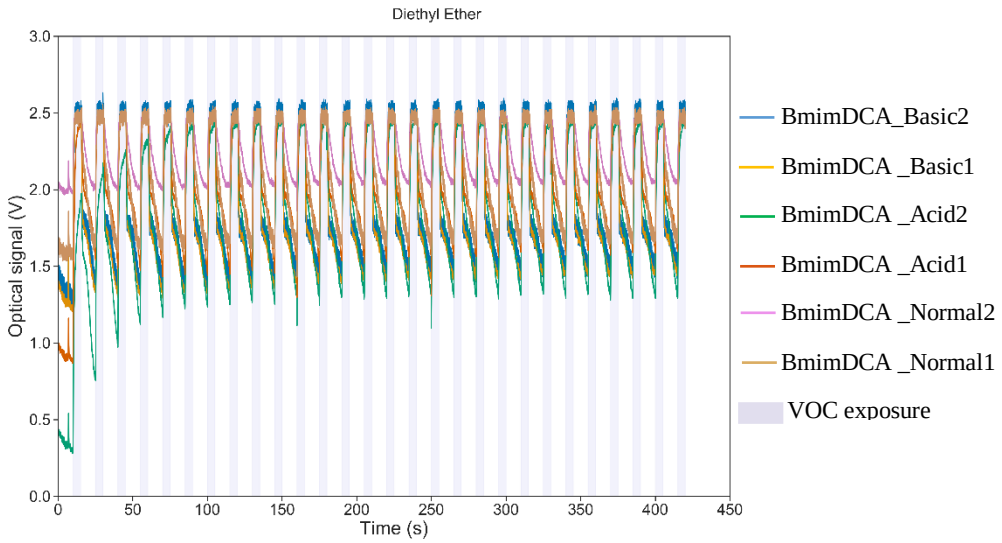
Diethyl Ether
Optical signal (V)
Time (s)
BmimDCA_Basic2
BmimDCA _Basic1
BmimDCA _Acid2
BmimDCA _Acid1
BmimDCA _Normal2
BmimDCA _Normal1
VOC exposure

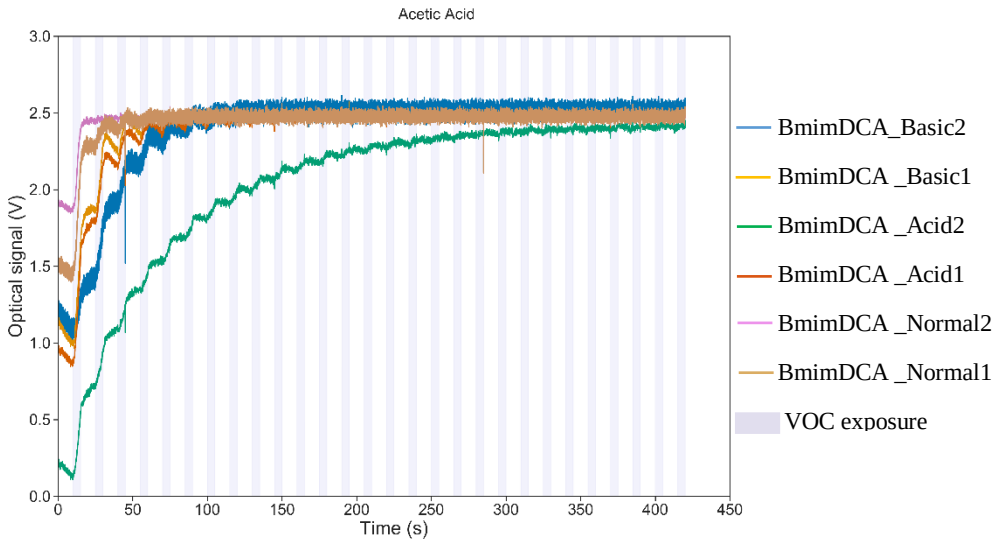
Acetic Acid
Optical signal (V)
Time (s)
BmimDCA_Basic2
BmimDCA _Basic1
BmimDCA _Acid2
BmimDCA _Acid1
BmimDCA _Normal2
BmimDCA _Normal1
VOC exposure

6) No surfactant

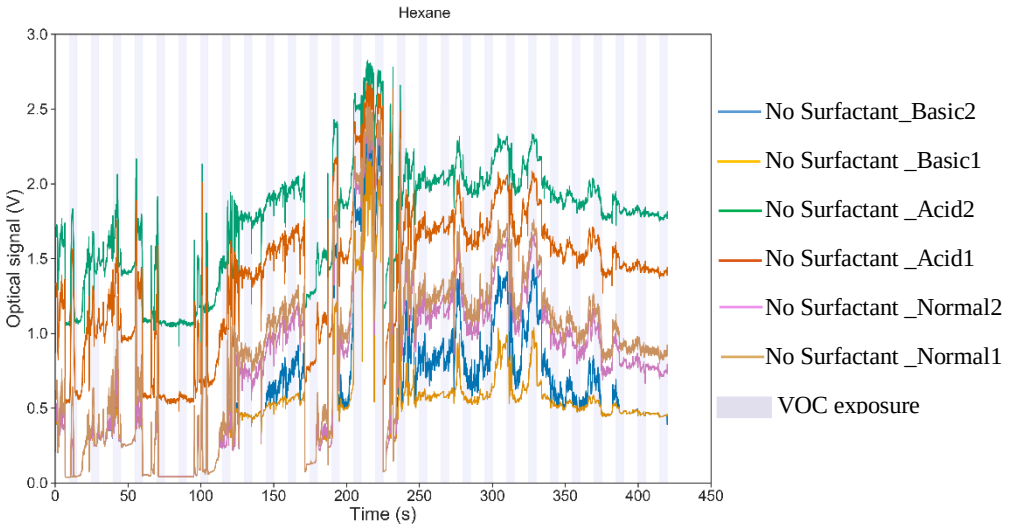

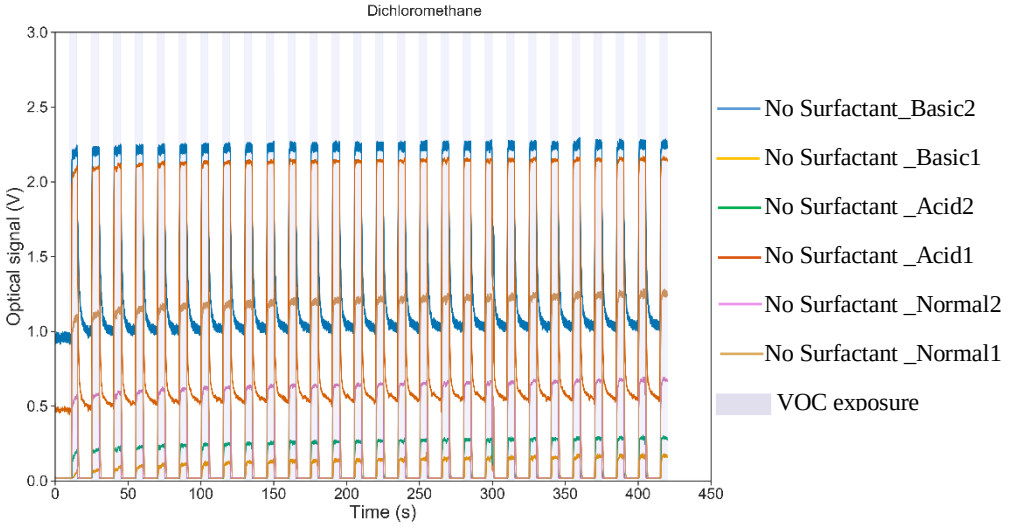

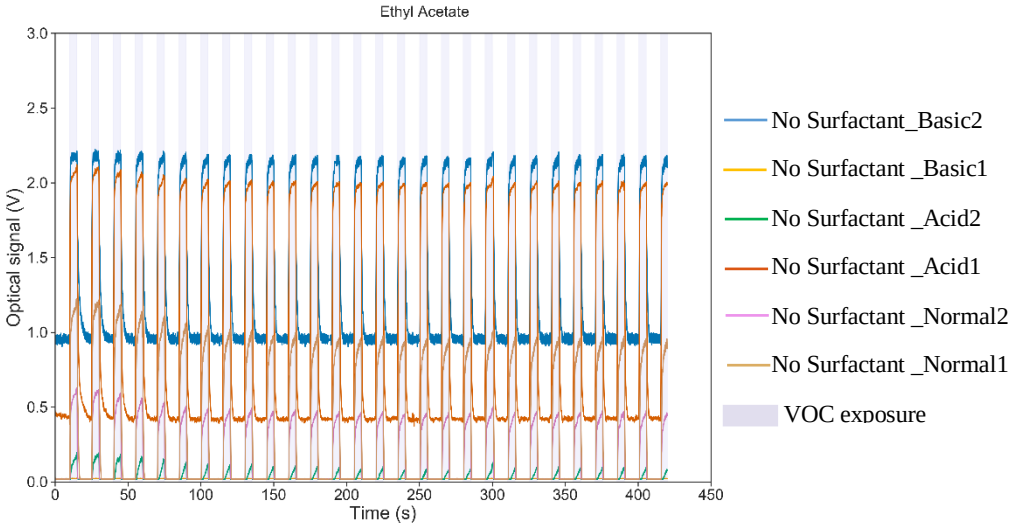

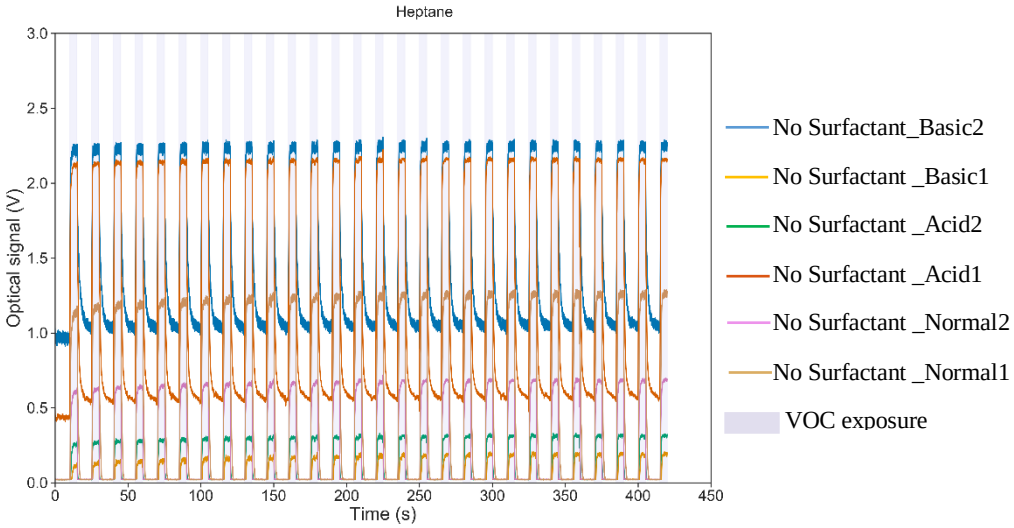
Heptane
Optical signal (V)
Time (s)
No Surfactant_Basic2
No Surfactant _Basic1
No Surfactant _Acid2
No Surfactant _Acid1
No Surfactant _Normal2
No Surfactant _Normal1
VOC exposure

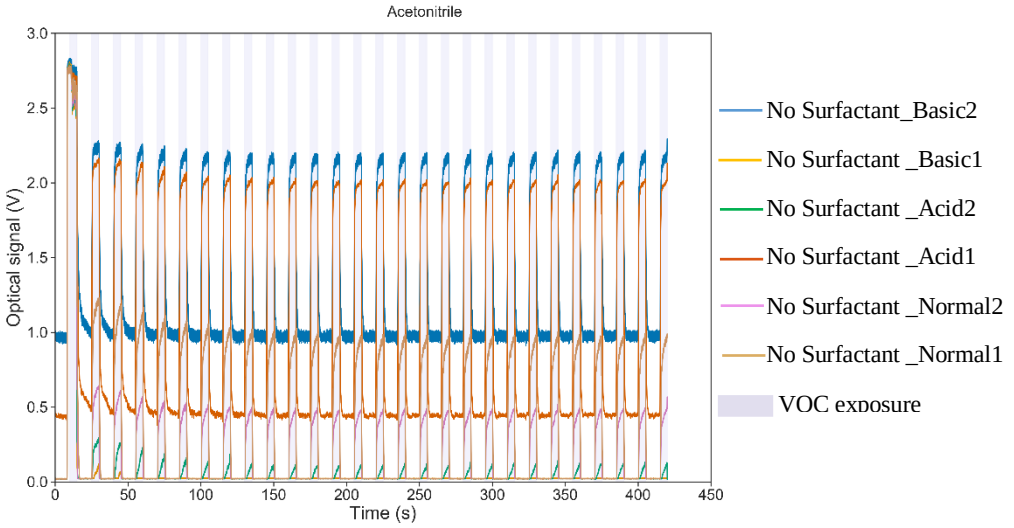
Acetonitrile
Optical signal (V)
Time (s)
No Surfactant_Basic2
No Surfactant _Basic1
No Surfactant _Acid2
No Surfactant _Acid1
No Surfactant _Normal2
No Surfactant _Normal1
VOC exposure

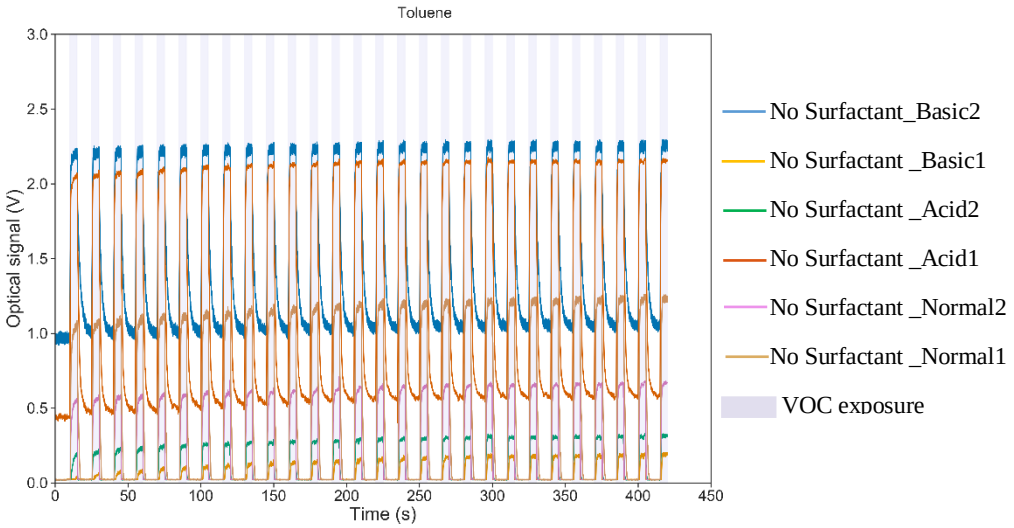
Toluene
Optical signal (V)
Time (s)
No Surfactant_Basic2
No Surfactant _Basic1
No Surfactant _Acid2
No Surfactant _Acid1
No Surfactant _Normal2
No Surfactant _Normal1
VOC exposure

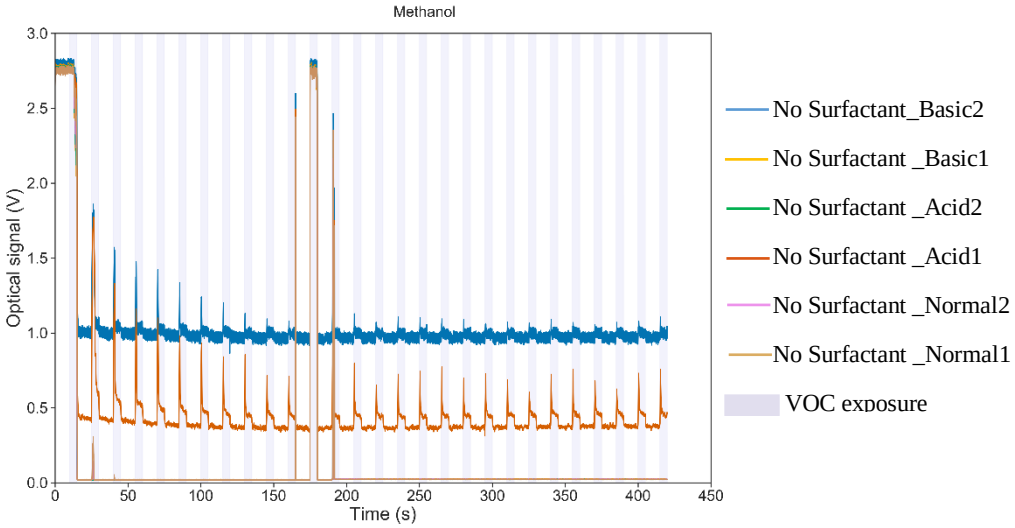
Methanol
Optical signal (V)
Time (s)
No Surfactant_Basic2
No Surfactant _Basic1
No Surfactant _Acid2
No Surfactant _Acid1
No Surfactant _Normal2
No Surfactant _Normal1
VOC exposure

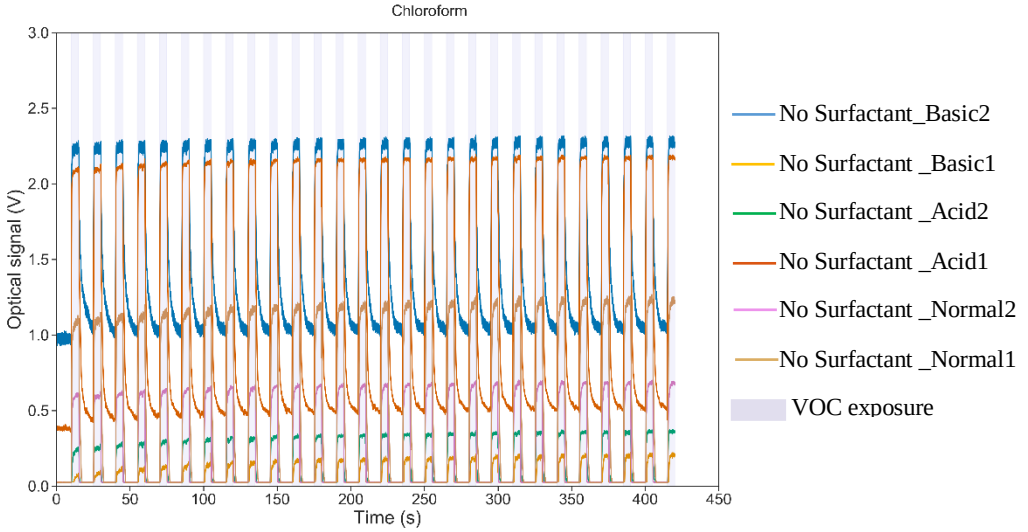
Chloroform
Optical signal (V)
Time (s)
No Surfactant_Basic2
No Surfactant _Basic1
No Surfactant _Acid2
No Surfactant _Acid1
No Surfactant _Normal2
No Surfactant _Normal1
VOC exposure

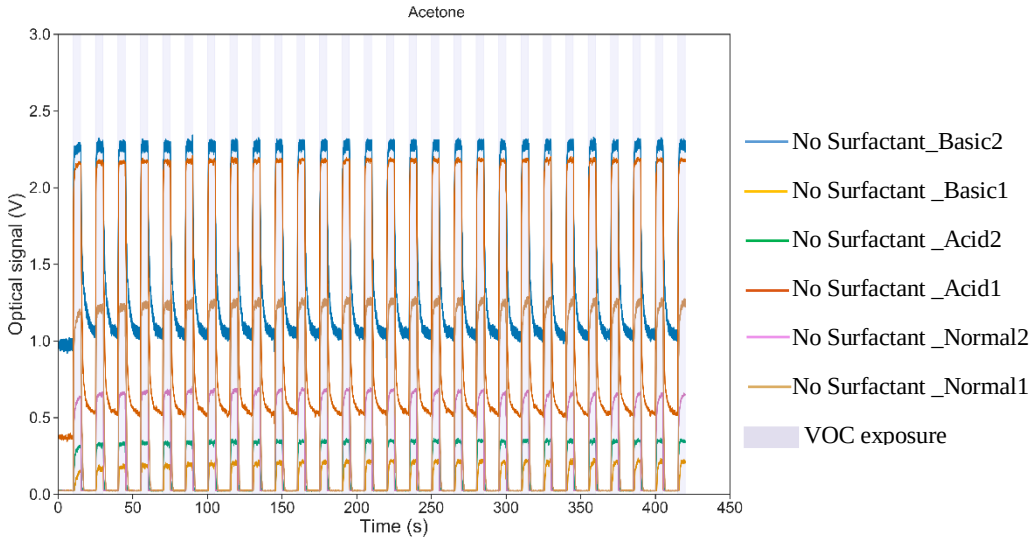
Acetone
Optical signal (V)
Time (s)
No Surfactant_Basic2
No Surfactant _Basic1
No Surfactant _Acid2
No Surfactant _Acid1
No Surfactant _Normal2
No Surfactant _Normal1
VOC exposure

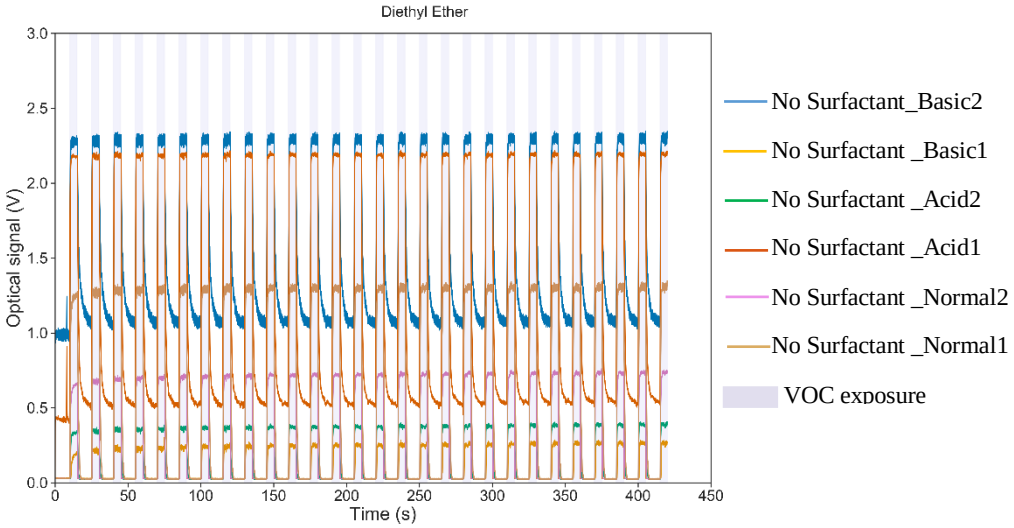
Diethyl Ether
Optical signal (V)
Time (s)
No Surfactant_Basic2
No Surfactant _Basic1
No Surfactant _Acid2
No Surfactant _Acid1
No Surfactant _Normal2
No Surfactant _Normal1
VOC exposure

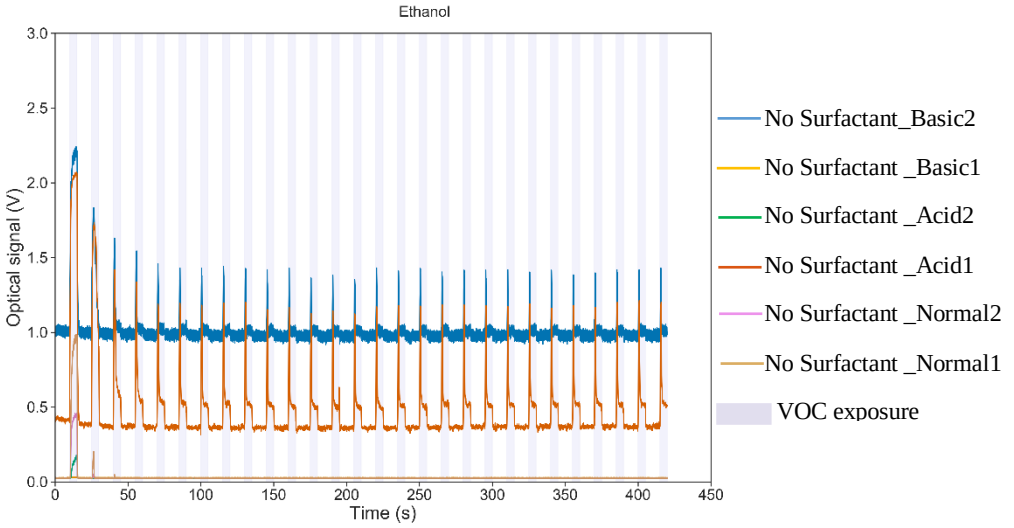
Ethanol
Optical signal (V)
Time (s)
No Surfactant_Basic2
No Surfactant _Basic1
No Surfactant _Acid2
No Surfactant _Acid1
No Surfactant _Normal2
No Surfactant _Normal1
VOC exposure

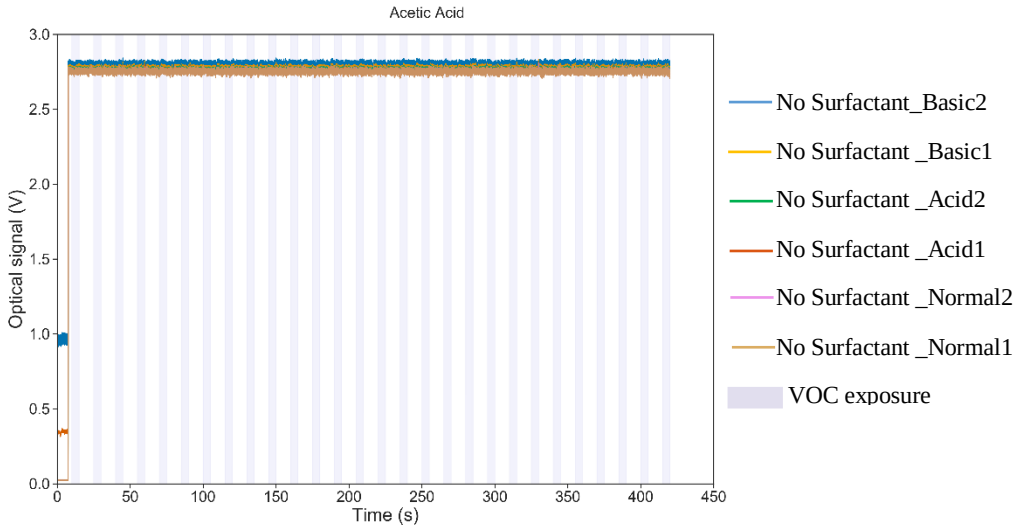
Acetic Acid
Optical signal (V)
Time (s)
No Surfactant_Basic2
No Surfactant _Basic1
No Surfactant _Acid2
No Surfactant _Acid1
No Surfactant _Normal2
No Surfactant _Normal1
VOC exposure

H – E-nose Features – VOCs scores for all tested gels and confusion matrices

1) [C_{12}mim][Cl]

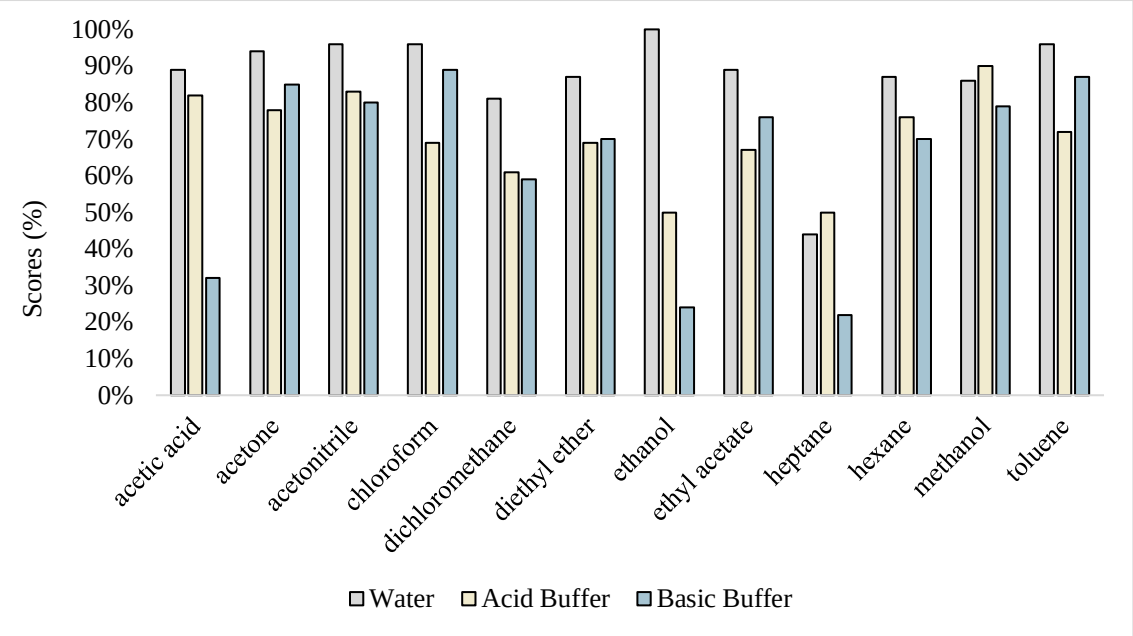

VOC/ Medium	Water	Acid Buffer	Basic Buffer
Acetic Acid	89%	82%	32%
Acetone	94%	78%	85%
Acetonitrile	96%	83%	80%
Chloroform	96%	69%	89%
Dichloromethane	81%	61%	59%
Diethyl Ether	87%	69%	70%
Ethanol	100%	50%	24%
Ethyl Acetate	89%	67%	76%
Heptane	44%	50%	22%
Hexane	87%	76%	70%
Methanol	86%	90%	79%
Toluene	96%	72%	87%

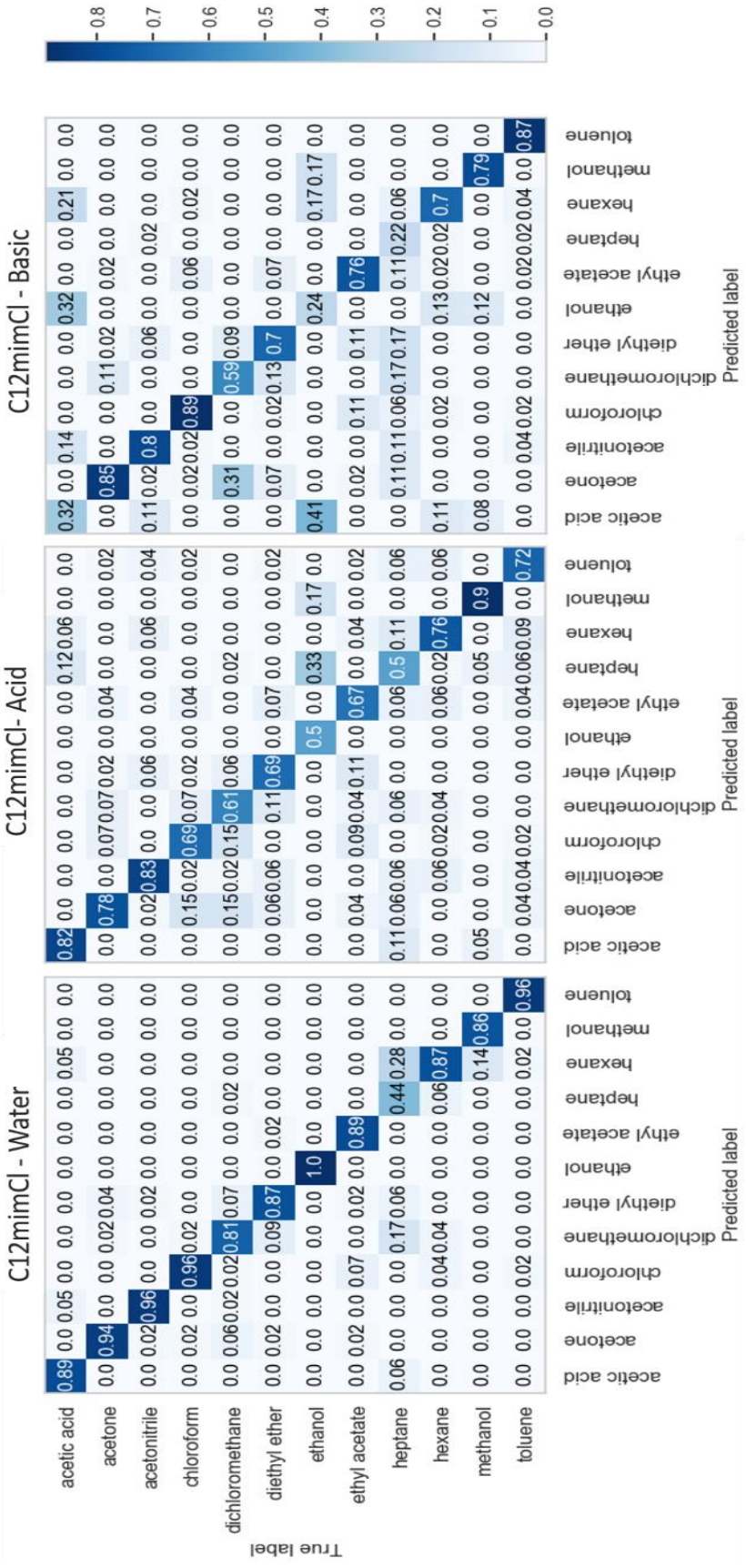

Figure 0.5. Confusion matrices for [C_{12}mim][Cl] with different pH means

2) SDS

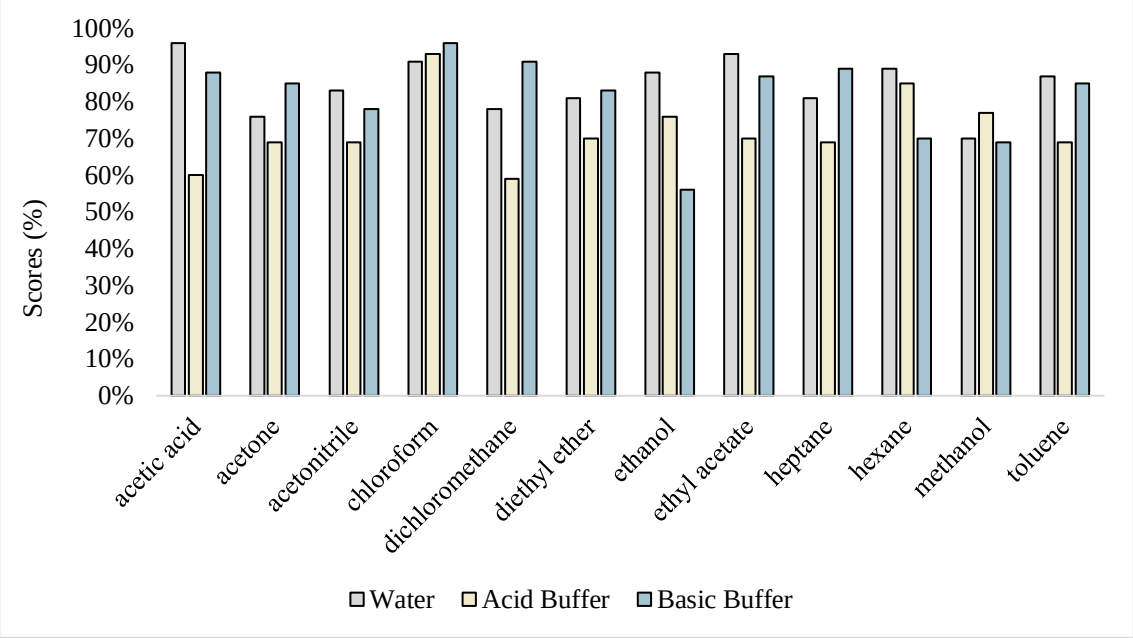

VOC/ Medium	Water	Acid Buffer	Basic Buffer
Acetic Acid	96%	60%	88%
Acetone	76%	69%	85%
Acetonitrile	83%	69%	78%
Chloroform	91%	93%	96%
Dichloromethane	78%	59%	91%
Diethyl Ether	81%	70%	83%
Ethanol	88%	76%	56%
Ethyl Acetate	93%	70%	87%
Heptane	81%	69%	89%
Hexane	89%	85%	70%
Methanol	70%	77%	69%
Toluene	87%	69%	85%

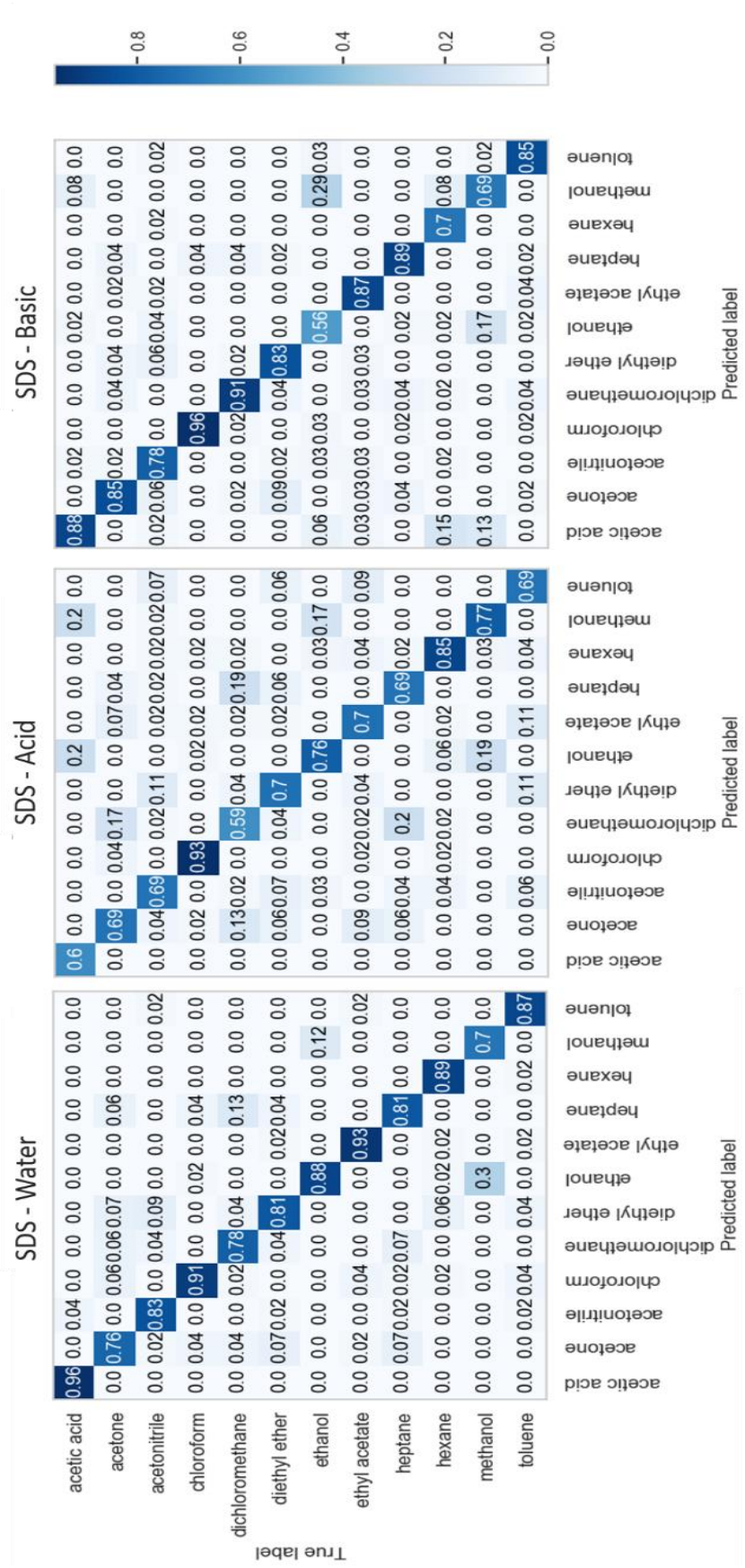

Figure 0.6. Confusion matrices for SDS with different pH means

3) [C_{12}mim][DS]

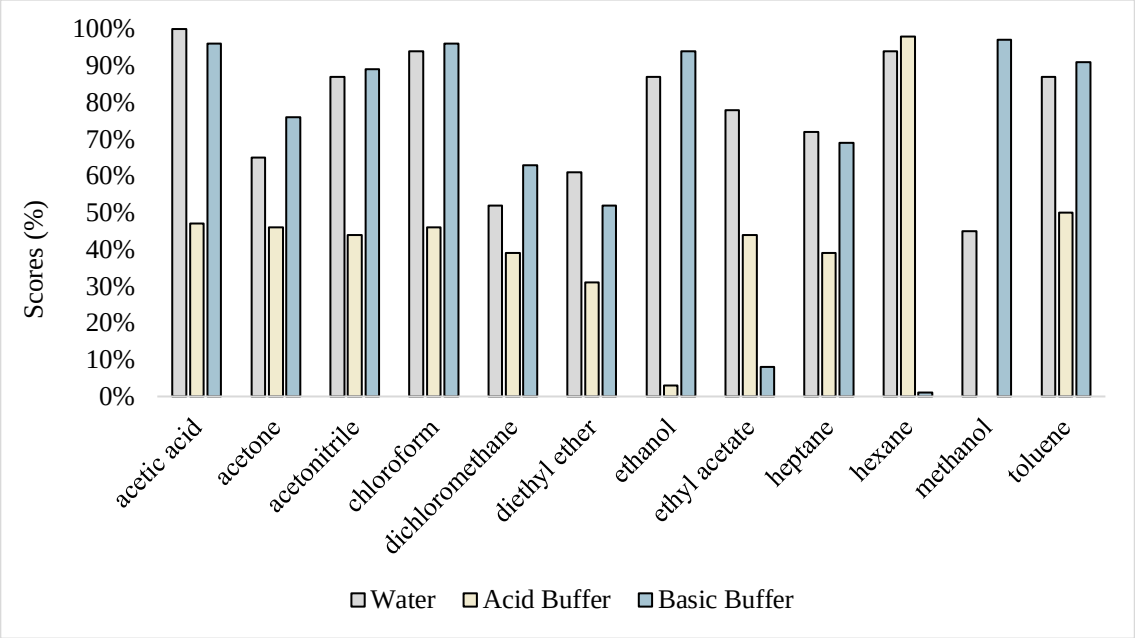

VOC/ Medium	Water	Acid Buffer	Basic Buffer
Acetic Acid	100%	47%	96%
Acetone	65%	46%	76%
Acetonitrile	87%	44%	89%
Chloroform	94%	46%	96%
Dichloromethane	52%	39%	63%
Diethyl Ether	61%	31%	52%
Ethanol	87%	3%	94%
Ethyl Acetate	78%	44%	8%
Heptane	72%	39%	69%
Hexane	94%	98%	1%
Methanol	45%	0%	97%
Toluene	87%	50%	91%

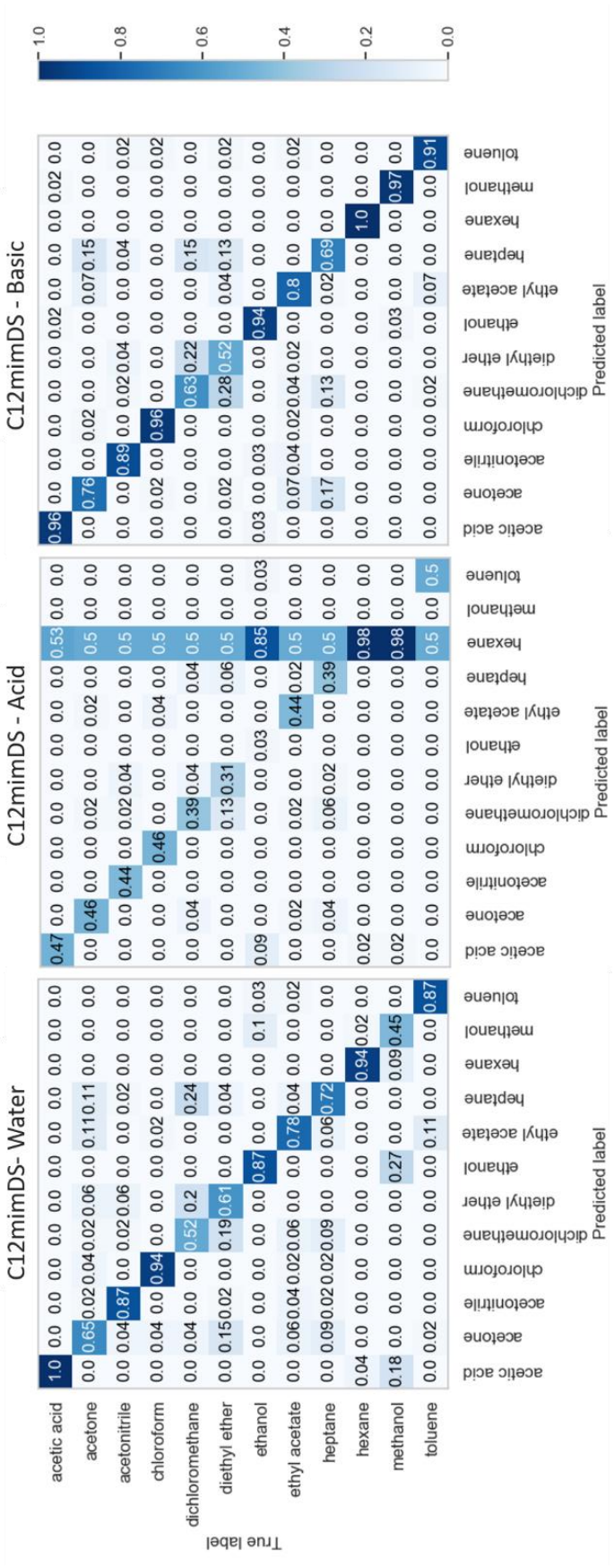

Figure 0.7. Confusion matrices for [C_{12}mim][DS] with different pH means

4) [Bmim][Cl]

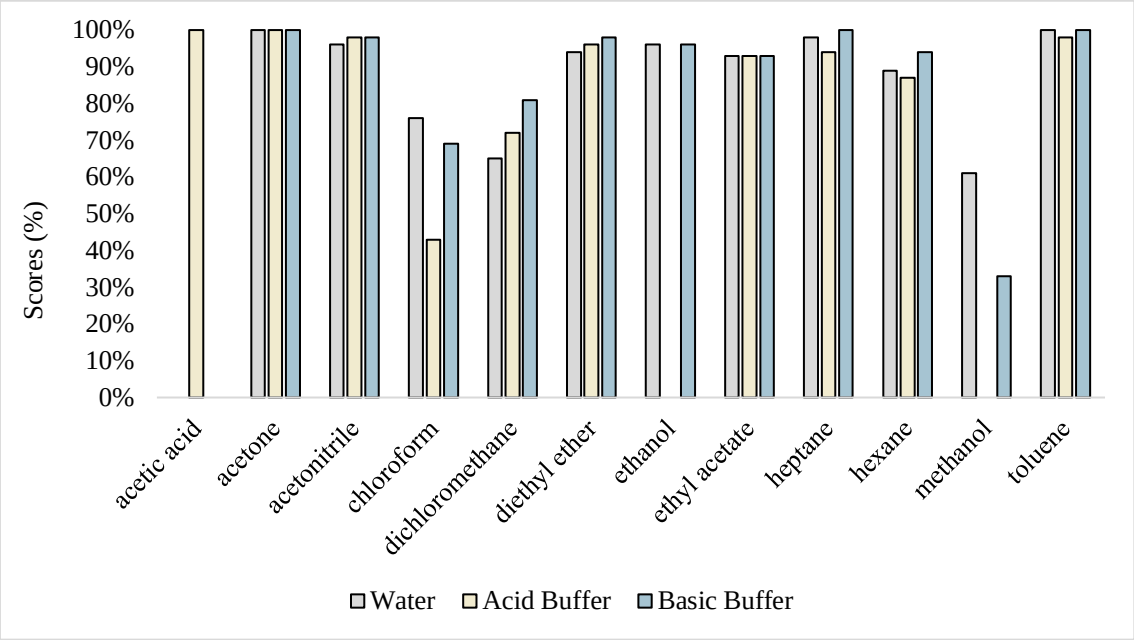

VOC/ Medium	Water	Acid Buffer	Basic Buffer
Acetic Acid	0%	100%	0%
Acetone	100%	100%	100%
Acetonitrile	96%	98%	98%
Chloroform	76%	43%	69%
Dichloromethane	65%	72%	81%
Diethyl Ether	94%	96%	98%
Ethanol	96%	0%	96%
Ethyl Acetate	93%	93%	93%
Heptane	98%	94%	100%
Hexane	89%	87%	94%
Methanol	61%	0%	33%
Toluene	100%	98%	100%

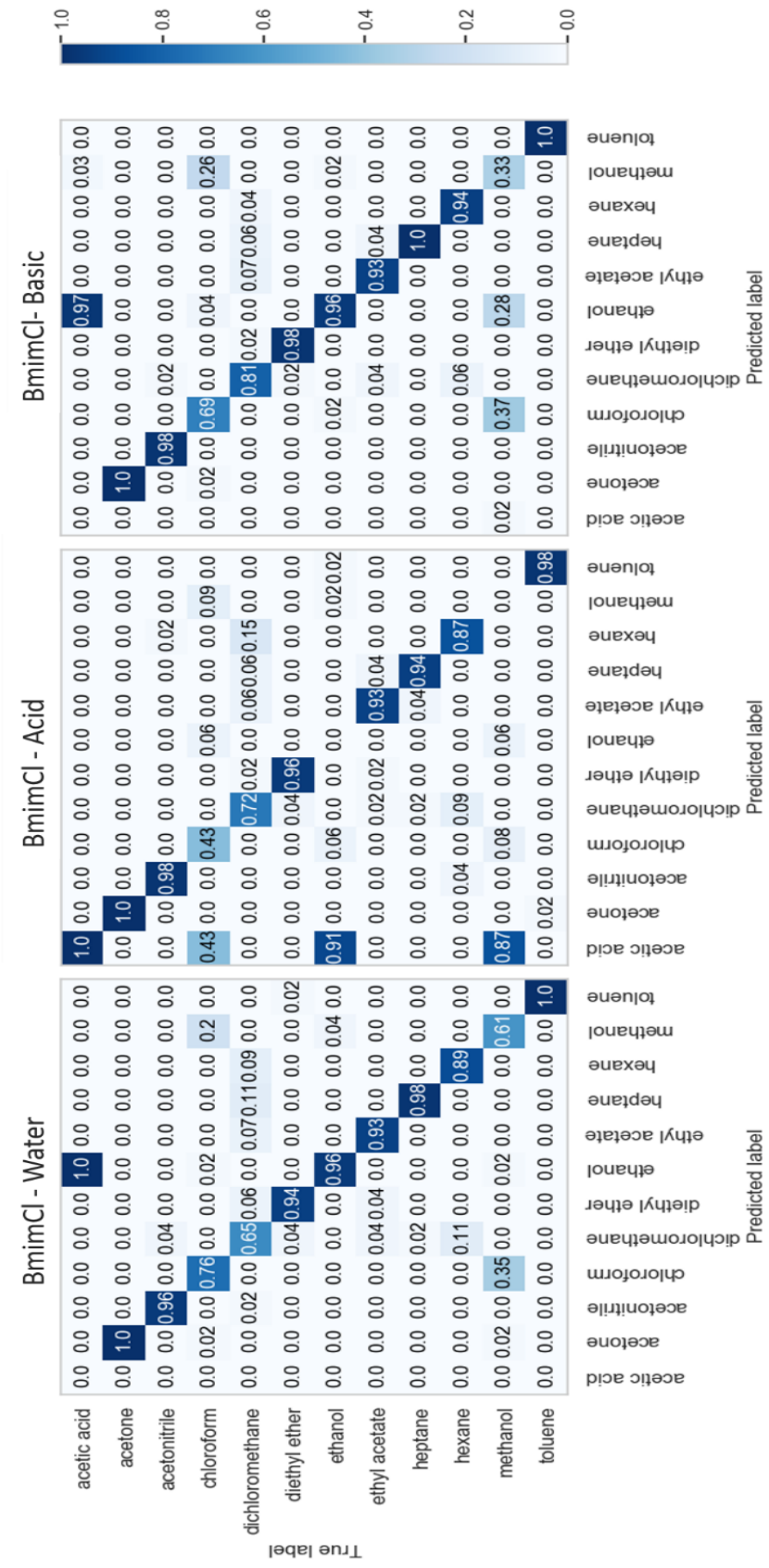

Figure 0.8. Confusion matrices for [Bmim][Cl] with different pH means

5) [Bmim][DCA]

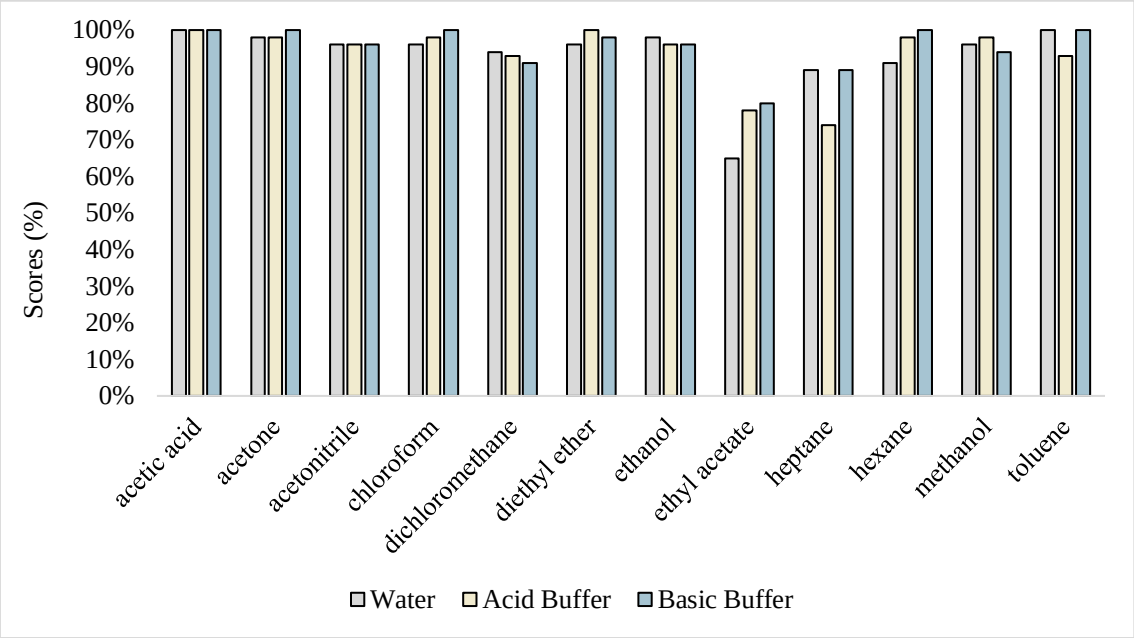

VOC/ Medium	Water	Acid Buffer	Basic Buffer
Acetic Acid	100%	100%	100%
Acetone	98%	98%	100%
Acetonitrile	96%	96%	96%
Chloroform	96%	98%	100%
Dichloromethane	94%	93%	91%
Diethyl Ether	96%	100%	98%
Ethanol	98%	96%	96%
Ethyl Acetate	65%	78%	80%
Heptane	89%	74%	89%
Hexane	91%	98%	100%
Methanol	96%	98%	94%
Toluene	100%	93%	100%

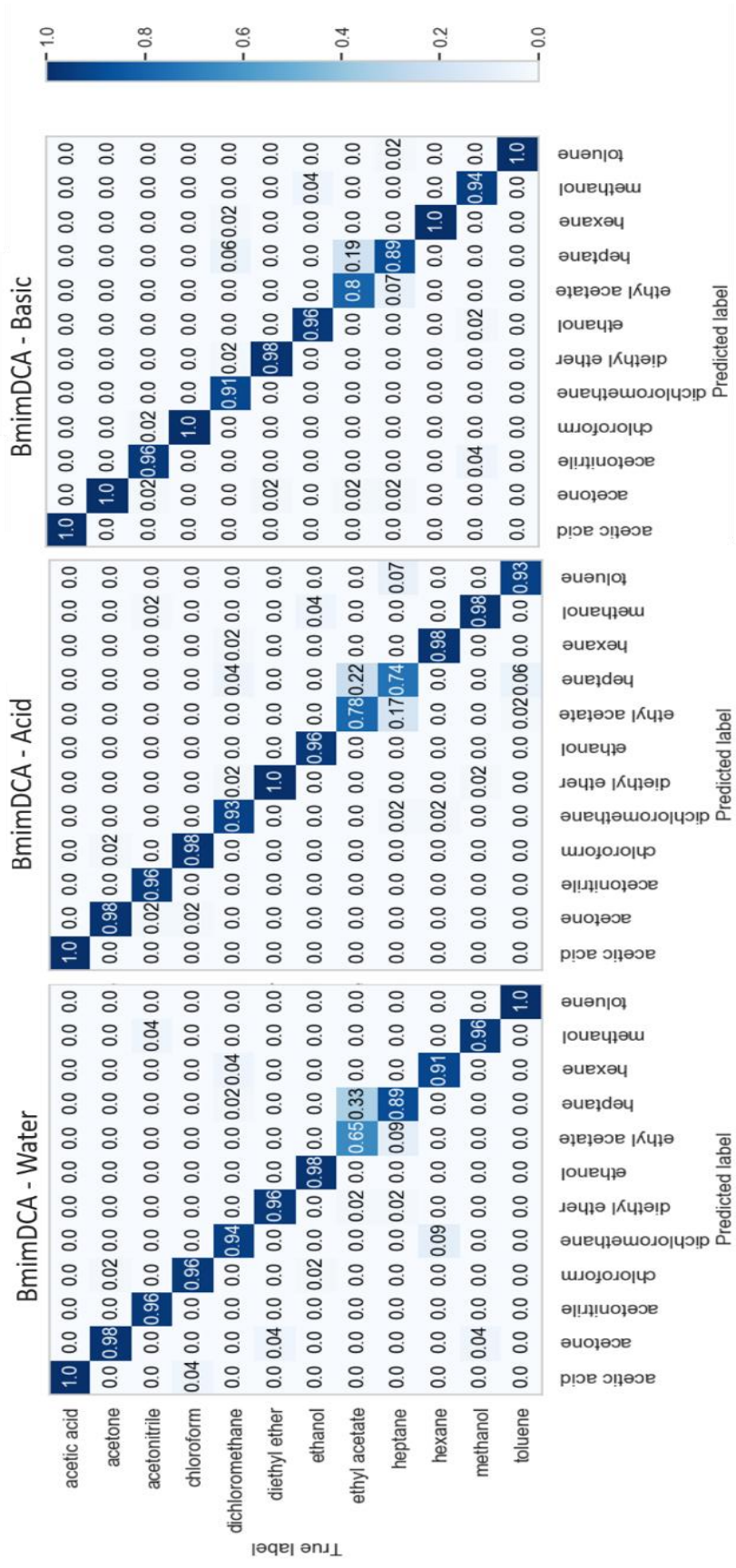

Figure 0.9. Confusion matrices for [Bmim][DCA] with different pH means

6) No Surfactant

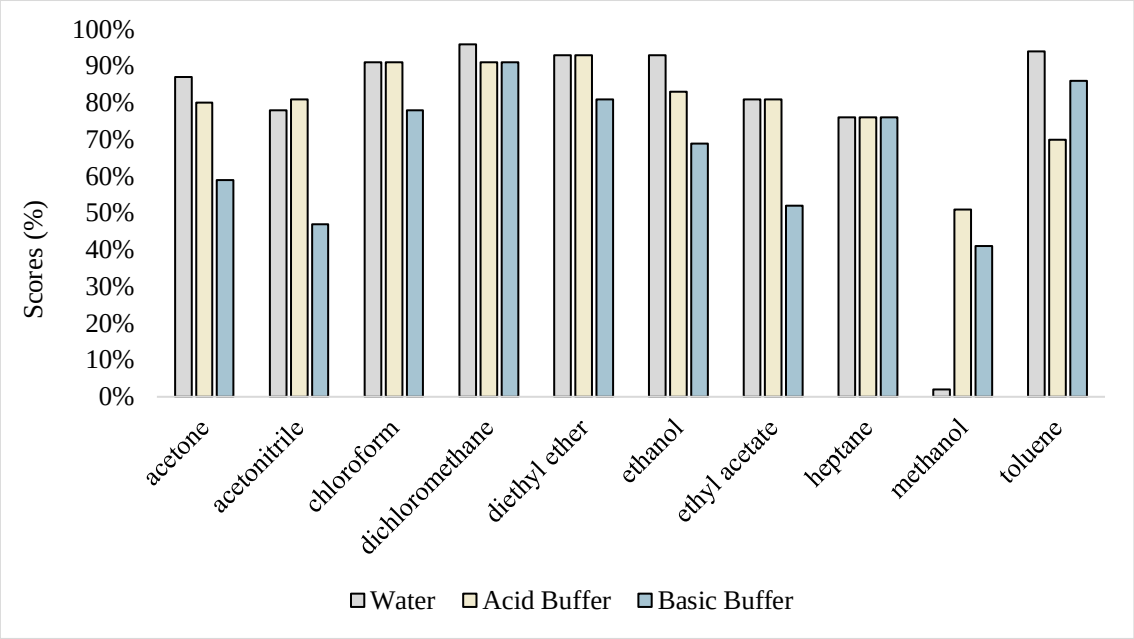

VOC/ Medium	Water	Acid Buffer	Basic Buffer
Acetic Acid	87%	80%	59%
Acetone	78%	81%	47%
Acetonitrile	91%	91%	78%
Chloroform	96%	91%	91%
Dichloromethane	93%	93%	81%
Diethyl Ether	93%	83%	69%
Ethanol	81%	81%	52%
Ethyl Acetate	76%	76%	76%
Heptane	2%	51%	41%
Hexane	94%	70%	86%
Methanol	-	-	-
Toluene	-	-	-

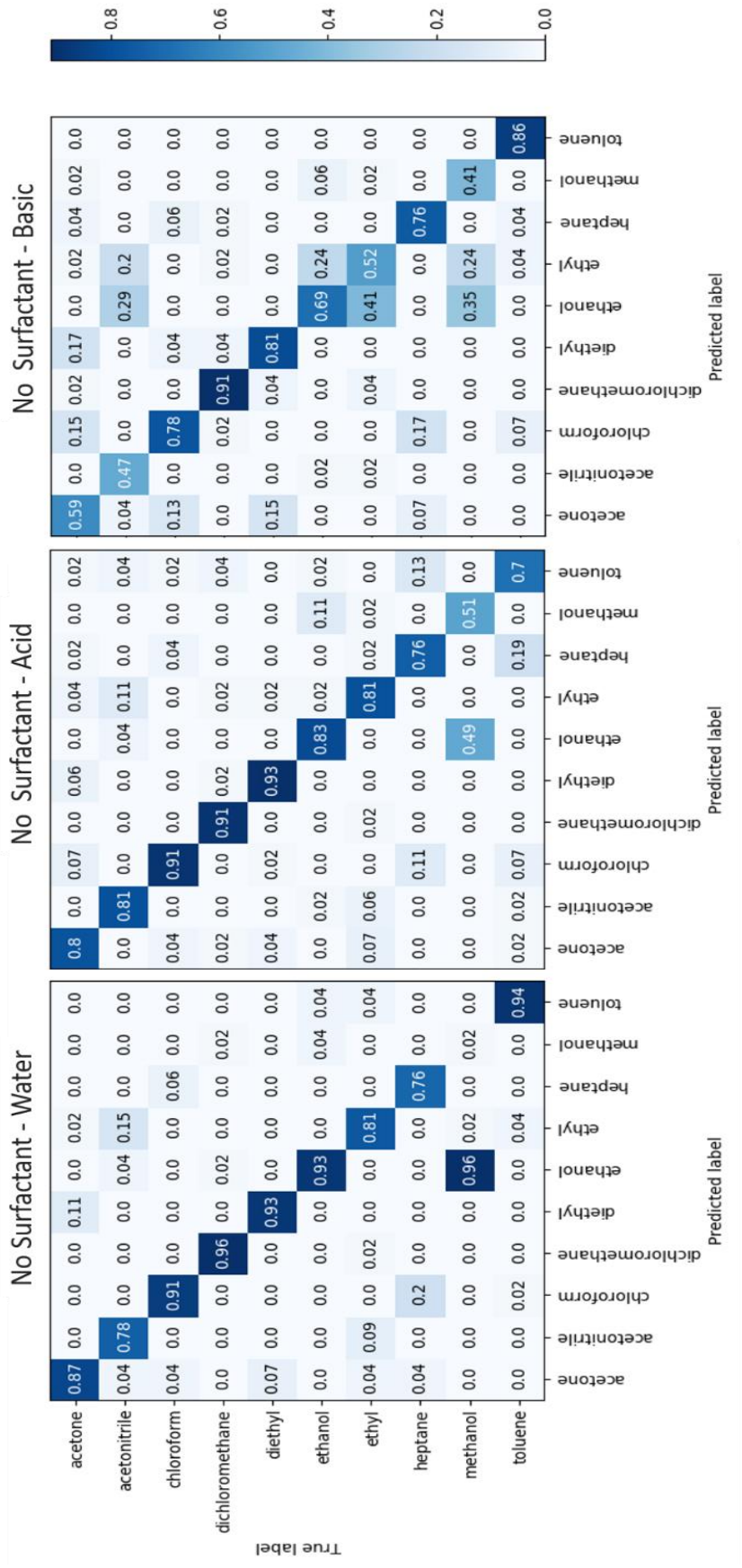

Figure 0.10. Confusion matrices for the different pH means for the case of no surfactant

I – E-nose Sensors Tiles

1) [C_{12}mim][Cl]

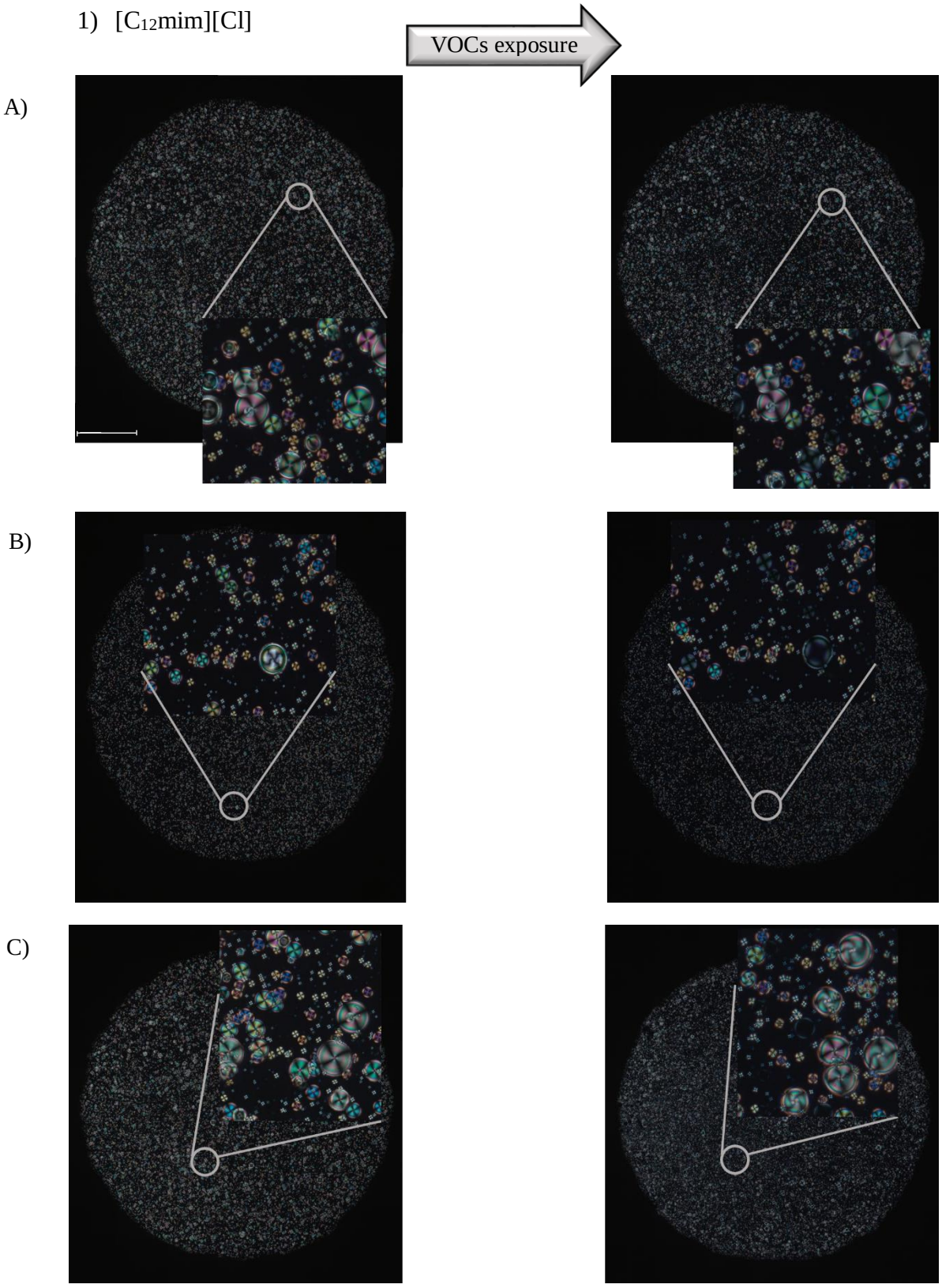

Figure 0.11. Tiles Before and after the VOCs exposure, for [C_{12}mim][Cl] sensors; A) Gels made within an aqueous mean; B) Gels made within an acid mean; C) Gels made within a basic mean. The scale bar represents 500 um

2) SDS

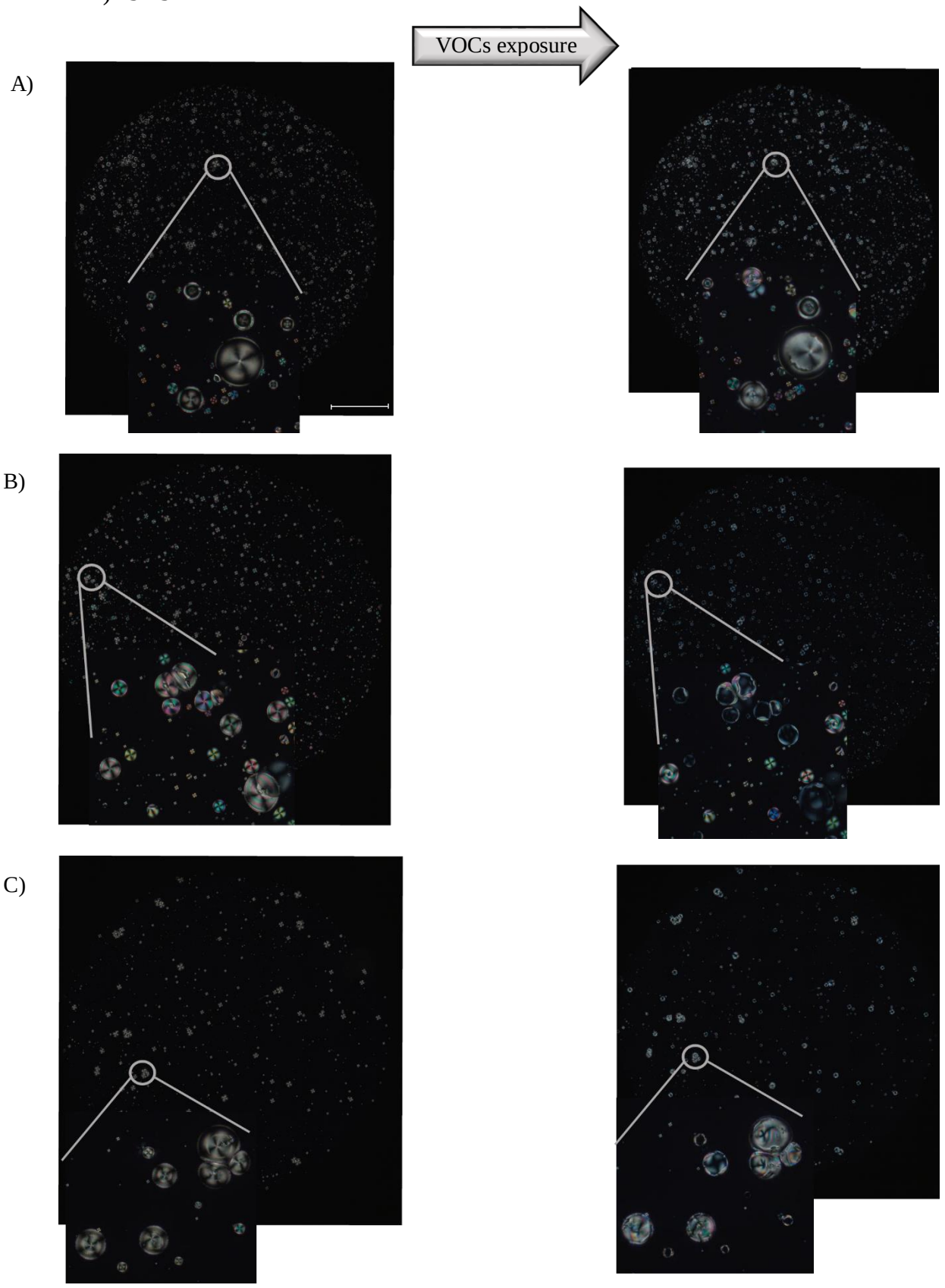

Figure 0.12. Tiles Before and after the VOCs exposure, for SDS sensors; A) Gels made within an aqueous mean; B) Gels made within an acid mean; C) Gels made within a basic mean. The scale bar represents 500 um

3) [C_{12}mim][DS]

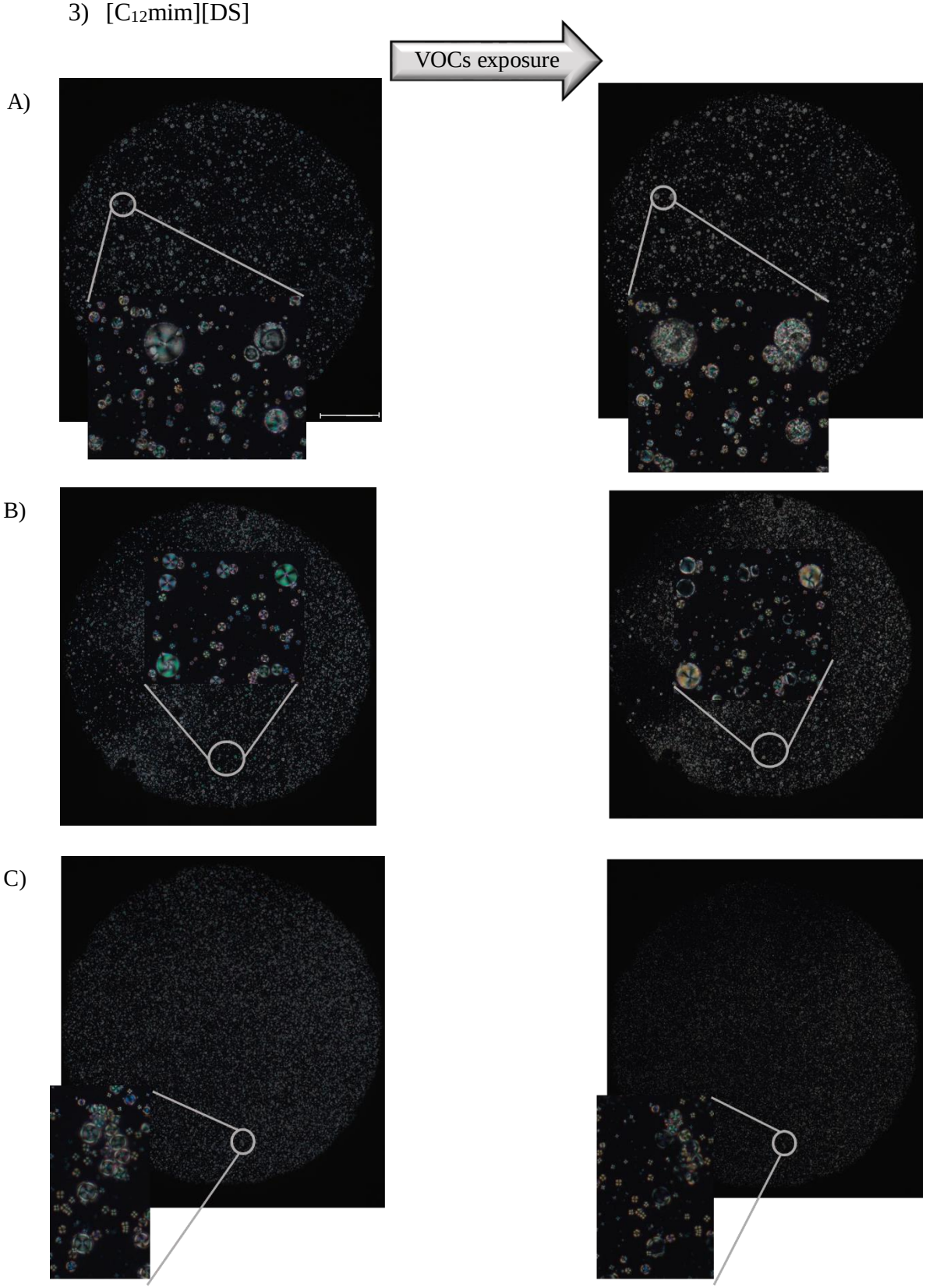

Figure 0.13. Tiles Before and after the VOCs exposure, for [C_{12}mim][DS] sensors; A) Gels made within an aqueous mean; B) Gels made within an acid mean; C) Gels made within a basic mean. The scale bar represents 500 um

4) [Bmim][Cl]

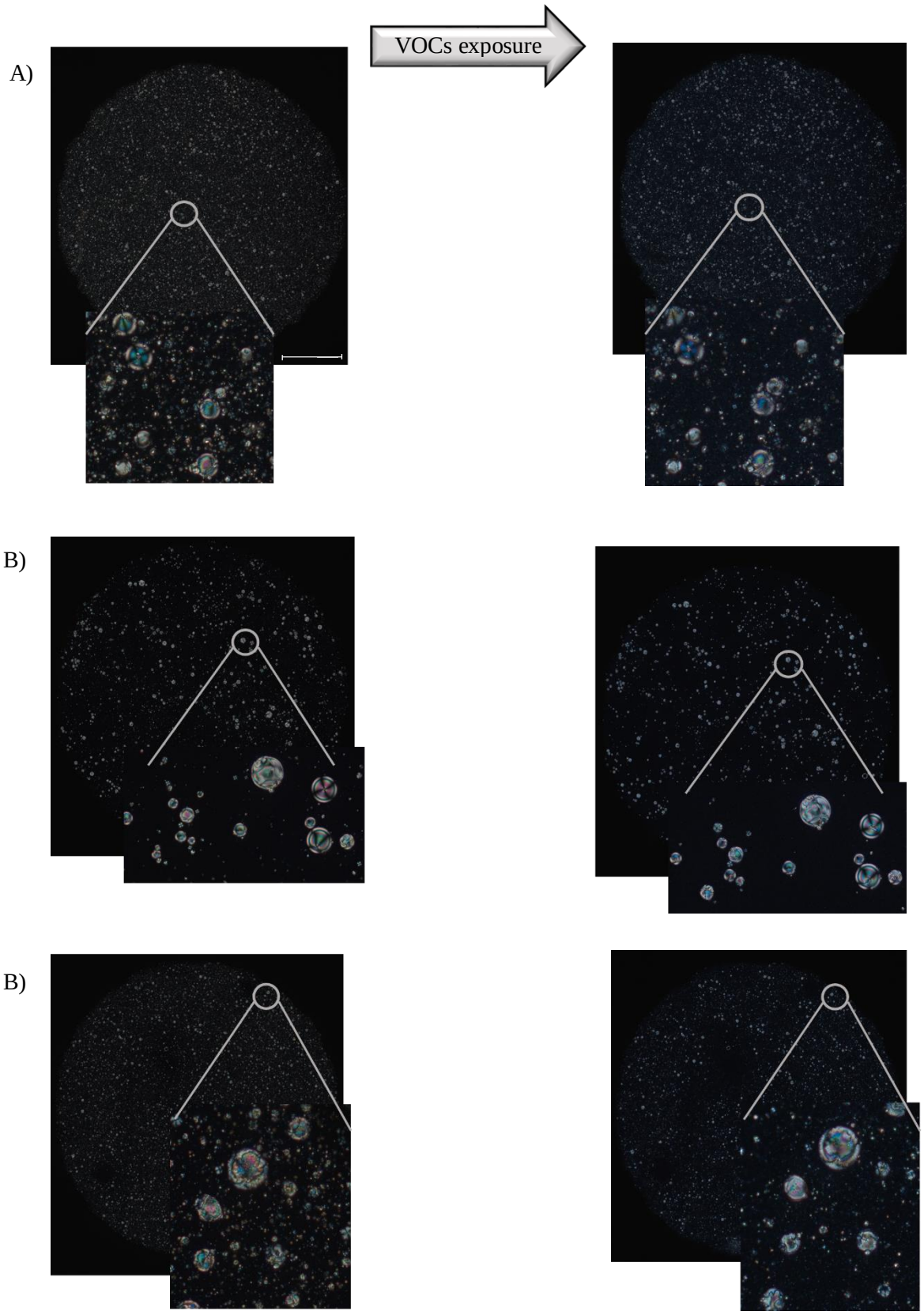

Figure 0.14. Tiles Before and after the VOCs exposure, for [Bmim][Cl] sensors; A) Gels made within an aqueous mean; B) Gels made within an acid mean; C) Gels made within a basic mean. The scale bar represents 500 um

5) [Bmim][DCA]

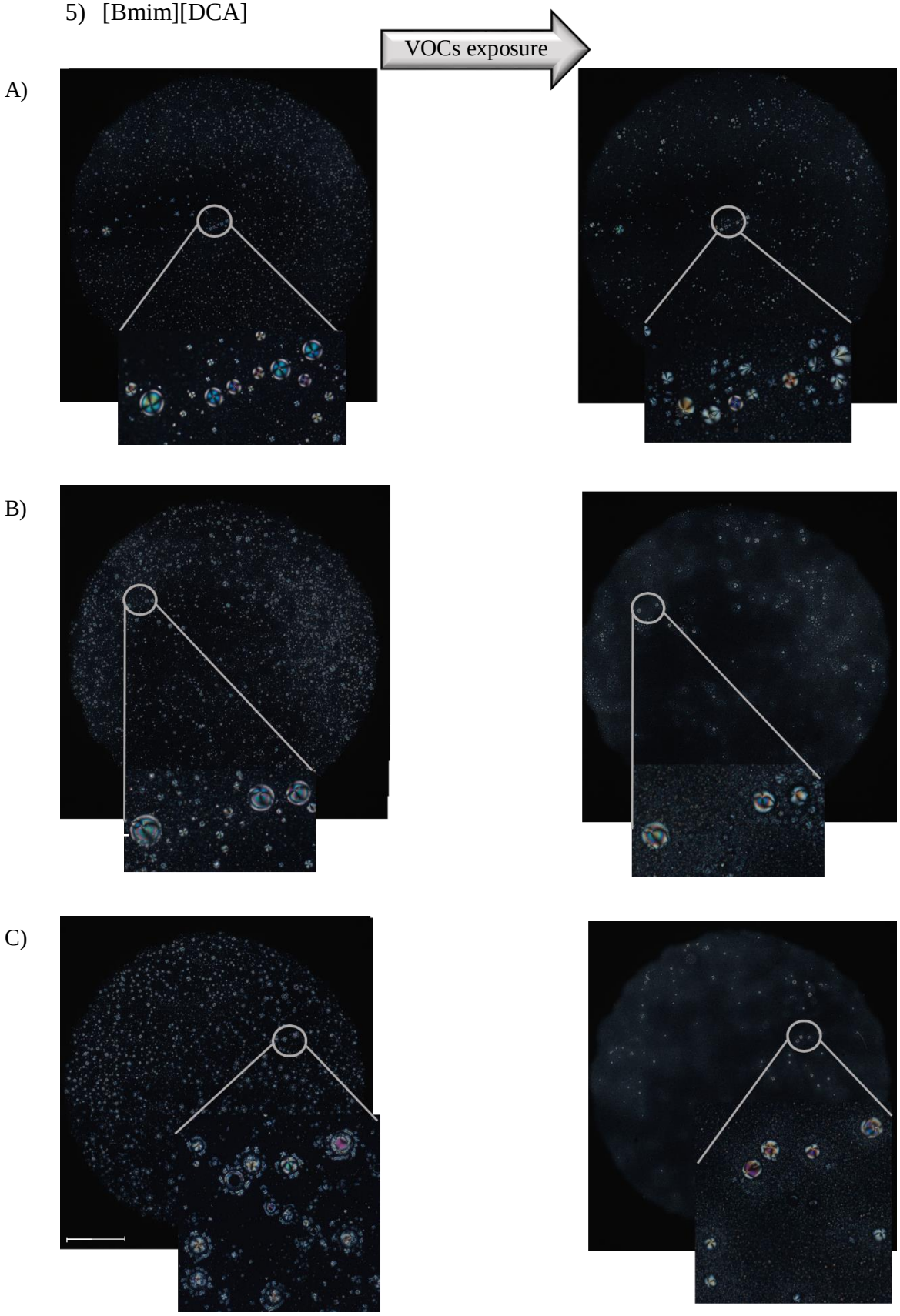

Figure 0.15. Tiles Before and after the VOCs exposure, for [Bmim][DCA] sensors; A) Gels made within an aqueous mean; B) Gels made within an acid mean; C) Gels made within a basic mean. The scale bar represents 500 um

6) No surfactant

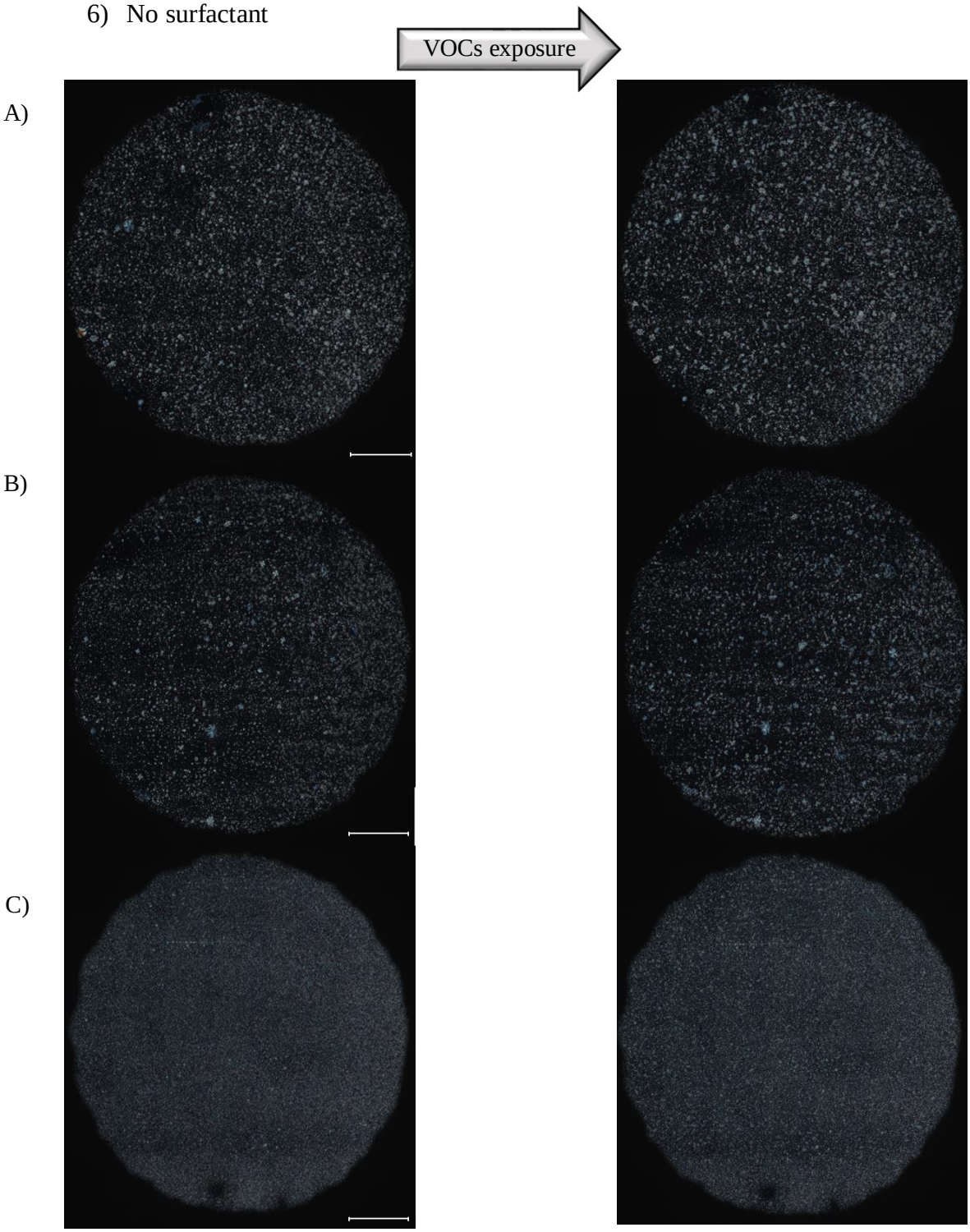

Figure 0.16. Tiles Before and after the VOCs exposure, for the no surfactant case sensors; A) Gels made within an aqueous mean; B) Gels made within an acid mean; C) Gels made within a basic mean. The scale bar represents 500 um